This is to certify that the
dissertation entitled

D2 RECEPTOR-MEDIATED REGULATION OF GENE EXPRESSION IN TUBEROINFUNDIBULAR DOPAMINE NEURONS

presented by

YVONNE MARIE WILL-MURPHY

has been accepted towards fulfillment
of the requirements for the

Ph.D. degree in Pharmacology and Toxicology

Ruth J. Lookingland
Major Professor's Signature

5-14-04
Date

D2 RECEPTOR-MEDIATED REGULATION OF GENE EXPRESSION IN TUBEROINFUNDIBULAR DOPAMINE NEURONS

By

Yvonne Marie Will-Murphy

A DISSERTATION

Submitted to
Michigan State University
in partial fulfillment of the requirements
for the degree of

DOCTOR OF PHILOSOPHY

Department of Pharmacology and Toxicology

2004

ABSTRACT

D2 RECEPTOR-MEDIATED REGULATION OF GENE EXPRESSION IN TUBEROINFUNDIBULAR DOPAMINE NEURONS

By

Yvonne Marie Will-Murphy

Activation of D2 receptors with selective agonists, such as quinelorane, stimulates the synthesis and release of dopamine (DA) from tuberoinfundibular (TI) DA neurons through an afferent neuronal system involving tonically active dynorphin neurons via kappa opioid receptors. Is the D2 receptor activation of TIDA neurons is accompanied by an increase in genomic expression in these neurons?

The purpose of this dissertation was to characterize D2 receptor-mediated regulation of gene expression in TIDA neurons located in the dorsomedial arcuate nucleus (DM-ARC) using a combination of anatomical, immunohistochemical, molecular and pharmacological experimental approaches to answer the following questions: 1) Are there sexual differences in the distribution of TIDA neurons and in Fos and related antigens (FRA) expression in these neurons? 2) Do D2 receptors regulate immediate early gene expression in TIDA neurons? 3) Do kappa opioid receptors mediate D2 receptor regulation of Fos expression in TIDA neurons? 4) Do D2 receptors regulate TH gene expression in TIDA neurons? and 5) Does Fos play a role in the regulation of TH gene expression in TIDA neurons?

1. There were no sexual differences in the number of TIDA neurons but the the percentage of these neurons containing FRA-IR nuclei was 2-3 times higher in females than in males.

2. Acute administration of the D2 agonist quinelorane caused a time-related increase in the percentage of TIDA neurons expressing Fos. This effect was blocked by administration of the D2 antagonist, raclopride.

3. The kappa receptor agonist U50-488 had no effect per se, but reversed the stimulatory effects of quinelorane on Fos expression in TIDA neurons. This suggests that D2 receptor-mediated regulation of Fos in these neurons involves inhibition of endogenous dynorphin release and thus the loss of tonic inhibition of gene expression.

4. Quinelorane significantly increased TH mRNA in TIDA neurons and this effect was blocked by raclopride. Thus, D2 receptors regulate TH gene expression in TIDA neurons.

5. c-fos antisense blocked the quinelorane-induced activation of TH mRNA expression in TIDA neurons, whereas c-fos sense and nonsense were without effect. These results reveal that Fos, at least in part, mediates the activation of TH gene expression in TIDA neurons.

This work is lovingly dedicated to my husband Frank,
my son Conor,
my parents Kurt and Gerry Will and
my Godparents Lou and Karen Mihalyfy

ACKNOWLEDGEMENTS

First and foremost, I wish to thank my thesis advisor and mentor, Dr. Keith Lookingland. I will be forever grateful for all of your time, advice, and support. This has been a very long road and I thank you for believing in me. I will always remember your slogan, "You can do it!"

In addition, I would like to give a special thanks to my guidance committee Drs. Kenneth Moore, William Falls, Norbert Kaminiski, and John Thornburg. I am grateful for their advice, support, and patience.

There have been several post-doctoral fellows and senior students in the lab that I would like to thank: Chris McMahon, Sun Cheung, Rob Durham, Ken Hentschel and John Morris. Even through the long days crouched over swirling plates of brain tissue, you always found a way to make me laugh. Our "unofficial" lab meetings will not be forgotten.

I would like to thank the technicians Erika Bronz, and Tom "Bubba" Ingram for providing technical assistance. A special thanks goes to Mark Jacob for going above and beyond the call of duty. From washing dishes to creating computer artwork to making the HPLC room a 70's haven, you are a man of a many talents. I wish you luck in the medical field.

I would like to recognize the front office staff, Diane Hummel, Nelda Carpenter, Mickie Vanderlip, Faye Spencer, and Jeff Nobis for assisting me with all of my complicated administrative dilemmas.

I would like to acknowledge Dr Joan Mattson. Thank you for introducing me to the world of science and medicine.

Finally I would like to thank my husband Frank, my parents Kurt and Gerry Will, my Godparents Karen and Lou Mihalyfy and the Murphy family for all the love, support and encouragement to see me through to the end. Thank you for always believing in me. I could never have done it without you.

TABLE OF CONTENTS

LIST OF TABLES

LIST OF FIGURES

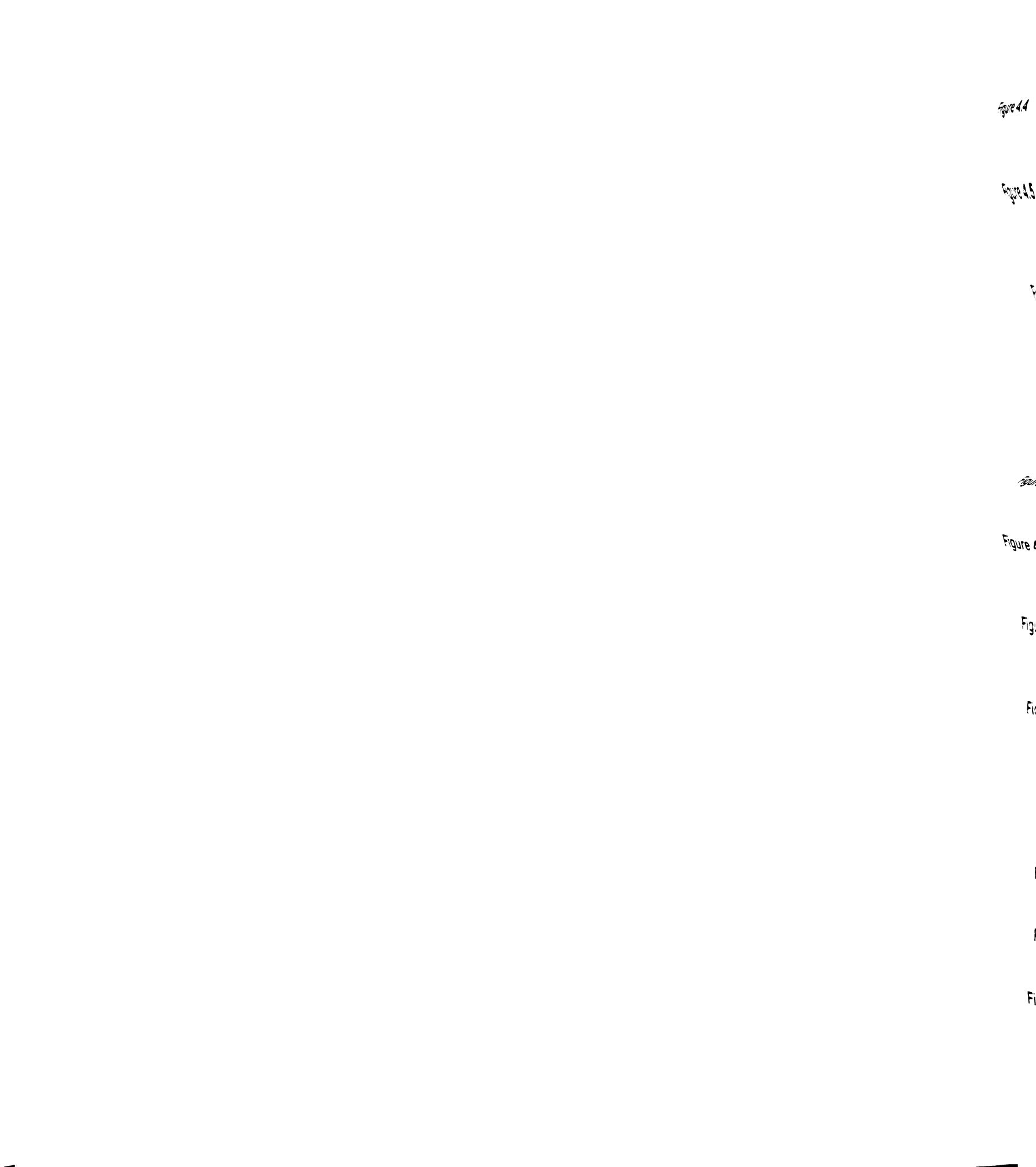

Figure 5.2

Figure 5.3

Figure 5

Figu

Fi

Fi

Figure 5.14

Figure 5.1

Figure e

Figu

Fi

F

F

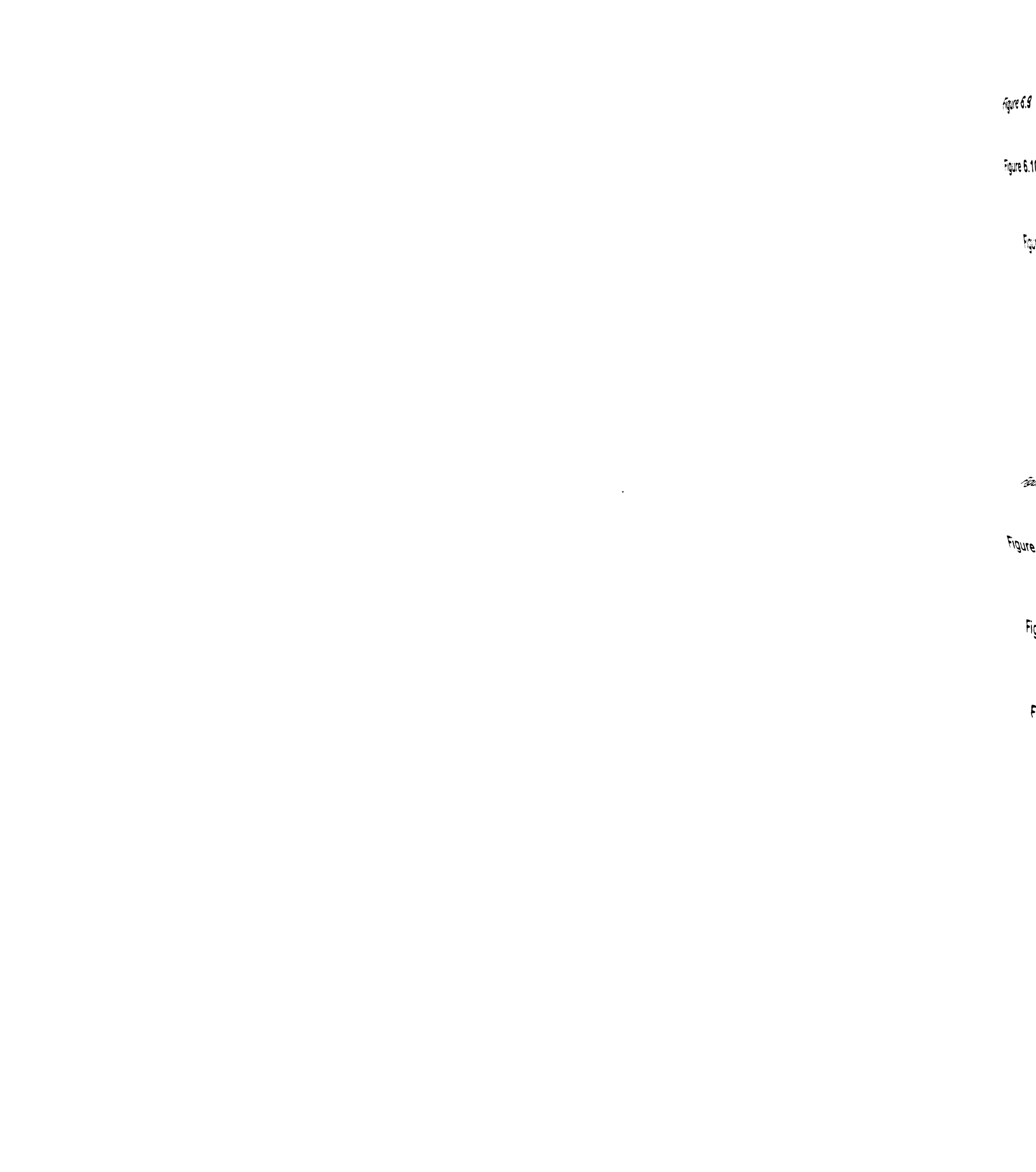

ABBREVIATIONS

2-DG	2-deoxyglucose
3V	third ventricle
ABC	avidin-biotin complex
AL	anterior lobe of the pituitary
AMPA	alpha-amino-3-hydroxy-5-methylisoxazole-4-proprionic acid
AP	alkaline phosphatase
AP-1	activated protein 1
AP-2	activated protein 2
ARC	arcuate nucleus
AS	antisense
ATF-1	activating transcription factor-1
cAMP	cyclic adenyl monophosphate
CC	corpus callosum
CaRE	calcium response element
CRE	cyclic AMP response element
CRE-2	cyclic AMP response element 2
CREB	cyclic AMP response element binding protein
CREM	cAMP response element modulator
CSF	cerebrospinal fluid
DA	dopamine
DAB	3,3'-diaminobenzidine
DD	DOPA decarboxylase
ddH_2O	double distilled water
DEPC	diethylpyrocarbonate
DM	dorsomedial
DMN	dorsomedial hypothalamic nucleus
DNA	deoxyribonucleic acid
DOPA	3,4-dihydroxyphenylalanine
DOPAC	3,4-dihydroxyphenylacetic acid
DYN	dynorphin
Egr1	early growth response 1
EtOH	ethanol
f	fornix
FRA	Fos and its related antigens
GABA	gamma aminobutyric acid
GBL	gamma butyrolactone
h	hour(s)
HEPT	heptamer
HIF	hypoxia-inducible factor
HIPP	hippocampus
ic	internal capsule
ICV	intracerebroventricular
IEG	immediate early gene
IHDA	incertohypothalamic dopamine

IL	intermediate lobe of the pituitary
InfS	infundibular stalk
ip	intraperitoneal
IR	immunoreactive
K+	potassium
Kg	kilogram(s)
MAO	monoamine oxidase
ME	median eminence
mg	milligram(s)
min	minute(s)
ml	milliliters
mm	millimeters
mRNA	messenger ribonucleic acid
mt	mammillothalamic tract
MZI	medial zona incerta
NIH	National Institutes of Health
NL	neural lobe of the pituitary
NMDA	N-methyl-D-aspartate
nmol	nanomoles
nor-BNI	nor-binaltorphimine
Norepi	norepinephrine
NS	nonsense
OCT	octamer
Opt	optic tract
OX	optic chiasm
PBS	phosphate buffered saline
PC-12	pheochromocytoma cells 12
PF	paraformaldehyde
PKA	protein kinase A
PKC	protein kinase C
Ppit	posterior lobe of the pituitary
PRL	prolactin
RNA	ribonucleic acid
S	sense
sc	subcutaneous
SCN	suprachiasmatic nucleus
SEM	standard error of the mean
SOX	supraoptic descussation
Sp	specificity protein
SP-1	specificity protein 1
SRE	serum response element
SRF	serum response factor
ST	striatum
TBS	tris buffered saline
TF's	transcription factors
TH	tyrosine hydroxylase

TIDA	tuberoinfundibular dopamine
TPA	12-O-tetradecanoyl-phorbol-13-acetate
TX	triton X
V	vehicle
VL	ventrolateral
VMla	lateral anterior part of the ventromedial nucleus
VMlp	lateral posterior part of the ventromedial nucleus
VMma	medial anterior part of the ventromedial nucleus
VMmp	medial posterior part of the ventromedial nucleus
VMN	ventromedial hypothalamic nucleus
μg	microgram(s)
μL	microliter(s)
ZI	zona incerta

CHAPTER

GENERAL

Th

ac

be

ar

CHAPTER ONE

GENERAL INTRODUCTION

The mammalian brain contains several different dopaminergic neuronal systems classified alphanumerically based on anatomical distribution of their perikarya (Dahlström and Fuxe, 1964; **Figure 1.1**). These systems differ in their function and how they are regulated (e.g. via autoreceptors, long loop neuronal circuits or hormones). All dopamine (DA) neurons, however, have the same intracellular enzyme systems involved in the synthesis and metabolism of DA (Lookingland and Moore, 1995).

The mesotelencephalic DA system, which consists of the nigrostriatal and the mesolimbic systems, is the best studied of the DA neurons. Neurons of the nigrostriatal system originate from perikarya in the substantia nigra (A8 and A9) and project to the striatum, which consists of the caudate nucleus and putamen. These neurons are involved in the modulation of muscle movement; destruction of these neurons can lead to Parkinson's disease. The cell bodies of the mesolimbic system are located in the ventral tegmental area (A10) and terminate in the nucleus accumbens and other subcortical structures such as the lateral septum and olfactory tubercle. These neurons are involved in mediating emotionally-driven affective behaviors and dysfunction in this system is proposed to play a role in schizophrenia. Treatments of Parkinson's disease and schizophrenia have typically utilized agonists and antagonists that act at specific DA receptors. However, DA receptors regulate other neurological functions

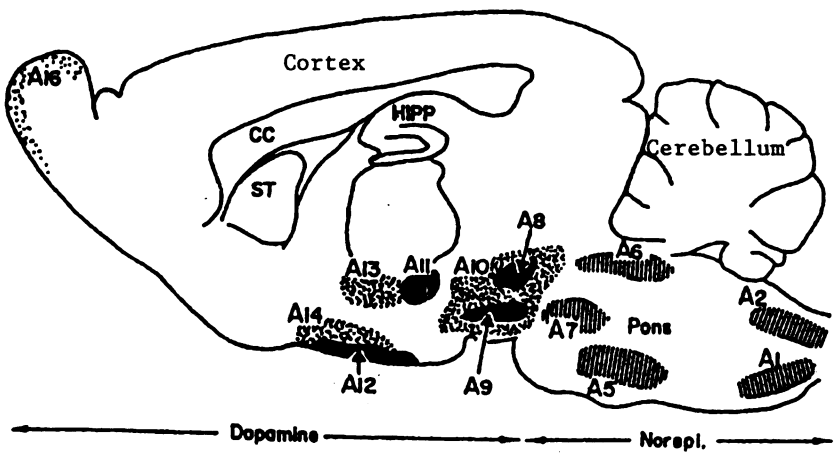

Figure 1.1 Sagittal section of the rat brain schematically depicting the location of catecholamine-containing cell bodies (Moore, 1987). Cell groups A1-A7 are noradrenergic and groups A8-A16 are dopaminergic (Dahlström and Fuxe, 1964). Abbreviations: CC, corpus callosum; HIPP, hippocampus; Norepi, norepinephrine; ST, striatum.

outside the mesotelencephalic system, which can result in unwanted side effects by acting at non-targeted DA neuronal systems such as those in the diencephalon.

The diencephalic DA systems consist of neurons located in the subthalamus (A11 and A13) and the hypothalamus (A12, A14 and A15). Much less is understood about the regulation of these neuronal systems that originate in the diencephalon compared to those that originate in the mesotelencephalic DA systems. Interestingly, the numbers of DA neurons in the diencephalon are similar to the numbers in the mesotelencephalic system (Van Den Pol et al., 1984). While much is still to be learned about the regulation of various DA neuronal systems in the diencephalon, it is known that some of these neurons play an important role in regulating the secretion of pituitary hormones. The focus of the experiments described in this thesis is the regulation of tuberoinfundibular (TI) DA neurons by DA receptors. The incertohypothalamic (IH) DA system is incorporated to highlight the differences in the regulation of TIDA neurons compared to DA neurons that are regulated by DA autoreceptors.

Tuberoinfundibular Dopamine Neurons

Anatomy and Function

The perikarya of the TIDA neurons (A12) are located in the arcuate nucleus (ARC) and their axons project ventrally and terminate in the median eminence (ME) (**Figure 1.2**). The cytoarchitecture consists of various layers: the subependymal and internal and external layers (Löfström et al., 1976; Mezey

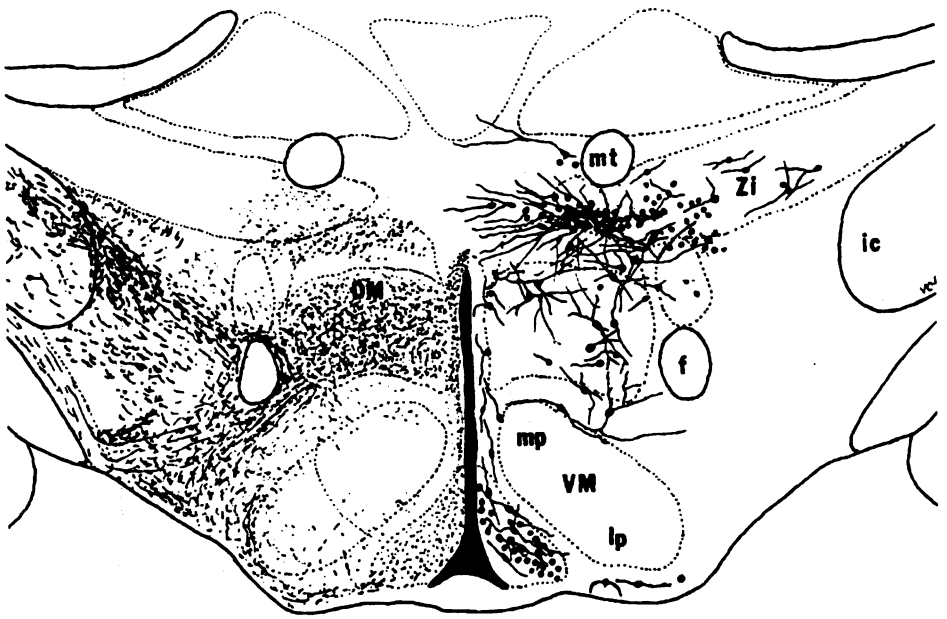

Figure 1.2 . Frontal section of the rat brain schematically depicting the location of TIDA neurons in the arcuate nucleus and the IHDA neurons of the medial zona incerta in the middle hypothalamus (Chan-Palay et al., 1984). The left side of the figure shows the topography of TH-IR fibers and terminals; the right side shows the location of the TH-IR cell bodies. Abbreviations: DM, dorsomedial hypothalamic nucleus; f, fornix; ic, internal capsule; mt, mammillothalamic tract; VMlp, lateral posterior part of the ventromedial nucleus; VMmp, medial posterior part of the ventromedial nucleus; ZI, zona incerta.

and Palkovits, 1982). The subependymal layer contains noradrenergic axon terminals while the external layer is comprised of those containing DA (Löfström et al., 1976). The external layer is further divided into the medial and lateral palisade zones. From there, DA is released, diffuses into the hypophysial portal blood system, and is carried to the anterior pituitary. DA acts on D2 receptors located on pituitary lactotrophs to inhibit the secretion of prolactin (PRL).

The ARC is a relatively long structure (approximately 1.5 to 2.0 mm) in the rat (Paxinos and Watson, 1986) with a majority of the DA neurons located in the rostral half of the ARC and some scattered in the caudal half (Björklund and Nobin, 1973). Because of this, the ARC can be divided into rostral, middle and caudal regions. These neurons have a regular dorsoventrally oriented projections and connect each portion of the ARC to a corresponding part of the ME (Lindvall and Björklund, 1978). The axons originate from one of the main dendritic shafts or from the cell bodies and course ventromedially towards the ME (Chan-Palay et al., 1984).

In addition to dividing the ARC rostrocaudally, the neurons are distributed in such a way that they can also be located in either the dorsomedial (DM) or ventrolateral (VL) ARC (**Figure 1.3**). Anatomical, histochemical, and biochemical evidence suggest that these regions contain separate populations of TIDA neurons. The perikarya of TIDA neurons in the DM-ARC are small and display dark immunostaining of tyrosine hydroxylase (TH), indicative of abundant TH protein (the rate limiting enzyme in DA synthesis). The dendrites have a dorsoventral orientation, and the terminals project to both medial and lateral

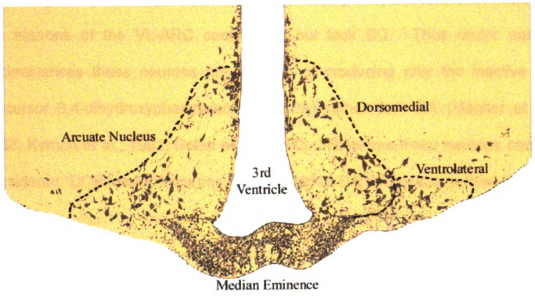

Figure 1.3. Frontal section of the rat brain schematically depicting the distribution of tyrosine hydroxylase immunoreactive neurons in the dorsomedial and ventrolateral subdivisions of the arcuate nucleus (Fuxe et al., 1985).

portions of the ME (Selmanoff, 1981; Van den Pol et al., 1984). The neurons of the VL-ARC, however, are larger and have pale TH immunostaining. These neurons have dendrites with mediolateral orientations (Van den Pol et al., 1984) and their axon terminals extend only to the lateral portion of the ME (Everitt et al., 1986). In the DM-ARC, the TIDA neurons contain both TH and DOPA decarboxylase (DD) enzymes, which are necessary to synthesize DA. However, the neurons of the VL-ARC contain TH but lack DD. Thus under normal circumstances these neurons are capable of producing only the inactive DA precursor 3,4-dihydroxyphenylalanine (DOPA) rather than DA (Meister et al., 1988; Komori et al., 1991; Balan et al., 2000). Therefore these neurons can be considered "DOPA-ergic" neurons, as opposed to DA neurons, and their function is unknown.

Incertohypothalamic Dopamine Neurons

Anatomy and Function

The cell bodies of the IHDA system (A13) are located in the rostral portion of the medial zona incerta (MZI) just ventral to the mammillothalamic tract (**Figure 1.2**). Early studies using glyoxylic acid histochemical fluorescence techniques reported that this system consists of short DA neurons that project to the anterior, dorsomedial and posterior regions of the hypothalamus (Björklund et al., 1975). Later studies using tract-tracing (Wagner et al., 1995; Cheung et al., 1998) and neurochemical techniques (Eaton et al., 1994b) revealed that IHDA neurons project to various areas within the hypothalamus, such as the

paraventricular nucleus, as well as outside the hypothalamus, specifically the central amygdala and horizontal diagonal band of Broca. The DA terminals in the paraventricular nucleus originate exclusively from the IHDA neurons; however, these neurons provide only a portion of the DA innervation to the central amygdala and horizontal diagonal band (Cheung et al., 1998). These studies also revealed that the cell bodies of the IHDA neurons projecting the paraventricular nucleus, central amygdala, and horizontal diagonal band are not organized into distinct groups within the MZI (Cheung et al., 1998).

There is very little information regarding the function of IHDA neurons, but their widespread projections to various regions in the brain suggest that these neurons have an integrative function. The rostral zona incerta is involved in processing afferent sensory information from such brain regions as the hypothalamus, thalamus, and brain stem, and coordinating specific biological responses (Ma et al., 1997). In addition examination of projection sites of IHDA neurons may offer some insight to their function.

The paraventricular nucleus contains corticotropin-releasing hormone perikarya and is involved with neuronal regulation of hypothalamic-pituitary-adrenal axis. Activation of DA receptors stimulates corticotropin-releasing hormone mRNA expression in the paraventricular nucleus (Eaton et al., 1996) while central administration of corticotropin-releasing hormone increases DA metabolism in the paraventricular nucleus (Pan et al., 1995). This suggests that IHDA neurons participate in neuronal regulation of the hypothalamic-pituitary-

adrenal axis, which is involved with the stress response and the release of cortisol.

The horizontal diagonal band contains gonadotropin-releasing hormone neurons that may be the target for the IHDA neurons. The MZI has been implicated in the regulation of luteinizing hormone and ovulation. Direct injection of DA into the MZI increases luteinizing hormone secretion, which in turn regulates ovulation (MacKenzie et al., 1984; James et al., 1987). In contrast, lesions of the MZI block the proestrous surge of luteinizing hormone (Sanghera et al., 1991) and disrupt the estrous cycle (MacKenzie et al., 1984).

Neurochemical Events in Dopamine Nerve Terminals

Figure 1.4 represents the neurochemical events in DA nerve terminals. DA synthesis begins with the active transport of dietary tyrosine into the nerve terminal which is then converted to DOPA by the rate-limiting enzyme TH. DOPA is then rapidly decarboxylated to DA by DD to form cytosolic DA. The majority of newly synthesized cytosolic DA is packaged into synaptic vesicles and stored for release. Some of the DA is metabolized by monoamine oxidase (MAO) to form 3,4-dihydroxyphenylacetic acid (DOPAC) which reflects DA release from DA neurons.

There is a tight coupling of synthesis, release, and metabolism due to the regulation of TH by end product inhibition that maintains a steady state of releasable DA in the terminals. Once DA is released, there is a loss of the end product inhibition and the synthesis of DA increases. The coupling between DA

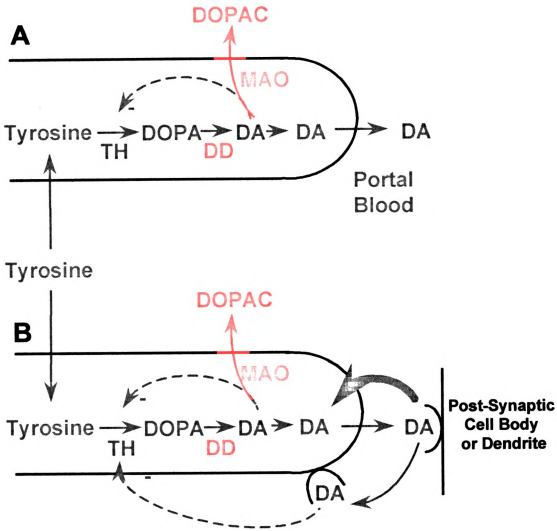

Figure 1.4. Schematic diagram of the neurochemical events in **A.** TIDA neurons and **B.** IHDA neurons. Dietary tyrosine is transported into the nerve terminal where it is converted by the rate-limiting enzyme, TH to DOPA. DOPA is rapidly decarboxylated by DD to form DA. Newly synthesized DA is stored within vesicles until release upon arrival of action potentials. Excess non-vesicular DA is metabolized by MAO to DOPAC. Abbreviations: DA, dopamine; DD, DOPA decarboxylase; DOPA, 3,4-dihdroxyphenylalanine; DOPAC 3,4-dihydroxyphenylacetic acid; MAO, monoamine oxidase; TH, tyrosine hydroxylase.

release, synthesis and metabolism allows two methods to neurochemically estimate DA neuronal activity. The first method measures the concentration of the DOPAC in terminal regions of DA neurons as an index of neuronal activity (Lookingland et al., 1987). The second method uses the synthesis of DA as an estimate of activity by measuring DOPA accumulation following the administration of a DD inhibitor (Carlsson et al., 1972).

There are three major differences between the TIDA neuronal system and the other dopaminergic neuronal systems such as the IHDA system following the release of DA. These differences are related to the unique architecture of TIDA neurons. First in the IHDA system, DA is released into a synapse where it can bind to post-synaptic receptors, unlike the TIDA system where DA is released and diffuses into the hypophysial portal blood system. The synaptic actions of DA released from IHDA neurons are terminated predominately via high affinity reuptake pumps on the DA nerve terminals. DA can be repackaged into synaptic vesicles for re-release, metabolized to DOPAC, or can feedback to inhibit DA synthesis. TIDA neurons lack high affinity reuptake pumps; however, there is evidence that these neurons have a low affinity reuptake system. The functional significance of this system is not known since little to no DA is taken-up and metabolized to DOPAC in the median eminence (Demarest and Moore, 1979b; Annunziato et al., 1980). Finally, in addition to acting at post-synaptic DA receptors, DA released from IHDA neurons also acts at pre-synaptic autoreceptors which further inhibits the synthesis and release of DA from these neurons. In contrast, TIDA neurons lack pre-synaptic autoreceptors as

demonstrated by neurochemical (Lookingland and Moore, 1984; Gunnet et al., 1987), *in situ* hybridization (Weiner et al., 1991; Fox et al., 1993) and microdialysis studies (Timmerman et al., 1995) and are unresponsive to first generation DA agonists that act pre-synaptic DA receptors (Gudelsky and Moore, 1976; Demarest and Moore, 1979a).

Regulation of Tuberoinfundibular and Incertohypothalamic Dopamine Neuronal Activity

Sexual Differences

There are marked differences in the activities of TIDA neurons of male and female rats. Although there are no sexual differences in the density of TIDA nerve terminals (as reflected in the concentration of DA in the ME; Gunnet et al., 1986b), the rate of turnover, synthesis and metabolism of DA in this region and the concentration of DA in the hypophysial portal blood is 2-3 times higher in female than in male rats (Demarest et al., 1981; Gudelsky and Porter, 1981). This difference is due in part to a greater responsiveness of TIDA neurons to positive feedback effects of circulating PRL in females versus males (Demarest and Moore, 1981) and the effects of gonadal steroids (Gunnet et al., 1986b). TIDA neuronal activity is decreased in the female and increased in the male after castration, and these effects are reversed by replacement with estrogen or with testosterone, respectively (Gunnet et al., 1986b; Toney et al., 1991). The stimulatory effect of estrogen on TIDA neuronal activity in female rats is mediated through its positive influence on circulating PRL concentrations (Toney et al., 1992). In males, however, the inhibitory effects of testosterone on TIDA neurons

is PRL independent (Toney et al., 1991) and may possibly occur through an indirect neuronal mechanism involving dynorphin neurons (Manzanares et al., 1992a).

Unlike the TIDA neurons, IHDA neurons are not responsive to experimentally-induced changes in circulating levels of gonadal steroids. There is no sexual difference in the basal activity of the IHDA neurons, and neither castration nor steroid hormone treatment alters the activity of these neurons in male or female rats (Gunnet et al., 1986a).

Effects of Prolactin

As depicted in **Figure 1.5**, DA released from TIDA neurons in the ME diffuses into the portal blood and is transported to the anterior pituitary where it tonically inhibits the secretion of PRL from anterior pituitary lactotrophs. PRL, in turn, can feed back to activate TIDA neurons. Under normal physiological situations, the activity of TIDA neurons is regulated to large extent by circulating levels of PRL. TIDA neuronal activity is reduced during periods of hypoprolactinemia caused by either hypophysectomy, or administration of DA agonists or PRL antibody (Gudelsky and Porter, 1980; Demarest and Moore, 1981; Arbogast and Voogt, 1991; Hentschel et al., 2000a). During periods of increased circulating levels of PRL following the administration of exogenous PRL, DA antagonists, estrogen or implantation of pituitary tissue, TIDA neuronal activity is increased (Moore et al., 1980; Selmanoff, 1981; Morgan et al., 1982; Moore et al., 1985).

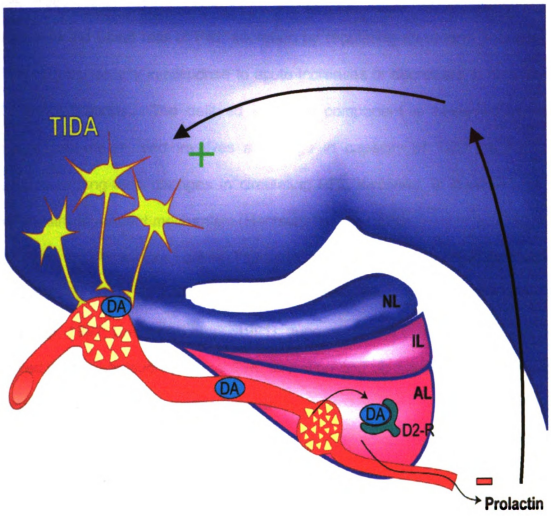

Figure 1.5. Schematic representing a sagittal section of the rat brain (Modified from Fuxe et al., 1985). TIDA neurons release DA in the ME, where it diffuses into the hypophysial portal blood system and is transported to the anterior pituitary. DA binds to D2 receptors on lactotrophs and inhibits prolactin secretion. Systemic prolactin can also feedback and activate these neurons, thus inhibiting its own secretion. Abbreviations: AL, anterior lobe of the pituitary; DA, dopamine; D2-R, D2 receptor; IL, intermediate lobe of the pituitary; NL, neural lobe of the pituitary, TIDA, tuberoinfundibular dopamine neurons.

There are two components to the activation of TIDA neurons by PRL: a rapid tonic component and a delayed inductive component (Demarest et al., 1984, 1985, and 1986). The tonic component, observed in female rats, determines the basal rate of PRL secretion by regulating short-term changes in TIDA neuronal activity in response to acute increases or decreases in circulating PRL concentrations. The delayed inductive component is observed in both females and males, and involves a change in capacity of TIDA neurons in response to long-term changes in circulating PRL involving, at least in part, a neurotensin-dependent mechanism (Hentschel et al., 1998).

The IHDA neurons, unlike TIDA neurons, do not respond to circulating levels of PRL. They also do not respond to chronic elevations of PRL (Arbogast and Voogt, 1991; Selmanoff et al., 1991), suggesting that these neurons are not involved in the regulation of basal PRL secretion and do not mediate the effects of increased PRL in reproductive function.

DA Receptor Regulation

Major ascending mesotelencephalic DA neurons are regulated by DA receptor-mediated mechanisms consisting of autoreceptors and long loop neuronal feedback circuits. Autoreceptors are located on cell membranes of nerve terminals, cell bodies, and dendrites (Lookingland and Moore, 1984; Fuxe et al., 1985). Somatodendritic autoreceptors regulate neuronal firing whereas terminal autoreceptors exert effects on DA synthesis and release. Activation of these receptors leads to inhibition, while blockade results in stimulation. Long

loop neuronal feedback comes into play following stimulation of postsynaptic receptors. For example, GABA neurons project from the striatum to the substantia nigra where they communicate with the DA cell bodies of the nigrostriatal system. As DA is released and stimulates the post-synaptic receptors, the striatal GABA neurons exert a negative feedback effect on the DA cell firing (Roth and Elsworth, 1995).

In addition to the mesotelencephalic system, IHDA neurons of the MZI are regulated by DA receptor-mediated mechanisms as demonstrated by neurochemical studies using DA receptor agonists and antagonists (Lookingland and Moore, 1984). DA agonists (such as apomorphine) decrease and DA antagonists (such as haloperidol and raclopride) increase IHDA neuronal activity (Tian et al., 1991; Eaton et al., 1992).

TIDA neurons, however, are different in that they are primarily regulated by PRL. Early studies demonstrated that acute administration of first generation DA agonists (apomorphine and bromocriptine) and antagonists (haloperidol) had no direct effect on TIDA neurons (Gudelsky et al., 1978; Demarest and Moore, 1979) suggesting that TIDA neurons do not have autoreceptors (Moore, 1987). However, these neurons are responsive to these drugs in a delayed manner as a result of their ability to alter circulating concentrations of PRL (Moore and Lookingland, 1995).

The discovery of multiple DA receptor subtypes has led to research identifying their specific roles and function in the mesotelencephalic DA system. This research has, in turn, initiated the development of more selective drugs with

the goal of more effective clinical management of the treatment of neuropsychiatric diseases (such as Parkinson's disease and schizophrenia) with reduced unwanted side effects. The DA receptor subtypes have been divided into two main categories, D1 and D2. The D1 family consists of D_1 and D_5 receptors, which are found post-synaptically. Activation of these receptors stimulates the production of cAMP through a G_s protein. The D2 family of receptors includes D_2, D_3, and D_4 receptors. These receptors are found both pre- and post-synaptically and are linked to G_i proteins, inhibiting cAMP (Spano et al., 1978; Kebabian and Calne, 1979; Vallone et al., 2000).

DA autoreceptors are inhibitory and thus have been categorized as D2 receptors. Systemic administration of selective D2 agonist quinelorane decreases neuronal activity in DA neuronal systems regulated by DA receptors (Foreman et al., 1989; Eaton et al., 1994a). However, quinelorane stimulates TIDA neuronal activity (Berry and Gudelsky, 1991; Eaton et al., 1993). Considering the lack of response by TIDA neurons following the administration of classical DA agonists, and that D2 receptors typically exert inhibitory effects, the results were unexpected. The D2 receptor antagonist raclopride is able to reverse the effects of quinelorane, leading to the conclusion that this stimulatory effect is mediated through D2 receptors (Eaton et al., 1993). If this effect is mediated through pre-synaptic autoreceptors then TIDA neuronal activity should decrease as seen in other DA neuronal systems. D2 agonists can also act on D2 receptors on pituitary lactotrophs to decrease PRL secretion; however,

decreases in PRL would feedback on TIDA neurons and decrease, not increase neuronal activity.

This response is different from what is seen with autoreceptor regulation, raising the question of how D2 receptors mediate these effects? If this is not mediated through autoreceptors or changes in PRL secretion, then it must be through an indirect neuronal system. Medial basal hypothalamic deafferentation lesions, designed to surgically isolate TIDA neurons from the rest of the brain, were able to block the stimulatory effects of quinelorane on these neurons (Durham et al., 1996). These studies demonstrated that the stimulatory effect of D2 receptor activation on TIDA neuronal activity is mediated through a neuronal system originating outside the mediobasal hypothalamus. This neuronal system must involve projection neurons that are acting through the activation of a quiescent stimulatory neuronal system or through the suppression of a tonically active inhibitory neuronal system. Because D2 receptors exert inhibitory effects on their target cells, it is more likely that D2 receptors would inhibit or turn off an active system as opposed to turning on a stimulatory system.

Kappa Opioid Receptor Regulation

There are three classes of endogenous opioid peptides: β-endorphin, enkephalin, and dynorphin. Dynorphins were originally isolated and characterized from porcine hypothalamus and pituitary (Goldstein et al., 1979; Goldstein et al., 1981) and consist of a group of peptides, dynorphin A, dynorphin B and dynorphin$_{1-8}$ (the amino-terminal octapeptide fragment of dynorphin A), that are

all derived from the preprodynorphin gene. Early studies using radioimmunoassay detected dynorphin A and dynorphin$_{1-8}$ throughout the brain (Cone et al., 1983) including the hypothalamus (Zamir et al., 1984). These studies examined microdissected regions of the brain rather than individual neurons. Later studies used *in situ* hybridization to achieve cellular resolution and demonstrated prodynorphin mRNA throughout the hypothalamus including the ARC, dorsomedial nucleus, paraventricular nucleus, and ventromedial nucleus (Merchenthaler et al., 1997), suggesting a neuroendocrine function of dynorphin. One area found to be devoid of prodynorphin mRNA was the MZI (Merchenthaler et al., 1997).

Dynorphin is involved in the regulation of nociception, diuresis, feeding, and secretion of hormones including vasopressin, alpha-melanocyte-stimulating hormone, and PRL (Mansour et al., 1988; Dhawan et al., 1996). Dynorphin acts at kappa opioid receptors (Chavkin et al., 1982) which are members of the seven transmembrane G protein coupled receptors (Mansour et al., 1995). Specifically these receptors are linked to inhibitory $G_{i/o}$ proteins which when activated leads to decreases in adenylate cyclase activity and cAMP, and increases in K^+ conductance (Childers, 1991; Childers et al., 1998b; Takekoshi et al., 2000). Kappa receptor mRNA (Merchenthaler et al., 1997) and binding sites (Mansour et al., 1988) have been detected in many regions of the diencephalon including the ARC, dorsomedial nucleus, paraventricular nucleus, and ventromedial nucleus, but not in the MZI.

There is some debate concerning subtypes of kappa opioid receptors. Early pharmacological studies have suggested the existence of several kappa receptor subtypes, κ_1, κ_2 and κ_3 (Iyengar et al., 1986; Zukin et al., 1988; Cheng et al., 1992). The pharmacology of the cloned kappa opioid receptor corresponds to the κ_1 receptor with high affinity for agonists such as U50-488 and dynorphin, and antagonists like nor-binaltorphimine (nor-BNI) (Dhawan et al., 1996; Childers et al., 1998a). Nonselective ligands have been shown to bind to κ_2 receptors, but these ligands also have mu receptor antagonist properties (Fowler and Fraser, 1994). The pharmacological profiles of κ_2 and κ_3 receptors are still poorly defined and molecular cloning data have yet to provide evidence of kappa receptor subtypes. Thus to date no specific κ_2 or κ_3 agonists or antagonists have been developed.

Drugs that activate kappa receptors exert only inhibitory actions on diencephalic DA neurons, but the degree of inhibition is generally dependent upon the level of activity of these DA neurons. Kappa receptor agonist U50-488 decreases elevated TIDA neuronal activity found under basal conditions in female rats, but has no effect on the activity in male rats (Manzanares et al., 1992a). Conversely, the kappa opioid receptor antagonist nor-BNI increases TIDA neuronal activity in gonadally-intact male rats, but not females. Similarly, central administration of dynorphin antibodies also leads to increases in neuronal activity in male rats (Manzanares et al., 1992b). These studies concluded that dynorphin tonically inhibits TIDA neurons via kappa opioid receptors in male rats, but not in females (Manzanares et al., 1992a). This sexual difference is due to

the effects of estrogen. Estrogen acts in females via a prolactin-independent mechanism to suppress kappa opioid receptor mediated inhibition of TIDA neurons, possibly by decreasing the release of endogenous dynorphin (Wagner et al., 1994).

Because dynorphin acting via kappa opioid receptor tonically inhibits TIDA neurons, further studies were carried out to determine if these neurons played a role in D2 receptor regulation of TIDA neurons. U50-488 reverses the stimulatory effects of quinelorane on TIDA neurons demonstrating that dynorphin neurons via kappa opioid receptors mediate the effects of D2 receptor regulation of TIDA neurons (Durham et al., 1996).

The IHDA neurons, unlike the TIDA neurons, do not respond to kappa receptor agonists or antagonists (Tian et al., 1992). This is consistent with studies demonstrating a lack of dynorphin-IR and kappa receptor mRNA and binding in the MZI. These results demonstrate that IHDA neurons are not regulated by kappa receptors. Instead, these neurons are regulated by mu receptors (Tian et al., 1992).

Regulation of Immediate Early Gene Expression

For over a decade, inducible transcription factors have been studied and have become a tool for mapping neuronal activity. Using immunohistochemistry to identify neurons expressing specific transcription factors gained popularity because other techniques could not differentiate the activity of individual neurons. Neurochemistry, as described earlier, uses levels of neurotransmitters

and/or their metabolites to examine the changes in activity of neuronal populations or subpopulations. 2-Deoxyglucose (2-DG) involves glucose utilization as an index of metabolic requirements, but as with neurochemistry, this technique reveals brain regions that are activated by specific stimuli. The disadvantage of these techniques is the lack of cellular resolution. Electrophysiology studies allow for the study of individual neurons, however the neurons are not typically identified neurochemically. Transsynaptic stimulation of neurons can activate two different mechanisms by which they process and transmit information. First is electrophysiological activity, which occurs in milliseconds to immediately process and convey information about the stimulus. Secondly, is the longer-acting second messenger signal cascade which occurs over minutes to hours. This mechanism evokes the production of transcription factor proteins which initiate transcription and/or repression of other genes, thereby altering the responses of neurons to subsequent stimuli (Biguet et al., 1991; Sheng and Greenberg, 1990; Herdegen and Leah, 1998).

So what are these transducible transcription factors? The discovery and subsequent research began in 1911, when Peyton Rous isolated a factor (later named the Rous sarcoma virus) from tumor infiltrate that caused sarcoma in chickens when they were injected with it (Wyke, 1983). In 1966 other researchers discovered another factor from osteosarcoma in a mouse that could induce osteosarcomas in younger mice when injected with it. This factor was later identified as viral particles and named FBJ-MSV (Finkel et al., 1966). Later in the 1960's the virus was analyzed and a gene was identified that was believed

to allow the virus to cause sarcomas *in vivo*. The term, "oncogene," meaning cancer-causing gene, was coined. It was discovered in the early 1970's the gene was found in all DNA of vertebrates (Stehelin et al., 1976). Oncogenes were derived from normal cellular genes, termed proto-oncogenes through recombination with viruses (Bishop, 1985). The invading virus "captures" the gene from the DNA of the infected cell. Under normal conditions, proto-oncogenes do not cause cancer because they are in a restrictive environment. However, there can be overexpression of oncogenes when they are in virally infected cells because there usually are not the regulatory elements present that can regulate growth. These are retroviral oncogenes that induce cellular transformation by RNA tumor viruses (Curran and Morgan, 1995). Tumors result from unregulated and uncontrolled growth and cell division from overexpression of oncogenes. It wasn't until 1982 that the FBJ-MSV was determined to be v-fos (Curran and Teich, 1982). Its cellular component (c-fos) was identified a short time later, and discovered to have DNA binding properties and gene activator properties (Curran et al., 1983).

Around the same time, Jun was first described as the oncogene of the avian sarcoma virus 17 (ASV 17). It is a retrovirus capable of causing fibrosarcomas in chickens. The name Jun came from ju-nana which is Japanese for number 17. The cellular component was isolated from human cells and found to be a major part of the AP-1 site in mouse rat and chicken (Herdegen and Leah, 1998).

Immediate early genes were first characterized in non-neuronal cells when researchers were trying to identify genes responsive to growth factors that induce cells to re-enter the cell cycle from the resting G_0 phase. This lead to the discovery of genes that were induced within minutes of growth factor stimulation (Sheng and Greenberg, 1990) including the Fos and Jun protein families. Fos family consists of Fos, FosB, FRA-1, and FRA-2 proteins. The Jun family consists of c-Jun, JunB and JunD. All immediate early genes share some common characteristics. Under basal conditions, immediate early genes have low expression, but are rapidly induced, sometimes within minutes, following stimulation. The induction of transcription is transient and independent of protein synthesis indicating that the factors responsible for inducing the immediate early gene preexist in the cell. However, new protein synthesis is required to turn off transcription of immediate early genes. The fact that immediate early gene expression is tightly controlled at the level of transcription and translation and by post-translational modification suggests a regulatory role for protein products in cellular response to external stimuli.

Fos family members differ in their time frame of induction. Fos is the first to be induced by acute challenges with the mRNA expression peaking at 15 minutes and the protein at a maximal level at 1-2 h and returning to basal levels by 4-6 h (Kovács, 1998). FosB is also induced following acute stimuli, but has a delayed induction and a longer half-life (approximately 9 h) (Kovács, 1998; Herdegen and Leah, 1998). FRA-1 and FRA-2 also have a delayed induction with their proteins gradually accumulating in the nucleus, especially after

repeated and chronic stimulation (Kovács, 1998; Herdegen and Leah, 1998). Like the Fos proteins, the Jun proteins also differ in their half lives and induction. c-Jun and JunB are similar to Fos in that they are both induced quickly and their protein half lives are 1 ½ to 2 h (Herdegen and Leah, 1998). Interestingly c-Jun expression can last up to 6 h due to cis activation. JunD has a higher basal expression and longer half life compared to c-Jun and JunB with the half-life of the mRNA of 6 h.

All Fos and Jun proteins have a leucine zipper, the conserved dimerization domain that allows strong protein-protein interactions (Kouzarides and Ziff, 1988 and 1989). All Fos and Jun proteins form heterodimers, and Jun proteins can form homodimers but this combination has less affinity for the DNA binding site compared to the heterodimers (Vogt and Bos, 1990). However, Fos proteins can not form homodimers because the structure of their leucine zippers and flank regions (Kouzarides and Ziff, 1988; Herdegen and Leah, 1998) . The Fos/Jun dimers contain a DNA binding region that lies adjacent to the leucine zipper (Abate et al., 1990) which binds directly to DNA elements that contain the conserved sequence ATGACTCA (Dragunow and Hughes, 1995). This sequence was first identified as phorbol-ester inducible promoter element and binding site for transcription factor named activator protein-1 (AP-1) which was later determined to consist of Fos/Jun dimers (Curran and Franza, 1988; Hirai et al., 1990; Ryder et al., 1988; Zerial et al., 1989).

There are two signaling pathways for Fos induction following the activation of receptors, the inositol phosphate-protein kinase C (PKC) pathway and the

calcium pathway. Stimulation by serum, growth factors and PKC activators leads to the phosphorylation of the constitutive transcription factor serum response factor (SRF; Treisman, 1986 and 1992). SFR forms a homodimer and binds to the serum response element (SRE) site on the *c-fos* gene promoter. Following exposure to calcium or stimulators of cAMP formation (such as forskolin), the constitutive transcription factor cAMP response element binding protein (CREB) becomes activated (Fisch et al., 1987) through phosphorylation by CaM kinase I and II (Sheng et al., 1991) and protein kinase A (PKA; Gonzalez and Montminy, 1989). CREB forms a homodimer and binds to the cAMP/Ca^{+2} response element (CRE/CaRE) site on the *c-fos* gene promoter. Once bound to the DNA, SRE or CREB leads to the induction of *c-fos* mRNA, which can be seen as early as 15 minutes after stimulation. *c-fos* mRNA is translated to Fos protein in the cytoplasm of the cell and translocates to the nucleus. Fos then dimerizes with a Jun protein and binds to the AP-1 site on the long term gene promoter (Dragunow and Hughes 1995). These intracellular events are summarized in **Figure 1.6**.

All Fos and Jun proteins can dimerize with one another, but each heterodimer has different effects on gene expression and different transactivational abilities. Fos/c-Jun heterodimers increase whereas Fra-1/c-Jun decrease DNA stability and have low or no transactivational activity (Suzuki et al., 1991). There are many stimuli of Fos expression in neurons such as seizures, hypoxia/ischemia, memory formation, stress, sensory stimulation, circadian rhythms (Dragunow and Hughes, 1995). Expression of Fos and its

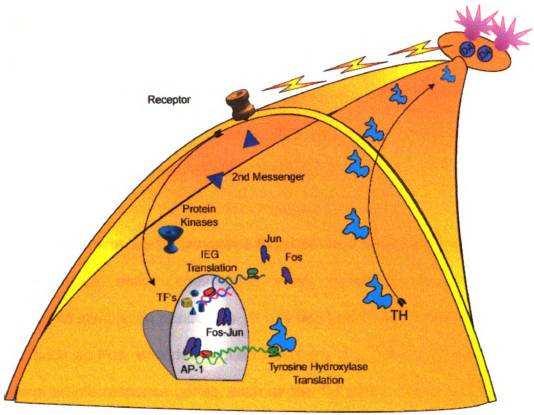

Figure 1.6. Schematic diagram depicting intracellular events in TH neurons (Modified from Hughes and Dragunow, 1995). Stimulation of a receptor leads to the activation of second messengers and a phosphorylation cascade. Constitutive transcription factors are covalently modified and translocate to the nucleus where they stimulate the synthesis of immediate early genes such as *c-fos*. Fos protein translocates into the nucleus, dimerizes with a Jun protein and binds to the AP-1 site located within the TH gene promoter. TH protein is then transported to its site of action in the axon terminal. Abbreviations: AP-1, activator protein-1; DA, dopamine; IEG, immediate early gene; TF's, transcription factors; TH, tyrosine hydroxylase.

related antigens has been correlated with neuronal activity (Hoffman et al., 1993). Utilizing IEG as an index of neuronal activity it is possible to glean insight into the anatomical identification of populations of neurons responsive to pharmacological and physiological manipulations (Yang et al., 1999). Using this approach subpopulations of chemically similar neurons can be identified within a given brain region (Hoffman et al., 1993; Cheung et al., 1997) and then changes in the number of active neurons within that subpopulation can be determined (Hoffman et al., 1993; Hentschel et al., 2000b).

Regulation of Tyrosine Hydroxylase Expression in Dopamine Neruons

Immediate early genes have been shown to be responsive to transsynaptic stimulation of neurons. It has been proposed that immediate early genes, such as Fos, encode regulatory proteins that control the expression of long term or late response genes, such as the TH gene. The products of these long term genes are believed to serve more specific functions in the neuronal response, such as the synthesis of DA.

TH is the rate-limiting enzyme in DA synthesis. The catalytic activity of this molecule determines the synthetic rate of DA in the TIDA system (Wang et al., 1993). It can be regulated in the short term by altering the enzyme itself or in the medium or long term through the regulation of gene expression and/or synthesis of new protein (Biguet et al., 1991; Herdegen and Leah, 1998).

The short term regulation of the TH enzyme consists of feedback inhibition, allosteric regulation by polyanions, enzyme phosphorylation and

enzyme stability. TH utilizes tyrosine, oxygen and tetrahydrobiopterin to begin the synthesis of DA. One form of feedback inhibition is reversible and involves DA binding to TH, thus preventing tetrahydrobiopterin from binding to TH and inhibiting further DA synthesis. TH enzymatic activity can also be decreased when the active site of TH is bound by a DA/ferric iron complex (Okuno and Fujisawa, 1991). Allosteric regulation is the modulation of enzyme activity at a site outside the active site of the protein. Heparin, phospholipids and polyanions have been demonstrated to increase TH activity by binding to the N-terminal regulatory domain of the TH protein and producing a conformational change that activates the enzyme (Daubner and Fitzpatrick, 1993; Daubner and Piper, 1995). In addition to allosteric regulation, TH is a substrate for direct phosphorylation by different protein kinases that can regulate its activity (Porter 1986; Arbogast and Voogt, 1995). *In vitro* studies have found at least seven different kinases that can phosphorylate TH (e.g. PKA, PKC, protein kinase G, and mitogen-activated protein kinase) at serine residues on the amino-terminal (Ser^{8}, Ser^{19}, Ser^{31}, and Ser^{40}) resulting in increased activity of the enzyme (Campbell et al., 1986; Haycock, 1990). While the activity of TH increases following phosphorylation, the stability actually decreases resulting in a shorter half-life (Gahn and Roskoski, 1995). In contrast, tyrosine, oxygen or inhibitors (e.g. DA) increase TH stability. One explanation is the inactive enzyme could be available for recruitment into the active pool. Reducing stability would provide a mechanism for readily reversing the phosphorylation activation of TH (Okuno and Fujisawa, 1991).

The long term regulation of TH consists of transcriptional regulation, alternative RNA processing, regulation of RNA stability and translational regulation. Alterations in TH gene expression have been reported in response to the administration of various drugs or manipulation of several endogenous hormone systems (Wang et al., 1993; Kedzierski et al., 1994; Rodriguez-Gomez et al., 1997; Najimi et al., 2002). During the past several years, the focus has become the study of promoter/enhancer sequences of the TH gene promoter (**Figure 1.7**) and the proteins that bind them to better understand transcriptional regulation of TH. The AP-1 site is found at base pairs (bp) -204 to -198 on the TH gene proximal promoter and is the binding site for Fos/Jun heterodimers. Various studies utilizing PC12 cells (a cell line derived from rat pheochromocytoma which produces DA and norepinephrine) have demonstrated the AP-1 site is responsive to depolarization (Nagamoto-Combs et al., 1997), calcium (Nagamoto-Combs et al., 1997), phorbol ester (e.g. 12-O-tetradecanoyl-phorbol-13-acetate (TPA); Icard-Liepkalns et al., 1992; Piech-Dumas et al., 2001), nerve growth factor (Gizang-Ginsberg and Ziff, 1990), hypoxia (Ringstedt et al., 1995; Norris and Millhorn, 1995), and muscarinic cholinergic agonists (Chen et al., 1996) leading to increases in TH mRNA levels. Preceding the increases in TH mRNA, phorbol ester, nerve growth factor, depolarization, and calcium lead to stimulation of Fos, c-Jun and sometimes JunB and JunD (Icard-Liepkalns et al., 1992; Gizang-Ginsberg and Ziff, 1990; Nagamoto-Combs et al., 1997; Sun and Tank, 2003; Nakashima et al., 2003).

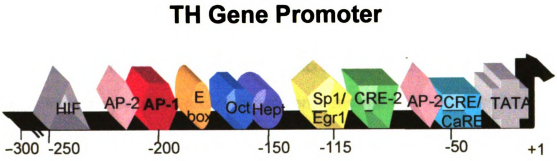

Figure 1.7. A schematic representation of the rat TH proximal gene promoter. The putative and functional elements involved in regulation of TH transcription are shown. **HIF:** Binding site for hypoxia-induced protein. **AP-2:** Binding site for AP-2 transcription factor found in adrenergic and noradrenergic neurons. **AP-1:** Highlighted in **red**; functional binding site for Fos/Jun; involved in stimulated expression. **E box:** Overlaps with AP-1 site and is involved with cell specificity. **Oct/Hept:** Binding site for Oct-2; represses expression. **Sp1/Egr1:** Binding sites for Sp1 and Egr1; involved in basal and stimulated expression. **CRE-2:** Binding site for CREB, involved in stimulated expression, works as a modulator possibly with CRE. **CRE/CaRE:** Binding site for cyclic AMP response element binding protein (CREB), regulates basal and cyclic AMP induced expression. **TATA box:** Conserved A•T-rich core promoter site. Abbreviations: AP, activated protein; CaRE, calcium response element; CRE, cAMP response element; Egr, early growth response; Hept, heptamer; HIF, hypoxia-inducible factor; Oct, octamer; Sp, specificity protein. Modified from Papanikolaou and Sabban, 2000.

The CRE site (bp -45 to -38) is involved in the basal transcription of the TH gene as well as cAMP-mediated gene induction in PC12 and neuroblastoma cell lines (Kim et al., 1993; Yang et al., 1998). This was determined to be regulated by PKA, but not phorbol ester-mediated induction which increase PKC (Kim et al., 1994). PKA phosphorylates and activates the constitutive transcription factor CREB, which can form homodimers or heterodimers with its protein family members cAMP response element modulator (CREM) or activating transcription factor-1 (ATF-1) and bind to the CRE site (reviewed in Herdegen and Leah, 1998). Further studies utilizing CREB antisense RNA expression vectors demonstrated that CREB, and not CREM and ATF, is essential for cAMP-mediated regulation of TH gene expression (Piech-Dumas and Tank, 1999). Interestingly, more recent experiments showed that TPA stimulates the TH gene promoter via the CRE, in addition to AP-1 (Piech-Dumas et al., 2001). The CRE is also responsive to calcium (Nagamoto-Combs et al., 1997), and nicotinic and muscarinic cholinergic agonists (Chen et al., 1996) leading to increases of TH mRNA in cell lines.

Like the CRE site the CRE-2 site (bp -97 to -90) is responsive to cAMP and TPA (Best et al., 1995; Best and Tank, 1998). However, this site plays a modulatory role and requires a downstream element (possibly CRE). The transcription factors that bind to this site have yet to be determined.

The specific protein-1 (Sp-1) and early growth response-1 (Egr-1) response elements overlap (bp -127 to -107) and bind Sp-1 and Egr-1 proteins. This site is interesting in that Sp-1 and Egr-1 play different roles. Sp-1 binds to

the promoter and participates in the basal expression of the TH gene, possibly along with the CRE site, but is not affected by cAMP or TPA (Yang et al., 1998). However, after the stimulation of PC12 cells with TPA, Egr-1 is induced, binds to the Sp-1/Egr-1 binding site (displacing Sp-1) and leads to the stimulation of TH mRNA. Like the CRE-2 site, Egr-1 is believed to play a modulatory role, possibly with the AP-1 site (Nakashima et al., 2003).

The hypoxia-inducible factor (HIF) response element is the binding site for hypoxia-induced protein (HIP) in response to hypoxia and may work in conjunction with AP-1 (Norris and Millhorn, 1995). The heptamer (Hept) response element can bind octamer-2 (Oct-2) protein and repress TH gene expression (Yoon and Chikaraishi, 1992; Dawson et al., 1994). Subsequently, deletion or mutation of the Hept site results in increased TH promoter activity. Adjacent to Hept is the Oct response element, which also binds the Oct-2 protein. Interestingly mutation of this binding site has no effect on TH gene expression (Goc and Stachowiak, 1994).

In humans, alternative splicing results in 4 isoforms of TH in the brain which may confer specificity for axonal transport proteins (Lewis et al., 1993). These isoforms may also be regulated by different signaling pathways (Haycock and Wakade, 1992). More research needs to be carried out to fully understand the functional role of these isoforms.

The stability of TH mRNA and translational regulation are two other areas that are being explored. Various stimulators of TH gene expression such as TPA and hypoxia can increase the half-life of TH mRNA or increase mRNA stability

(Fossom et al., 1992; Vyas et al., 1990; Czyzyk-Krzeska et al., 1994b). The increased stability may be due to a RNA-protein interaction (Czyzyk-Krzeska et al., 1994a). A 66 kDA protein has been shown to bind to a sequence in the 3'-untranslated region of TH mRNA that could protect the mRNA from degradation by nucleases. While increases in TH mRNA can lead to increases in the amounts of protein and in enzyme activity, this is not always true. An increase of five to fifty-fold of TH mRNA content following experimental stimulation may only lead to a two to three-fold increase or even no change in TH-IR or enzyme activity (Baruchin et al., 1990; Kaneda et al., 1991). One hypothesis is while there is an increase in TH mRNA content and stability, not all of the mRNA is "loaded" onto ribosomes for translation to protein (Kumer and Vrana, 1996).

HYPOTHESIS

The overall goal of studies described in this dissertation is to test the hypothesis that acute changes in the activity of TIDA neurons following stimulation of D2 receptors, via a mechanism involving kappa opioid receptors, leads to changes in immediate early and long term gene expression in these neurons. In addition, the expression of long term genes is preceded by and dependent on the expression of these immediate early genes.

SPECIFIC AIMS

1. Determine if there are sexual differences in the distribution of TH-IR neurons and the basal level of FRA expression in subdivisions of the ARC.
2. Determine if D2 receptors regulate immediate early gene expression in TIDA neurons
3. Determine the role of kappa opioid receptors in D2 receptor regulation of Fos expression in TIDA neurons.
4. Determine if D2 receptors regulate TH gene expression in TIDA neurons.
5. Assess the role of Fos in the regulation of TH gene expression in TIDA neurons.

CHAPTER TWO

MATERIALS AND METHODS

A. Animals

All experiments were performed using gonadally-intact male and female Long-Evans rats weighing 175-225 g purchased from either Harlan Breeding Laboratories (Indianapolis, IN) or Charles River Laboratories (Wilmington, MA). Animals were housed 2 – 3 per cage in a temperature- (22 ± 1°C) and light- (lights on between 06:00h and 20:00h) controlled environment with food (Harlan Teklad Rodent Diet; Bartonville, IL) and tap water provided ad libitum. In experiments involving female rats, estrous cycles were monitored daily by vaginal lavage, and only diestrous females exhibiting two consecutive cycles were used.

B. Drugs

Dosages of all drugs were based on their respective salts. Quinelorane (Research Biochemicals International; Natick, MA) and S-(-)-raclopride L-tartrate salt (raclopride; Sigma Chemical Company; St. Louis, MO) were dissolved in 0.9% saline. Nor-binaltorphimine dihydrochloride (Nor-BNI; Sigma Chemical Company) and trans-(±)-3,4-dichloro-N-methyl-N-(2-[1-pyrrolidinyl]cyclohexyl)-benzeneacetamide methanesulfonate salt (U-50488H; Sigma Chemical Company) were dissolved in distilled water. Doses and routes of administration of drugs are indicated in **Table 2.1** and the legends of the appropriate figures.

Table 2.1 List of drugs used, and their pharmacological properties, doses, vehicles, routes of administration and sources.

Drug	Pharmacological Properties	Dose	Vehicle	Route	Source
Quinelorane	D2 receptor agonist	100 μg/kg	0.9% saline	ip	Research Biochemicals International, Natick, MA
Raclopride	D2 receptor antagonist	3 mg/kg	0.9% saline	ip	Sigma Chemical Co, St Louis, MO
nor-BNI	κ opioid receptor antagonist	12.5 μg/rat	ddH_2O	icv	Research Biochemicals International, Natick, MA
U50488	κ opioid receptor agonist	10 mg/kg	ddH_2O	sc	Sigma Chemical Co, St Louis, MO

C. Anesthetic Agents

Ketamine hydrochloride (Fort Dodge Animal Health; Fort Dodge, IA) and xylazine (The Butler Company; Columbus, OH) were used as an anesthetic and muscle relaxer, respectively, prior to intracerebroventricular (icv) cannulation surgery. This solution was prepared by combining 8 ml of 100 mg/ml ketamine (final concentration 80 mg/ml), 1 ml of 100 mg/ml xylazine (final concentration 10 mg/ml) and 1 ml of 0.9% saline. Equithesin was used euthanize rats prior to perfusion in the immunohistochemistry studies. Equithesin was prepared by first dissolving 42.51g chloral hydrate, 9.72g pentobarbital, and 21.26g magnesium sulfate in 443.4 ml propylene glycol, followed by 120 ml 95% EtOH. The total volume was brought to 1000 ml with ddH_2O (Nielsen and Moore 1982).

D. Oligonucleotides

c-fos antisense, sense, and nonsense oligonucleotides were made, purified, and lyophilized by Macromolecular Facilities in the Department of Biochemistry at Michigan State University. They were reconstituted with sterile 0.9% saline, aliquoted and frozen at –20°C. All 15 mer sequences were phosphorothioated, which replaces internucleotide oxygen molecules with sulfur to ensure stability and resistance to nucleases once injected into the brain (Wahlestedt 1994). *c-fos* oligonucleotides that are completely phosphorothioated and complimentary to the translation start site of *c-fos* mRNA are the most effective (Hooper et al 1994). The sequences are listed in **Table 2.2**. The sense oligonucleotide had the same base sequence found in the targeted mRNA and

therefore could not bind with it. The nonsense oligonucleotide was made by using the same G:C:T:A content of the antisense probe and switching the position of the bases.

Table 2.2 List of base sequences for *c-fos* antisense, sense, and nonsense oligonucleotides (Moller et al 1994).

Oligonucleotide	**Sequence**
c-fos antisense	5'-GAA CAT CAT GGT CGT-3'
c-fos sense	5'-ACG ACC ATG ATG TTC-3'
c-fos nonsense	5'-GTA CCA ATC GGG ATT-3'

E. Stereotaxic Implantation of Intracerebroventricular Guide Cannula

Rats in studies requiring intracerebroventricular (icv) injection were anesthetized with ketamine/xylazine (80:10 mg/kg; ip). Rats were assessed for surgical anesthesia by pinching a back toe. The absence of a reflex movement was determined as sufficient anesthesia to begin the procedure. The surgical site was shaved and cleaned with betadine scrub. The rats were placed in a stereotaxic frame (David Kopf Instruments; Tujunga, CA) with the incisor bar set 2.4 mm below the horizontal plane. A 23-gauge stainless steel guide cannula was implanted into the right lateral ventricle (1.4 mm lateral to the midline at bregma and 3.2 mm below the dura mater surface) and anchored to the skull with stainless steel screws and dental cement. Animals were allowed to recover for 5 to 7 days prior to the experiment. On the day of the experiment, 3 μl of the compound or its respective vehicle was injected icv with a 5 μl Hamilton syringe

connected to a 30 gauge stainless steel injector needle which protruded 1 mm beyond the end of the cannula guide and into the right lateral ventricle. Placement of each cannula was verified histologically, and only those animals with correct cannula placement were included in the study.

F. Dual Immunohistochemistry Using Fluorescent Rhodamine and Nickel Intensified Diaminobenzidine (DAB)

1. Tissue Preparation

Rats were anesthetized with Equithesin (4 ml/kg; ip) and perfused through the aorta with 0.9% saline at 4°C for 2 min, followed by 4% paraformaldehyde (PF) in 0.1M phosphate buffer saline (PBS; pH 7.4) at 4°C for 15 min. The brains were removed from the skull and postfixed in 4% PF/PBS at 4°C overnight. The brains were then placed in 0.1M PBS containing 20% sucrose for 24-48 h and finally in 0.1M PBS containing 40% sucrose for cryoprotection at 4°C for at least 24 h prior to sectioning.

A cryostat (IEC Microtome, International Equipment; Needham Heights, MA) was used to slice 30 μm sections through the frontal plane of the arcuate nucleus (ARC), beginning at approximately 2.0 mm posterior from bregma. One plate of 10 wells containing 0.05M Tris buffer saline pH 7.6 (TBS) at 4°C were prepared for each brain. Six to eight consecutive sections were collected into each of the 10 wells. All of the sections were then processed for dual immunohistochemistry to detect Fos and related antigens (FRA's) and TH.

2. Detection of Fos Related Antigens (FRA) and Tyrosine Hydroxylase (TH)

Sections were initially rinsed 3 times for 5 min each in TBS with 0.3% of the detergent Triton X 100 (TX; Research Products International Corp., Elk Grove Village, IL) with mild agitation on a Gyrotory Shaker (model G2; New Brunswick Scientific Company; Edison, NJ). Unless otherwise specified, tissue sections were lightly agitated at all steps at room temperature. Sections were incubated in 3% normal donkey serum (Sigma) in TBS/TX for 30 min to block non-specific binding of the secondary antiserum.

Anti-FRA antiserum (Genosys Biotechnologies; The Woodlands, TX) was generated in sheep against a synthetic peptide derived from a conserved region of mouse and human c-fos gene common to all FRA genes including Fos, Fos B, FRA1, and FRA2. The sections were incubated in the anti-FRA antiserum diluted to 1:2500 with TBS/TX containing 1.5% normal donkey serum for 40 h at 4°C. Sections were rinsed in TBS/TX 3 times for 5 min each to remove excess primary antibody and incubated with secondary biotinylated donkey anti-sheep IgG antiserum (Accurate Chemical and Scientific Corp; Westbury, NY) diluted 1:200 in TBS/TX for 1 h. Excess secondary antibody was removed with 3 TBS/TX rinses 5 min each. Sections were then labeled with an avidin-biotin complex (ABC Elite kit; Vector Laboratories; Burlingame, CA) consisting of avidin D and biotinylated horseradish peroxidase. Sections were rinsed of excess avidin-biotin complex with 3 rinses of TBS/TX. FRA protein was localized with a DAB substrate kit (Vector Laboratories) consisting of 3,3'-diaminobenzidine (DAB), nickel sulfate, and hydrogen peroxide. Cells positive for FRA proteins

contained a black insoluble precipitate localized in the nucleus. Sections were washed in TBS/TX 6 times for 5 min each and then blocked with 3% normal horse serum (Sigma) in TBS/TX for 30 min to prevent non-specific binding with the secondary antibody.

The primary antiserum used to detect tyrosine hydroxylase (TH) was a monoclonal anti-TH antiserum (Incstar Corp; Stillwater, MN) generated in mouse against a fragment of purified TH isolated from rat PC12 cells. The epitope was derived from the midportion of the TH molecule where extensive species homology exists. There was no cross reactivity with dihydropterdine reductase, dopamine β-hydroxylase, tryptophan hydroxylase, phenylalanine hydroxylase, or phenylethanolamine-N-methyltransferase.

Sections were incubated in the primary anti-TH antiserum diluted 1:1000 in TBS/TX containing 1.5% normal horse serum for 40 h at 4°C. Excess primary antibody was washed from the tissue with 3 rinses of TBS/TX. The primary antibody was labeled with secondary biotinylated horse anti-mouse IgG antisera (Vector Laboratories) diluted 1:200 with TBS/TX for 1 h. Sections were rinsed 3 times with TBS/TX. The chromogen solution to label the TH was tetramethyl-rhodamine isothiocyanate-tagged avidin D (Vector Laboratories) diluted 1:500 in TBS/TX. The sections were incubated in this solution for 1 h in darkness, and the excess chromogen was washed away with 3 rinses of TBS/TX. Neurons positive for TH contained a fluorescent red-orange cytoplasm. Tissue sections were stored in 24 well plates with TBS at 4°C until mounted onto gelatin-coated glass microscope slides.

3. Slide Preparation and Tissue Mounting

Before sections were mounted onto glass microscope slides, the slides were cleaned and gelatin coated (or subbed). Slides were soaked in soapy distilled water for 1 h and rinsed thoroughly with ddH_2O. Slides were dipped once in subbing solution consisting of 1.88g gelatin and 0.188g chromium potassium sulfate dissolved in 750 ml ddH_2O at 60°C. Slides were allowed to dry for approximately 1 h and dipped again into the subbing solution. The slides were air dried overnight before use.

Sections were free-floated in a petri dish of TBS and mounted onto gelatin-coated slides. The slides were allowed to air-dry overnight, dehydrated in a series of ethanols (70%, 95%, and 100%) for 10 min each, and delipidated in xylene for 15 min. Slides were coverslipped using DPX mounting media and air dried overnight.

4. Quantification and Analysis

Each slide was coded to eliminate bias during counting. Sections were viewed using a Leitz Laborlux S microscope under bright field microscopy (Leica; Wetzlar, Germany) to identify DAB-nickel labeled FRA nuclei, and under dark field fluoromicroscopy (model 103 mercury lamp housing, Leitz) to visualize the red-orange rhodamine labeled TH neurons (**Figure 2.1**).

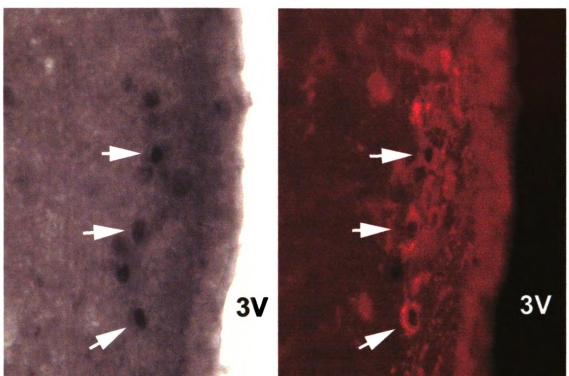

Figure 2.1 High power (400X) computer-captured image of a section through the arcuate nucleus (ARC) immunohistochemically processed using fluorescent rhodamine for the detection of TH and nickel intensified DAB for FRA. Fluorescent TH-IR neurons under dark field microscopy (**Left Panel**) and the same image under bright field microscopy (**Right Panel**) showing black FRA-IR nuclei. Arrows demonstrate TH-IR neurons containing FRA-IR nuclei. 3V, third ventricle.

Figure 2.2 Three representative frontal sections through the hypothalamus depicting the rostral, middle, caudal regions of the arcuate nucleus (ARC). Distances posterior to bregma for these regions were approximately 2.3 mm for rostral ARC, 2.8 mm for middle ARC, and 3.3 for caudal ARC (Paxinos and Watson 1998). 3V, third ventricle; A13, incertohyphothalamic dopamine neurons; ARC, arcuate nucleus; DMN, dorsomedial hypothalamic nucleus; ME, median eminence; opt, optic tract; VMN, ventromedial hypothalamic nucleus; ZI, zona incerta.

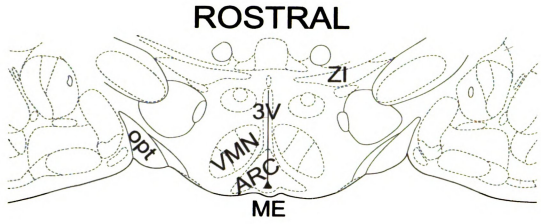
ROSTRAL
ZI
3V
opt
VMN
ARC
ME

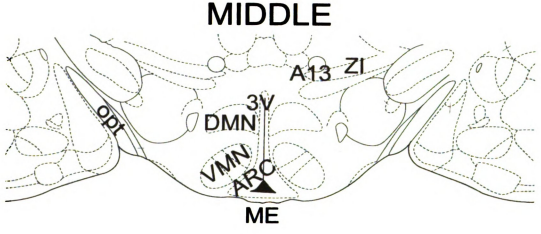
MIDDLE
A13
ZI
3V
opt
DMN
VMN
ARC
ME

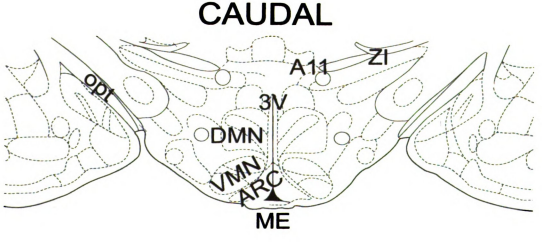
CAUDAL
A11
ZI
opt
3V
DMN
VMN
ARC
ME

The total number of TH-IR neurons and the number of TH-IR neurons expressing FRA-IR nuclei were counted bilaterally for each section of the rostral, middle, and caudal regions of the dorsomedial (DM) and ventrolateral (VL) ARC (**Figure 2.2**). The mean values for each animal were calculated, and the numbers of TH-IR neurons with FRA-IR nuclei were expressed as a percentage of the total number of TH-IR neurons in each region.

G. Dual Immunohistochemistry Using DAB and Nickel Intensified DAB

1. Characterization of Anti-Fos Antisera

Previous immunohistochemical studies performed in our laboratory utilized a nonspecific antibody that identified not only Fos, but also related transcription factors FosB, Fra-1 and Fra-2. While it is possible to identify increases or decreases in neuronal responsiveness by measuring FRA, it is not possible to determine which transcription factor(s) is (are) being expressed since each gene is induced by different types of stimuli and has a different half-life. Activation of D_2 receptors increases TIDA neuronal activity within 30 min. If acute stimulation of these neurons can induce a Fos family member, it would seem logical that it would be one that is induced following acute challenges. *c-fos* is the most rapidly induced and most transient of the Fos family, thus it was chosen as the immediate early gene to be studied. An antiserum (c-Fos 4) from Santa Cruz Biotechnology (Santa Cruz, CA) has been used successfully to specifically label Fos while not cross reacting with Fra-1, Fra-2, or Fos B (Moller et al., 1994; Li and Rowland, 1996; Grzanna et al., 1998; Yang et al., 1999). A second antisera (c-Fos H125) specific for Fos was also offered by Santa Cruz Biotechnology.

Both anti-Fos antisera were characterized to determine the optimal labeling of Fos. These are affinity-purified rabbit polyclonal antibodies that react with Fos of mouse, rat and human, but are non cross-reactive with Fos B, Fra-1, or Fra-2. The epitope for c-Fos 4 antibody corresponds to an amino acid sequence mapping at the amino terminus of c-Fos p62 of human origin. The epitope for c-Fos H125 antibody corresponds to amino acids 210-335 mapping at the carboxy terminus of c-Fos of human origin.

Cryoprotected, quinelorane-treated tissue sections were removed from the –20°C freezer and allowed to warm to room temperature prior to processing. Sections were rinsed in 3% H_2O_2 to reduce endogenous peroxidase activity and in 1% sodium borohydride to neutralize aldehydes. Sections were incubated in 3% normal goat serum to prevent nonspecific binding of the secondary antibody, followed by an avidin-biotin blocking kit (Vector Laboratories) to block endogenous biotin sites.

A series of dilutions (1:1000, 1:3000, 1:10,000, 1:30,000, 1:100,000, 1:300,000) for each Fos antisera were prepared in TBS/TX containing 1.5% normal goat serum. Sections were incubated in their respective antibody dilution with mild agitation for 40 h at 4°C. Sections were washed in TBS 6 times for 10 min each. Sections were then incubated with secondary antibody biotinylated goat anti-rabbit IgG (Jackson Immunoresearch Laboratories; West Grove, PA) diluted 1:500 in TBS/TX for 2 h at room temperature. Excess antibody was rinsed away with TBS 6 times for 10 min each. Sections were incubated with an avidin-biotin complex (ABC Elite Kit; Vector Laboratories) consisting of avidin D

and biotinylated horseradish peroxidase and rinsed 3 times with TBS and 3 times with 0.175M sodium acetate. The chromogen solution consisted of 0.01% hydrogen peroxide, 0.05% DAB, and nickel sulfate in 0.175M sodium acetate (Hsu et al 1981); (Hsu and Soban 1982). Sections were incubated for 3 min in the chromogen solution, then rinsed 3 times in 0.175M sodium acetate and 3 times in TBS. Cells positive for Fos protein contained a black insoluble precipitate localized within the nucleus. Sections were stored in TBS at 4°C until mounted onto gelatin-coated slides.

Sections were free-floated in a petri dish of TBS, mounted onto gelatin-coated slides, and allowed to air-dry overnight. The sections were then dehydrated in a series of ethanols (70%, 95%, 100%) and delipidated in 2 xylene baths for 10 min each. Slides were coverslipped using DPX mounting media and air dried overnight.

The background of tissue sections from the 1:1000 and 1:3000 dilutions of both Fos antibodies was very dark, making it difficult to visualize the cells in the ARC. There was distinct nuclear labeling with c-Fos 4 antibody, but there was also nonspecific cytoplasmic staining throughout the brain sections with c-Fos H125 antibody. At the 1:10,000 dilution, there were changes in staining intensity of the background and cells for both Fos antibodies. The background was lighter and it was easier to visualize Fos-IR cells. However there was a decrease in staining intensity in cells located in the ARC and in the number of labeled cells. At the 1:30,000 dilution, these changes were even more dramatic with a significant decrease in the numbers of cells labeled and staining intensity. There

was no Fos-IR at the 1:100,000 or 1:300,000 dilutions with either anti-Fos antiserum. Upon reviewing these slides, the c-Fos 4 antibody was chosen for future immunohistochemical studies since it resulted in specific and distinct labeling of nuclei while c-Fos H125 resulted in nonspecific cytoplasmic labeling. Because the background was too dark at the 1:3000 dilution and the numbers of Fos-IR nuclei decreased in the ARC at the 1:10,000 dilution, a compromise was made and the dilution of 1:5000 was chosen for future studies.

2. Characterization of Anti-TH Antiserum

Anti-TH antiserum (Chemicon International Inc, Temecula, CA) is an affinity-purified rabbit polyclonal antibody produced in rat adrenal medullary tumor tissue. It reacts with TH of monkey, rat, hamster, human and bovine and has no cross reactivity with dopamine-β-hydroxylase or DOPA-decarboxylase.

A series of dilutions (1:1000, 1:3000, 1:10,000, 1:30,000, 1:100,000, 1:300,000) of anti-TH antibody was prepared in TBS/TX containing 1.5% normal goat serum. Sections were incubated in their respective antibody dilution with mild agitation for 40 h at 4°C. Sections were washed in TBS 6 times for 10 min each to remove excess primary antibody and then incubated with secondary antibody biotinylated goat anti-rabbit IgG (Jackson Immunoresearch Laboratories) diluted 1:500 in TBS/TX for 2 h at room temperature. Sections were washed in TBS 6 times for 10 min each to remove excess primary antibody, labeled with an avidin-biotin complex (ABC Elite Kit; Vector Laboratories) to amplify the signal, and rinsed 3 times with TBS and 3 times with 0.05M TBS (pH

7.2). Sections were incubated in a chromogen solution containing 0.01% H_2O_2 and 0.05% DAB in 0.05M TBS (pH 7.2) for 5 min. The reaction was quenched with 3 rinses of 0.05M TBS (pH 7.2) and 3 rinses of TBS. Cells positive for TH contained a brown insoluble precipitate in the cytoplasm. Sections were stored in 24 well plates containing TBS at 4°C until mounted onto gelatin-coated glass microscope slides.

Sections were free-floated in a petri dish of TBS, were mounted onto gelatin-coated slides, and allowed to air-dry overnight. The sections were then dehydrated in a series of ethanols (70%, 95%, 100%) and delipidated in 2 xylene baths for 10 min each. Slides were coverslipped using DPX mounting media and air dried overnight.

The background of sections from 1:1000 and 1:3000 dilutions was very dark making it difficult to differentiate specifically labeled TH cells from background. At the 1:10,000 dilution, the TH-IR cells in the ARC were countable, but the background was still not optimal for dual immunohistochemistry. The staining intensity and numbers of TH-IR cells decreased at the 1:30,000 dilution. TH-IR was very pale at 1:100,000 and completely disappeared at the 1:300,000 dilution. Because the 1:10,000 dilution was too dark for dual immunohistochemistry and there was a decrease in the numbers of labeled cells at 1:30,000, the dilution 1:20,000 was chosen for future experiments.

3. Tissue Preparation

Following appropriate treatments, rats were anesthetized with Equithesin (4 ml/kg; ip) and perfused through the aorta with 0.9% saline at 4°C for 2 min, followed by 4% PF/PBS (pH 7.4) at 4°C for 15 min. The brains were removed from the skull and postfixed in 4% PF/PBS at 4°C overnight. The brains were then placed in 0.1M PBS containing 20% sucrose for cryoprotection at 4°C until slicing.

A cryostat (IEC Minotome, International Equipment; Needham Height, MA) was used to prepare 30 μm sections through the frontal plane of the ARC. Sections were placed in 24 well culture plates containing TBS at 4°C. Four sections each representing the rostral, middle, and caudal ARC (12 sections total) were chosen macroscopically (**Figure 2.2**) from each rat and prepared for dual immunohistochemistry.

Sections were rinsed in 3% H_2O_2 to reduce endogenous peroxidase activity and in 1% sodium borohydride to neutralize aldehydes. Sections were incubated in 3% normal goat serum to prevent nonspecific binding of the secondary antibody. Sections were incubated in 1% avidin D solution to block endogenous biotin binding sites, followed by a 1% biotin solution to block the remaining biotin sites on the avidin (Avidin-Biotin Blocking Kit, Vector Laboratories).

4. Detection of Fos and TH

Neurons containing Fos were identified by incubating sections for 40-64 h at 4°C in primary rabbit anti-c-Fos antiserum diluted to 1:5000 in TBS/TX containing 1.5% normal goat serum. Sections were washed in TBS 6 times for 10 min each. Sections were then incubated with secondary antibody biotinylated goat anti-rabbit IgG (Jackson Immunoresearch Laboratories; West Grove, PA) diluted 1:500 in TBS/TX for 2 h at room temperature. Excess antibody was rinsed away with TBS 6 times for 10 min each. Sections were incubated with an avidin-biotin complex (ABC Elite Kit; Vector Laboratories) consisting of avidin D and biotinylated horseradish peroxidase, rinsed 3 times with TBS and 3 times with 0.175M sodium acetate. The chromogen solution consisted of 0.01% hydrogen peroxide, 0.05% DAB, and nickel sulfate in 0.175M sodium acetate (Hsu, Raine, and Fanger 1981); (Hsu and Soban 1982). Sections were incubated for 3 min in the chromogen solution and then rinsed 3 times in 0.175M sodium acetate and 3 times in TBS. Cells positive for Fos protein contained a black insoluble precipitate localized within the nucleus. Sections were incubated in 3% normal goat serum in TBS/TX for 40 min to prevent non-specific binding by the secondary antibody.

Sections were incubated in primary rabbit anti-TH (Chemicon) for 40-64 h diluted 1:20,000 in TBS/TX containing 1.5% normal goat serum. Sections were then incubated with secondary antibody biotinylated goat anti-rabbit IgG (Jackson Immunoresearch Laboratories) diluted 1:500 in TBS/TX for 2 h at room temperature. Sections were washed in TBS 6 times for 10 min each to remove

excess primary antibody, labeled with an avidin-biotin complex (ABC Elite Kit; Vector Laboratories) to amplify the signal, and rinsed 3 times with TBS and 3 times with 0.05M TBS (pH 7.2). Sections were incubated in a chromogen solution containing 0.01% H_2O_2 and 0.05% DAB in 0.05M TBS (pH 7.2) for 5 min. The reaction was quenched with 3 rinses of 0.05M TBS (pH 7.2) and 3 rinses of TBS. Cells positive for TH contained a brown insoluble precipitate in the cytoplasm (Figure 2.3). Sections were stored in 24 well plates containing TBS at 4°C until mounted onto gelatin-coated glass microscope slides.

5. Tissue Mounting

Sections were free-floated in a petri dish of TBS, mounted onto gelatin-coated slides, and allowed to air-dry overnight. The sections were then dehydrated in a series of ethanols (70%, 95%, 100%) and delipidated in 2 xylene baths for 10 min each. Slides were coverslipped using DPX mounting media and air dried overnight.

6. Quantification and Analyses

Each slide was coded to eliminate bias during counting. Sections were viewed using a Leitz Laborlux S microscope under bright field microscopy (Leica; Wetzlar, Germany). Neurons containing Fos protein had black stained nuclei and neurons with TH immunoreactivity had a brown cytoplasm (**Figure 2.3**).

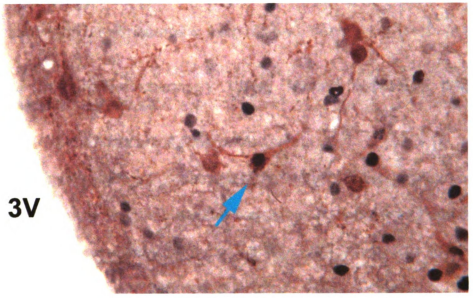

Figure 2.3 High power (400x) computer-captured image of a section through the arcuate nucleus (ARC) immunohistochemically processed using DAB for the detection of TH and nickel intensified DAB for Fos under bright field microscopy. TH-IR is identified by cells containing brown cytoplasm and Fos-IR is identified by black stained nuclei. Arrow represents a TH-IR neuron colocalized with Fos-IR nuclei. 3V, third ventricle.

The total numbers of TH-IR neurons and TH-IR neurons containing Fos-IR nuclei were counted bilaterally in the DM and VL subregions of the rostral, middle, and caudal ARC. Mean values for each animal were calculated, and the numbers of TH-IR neurons with Fos-IR nuclei were expressed as a percentage of the total number of TH-IR neurons in each region.

H. Dual Immunohistochemistry Using Nickel Intensified DAB and Alkaline Phosphatase

1. Characterization of Anti-Fos Antisera

The staining with Anti-Fos antisera from Santa Cruz was variable between lot numbers so it was difficult to achieve consistent, distinct nuclear labeling with a pale transparent tissue background. It was decided to test another Fos antibody also commonly used in several other studies (Hoffman et al., 1992; Dragunow et al., 1994; Carr et al., 1999). The antiserum is affinity-purified rabbit polyclonal antibody that reacts with Fos of mouse, rat and human, but is non cross-reactive with the 39 kDa Jun protein. The epitope corresponds to residues 4 to 17 of human *fos*.

To characterize this antisera, cryoprotected, quinelorane-treated tissue sections were removed from the –20°C freezer and allowed to warm to room temperature prior to processing. Sections were rinsed in 3% H_2O_2 to reduce endogenous peroxidase activity and in 1% sodium borohydride to neutralize aldehydes. Sections were incubated in 3% normal goat serum to prevent nonspecific binding of the secondary antibody. Sections were incubated in 1% avidin D solution to block endogenous biotin binding sites, followed by a 1%

biotin solution to block the remaining biotin sites on the avidin (Avidin-Biotin Blocking Kit, Vector Laboratories).

A series of dilutions (1:1000, 1:3000, 1:10,000, 1:30,000, 1:100,000, 1:300,000) of Fos antiserum were prepared in TBS/TX containing 1.5% normal goat serum. Sections were incubated with mild agitation for 40 h at 4°C. Sections were washed in TBS 6 times for 10 min each and then incubated with secondary antibody biotinylated goat anti-rabbit IgG (Jackson Immunoresearch Laboratories; West Grove, PA) diluted 1:500 in TBS/TX for 2 h at room temperature. Excess antibody was rinsed away with TBS 6 times for 10 min each. Sections were incubated with an avidin-biotin complex (ABC Elite Kit; Vector Laboratories) consisting of avidin D and biotinylated horseradish peroxidase and rinsed 3 times with TBS and 3 times with 0.175M sodium acetate. The chromogen solution consisted of 0.01% hydrogen peroxide, 0.05% DAB, and nickel sulfate in 0.175M sodium acetate (Hsu, Raine, and Fanger 1981); (Hsu and Soban 1982). Sections were incubated for 3 min in the chromogen solution and rinsed 3 times in 0.175M sodium acetate and 3 times in TBS. Cells positive for Fos protein contained a black insoluble precipitate localized within the nucleus.

Sections were free-floated in a petri dish of TBS, were mounted onto gelatin-coated slides, and allowed to air-dry overnight. The sections were then dehydrated in a series of ethanols (70%, 95%, 100%) and delipidated in 2 xylene baths for 10 min each. Slides were coverslipped using DPX mounting media and air dried overnight.

The background of the tissue sections was very dark in the 1:1000 and 1:3000 dilutions. Nonspecific cytoplasmic labeling was present and it was difficult to identify the labeled cells in the ARC. Sections incubated in the 1:10,000 dilution had specific nuclear labeling of Fos and the background was pale enough to count the numbers of labeled cells. The background of the tissue continued to become lighter at the 1:30,000 dilution and the numbers of labeled nuclei decreased especially in the ARC. Fos-IR was not present in the ARC at 1:100,000 and 1:300,000 dilutions. Taken together, these observations determined that the 1:10,000 dilution would yield the best results for dual immunohistochemical studies.

2. *Characterization of Alkaline Phosphatase Immunohistochemical Staining Technique*

While the IHC protocol utilizing DAB with nickel intensification and DAB is widely and successfully used, there were some instances where the same lot and dilution of antibodies resulted in blackish-brown cells that were too dark to differentiate. Under these conditions it was difficult to identify which cells were specifically labeled with TH, which had nonspecific cytoplasmic labeling of Fos, and which cells were truly dual labeled. Another immunohistochemical method employing the avidin/biotin complex amplification method offered by Vector Laboratories utilizes alkaline phosphatase as the enzyme marker instead of hydrogen peroxidase. There are four different substrate kits available as adjunctive reagents to the ABC kit, producing a red, black, blue, or purple/blue precipitate. Using the red precipitate as the chromogen to identify TH would offer

greater contrast to the black precipitate of localized Fos nuclei, thereby facilitating better differentiation.

When the DAB protocol was optimized by Dr. Chris McMahon, various studies were carried out using different dilutions of the avidin/biotin complex reagents and DAB reagents. The final recipe for the avidin/biotin complex is one quarter of the recommended recipe by Vector. In addition, the DAB reagent kit was no longer used and instead reagents were made fresh. Therefore, in order to optimize the alkaline phosphatase protocol, a dilution study of the avidin/biotin-AP and alkaline phosphatase reagent kits was carried out.

Sections were incubated in primary rabbit anti-TH (Chemicon International Inc.) for 40 h diluted 1:20,000 in TBS/TX containing 1.5% normal goat serum. Excess primary antibody is washed away with TBS 6 times 10 min each. Sections were then incubated with secondary antibody biotinylated goat anti-rabbit IgG (Jackson Immunoresearch Laboratories) diluted 1:500 in TBS/TX for 2 h at room temperature and rinsed with TBS 6 times for 10 min each. Three dilutions of avidin/biotin complex (ABC-AP Kit; Vector Laboratories) consisting of avidin DH and biotinylated alkaline phosphatase H were prepared. The first was made according to the manufacturer's protocol in a dilution of 1:1. The next two solutions were 1:2 and 1:4 dilutions of the original. Sections were incubated the appropriate avidin-biotin complex dilution for 2 h, and rinsed 3 with TBS and 3 times with 0.1M TBS (pH 8.5) 10 min each. Three sets of the alkaline phosphatase substrate kits (Vector Laboratories) were prepared. The first solution was prepared according to the manufacturer's protocol (1:1), the second

was a 1:2 dilution and the third was a 1:4 dilution of the original. The TH protein was localized using the appropriate substrate dilution and the endogenous alkaline phosphatase inhibitor levamisole in 0.1M TBS (pH 8.5) for 30 min in the dark. The reaction was quenched with 3 washes in 0.1M TBS (pH 8.5) and 3 washes in TBS. A pinkish-red precipitate formed in the cytoplasm of cells positive for TH.

Sections were free-floated in a petri dish of TBS, were mounted onto gelatin-coated slides, and allowed to air-dry overnight. The sections were then dehydrated in a series of ethanols (70%, 95%, 100%) and delipidated in 2 xylene baths for 10 min each. Slides were coverslipped using DPX mounting media and air dried overnight.

While the background staining of the tissue sections was low in all 9 nine dilutions, the TH-IR was best visualized using the avidin/biotin complex at a dilution of 1:1 and alkaline phosphatase reagent kit at a dilution of 1:1. The staining intensity of TH was the lightest with the 1:4 dilution of avidin/biotin complex and the 1:4 dilution of the reagent kit.

3. Tissue Preparation

Following appropriate treatments, rats were anesthetized with Equithesin (4 ml/kg; ip) and perfused through the aorta with 0.9% saline at 4°C for 2 min, followed by 4% PF/PBS (pH 7.4) at 4°C for 15 min. The brains were removed from the skull and postfixed in 4% PF/PBS at 4°C overnight. The brains were

then placed in 0.1M PBS containing 20% sucrose for cryoprotection at 4°C until slicing.

A cryostat (IEC Minotome, International Equipment; Needham Height, MA) was used to prepare 30 μm sections through the frontal plane of the ARC beginning at approximately 2.0 mm posterior to bregma. Sections were placed in 24 well culture plates containing TBS at 4°C. Four sections each representing the rostral, middle, and caudal ARC (12 sections total) were chosen macroscopically from each rat and prepared for dual immunohistochemistry.

Sections were rinsed in 3% H_2O_2 to reduce endogenous peroxidase activity and in 1% sodium borohydride to neutralize aldehydes. Sections were incubated in 3% normal goat serum to prevent nonspecific binding of the secondary antibody. Sections were incubated in 1% avidin D solution to block endogenous biotin binding sites, followed by a 1% biotin solution to block the remaining biotin sites on the avidin (Avidin-Biotin Blocking Kit, Vector Laboratories).

4. Tissue Staining Using Nickel Intensified DAB and Alkaline Phosphatase

Neurons containing Fos were identified by incubating sections for 40-64 h at 4°C in primary rabbit anti-c-Fos antiserum (Oncogene Research Products) diluted to 1:10,000 in TBS/TX containing 1.5% normal goat serum. Sections were washed 6 times for 10 min each in TBS with mild agitation. Sections were incubated with secondary antibody biotinylated goat anti-rabbit IgG (Jackson Immunoresearch Laboratories) 1:500 in TBS/TX for 2 h at room temperature and

rinsed 6 times in TBS for 10 min each. Secondary antibody was labeled with an avidin-biotin complex (ABC Elite Kit; Vector Laboratories) consisting of avidin D and biotinylated horseradish peroxidase. Excess avidin-biotin complex was washed away with 3 rinses of TBS and 3 rinses of 0.175M sodium acetate 10 min each. Fos protein was localized with a chromogen solution containing 0.01% hydrogen peroxide, 0.05% DAB, and nickel sulfate in 0.175M sodium acetate. Sections incubated in the chromogen for 3 min, and were washed 3 times in 0.175M sodium acetate and 3 times in TBS for 10 min each . Sections were then incubated in 3% NGS in TBS/TX for 40 min to prevent non-specific binding with the secondary antibody. Cells positive for Fos protein contained a black insoluble precipitate localized within the nucleus.

Sections processed for Fos protein were incubated in primary rabbit anti-TH (Chemicon International Inc.) for 40-64 h diluted 1:20,000 in TBS/TX containing 1.5% normal goat serum. Excess primary antibody is washed away with TBS 6 times 10 min each. Sections were then incubated with secondary antibody biotinylated goat anti-rabbit IgG (Jackson Immunoresearch Laboratories) diluted 1:500 in TBS/TX for 2 h at room temperature and rinsed with TBS 6 times for 10 min each. Secondary antibody was labeled with an avidin-biotin complex (ABC-AP Kit; Vector Laboratories) consisting of avidin DH and biotinylated alkaline phosphatase H. Sections were then rinsed 3 with TBS and 3 times with 0.1M TBS (pH 8.5) 10 min each. The TH protein was localized using the chromogen solutions in the alkaline phosphatase substrate kit (Vector Laboratories) and the endogenous alkaline phosphatase inhibitor levamisole in

0.1M TBS (pH 8.5) for 30 min in the dark. Sections were washed 3 times in 0.1M TBS (pH 8.5) and 3 times in TBS. A pinkish-red precipitate formed in the cytoplasm of cells positive for TH. Sections were stored in 24-well plates with TBS at 4°C until mounted onto gelatin-coated glass slides.

5. Tissue Mounting

Sections were free-floated in a petri dish of TBS, were mounted onto gelatin-coated slides and allowed to air dry overnight. The sections were then dehydrated in a series of ethanols (70%, 95%, 100%) and delipidated in 2 xylene baths for 10 min each. Slides were coverslipped using DPX mounting media and air dried overnight.

6. Quantification and Analyses

Each slide was coded to eliminate bias during counting. Sections were viewed using a Leitz Laborlux S microscope under bright field microscopy (Leica; Wetzlar, Germany). Neurons containing Fos protein had black stained nuclei and neurons with TH immunoreactivity had a pinkish-red cytoplasm (**Figure 2.4**).

The total numbers of TH-IR neurons and TH-IR neurons containing Fos-IR nuclei were counted bilaterally in the DM and VL subregions of the rostral, middle, and caudal ARC. Mean values for each animal were calculated, and the numbers of TH-IR neurons with Fos-IR nuclei were expressed as a percentage of the total number of TH-IR neurons in each region.

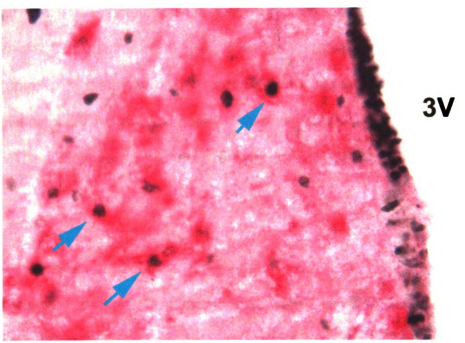

Figure 2.4 High power (400x) computer-captured image of a section through the arcuate nucleus (ARC) immunohistochemically processed using alkaline phosphatase for the detection of TH and nickel intensified DAB for Fos under bright field microscopy. TH-IR is identified by cells containing pinkish-red cytoplasm and Fos-IR is identified by black stained nuclei. Arrows represent TH-IR neurons colocalized with Fos-IR nuclei. 3V, third ventricle.

I. IN SITU HYBRIDIZATION HISTOCHEMICAL DETECTION OF TH mRNA

1. Slide Preparation

Prior to the experiment, the slides were cleaned and gelatin coated (subbed). Slides were soaked in soapy distilled water for 1 h and rinsed thoroughly with ddH_2O. Slides were soaked overnight in filtered 80% EtOH and rinsed with ddH_2O 5 times. Slides were dipped once in subbing solution consisting of 1.88g gelatin and 0.188g chromium potassium sulfate dissolved in 750 ml sterile, 0.1% diethylpyrocarbonate (DEPC)-treated ddH_2O at 60°C. Slides were allowed to dry for approximately 1 h and dipped again into the subbing solution. The slides were air dried overnight in a dust-free environment before use.

2. Tissue preparation

Following appropriate treatments, rats were decapitated and brains were quickly removed and frozen over dry ice. Fresh frozen brains were sectioned at a thickness of 30 μm in the frontal plane with a Hacker-Bright microtome cryostat (model OTF/AS/O; Hacker Instruments Inc., Fairfield, NJ) under RNase-free conditions. ARC sections were thaw-mounted onto sterile, RNase-free gelatin-coated subbed slides. Slides were stored in a slide box containing desiccant at -80°C until *in situ* hybridization processing. On the day of processing, one slide per animal containing 6 sections through the middle ARC (beginning approximately -2.8 mm posterior to bregma) was chosen macroscopically and placed in an autoclaved slide rack to thaw and airdry. In addition, 18 slides were

randomly chosen (approximately -2.0 mm posterior to bregma) as test slides (3 slides each for 6 weeks). Sections were fixed in 4% PF in sterile, DEPC-treated 1X PBS for 5 min, and then washed twice in sterile, DEPC-treated 1X PBS. Sections were then treated with sterile DEPC-treated 0.1M TEA/0.9% saline (pH 8.0) containing 0.25% acetic anhydride for 10 min. The acetic anhydride acetylates tissue to block positive charges on tissue and reduce nonspecific binding. Sections were dehydrated with gradient ethanols (70%, 80%, 95%, 100%) for 1 min each, delipidated in chloroform for 5 min and rehydrated in 100% and 95% ethanol for 1 min each. Slides were allowed to air dry.

3. Labeling the TH mRNA probe

A 48 mer TH mRNA probe complimentary to bases 1441-1488 with the sequence [5'-CGT GGG CCA GGG TGT GCA GCT CAT CCT GGA CCC CCT CCA AGG AGC GCT-3'] (Grima et al., 1985; Young et al., 1987) was synthesized and purified by the Macromolecular Facilities in the Department of Biochemistry at Michigan State University. A 5 μM stock of the probe was incubated with ^{35}S-dATP (New England Nuclear Life Science Products; Boston, MA), terminal transferase enzyme (Boehringer Mannheim Biochemicals; Indianapolis, IN), and cacoadylate buffer for 20 min at 37°C to 3' end label the probe. The tailing reaction was stopped with the addition of sterile, DEPC-treated Tris Base/EDTA buffer and yeast tRNA (Gibco BRL; Grand Island, NY).

4. Extraction of the Labeled Probe

For the first extraction, a phenol/chloroform/isoamyl alcohol (25:24:1) solution was added to the probe and the mixture was vortexed for 30 s and microfuged for 5 min. The aqueous layer was drawn off and transferred to a new sterile microfuge tube while the organic layer was discarded. For the second extraction, a chloroform/isoamyl alcohol (24:1) solution was added to the aqueous layer, and the solution was briefly vortexed and microfuged for 2 min. The aqueous layer was removed and transferred to a new sterile microfuge tube. Cold absolute ethanol and 3M sodium acetate were added to this aqueous phase and tubes were placed on ice for 45 min to initiate precipitation of the labeled TH mRNA probe. The precipitant was then spun in a Sorvall RC-5B Superspeed centrifuge (Du Pont Instruments; Hoffman Estates, IL) at 4000 rpm for 50 min at 0°C. The supernatant was poured off, and the pellet was allowed to dry for 1 h at room temperature. The pellet was resuspended with Tris base/EDTA buffer and 1M dithiothreitol (DTT; Sigma) and the amount of radioactivity was counted.

5. Counting Radioactivity

One μl of probe was added to 5 ml of Safety Solve scintillation fluid and the number of radioactive counts was determined using the Packard Tri-Carb 2100TR Liquid Scintillation Counter (Packard Instrument Co, Downers Grove, IL). Each tailing reaction was counted in duplicate and the counts were averaged. Calculations were carried out to determine the proper volume of hybridization buffer and 5M DTT to dilute the labeled TH mRNA probe to 20,000

cpm/μl. The hybridization buffer consisted of 50% formamide (Fluka), 500 μg/ml sheared single stranded DNA from salmon testes (Sigma), 250 μg/ml yeast tRNA (Gibco), 1X Denhardt's solution (0.02% Ficoll, 0.02% polyvinylpyrrolidone, 0.02% bovine serum albumin; Sigma), 10% Dextran sulfate (Sigma), and 4X saline/sodium citrate buffer (0.6M sodium chloride and 0.06M sodium citrate). Formamide lowers the effective melting temperature of nucleic acid duplex chains so that hybridization can occur at temperatures that preserve tissue morphology. The sheared single stranded DNA and yeast tRNA were used as non-homologous carriers. The Denhardt's solution was a mixture of proteins that stabilizes the TH mRNA probe and reduces nonspecific binding. Dextran sulfate was a large, non-reactive polymer that increased effective probe concentration at the tissue surface and helps reduce non-specific binding. DTT is an antioxidant that stabilizes ^{35}S attachment to the probe by maintaining the sulfur molecule in a reduced state. It also reduces the possibility of ^{35}S forming disulfide bonds with sulfur molecules in the tissue, thereby eliminating another source of non-specific probe binding.

6. Hybridization and Postwash

Sections previously fixed and dehydrated were incubated with hybridization solution. Twenty-five μl of hybridization solution per brain section was pipetted onto each slide and coverslipped with a sterile Hybri-Slip (Sigma). All slides were incubated in a humidity chamber in a Labline Imperial II incubator (Labline Instruments Inc, Melrose Park, IL) at 37°C for approximately 18 h.

Slides were removed from the incubator and soaked in 1X saline/sodium citrate buffer to remove the coverslips. The slides were transferred to a slide rack and soaked in 2X saline/sodium citrate buffer/50% formamide at 40°C 4 times 15 min each. The slides were rinsed in 1X saline/sodium citrate buffer at room temperature twice for 30 min each. The sections were then dehydrated in a series of ethanols containing 0.3M ammonium acetate (50%, 70%, 90%, 95%) and 100% EtOH, and allowed to air dry.

7. Emulsion Dip

In the darkroom under a No. 2 safelight filter, NTB2 photographic emulsion (Eastman Kodak Co., Rochester, NY) was liquefied in a warm water bath and diluted 1:2 with ddH2O. Dried slides were dipped into the emulsion and the excess was wiped from the back of the slide. The slides were placed in a vertical slide holder and allowed to dry for 1-2 h in a light-tight cardboard box. Dried slides were placed in small slide boxes containing a desiccant capsule, sealed with black electrical tape, and wrapped in aluminum foil. The boxes were then placed in a –20°C freezer to incubate.

8. Developing the Slides

Each week, a box of three test slides was removed from the freezer and developed to determine the extent of labeling of the TH mRNA. Once adequate labeling of TH mRNA was achieved (typically after a 4 – 6 week incubation), the experimental slides were removed from the freezer and allowed to warm to room

temperature for about 1 h. During this period, 300 ml each of Kodak D19 Developer and Kodak Fixer were prepared and cooled on ice to 17°C. In the darkroom under a No. 2 safelight filter, slides were removed from the black slide boxes and placed in a slide rack. The slides were developed in Kodak D19 for 2 min, washed in ddH_2O for 15 sec, and placed in Kodak Fixer for 3 min. The slides were then washed under slow running cool water for 30 min, counterstained with thionin, dehydrated in a series of ethanols (70%, 95%, 100%) and dilipidated in 2 baths of xylene for 10 min each. Slides were coverslipped using DPX mounting media and allowed to air dry overnight.

9. Quantification and Analysis

TH mRNA was visualized in sections using high-resolution darkfield optics (**Figure 2.5**; Darklite Illuminator, Micro Video Instruments Inc, Avon, MA). Images of labeled cells in the ARC are captured with the Spot 2 Digital Camera (Diagnostic Instruments, Inc.) on a Leitz Laborlux S microscope (Leica; Wetzlar, Germany). The number of silver grains over a chosen cell was counted using NIH Image program (version 1.62). The number of silver grains over the adjacent background of the same area size was also counted. The density of mRNA per cell was reported as a labeling ratio, which was calculated by dividing the number of silver grains over the cell by the average number of silver grains over the adjacent background. This ratio corrects for subtle differences in grain density due to differential thickness of the emulsion. A cell was considered labeled if the labeling density ratio was 3 or greater. Data included the total

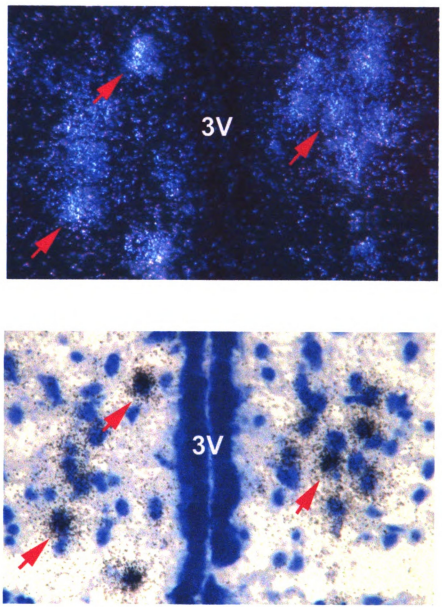

Figure 2.5 High power (400x) computer-captured images of a section through the arcuate nucleus (ARC) processed for TH mRNA using *in situ* hybridization. **Top Panel**: Localization of silver grains over the soma of cells containing TH mRNA under dark-field microscopy. **Bottom Panel**: Same image under bright-field microscopy demonstrating cells that are counterstained with thionin. Arrows represent thionin stained cells with silver grains localized over the soma. 3V, third ventricle.

number of labeled neurons and the average labeling ratio of those neurons resulting from bilateral quantification of DM-ARC and VL-ARC.

J. Statistical Analyses

Results from all experiments were expressed as the mean ± 1 SEM with the n equal to the number of experimental animals. Data that were nonparametric (i.e. did not follow a normal distribution) was transformed by taking the square root before analysis was carried out. Statistical analyses were conducted by one way analyses of variance followed by Student Newman Keuls test for least significant difference. Kruskal Wallis one way analysis of variance on ranks was carried out when data failed the equal variance test followed by Dunn's method to determine least significant difference. Differences were considered significant if the probability of error was less than 5%.

K. Images

Images in this dissertation are presented in color.

CHAPTER THREE

SEXUAL DIFFERENCES IN THE DISTRIBUTION OF TH-IR NEURONS AND EXPRESSION OF FOS AND RELATED ANTIGENS IN SUBDIVISIONS OF THE ARCUATE NUCLEUS

Introduction

The perikarya of the TIDA neurons are located in the ARC and their axons project ventrally and terminate in the ME. DA released at the ME diffuses into the hypophysial portal blood system, and is carried to the anterior pituitary. DA acts at D2 receptors located on pituitary lactotrophs to inhibit the secretion of PRL.

Early studies (conducted primarily in male rats) used histofluorescent (Löfström et al., 1976), electron microscopic (Ajika and Hökfelt, 1973), and biochemical techniques (Selmanoff, 1981) to demonstrate that the distribution of DA in the ME is not uniform. Higher levels of DA are located in the medial portion of the ME compared to the lateral portions (Selmanoff, 1981; Palkovits et al., 1982), and DA concentrations in both medial and lateral ME increase in a rostrocaudal gradient (Palkovits et al., 1982).

The ARC is a relatively long structure in the rat that can be sectioned into rostral, middle and caudal regions. In addition to dividing the ARC rostrocaudally, the TH-IR neurons are distributed in such a way that they can also be located in either the DM- or VL-ARC. These divisions are based on differences in size (Van den Pol et al., 1984), projection (Selmanoff, 1981; Van den Pol et al., 1984; Everitt et al., 1986) histochemistry, and biochemistry (Meister et al., 1988; Komori et al., 1991; Balan et al., 2000).

den Pol et al., 1984; Everitt et al., 1986) histochemistry, and biochemistry (Meister et al., 1988; Komori et al., 1991; Balan et al., 2000).

Basal activity of TIDA neurons is determined by the positive feedback effects of circulating levels of PRL. Changes in PRL secretion from the anterior pituitary lead to corresponding changes in the activity of TIDA neurons (Demarest et al., 1981). Neurochemical techniques have demonstrated no difference in the concentration of DA in the ME between male and female rats (Demarest et al., 1981; Gunnet et al., 1986) indicating there is no sexual difference in the density of DA innervation. However, there is greater turnover, synthesis, and metabolism of DA in the ME in females compared to males (Demarest et al., 1981; Gunnet et al., 1986; Lookingland et al., 1987), which corresponds to greater neuronal activity in females. This difference is due to the direct stimulatory effects of estrogen on PRL secretion in female rats (Moore et al., 1987), and the ability of testosterone to inhibit the basal activity of TIDA neurons, independent of PRL, in male rats (Toney et al., 1991).

One hypothesis for this sexual difference is that there are greater numbers of active neurons in females versus males. A second line of thought is that there are equal numbers of active neurons; however, each neuron is more active in females due to increased DA synthesis, which is the result of increases of TH mRNA (Arbogast and Voogt, 1990) and protein cycling (Porter, 1986b; Arbogast and Voogt, 1990) or a greater amount of phosphorylation of TH protein (Porter, 1986a).

Because most of what is known concerning the regulation of TIDA neurons is based on neurochemical estimates of DA synthesis and metabolism in axon terminals converging in the ME, it is not known if anatomically distinct subpopulations of these neurons respond differently to specific stimuli. Neurochemical techniques are useful tools for studying the effects of pharmacological and physiological manipulations on neuronal activity at axon terminals, yet there is a limitation. While this technique can sample the area of interest as a whole or even subpopulations of it (Selmanoff, 1981; Palkovits et al., 1982), it is not possible to discern changes in individual neurons.

2-DG can also be used to study neuronal activity in axon terminals. This technique permits quantitative and regionally localized analysis of glucose utilization, an index of metabolic requirements of actively firing neurons and neuronal terminals (Brown et al., 1996; Eells et al., 2000). Advantages of this technique are that most types of physiological stimuli increase 2-DG accumulation in the brain and there is the potential for demonstrating all of the brain regions involved with a specific stimulus (Sharp et al., 1993). However, increases in 2-DG uptake produced by synaptic stimulation occur primarily in presynaptic neuronal and possibly glial elements (Sharp et al., 1993). While the use of this technique can identify active brain regions, it does not allow for chemical differentiation between types of neurons, such as TH neurons from vasopressin neurons. Thus, as with neurochemistry, 2-DG provides an index of activity of nerve terminals and does not allow for cellular resolution (Komisaruk et al., 2000; Eells et al., 2000).

Electrophysiology studies allow for the study of cell bodies focusing on the electrical activities of individual neuroendocrine neurons. Earlier *in vivo* studies were laborious to carry out because of difficulty accessing these neurons located deep within the brain. In addition, it was not possible to verify probe location until after the experiment and the required use of anesthetic may have altered neuronal response (Pan et al., 1986). *In vitro* studies using brain slices remove these obstacles of electrophysiology and can provide information concerning individual neurons in specific brain regions. While a few studies have successfully labeled the neurons of interest (Wagner et al., 1998), most neurons remain unidentified (Lin et al., 1993; Pan et al., 1996).

Immunohistochemistry has become a useful technique to visualize and identify neurons and their projections, but which cells were active under specific stimuli was unknown. Through studies with the immediate early gene FRA, it was demonstrated that FRA expression provides a metabolic map of individual neuronal responses. FRA are immediate early genes that are rapidly and transiently expressed in a variety of tissues including the brain following such stimuli as growth factors, electrical stimulation and various stressors (Sagar et al., 1988; Hoffman et al., 1993; Hoffman et al., 1994). Thus, it has been used as a tool for mapping neuronal responses, localizing subpopulations of chemically similar neurons, and determining if there are changes in the numbers of active neurons in that subpopulation.

The goals of the studies in this chapter are two fold. First is to compare the numbers and the distribution of TH-IR neurons throughout the ARC in male

and female rats. Innervation of the ME by TIDA neurons, as estimated by DA concentrations, is equivalent in male and female rats. Thus there should be similar numbers of TH-IR neurons in males and females. Second is to calculate the percentage of those neurons expressing FRA. Previous studies have demonstrated that TIDA neuronal activity, as estimated by DOPAC concentrations in the ME, are two to three times greater in females compared to males. The working hypothesis is that if the expression of FRA correlates with neuronal activity, then female rats will have a greater number of TIDA neurons containing FRA in the ARC compared to male rats. For comparison IHDA neurons of the MZI were examined. Unlike TIDA neurons, there is no sexual difference in DA concentration or activity in axon terminals of IHDA neurons. These neurons are not responsive to gonadal steroids or PRL (Gunnet et al., 1986), but instead are regulated by DA receptor-mediated mechanisms (Lookingland and Moore, 1984). The numbers of TH-IR neurons in the MZI were determined and the percentage of those neurons expressing FRA calculated in male and female rats.

Materials and Methods

Gonadally intact female and male rats were used in these experiments. Care and handling of the rats was carried out as described in the **Material and Methods** in Chapter 2. The estrous cycles of female rats were monitored by daily vaginal lavage, and only diestrous females exhibiting two or more consecutive 4 to 5 day cycles were used in these experiments.

Untreated rats were anesthetized with Equithesin and perfused with 4% paraformaldehyde. Brains were removed and sectioned as described in **Materials and Methods** in Chapter 2. The identification of TH-IR neurons using fluorescent rhodamine and FRA-IR nuclei using nickel intensified DAB in the ARC and MZI was carried out using immunohistochemical procedures described in the **Materials and Methods** in Chapter 2. An indepth analysis of the entire length of the ARC was initially carried out by dividing the ARC into 10 regions spanning the area 1.8mm posterior to 3.96 mm posterior to bregma. Observations during initial analysis suggested that subsequent trends may exist in more defined subpopulations of TH-IR neurons within the ARC, thus the original slides were re-evaluated. For this analysis, the ARC was regrouped into rostral, middle, and caudal regions (2.3 mm, 2.8 mm and 3.3 mm posterior to bregma, respectively) and then further partitioned into DM-ARC and VL-ARC. FRA were localized with anti-FRA antiserum (Genosys Biotechnologies) generated against a synthetic peptide derived from a conserved region of the *c-fos* gene common to all FRA genes. The dilution used was 1:2500 in TBS/TX containing 1.5% normal donkey serum. TH was detected using a monoclonal anti-TH antiserum (Incstar Corp) generated in mouse against a midportion fragment of purified portion of TH isolated from PC-12 cells. The final dilution was 1:1000 in TBS/TX containing 1.5% normal horse serum.

Results

Figure 3.1 depicts the distribution of TH-IR neurons through representative sections of the ARC of male rats. The numbers of TH-IR neurons were significantly higher in the middle regions and continued through the caudal regions of the ARC. The percentage of TH-IR neurons expressing FRA in males were low in the rostral and more rostral middle regions of the ARC ranging from 3.3% to 6.1%, and significantly increased in the more caudal middle and caudal regions to a maximum level of 11.7% (**Figure 3.2**). In females, higher numbers of TH-IR neurons occurred in the rostral regions and declined in the caudal regions of the ARC (**Figure 3.3**). The percentage of TH-IR neurons expressing FRA remained relatively constant throughout the ARC ranging from 8.9-13.8% (**Figure 3.4**).

In addition to the sexual differences in the distribution of TH-IR neurons and FRA-IR nuclei within those neurons, there were visual clues that differences may be present within the dorsoventral regions of the ARC. The ARC was further analyzed by partitioning it into DM-ARC and VL-ARC.

In the DM-ARC, there was a significantly decreasing gradient in the numbers of TH-IR neurons that extended caudally in both males and females (**Figure 3.5**). The actual numbers of neurons within each rostrocaudal region was similar between male (64.6 rostral, 50.2 middle, and 41.0 caudal) and female (65 rostral, 54.9 middle, 33.6 caudal) indicating no sexual differences. The number of TH-IR neurons containing FRA-IR nuclei, however, was almost 3 times greater in the rostral DM-ARC of females (14.2%) compared to males

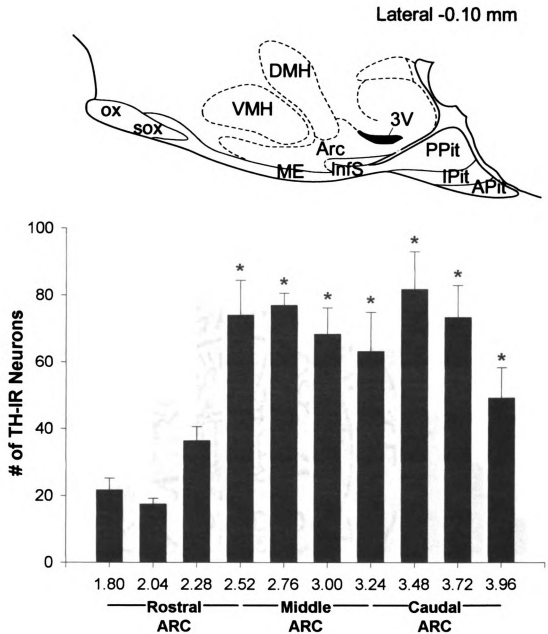

Figure 3.1 Distribution of TH-IR neurons throughout the rostro-caudal extent of the ARC in male rats. Coordinates for these regions extend from 1.80–3.96 mm posterior to bregma (Paxinos and Watson, 1997). Columns represent means and vertical lines + 1 SEM from 5 animals. *, Values that are significantly different ($p < 0.05$) from 1.80 mm posterior to bregma. 3V, third ventricle; APit, anterior lobe of pituitary; Arc, arcuate nucleus; DMH, dorsomedial hypothalamic nucleus; InfS, infundibular stalk; IPit, intermediate lobe of pituitary; ME, median eminence; ox, optic chiasm; PPit, posterior lobe of pituitary; sox, supraoptic decussation; VMH, ventromedial hypothalamic nucleus

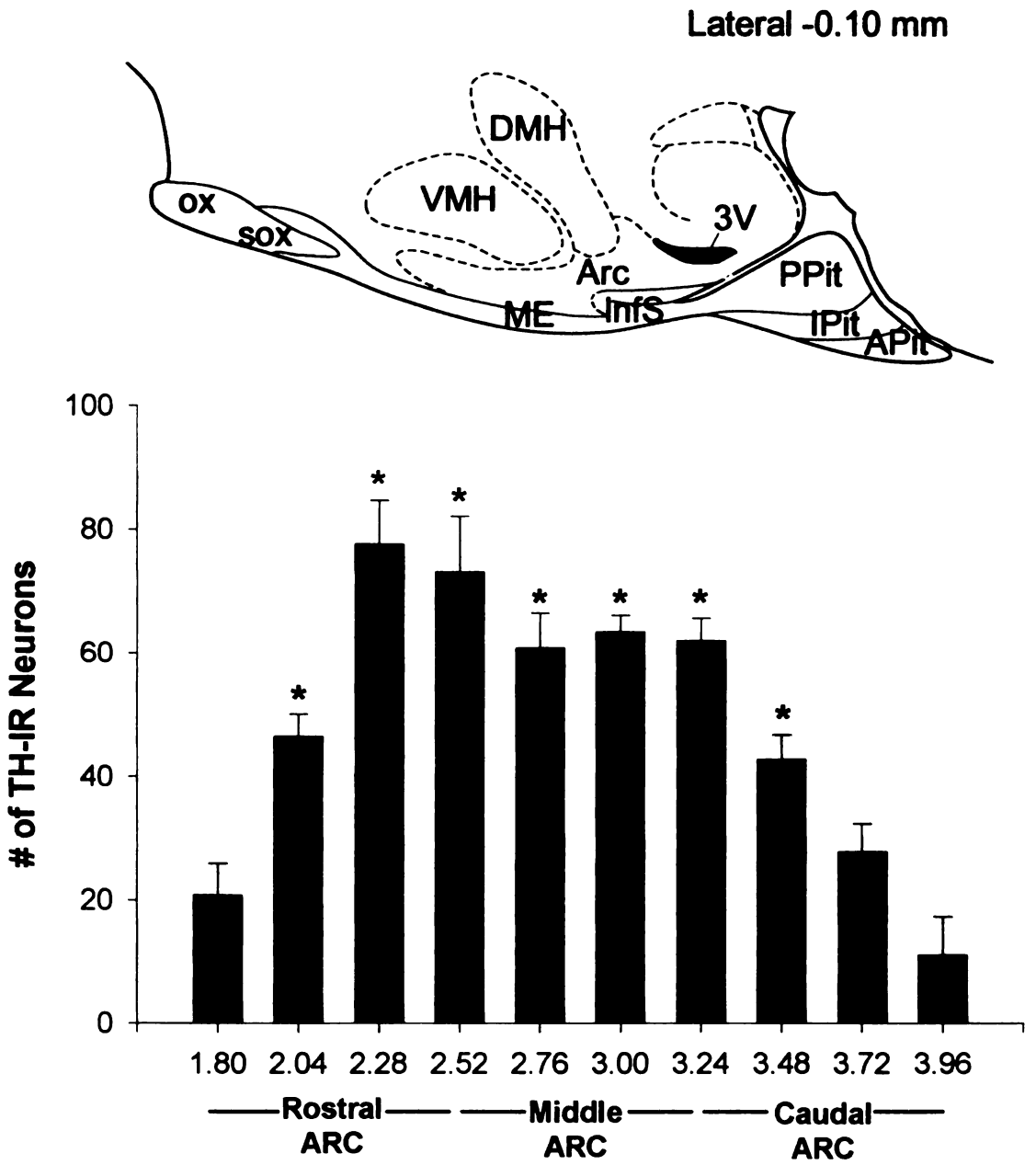

Figure 3.2 Distribution of TH-IR neurons throughout the rostro-caudal extent of the ARC in female rats. Coordinates for these regions extend from 1.80–3.96 mm posterior to bregma (Paxinos and Watson, 1997). Columns represent means and vertical lines + 1 SEM from 5 animals. *, Values that are significantly different ($p < 0.05$) from 1.80 mm posterior to bregma. Abbreviations are as defined in Figure 3.1.

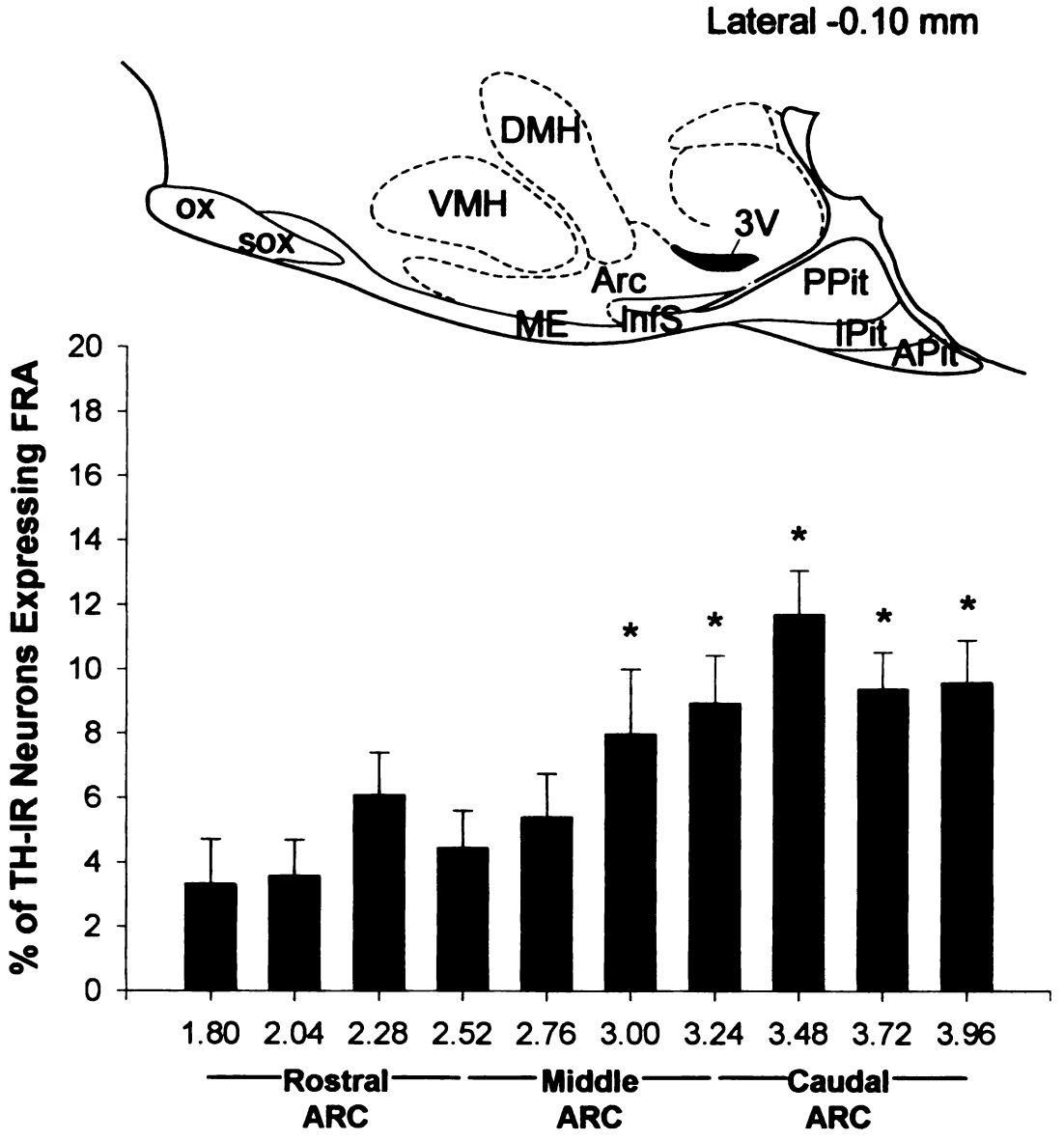

Figure 3.3 Percentages of TH-IR neurons expressing FRA throughout the rostro-caudal extent of the ARC in male rats. Coordinates for these regions extend from 1.80–3.96 mm posterior to bregma (Paxinos and Watson, 1997). Columns represent means and vertical lines + 1 SEM from 5 animals. *, Values that are significantly different ($p < 0.05$) from 1.80 mm posterior to bregma. Abbreviations are as defined in Figure 3.1.

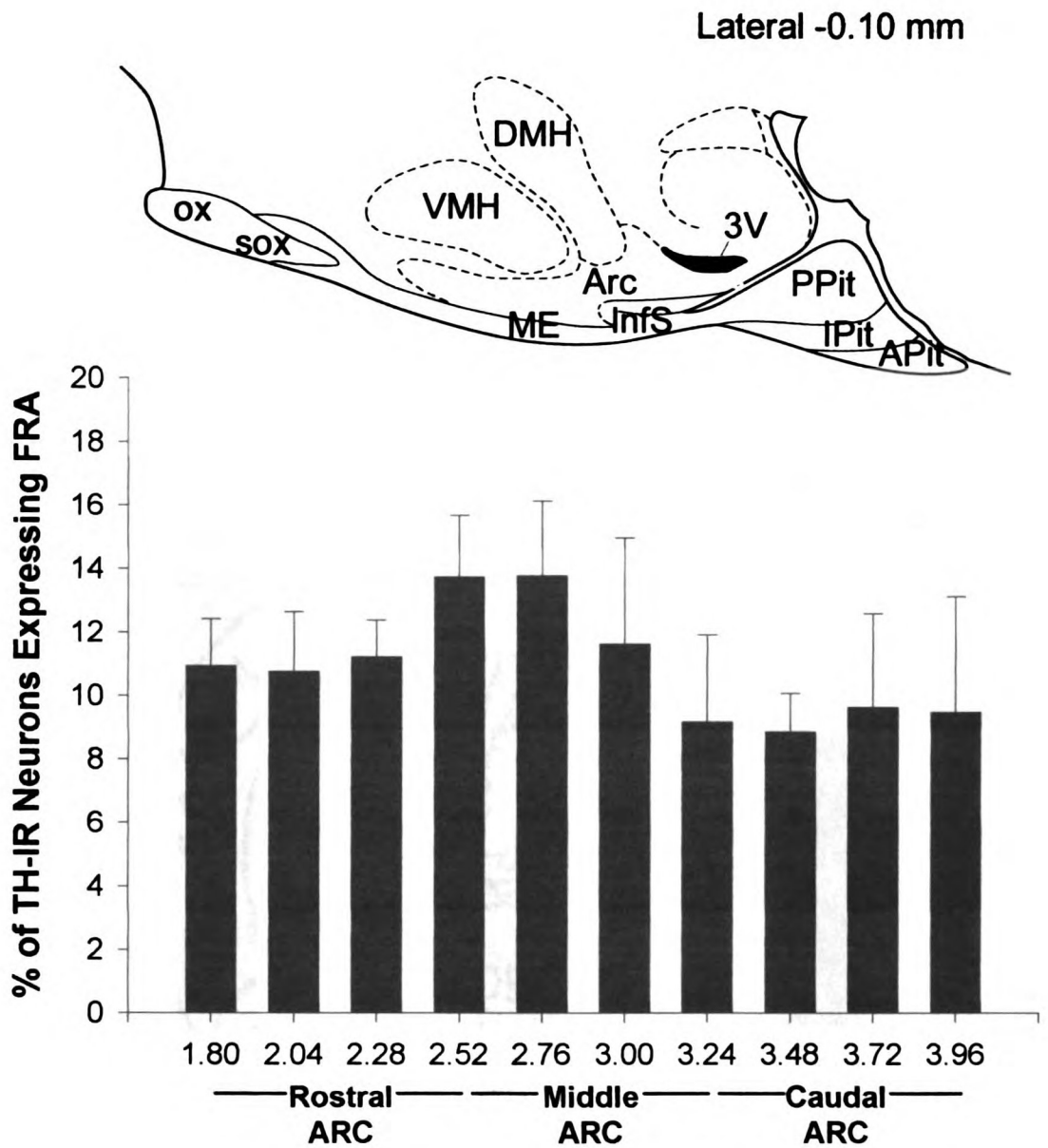

Figure 3.4 Percentages of TH-IR neurons expressing FRA throughout the rostro-caudal extent of the ARC in female rats. Coordinates for these regions extend from 1.80–3.96 mm posterior to bregma (Paxinos and Watson, 1997). Columns represent means and vertical lines + 1 SEM from 5 animals. Abbreviations are as defined in Figure 3.1.

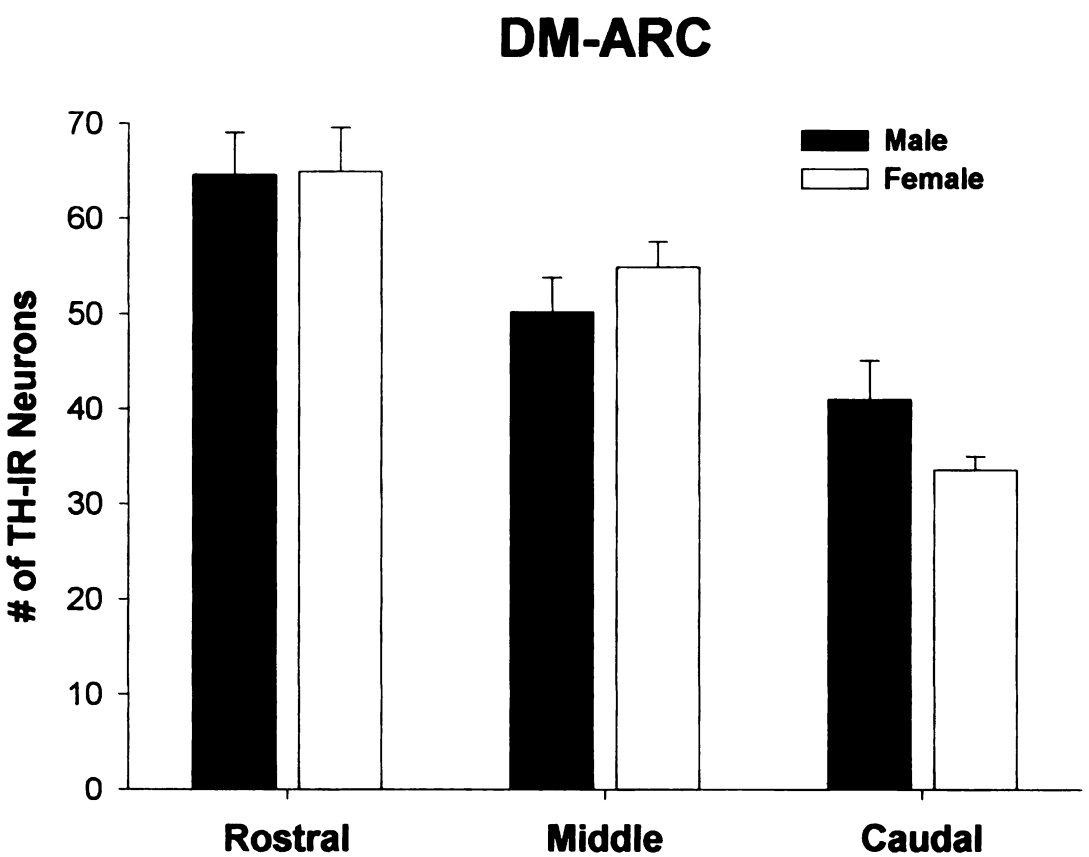

Figure 3.5 Comparison of the numbers of TH-IR neurons in the rostral, middle, and caudal regions of the DM-ARC in male (filled columns) and female rats (open columns). Coordinates for these regions of the ARC were approximately 2.3mm (rostral), 2.8 mm (middle), and 3.3 mm (caudal) posterior to bregma (Paxinos and Watson, 1997). Columns represent means and vertical lines + 1 SEM from 5 animals.

(5.2%). In the middle and caudal regions, the percentage of FRA-IR nuclei was similar between females (8.6% and 6.5%) and males (6.2% and 4.8%) (**Figure 3.6**).

Unlike the DM-ARC, there were differences in the number of TH-IR neurons between sexes in two of the subregions of the VL-ARC. The numbers of neurons were almost two times greater in male versus female rats in the middle and caudal VL-ARC (**Figure 3.7**). In the rostral VL-ARC, the numbers of neurons were relatively low in males (16.5 cells/section) and females (10.0 cells/section). **Figure 3.8** represents the percentage of TH-IR neurons expressing FRA-IR nuclei in the VL-ARC of males and females. The percentages were relatively constant throughout the rostrocaudal VL-ARC in both sexes (13-17%), but there was high variability in this area especially in the rostral VL-ARC.

In the MZI, the numbers of TH-IR neurons in males were comparable to the numbers in females (260 vs 235 cells/section) (**Figure 3.9, Bottom Panel**). However, this was a stark contrast to the numbers of TH-IR neurons within the DM-ARC or VL-ARC; the numbers of TH-IR neurons in the MZI ranged 4 to 20 times higher. As with the numbers of neurons, there was no difference between males and females in the percentage of TH-IR neurons containing FRA-IR nuclei (**Figure 3.9, Top Panel**). Unlike the ARC, however, the percent of FRA-IR nuclei in the MZI was very low, less than 1%.

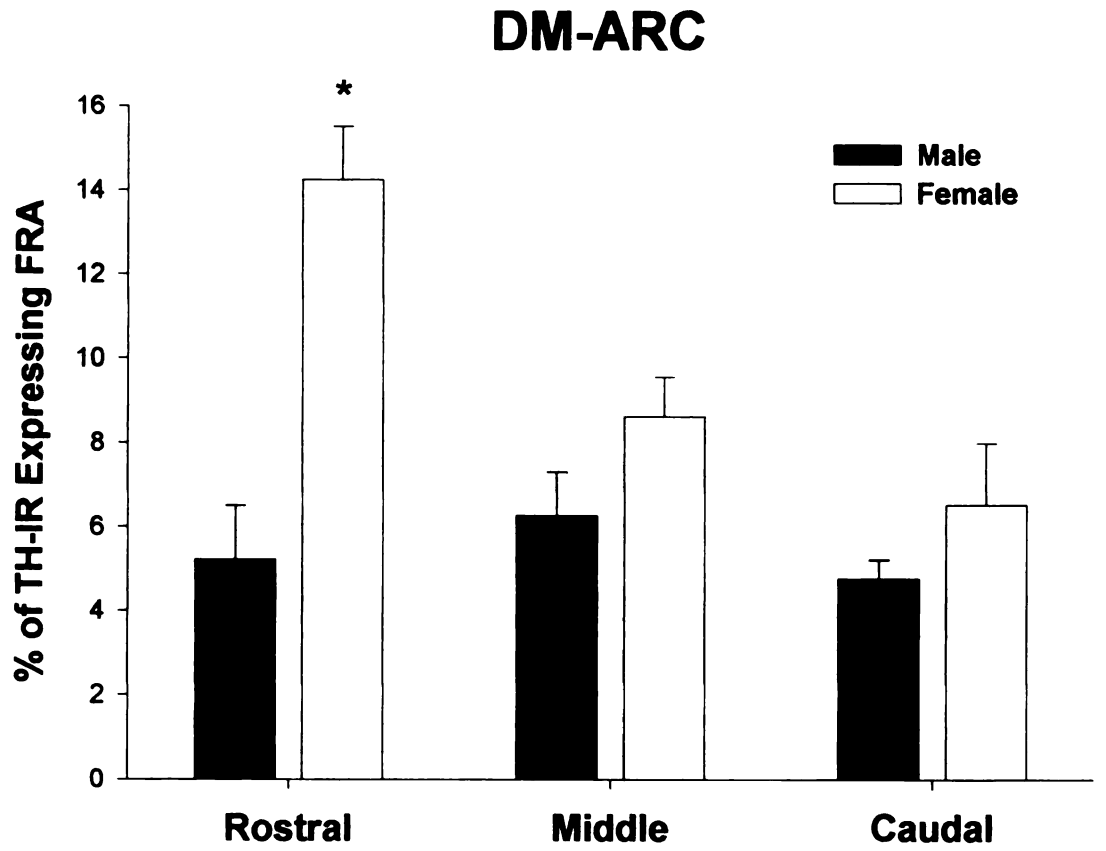

Figure 3.6 Comparison of the percent of TH-IR neurons expressing FRA in the rostral, middle, and caudal regions of the DM-ARC in male (filled columns) and female rats (open columns). Coordinates for these regions of the ARC were approximately 2.3mm (rostral), 2.8 mm (middle), and 3.3 mm (caudal) posterior to bregma (Paxinos and Watson, 1997). Columns represent means and vertical lines + 1 SEM from 5 animals. *, Values for females that are significantly higher ($p < 0.05$) than males.

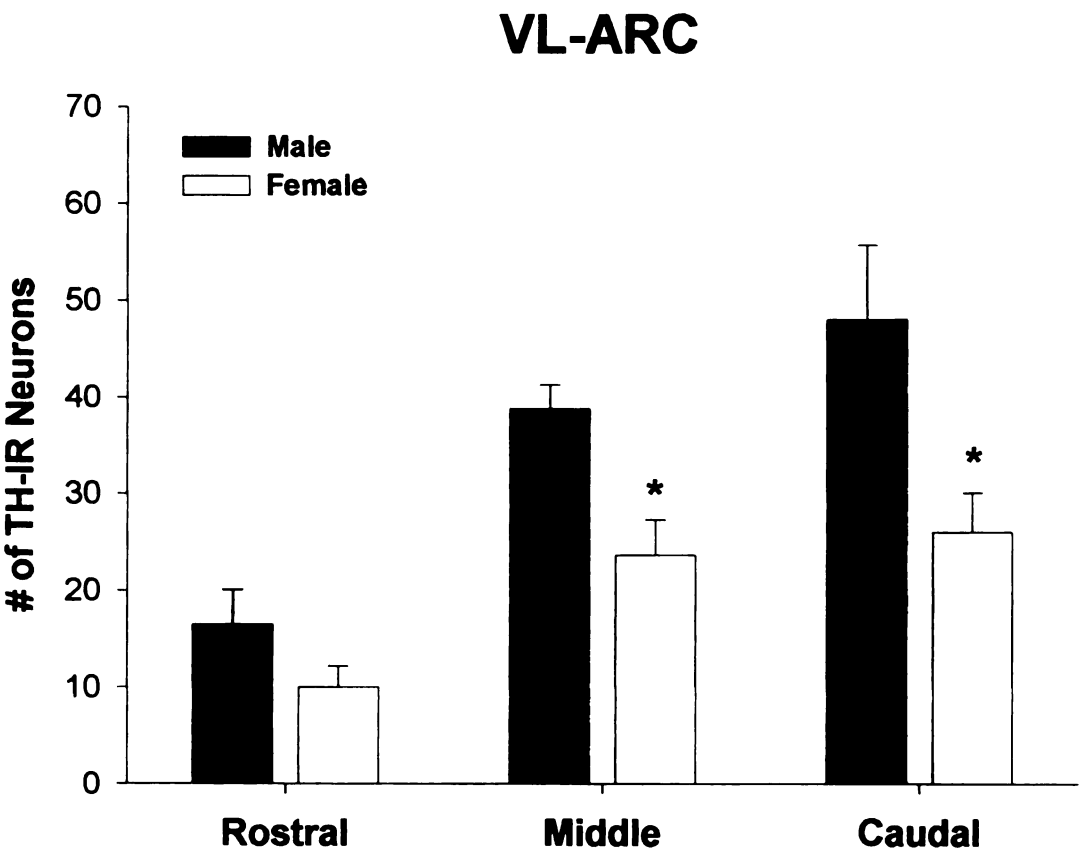

Figure 3.7 Comparison of the numbers of TH-IR neurons in the rostral, middle, and caudal regions of the VL-ARC in male (filled columns) and female rats (open columns). Coordinates for these regions of the ARC were approximately 2.3mm (rostral), 2.8 mm (middle), and 3.3 mm (caudal) posterior to bregma (Paxinos and Watson, 1997). Columns represent means and vertical lines + 1 SEM from 5 animals. *, Values for females that are significantly lower ($p < 0.05$) than males.

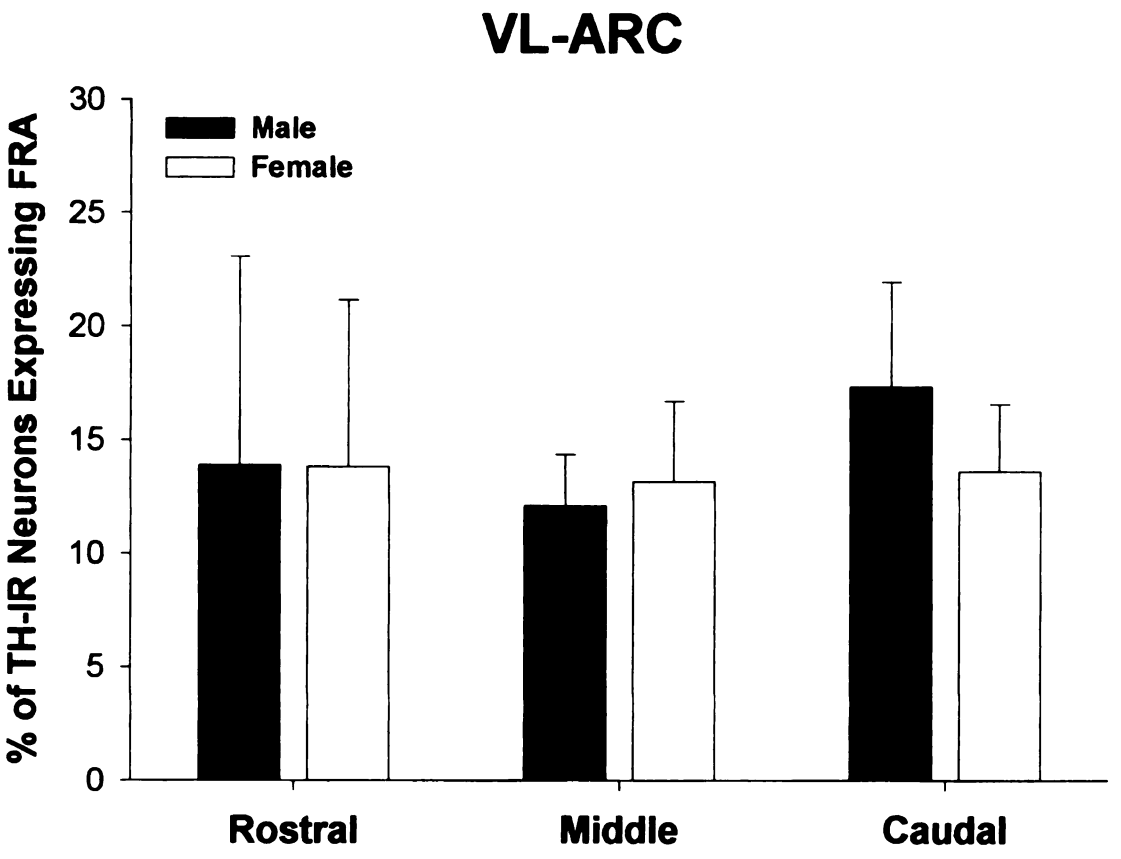

Figure 3.8 Comparison of the percent of TH-IR neurons expressing FRA in the rostral, middle, and caudal regions of the VL-ARC in male (filled columns) and female rats (open columns). Coordinates for these regions of the ARC were approximately 2.3mm (rostral), 2.8 mm (middle), and 3.3 mm (caudal) posterior to bregma (Paxinos and Watson, 1997). Columns represent means and vertical lines + 1 SEM from 5 animals.

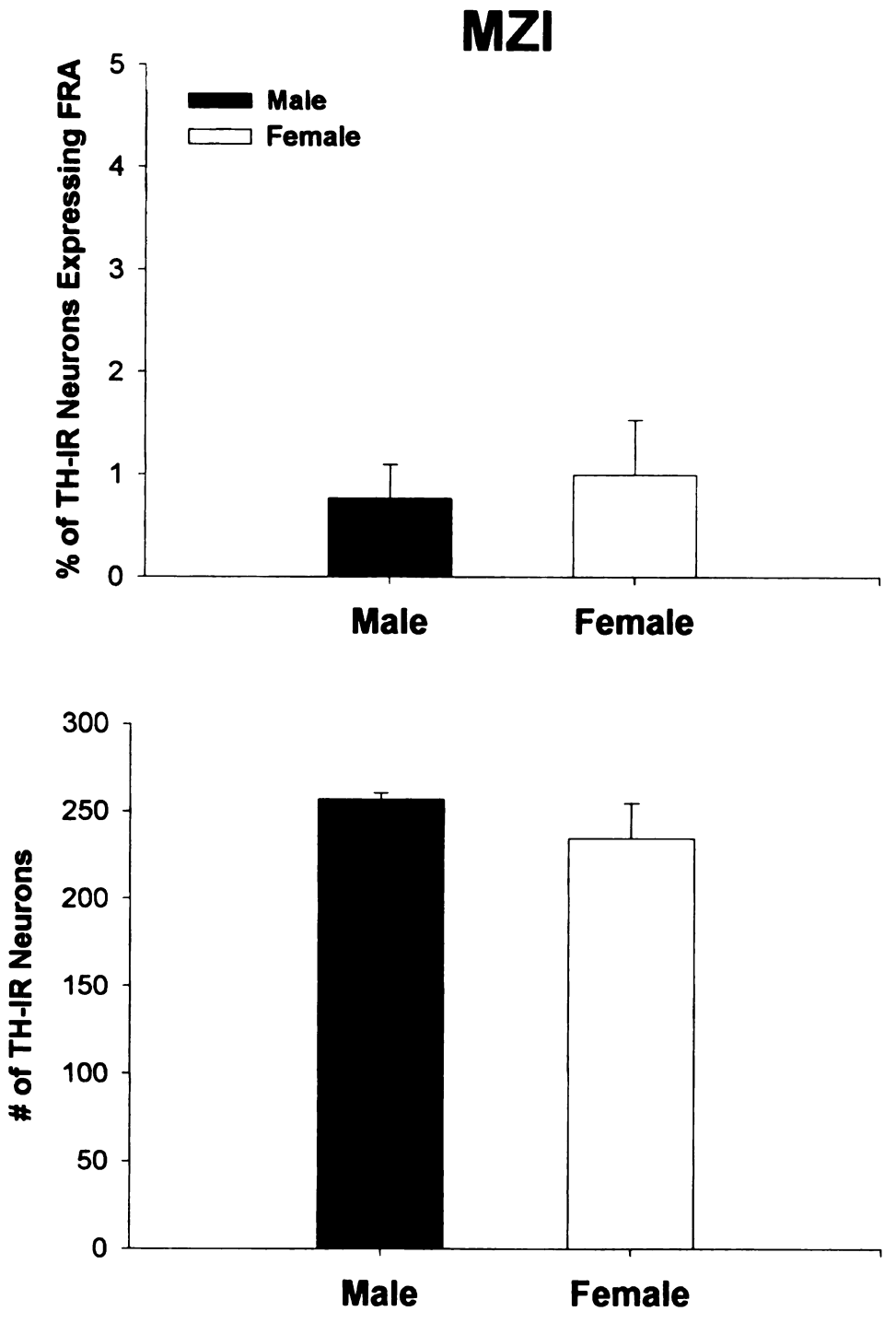

Figure 3.9 Comparison of the numbers of TH-IR neurons (**Bottom Panel**) and the percent of these neurons expressing FRA (**Top Panel**) in the MZI of male (filled columns) and female rats (open columns. Coordinates for this region was approximately 2.8 mm posterior to bregma (Paxinos and Watson, 1997). Columns represent means and vertical lines + 1 SEM from 5 animals.

Discussion

The goals of these studies were to determine the distribution of TH-IR neurons as well as the basal level of FRA expression in these neurons in the DM-ARC and VL ARC in male and diestrous female rats.

The overall numbers and distribution of TIDA neurons throughout the ARC correlate with previous studies describing the distribution of TH-IR neurons throughout the hypothalamus in male rats (Chan-Palay et al., 1984; Van den Pol et al., 1984). The results from initial studies presented here demonstrate an increase in numbers of TIDA neurons in a rostrocaudal gradient in the ARC of male rats. This correlates with DA concentrations, an indirect estimate of innervation, of the ME. Distribution studies of the ME divided the region into five rostrocaudal segments and compared DA concentrations (Palkovits et al., 1982). The ME has an increasing rostrocaudal gradient of DA with the maximum level located at the site of attachment of the pituitary stalk. TIDA neurons project ventrally and connect each portion of the ARC to a corresponding part of the ME (Lindvall and Björkland, 1978). Taken together these data indicate that there is an increase in innervation in the caudal portion of the ME in male rats. In females, there is a decrease in the numbers of TIDA neurons from the rostral to caudal portions of the ARC. While there are no published data describing the distribution of innervation in subdivisions of the ME in females, it would be logical that, like with male rats, the numbers of TIDA neurons would correlate with the innervation of the ME. Thus in females, one would anticipate that there would be greater DA concentrations and innervation in the rostral portion of the ME.

Expression of immediate early genes such as FRA have been shown to reflect activity of TIDA neurons of the ARC (Hoffman et al., 1994; Yang et al., 1999). FRA are stimulated through depolarization or ligand-mediated activation of membrane receptors located on neuronal soma or dendrites. This triggers a second messenger system (e.g. cyclic AMP and calcium) and phosphorylation cascade involving protein kinases A or C to activate constitutive transcription factors like CREB (Sheng and Greenberg, 1990; Sim et al., 1994). CREB induces the transcription and translation of immediate early genes like FRA. FRA dimerize with Jun proteins and bind to the AP-1 site (Curran and Franza, 1988) to regulate transcription and translation of long-term genes such as TH (Gizang-Ginsberg and Ziff, 1990; Icard-Liepkalns et al., 1992).

In males, there is an increase in the expression of FRA in the middle and caudal regions of the ARC. In contrast, the expression of FRA in female rats remains relatively constant throughout the ARC. These data suggest the presence of subpopulations of active TIDA neurons present in males that may subserve some gender-specific function which is absent or quiescent in females.

In the DM-ARC, there was a difference in distribution of TH-IR neurons in both males and females. There were a greater number of neurons in the rostral DM-ARC compared to the middle and caudal regions. Thus, the results presented here correlate with neurochemical studies demonstrating the density of innervation to the ME is the same for male and female rats (Gunnett et al., 1986).

Several studies have demonstrated that axon terminal activity, using neurochemical techniques (Lookingland et al., 1987), as well as glucose utilization, using 2-DG autoradiography (Brown et al., 1996), is 2-3 times greater in diestrous female rats compared to male rats under basal conditions. One explanation for the higher activity in females could simply be that an identical number of neurons are firing in males and females, but the rate is 2-3 times greater in females. A second possible explanation is that while the firing rate is constant, there are 2-3 times more neurons firing in females compared to males. By using FRA as an index of activity, it may be possible to identify which scenario accounts for the difference in female rats. It was the goal of these studies to determine if there were sexual differences in the expression of FRA that correlated with neurochemistry. If the percentage of TIDA neurons expressing FRA does correlate with neuronal activity, it should be 2-3 times greater in female rats compared to male rats. These results in **Figure 3.6** demonstrate that females have almost three times greater FRA expression in the rostral DM-ARC compared to males. This indicates that there are a greater number of neurons that are active in a subpopulation of TIDA neurons in female rats.

This difference is due to the effects of gonadal steroids as well as a difference in responsiveness of these neurons to PRL. Estrogen has a stimulatory effect on TIDA neuronal activity (Gunnet et al., 1986) as well as FRA expression (Cheung et al., 1997) via a mechanism mediated by PRL. Blockade of PRL secretion from the anterior pituitary prevents the estrogen-induced increases in TIDA neuronal activity (Toney et al., 1992). Furthermore, estrogen

increases synthesis of PRL by regulating gene transcription (Shull and Gorski, 1989) and disrupts the inhibitory actions of DA on PRL release from the anterior pituitary (Ferland et al., 1979). On the other hand, castration and hormone replacement studies demonstrated that testosterone has an inhibitory effect on both TIDA neuronal activity (Toney et al., 1991) and the expression of FRA (Cheung et al., 1997). Testosterone also attenuates the responsiveness of TIDA neurons to tonic stimulatory actions of PRL, but not the delayed activation by PRL (Toney, et al., 1991). Females are more sensitive to the stimulatory actions of PRL compared to males, and increases in PRL secretion stimulate DA release (Demarest and Moore, 1981) as well as FRA expression (Hentschel, 2000) in TIDA neurons of females to a greater extent than males. In addition, hypoprolactinemia decreases the activity of TIDA neurons in females, but decreases in PRL have almost no effect in males (Demarest and Moore, 1981).

In the VL-ARC, there is a sexual difference in the numbers of TH-IR neurons. The numbers of TH-IR neurons are greater in the middle and caudal aspects of the VL-ARC in males, but not in females. The neurons of the VL-ARC project to the lateral ME (Everitt et al., 1986). The TH-IR neurons of the VL-ARC are unique from those of the DM-ARC in that they lack the DD enzyme to convert DOPA to DA. Instead they only synthesize TH and are limited to producing only DOPA (Meister et al., 1988). This difference may indicate a physiological difference in the function of these "DOPA-ergic" neurons. Their exact function is not known; however, DOPA nerve terminals have been detected in vesicle-like aggregates in the external layer of the ME (Misu et al., 1996), and DD activity is

present in the vascular wall of the brain (Meister et al., 1988). This suggests that DOPA released from these neurons may be converted to DA at the level of the ME or in the portal blood system (Meister et al., 1988).

The expression of FRA in the VL-ARC is equal in males and females but highly variable. In the rostral portion of the VL-ARC this is most likely due to the low numbers of TIDA neurons. Nonetheless, this suggests that there is no sexual difference in the activity of these neurons.

For comparison, the numbers IHDA neurons of the MZI and the percentage of those neurons expressing FRA were examined in males and females. These neurons project to various areas of the brain including the paraventricular nucleus, horizontal limb of the diagonal band of Broca and central nucleus of the amygdala (Wagner et al., 1995; Eaton et al., 1994) and may play a role in luteinizing hormone secretion in female rats (MacKenzie et al., 1984). Compared to the ARC, the MZI has a significantly greater number of DA neurons, but significantly lower expression of FRA. The finding that there was no sexual difference in the number of IHDA neurons or in FRA expression correlates with previous neurochemical studies demonstrating that these neurons are not regulated by PRL or gonadal steroids and there is no sexual difference in basal activity of IHDA neurons (Gunnett et al., 1986b)

The results confirm the presence of subpopulations of TH-IR neurons that can be grouped into rostral, middle, and caudal DM-ARC and VL-ARC. In addition, there are sexual differences in FRA expression in TH-IR neurons in the rostral DM-ARC that coincide with differences in neurochemical activity of TIDA

neurons that terminate in the ME. These studies indicate that there are 2 to 3 times more TIDA neurons in the rostral DM-ARC that are active in female compared male rats. It is these TH-IR neurons in the DM-ARC that should be considered true TIDA neurons. In contrast the IHDA neurons of the MZI, which are regulated by DA-receptor mediated mechanisms (and not PRL or gonadal steroids as are TIDA neurons) demonstrate no sexual differences in the numbers or in the percentage of neurons expressing FRA.

CHAPTER FOUR

D2 RECEPTOR REGULATION OF IMMEDIATE EARLY GENE EXPRESSION IN TH-IR NEURONS IN SUBDIVISIONS OF THE ARCUATE NUCLEUS

Introduction

As discussed in Chapter Three, TIDA neurons are primarily regulated by prolactin, which is influenced by estrogen. This is in contrast to the mesotelencephalic DA neurons, which are regulated by DA receptor-mediated mechanisms consisting of autoreceptors and long loop neuronal feedback circuits. Several lines of evidence suggest TIDA neurons do not have autoreceptors, although there is controversy as to whether or not this is the case. TIDA neurons are unresponsive to nonselective DA agonists suggesting that TIDA neurons do not have DA autoreceptors (Moore, 1987). γ-Butyrolactone (GBL) disrupts impulse flow in DA neurons and thereby reduces the release of DA (Moore, 1987). In the mesotelencephalic and IHDA systems, less DA in the synapse leads to decreased activation of pre-synaptic autoreceptors and a disinhibition of TH (Demarest and Moore, 1979; Lookingland and Moore, 1984). The result is an increase in the rate of synthesis and concentration of DA in axon terminals. The increases of DA can be reversed with DA agonists (Moore, 1987). However, the concentration and rate of synthesis of DA does not increase in nerve terminals of the ME following GBL administration (Demarest and Moore, 1979; Lookingland and Moore, 1984; Gunnet et al., 1987).

Autoradiography and *in situ* hybridization studies have demonstrated D2 heteronuclear RNA and mRNA in many of the dopaminergic cell groups of the

hypothalamus including the MZI, but not the ARC (Weiner et al., 1991; Fox et al., 1993). Local infusion of selective D2 agonists and antagonists through microdialysis had no effect on DA and DOPAC levels in the medial basal hypothalamus (Timmerman et al., 1995). However, application of DA on rat hypothalamic brain slices inhibits single-unit activity of 70% of DM-ARC neurons suggesting that these neurons may contain autoreceptors (Lin and Pan, 1999). These neurons were not identified as being dopaminergic, however.

Following the discovery of receptor subtypes, in hopes of minimizing side effects often encountered, (i.e. dyskinesias) more specific DA receptor agonists and antagonists have been developed for the treatment of Parkinson's disease and schizophrenia. The receptor subtypes have been divided into two families: D1-like and D2-like. D1-like receptors are stimulatory and found post-synaptically, while D2-like receptors are inhibitory and found pre- and post-synaptically (Spano et al., 1978; Kebabian and Calne, 1979; Vallone et al., 2000). Autoreceptors fall into the D2-like category. Systemic administration of selective D2 agonists decreases neuronal activity in DA receptor-regulated mesotelencephalic systems neuronal systems (Foreman et al., 1989; Eaton et al., 1993; Durham et al., 1996). Surprisingly, D2 agonist effects on TIDA neurons result in an increase in activity (Eaton et al., 1993). This occurs independently of PRL and is mediated through tonically active afferent dynorphin neurons and kappa opioid receptors (Durham et al., 1996).

In addition to causing DA release from the axon terminal, stimulation of TIDA neurons can lead to changes in cellular events initiated by expression of

immediate early gene transcription factors. One set of immediate early genes that has been correlated with neuronal activity is FRA (Hoffman et al., 1993; Hoffman et al., 1994). FRA expression is increased throughout the brain following various pharmacological and physiological manipulations.

There are several lines of evidence demonstrating regulation of FRA expression via DA receptors in various brain regions. Haloperidol increases c-fos mRNA in the dorsolateral regions of the rat neostriatum via an action on post-synaptic D2 receptors (Merchant, et al., 1994). Quinelorane can reverse the stimulatory effects of haloperidol on *c-fos* (and *c-jun*) mRNA in the striatum (Rogue and Vincendon, 1992). Changes in FRA expression have also been demonstrated in the hypothalamus. In the paraventricular nucleus, quinelorane stimulates FRA expression in corticotropin-releasing hormone (CRH) neurons (Eaton, et al., 1996), while quinelorane inhibits FRA expression in somatostatin neurons of the periventricular nucleus (Cheung, et al., 1997). Fos expression also been studied in neonatal TH immunoreactive neurons cultured from the MZI (Sim, et al., 1994). These studies demonstrated that D_2 agonists can inhibit Fos expression and that a D2 antagonist can block this inhibition. Thus, the D_2 receptor system regulates Fos levels in IHDA neurons. However, no information is available regarding DA receptor-mediated regulation of gene expression in TIDA neurons.

The goal of these studies was to determine if D2 receptors regulate immediate early gene expression in TIDA neurons in male rats. The working hypothesis is that activation of D2 receptors stimulates Fos and Jun expression

in subpopulations of these neurons. Experiments in Chapter 3 used a nonspecific antibody that identified Fos, FosB, Fra-1 and Fra-2. By measuring FRA it is possible to identify increases and decreases in neuronal responsiveness (Hoffman et al., 1994); however, it is not possible to determine which transcription factor(s) is (are) being expressed, for each gene is induced by different types of stimuli and has a different half-life (Hoffman et al., 1992; Hughes and Dragunow, 1995; Kovacs, 1998). Activation of D2 receptors rapidly increases TIDA neuronal activity. If a Fos family member is induced by acute stimulation of these neurons, it is logical that it would be a protein that is induced following acute challenges. *c-fos* is the most rapidly induced by acute challenges (Hughes and Dragunow, 1995; Kovacs, 1998), thus it was chosen as the immediate early gene to be studied. To this end, the time course effects of quinelorane on Fos and c-Jun expression were determined. For comparison, the effects on Fos and c-Jun in the IHDA neurons of the MZI were also studied.

Materials and Methods

Gonadally intact male rats were used in these experiments. Care and handling of the rats was carried out as described in the **Materials and Methods** in Chapter 2. Following appropriate treatments, rats were anesthetized with Equithesin and perfused with 4% paraformaldehyde. Brains were removed and sectioned as described in **Materials and Methods** in Chapter 2. The identification of TH-IR neurons using diaminobenzidine or alkaline phosphatase and Fos-IR using nickel-intensified diaminobenzidine in the ARC and MZI was

carried out using immunohistochemical procedures in **Materials and Methods** in Chapter 2. The ARC sections were sorted into rostral, middle and caudal regions and then visually partitioned into DM-ARC and VL-ARC. Fos was localized with anti-Fos antiserum generated against the amino terminus of human c-Fos p62 (Santa Cruz) or against residues 4 to 17 of human *fos* (Oncogene). The dilution used was 1:5000 (Santa Cruz) or 1:10,000 (Oncogene) in TBS/TX containing 1.5% normal donkey serum. TH was detected using anti-TH serum (Chemicon) generated against rat adrenal medullary tumor tissue. The final dilution was 1:20,000 in TBS/TX containing 1.5% normal goat serum.

Results

Photomicrographs in **Figure 4.1** illustrate Fos expression in TH-IR neurons of middle DM-ARC 2 h after injection of either vehicle (**Top Panel**) or quinelorane-treated (**Bottom Panel**) male rats. These images show that Fos expression in TH-IR neurons is increased after quinelorane administration. **Figure 4.2** illustrates the time course effects of quinelorane on the percentage of TH-IR neurons expressing Fos in the DM-ARC. Quinelorane significantly increased Fos expression in a time dependent manner, reaching maximum levels at 2 h and returning to basal levels by 4 h in the rostral, middle and caudal regions of the DM-ARC. While the number of TH-IR neurons declines through the rostral-caudal extent of the DM-ARC, there were no changes in the numbers of TH-IR neurons at any time point after quinelorane within each region of the DM-ARC (**Figure 4.3**). In contrast, quinelorane caused significant decreases of

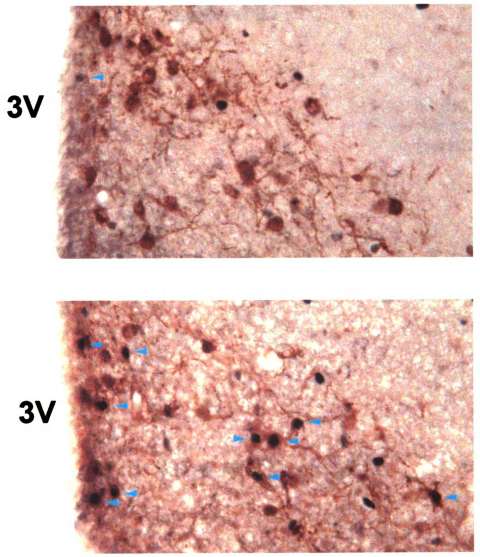

Figure 4.1 High power (400x) computer-captured images demonstrating increased Fos expression in TH-IR neurons of the DM-ARC 2 h following the administration of quinelorane. Rats were injected with either vehicle (**Top Panel**; 0.9% saline; 1 ml/kg; ip) or quinelorane (**Bottom Panel**; 100 μg/kg; ip) and sacrificed 2 h later. Arrowheads represent colocalization of brown TH-IR neurons containing black Fos-IR nuclei. 3V, third ventricle.

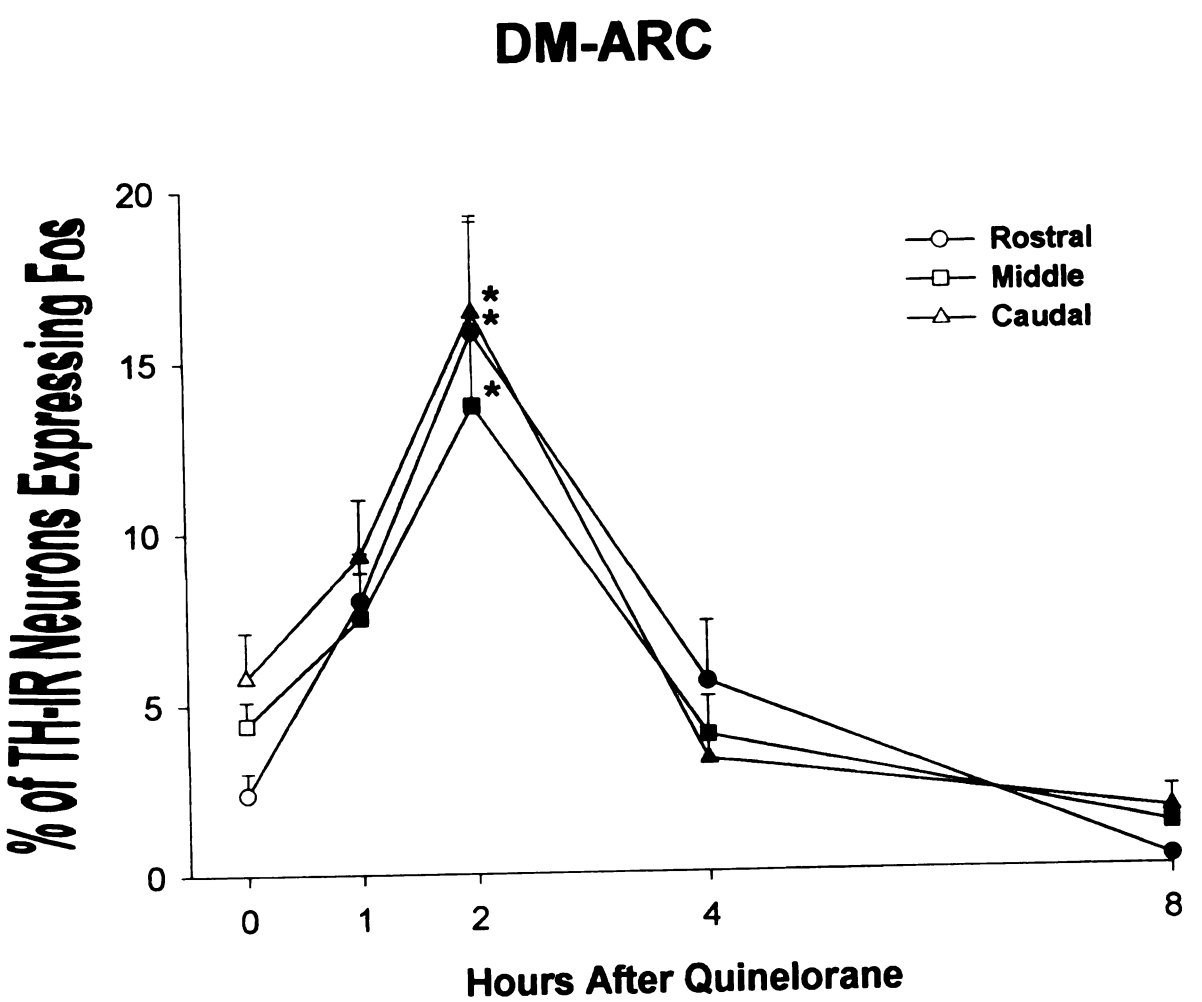

Figure 4.2 Time course effects of quinelorane on the percentage of TH-IR neurons expressing Fos in the rostral (circles), middle (squares), and caudal (triangles) regions of the DM-ARC. Rats were injected with quinelorane (filled symbols; 100 μg/kg; ip) and sacrificed 1, 2, 4 or 8 h later. Zero time controls (open symbols) were injected with 0.9% saline vehicle (1 ml/kg; ip) and sacrificed 2 h later. Symbols represent the means and vertical lines + 1 SEM from 6-8 animals. Where vertical lines are not depicted, 1 SEM is less than the radius of the symbol. *, Values for quinelorane-treated rats that are significantly different ($p<0.05$) from vehicle-treated controls.

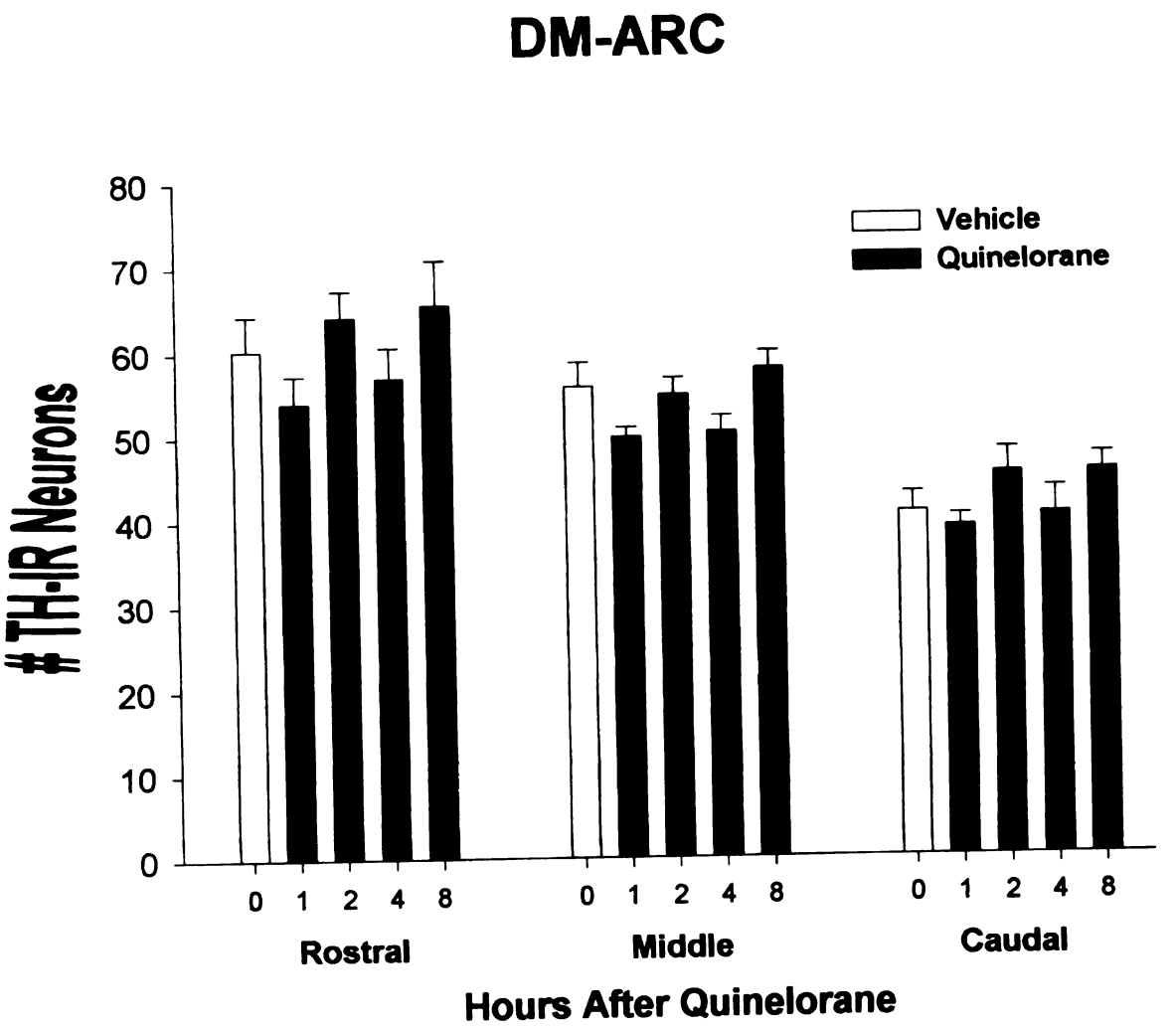

Figure 4.3 Time course effects of quinelorane on the numbers of TH-IR neurons in the rostral, middle, and caudal regions of the DM-ARC. Rats were injected with quinelorane (filled columns; 100 μg/kg; ip) and sacrificed 1, 2, 4 or 8 h later. Zero time controls (open columns) were injected with 0.9% saline vehicle (1 ml/kg; ip) and sacrificed 2 h later. Columns represent the means and vertical lines + 1 SEM from 6-8 animals.

Fos expression at 4 and 8 h throughout the rostral-caudal extent of the VL-ARC (**Figure 4.4**). As shown in **Figure 4.5**, there is an increasing gradient in the numbers of TH-IR neurons in vehicle-treated rats that extends caudally in the VL-ARC. As in the DM-ARC, there were no changes in the numbers of TH-IR neurons at any time point within each region of the VL-ARC. In the MZI, there was a gradual decrease in Fos expression following quinelorane such that there was a significant decrease in the percentage of TH-IR neurons with Fos-IR nuclei at the 8 h time point (**Figure 4.6**). Quinelorane had no effect on the numbers of TH-IR neurons in the MZI at any time point (**Figure 4.6**; **Inset**).

To determine if the effects of quinelorane on Fos were mediated through D2 receptors a study was carried out using the D2 receptor antagonist raclopride. Blockade of D2 receptors with raclopride had no effect *per se*, but reversed the stimulatory effects of quinelorane on Fos expression throughout the rostral-caudal extent of the DM-ARC (**Figure 4.7**). There were no changes in the numbers of TH-IR neurons following either raclopride or quinelorane (**Figure 4.8**). In the VL-ARC, there was a decreasing trend in the percent of TH-IR neurons expressing Fos-IR nuclei following raclopride and quinelorane administration, but there were no significant differences when compared to their respective control group (**Figure 4.9**). There were no changes in the numbers of TH-IR neurons in the VL-ARC following the administration of either raclopride or quinelorane (**Figure 4.10**). In the MZI raclopride increased Fos expression and the coadministration of quinelorane reversed this effect (**Figure 4.11**; **Top Panel**). Quinelorane alone had no effect on the percentage of TH-IR neurons

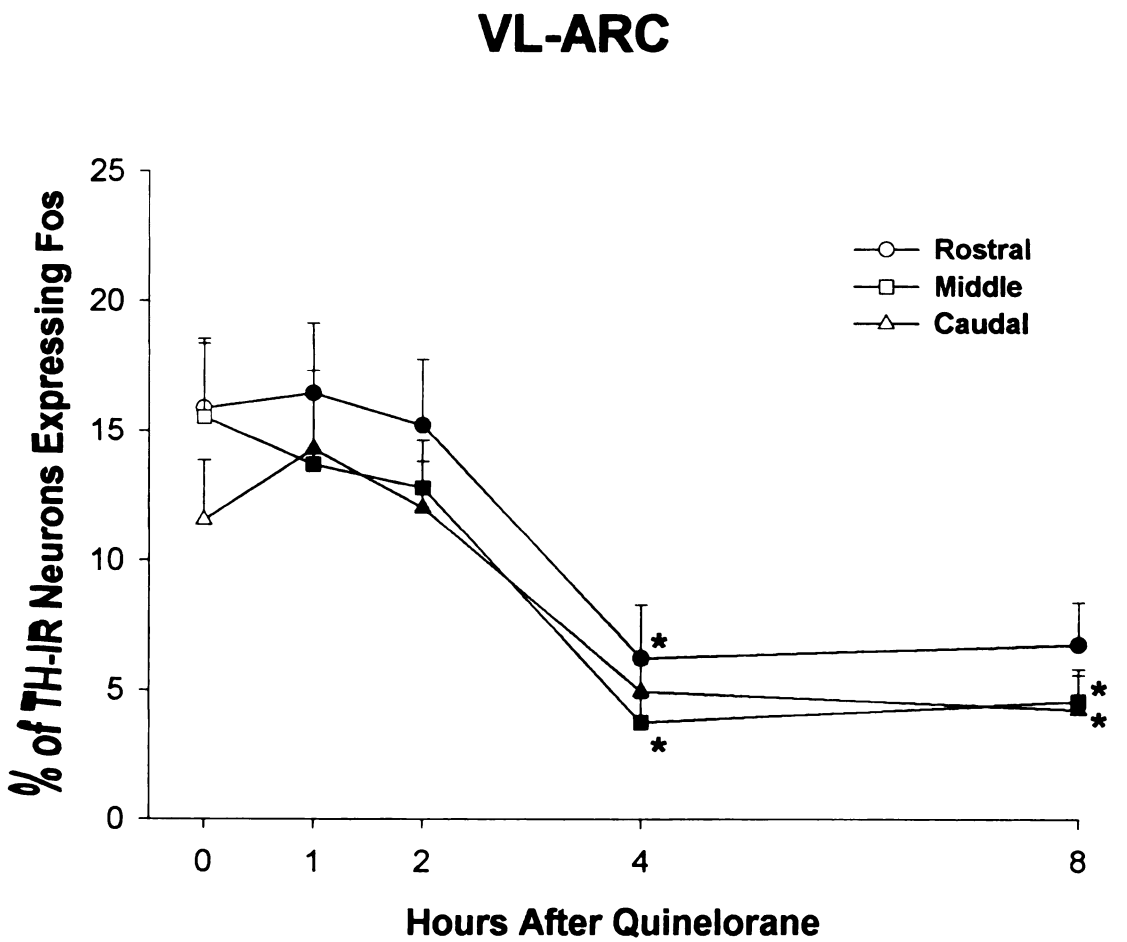

Figure 4.4 Time course effects of quinelorane on the percentage of TH-IR neurons expressing Fos in the rostral (circles), middle (squares), and caudal (triangles) regions of the VL-ARC. Rats were injected with quinelorane (filled symbols; 100 μg/kg; ip) and sacrificed 1, 2, 4 or 8 h later. Zero time controls (open symbols) were injected with 0.9% saline vehicle (1 ml./kg; ip) and sacrificed 2 h later. Symbols represent the means and vertical lines + 1 SEM-for 6-8 animals. *, Values for quinelorane-treated rats that are significantly different ($p<0.05$) form vehicle-treated controls.

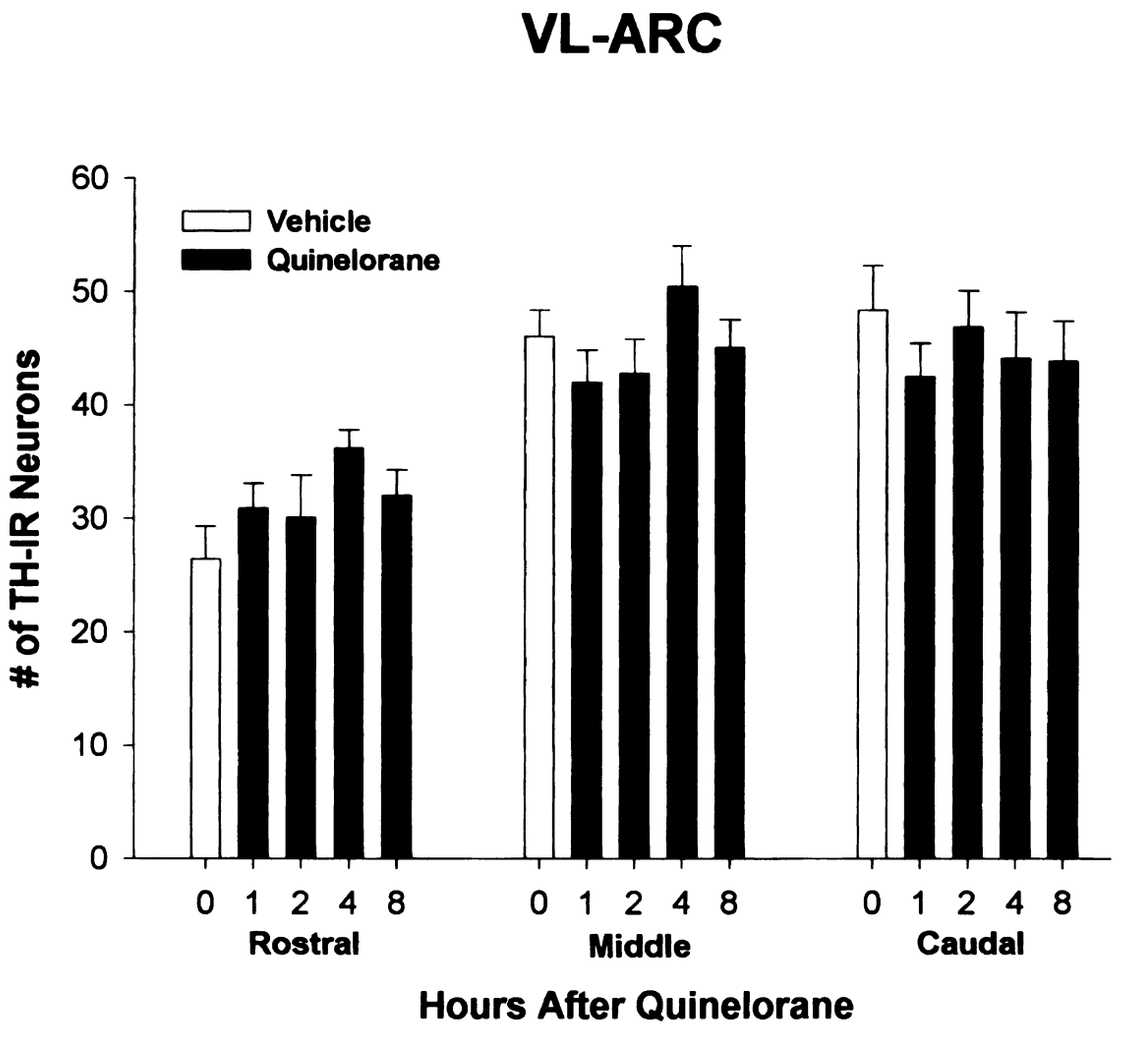

Figure 4.5 Time course effects of quinelorane on the numbers of TH-IR neurons in the rostral, middle, and caudal regions of the VL-ARC. Rats were injected with quinelorane (filled columns; 100 μg/kg; ip) and sacrificed 1, 2, 4 or 8 h later. Zero time controls (open columns) were injected with 0.9% saline vehicle (1 ml/kg; ip) and sacrificed 2 h later. Columns represent the means and vertical lines + 1 SEM from 6-8 animals.

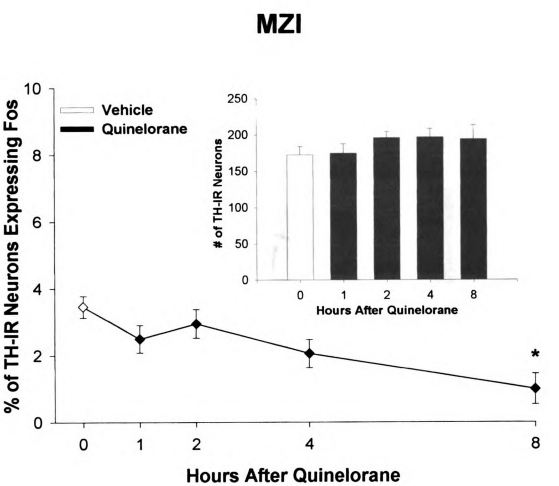

Figure 4.6 Time course effects of quinelorane on the numbers of TH-IR neurons (**Inset**) and the percentage of these neurons expressing Fos in the MZI. Rats were injected with quinelorane (filled symbols and columns; 100 μg/kg; ip) and sacrificed 1, 2, 4 or 8 h later. Zero time controls (open symbols and columns) were injected with 0.9% saline vehicle (1 ml/kg; ip) and sacrificed 2 h later. Symbols and columns represent the means and vertical lines + 1 SEM from 6-8 animals. *, Values for quinelorane-treated rats that are significantly different ($p<0.05$) from vehicle-treated controls.

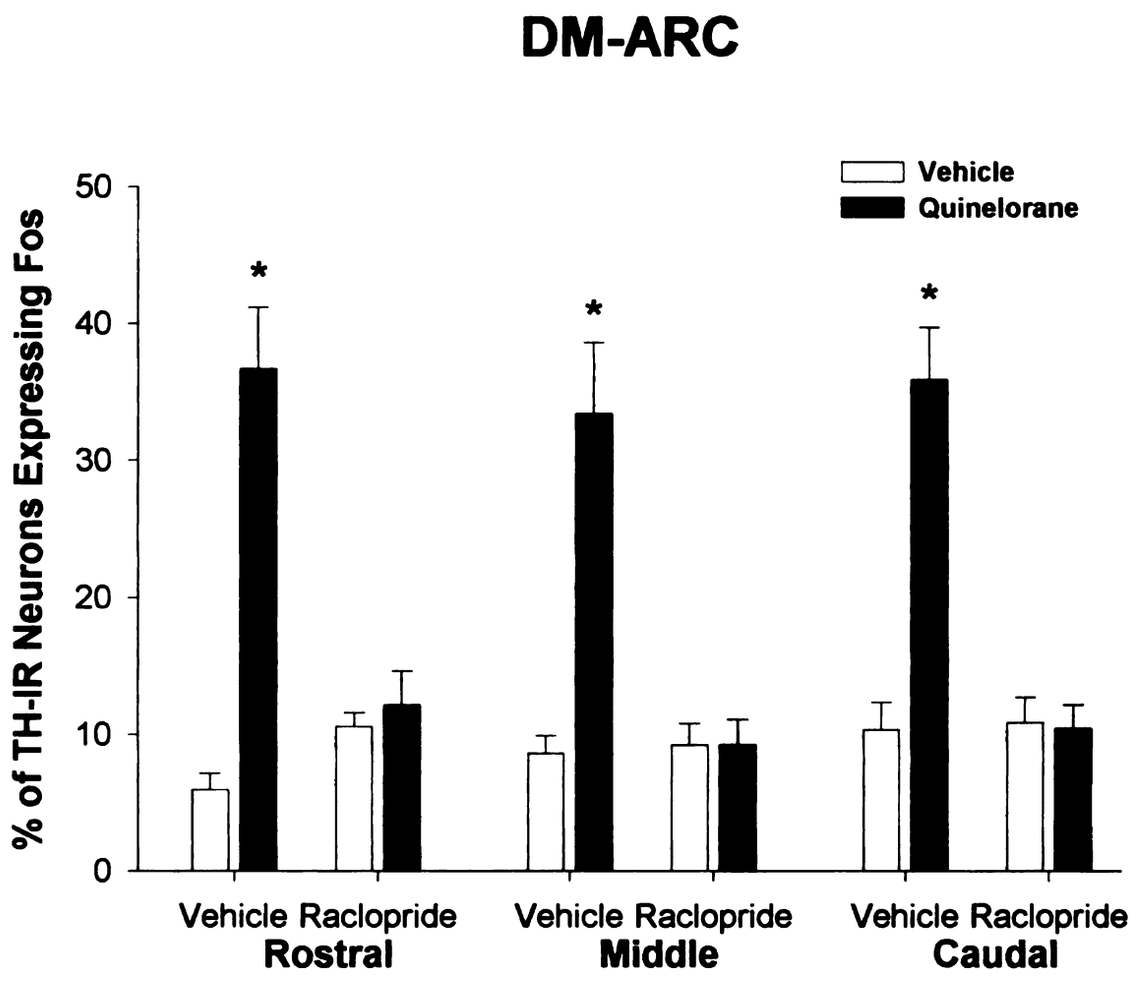

Figure 4.7 Effects of quinelorane on the percentage of TH-IR neurons expressing Fos in the rostral, middle and caudal regions of the DM-ARC of vehicle- or raclopride-treated rats. Rats were injected with either raclopride (3 mg/kg; ip) or its 0.9% saline vehicle (1 ml/kg; ip) 2 h prior to sacrifice, and with either quinelorane (100 μg/kg; ip) or its 0.9% saline vehicle (1 ml/kg; ip) 2 h prior to sacrifice. Columns represent the means and vertical lines + 1 SEM form 6-8 vehicle- (open columns) and quinelorane- (solid columns) treated rats. *, Values that are significantly different ($p<0.05$) from vehicle-treated rats.

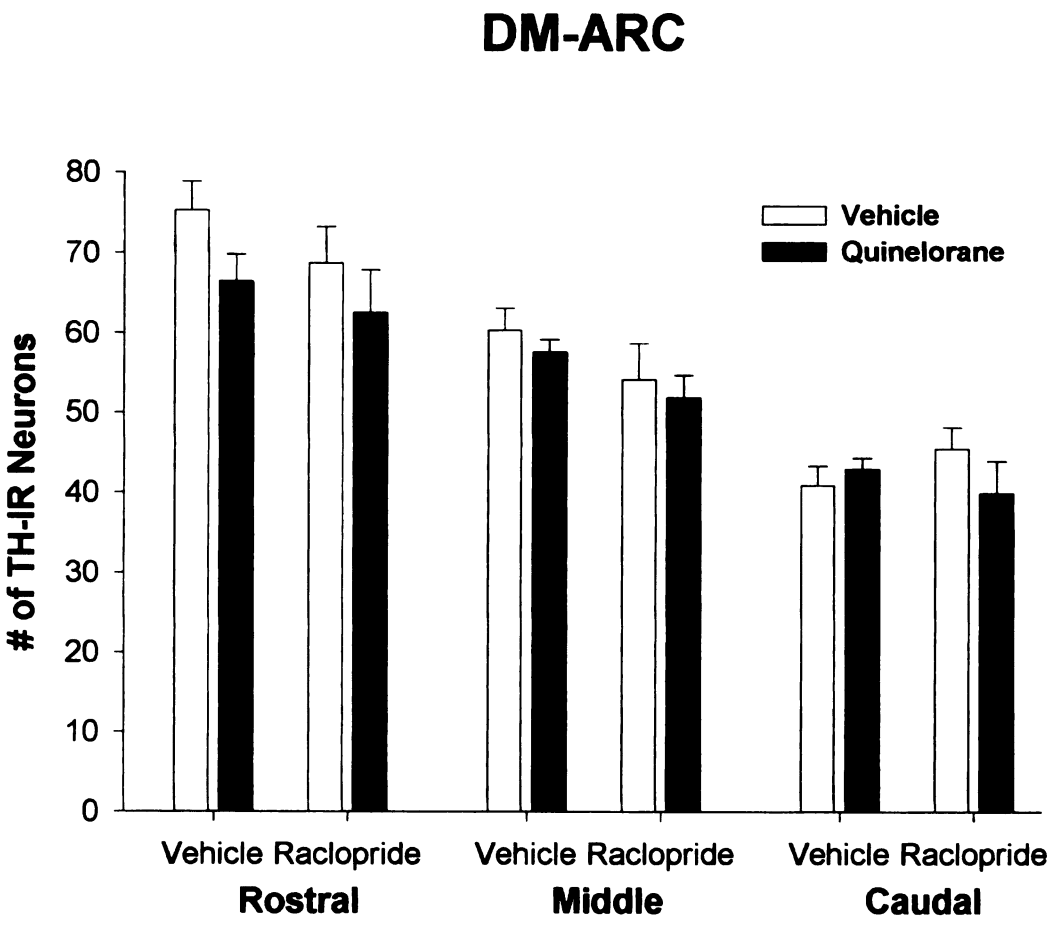

Figure 4.8 Effects of quinelorane on the numbers of TH-IR neurons in the rostral, middle and caudal regions of the DM-ARC of vehicle- or raclopride-treated rats. Rats were injected with either raclopride (3 mg/kg; ip) or its 0.9% saline vehicle (1 ml/kg; ip) 2 h prior to sacrifice, and with either quinelorane (100 μg/kg; ip) or its 0.9% saline vehicle (1 ml/kg; ip) 2 h prior to sacrifice. Columns represent the means and vertical lines + 1 SEM from 6-8 vehicle- (open columns) and quinelorane- (solid columns) treated rats.

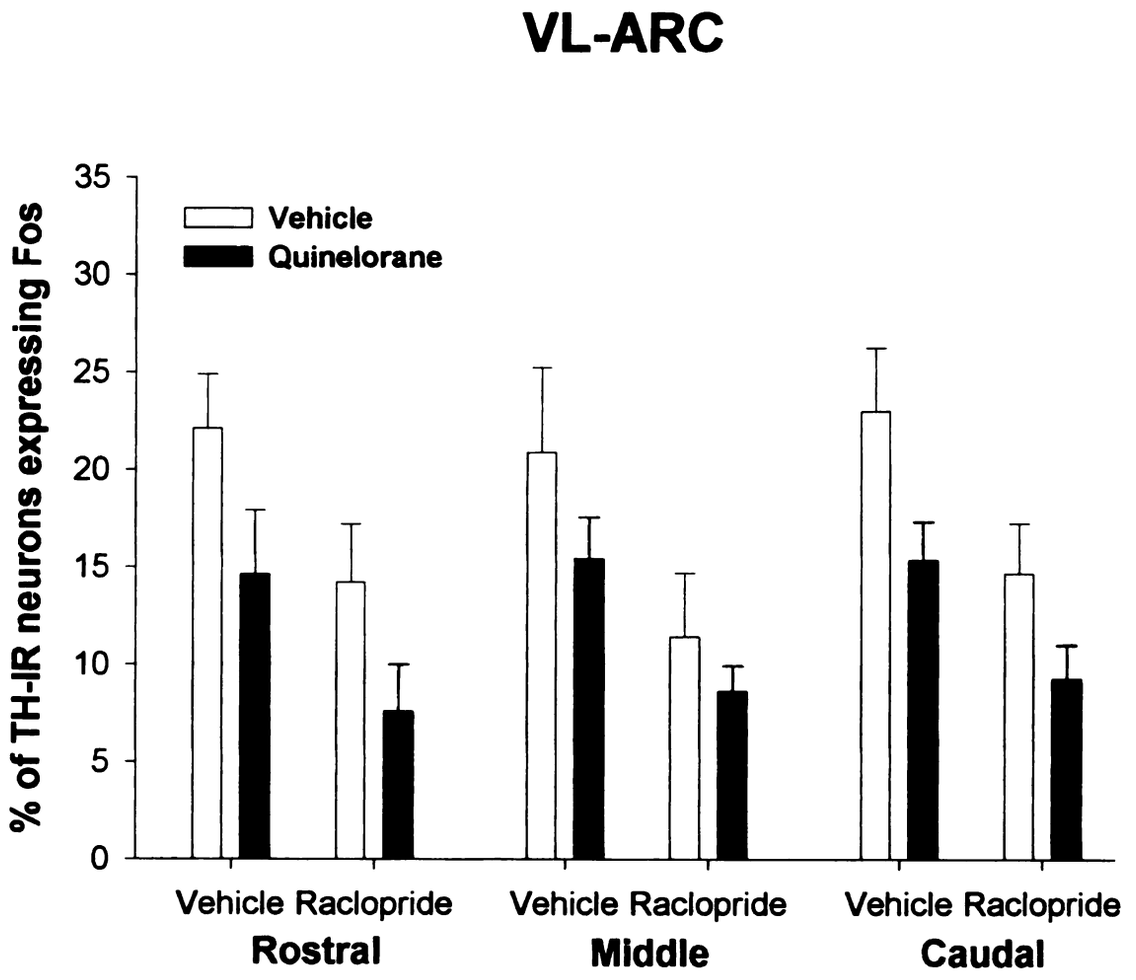

Figure 4.9 Effects of quinelorane on the percentage of TH-IR neurons expressing Fos in the rostral, middle and caudal regions of the VL-ARC of vehicle- or raclopride-treated rats. Rats were injected with either raclopride (3 mg/kg; ip) or its 0.9% saline vehicle (1 ml/kg; ip) 2 h prior to sacrifice, and with either quinelorane (100 μg/kg; ip) or its 0.9% saline vehicle (1 ml/kg; ip) 2 h prior to sacrifice. Columns represent means and vertical lines + 1 SEM form 6-8 vehicle- (open columns) and quinelorane- (solid columns) treated rats.

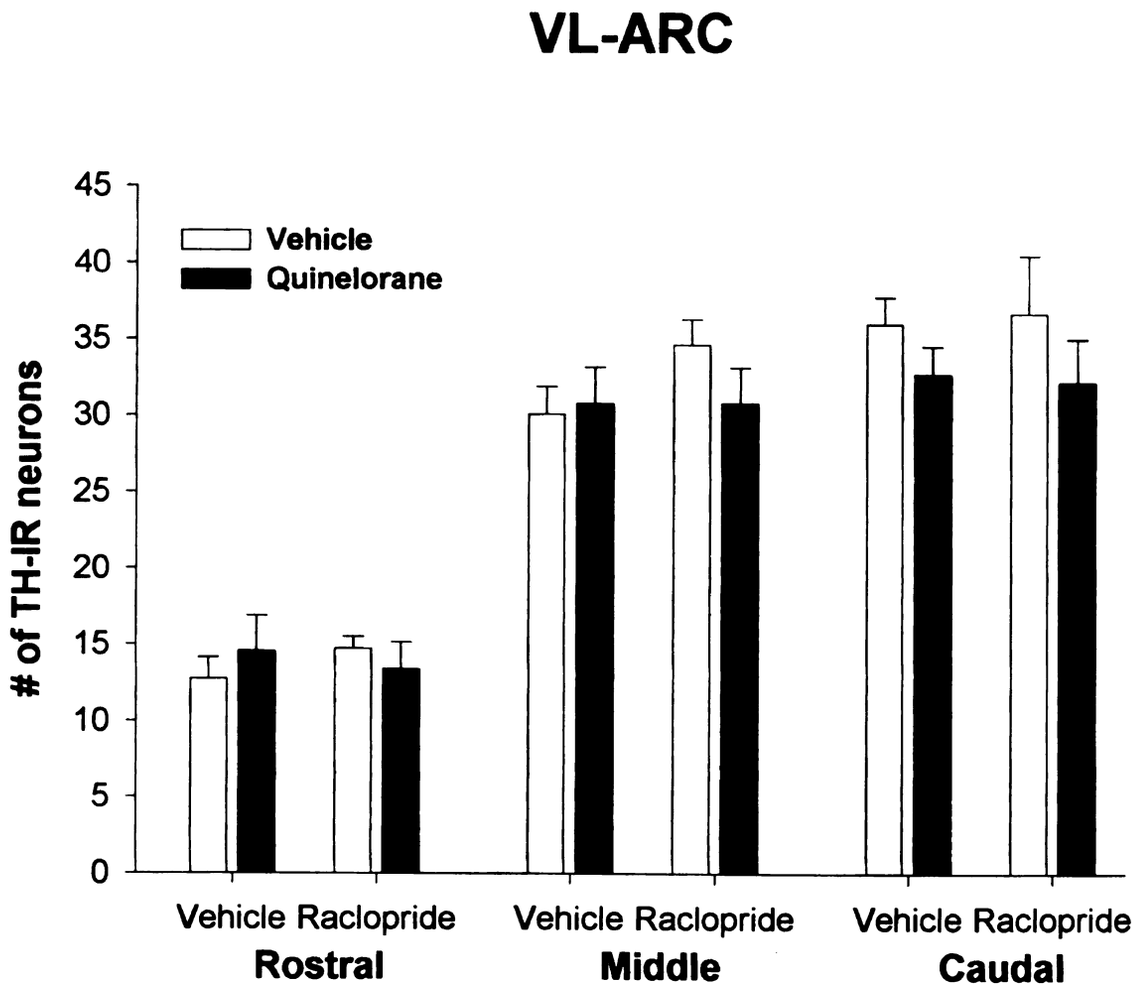

Figure 4.10 Effects of quinelorane on the numbers of TH-IR neurons in the rostral, middle and caudal regions of the VL-ARC of vehicle- or raclopride-treated rats. Rats were injected with either raclopride (3 mg/kg; ip) or its 0.9% saline vehicle (1 ml/kg; ip) 2 h prior to sacrifice, and with either quinelorane (100 μg/kg; ip) or its 0.9% saline vehicle (1 ml/kg; ip) 2 h prior to sacrifice. Columns represent the means and vertical lines + 1 SEM from 6-8 vehicle- (open columns) and quinelorane- (solid columns) treated rats.

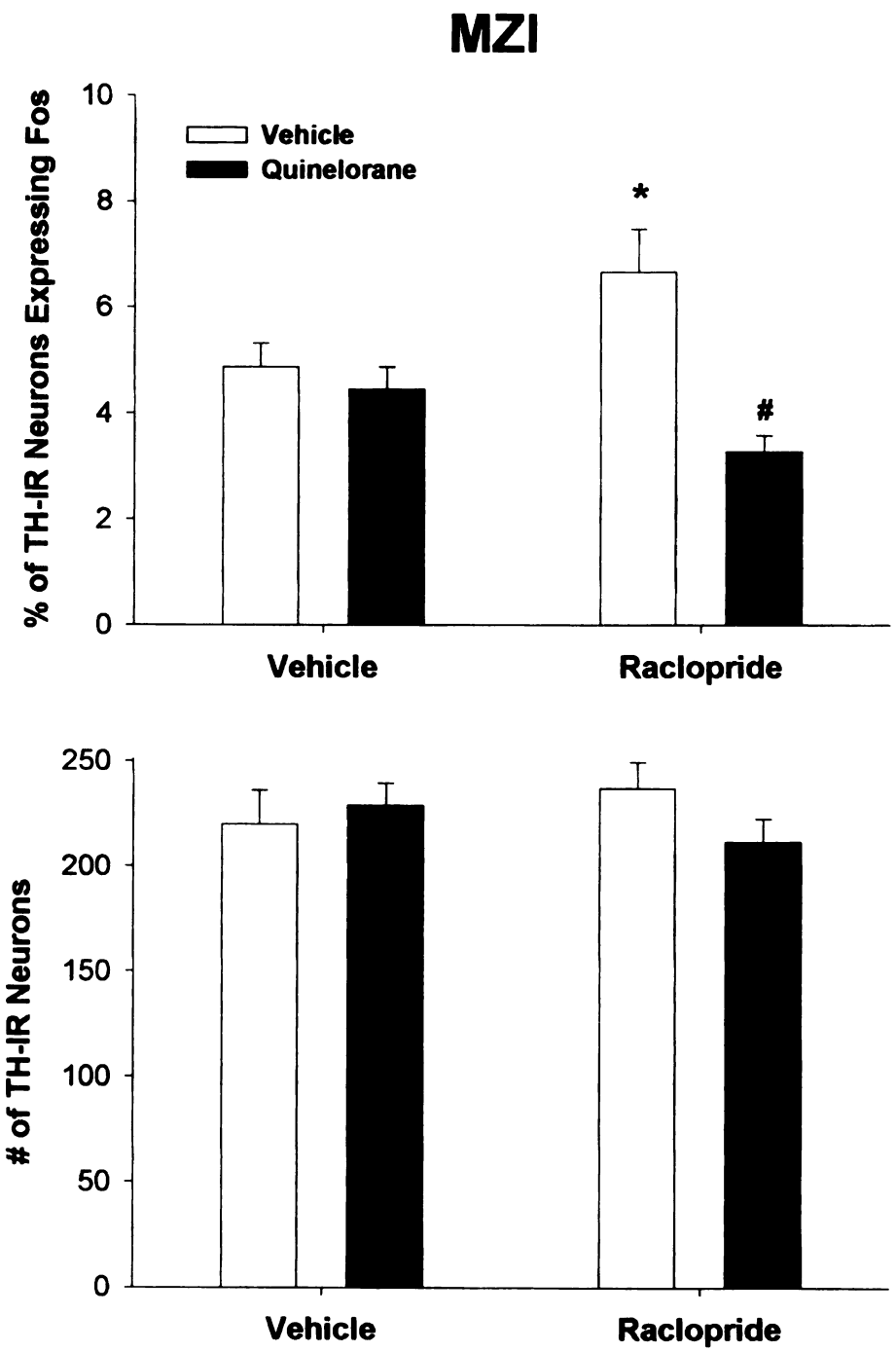

Figure 4.11 Effects of quinelorane on the numbers of TH-IR neurons (**Bottom Panel**) and the percentage of these neurons expressing Fos (**Top Panel**) in the MZI of vehicle- or raclopride-treated rats. Rats were injected with either raclopride (3 mg/kg; ip) or its 0.9% saline vehicle (1 ml/kg; ip) 2 h prior to sacrifice, and with either quinelorane (100 μg/kg; ip) or its 0.9% saline vehicle (1 ml/kg; ip) 2 h prior to sacrifice. Columns represent the means and vertical lines + 1 SEM from 6-8 vehicle- (open columns) and quinelorane- (solid columns) treated rats. *, Values that are significantly different ($p<0.05$) from vehicle-treated rats. #, Values that are significantly different ($p<0.05$) from raclopride-treated rats.

expressing Fos. There were no effects on the numbers of TH-IR neurons following the administration of either raclopride or quinelorane (**Figure 4.11**; **Bottom Panel**).

The TH-IR neurons of the VL-ARC did not respond to quinelorane and raclopride thus expression of Fos in these neurons is not regulated by D2 receptors. While the TH-IR neurons of the VL-ARC and the MZI were not responsive at 2 h, there was a gradual and late decrease in Fos expression. This suggests other factors such as the stress of receiving an intraperitoneal injection or circadian rhythm may account for the decrease in Fos expression. Restraint stress decreases DOPAC levels in the ME as demonstrated by neurochemical studies (Lookingland and Moore, 1988; Lookingland et al., 1990). Circadian rhythms also induce changes in TIDA neuronal activity in female rats as shown in neurochemical indices (Mai et al., 1994) and this is associated with a corresponding decrease in FRA expression (Lerant and Freeman, 1997). The circadian rhythm is regulated by the suprachiasmatic nucleus (SCN) and amplified by estrogen for the induction of the PRL surge. There is a decrease in TIDA activity over the afternoon corresponding to the PRL surge.

To determine if stress or time of day regulated Fos expression in TH-IR neurons in the VL-ARC, the time course effects of an intraperitoneal saline injection on Fos expression were examined. Uninjected animals served as controls in this experiment. Throughout the rostral-caudal extent of VL-ARC, there was no significant change at any time point after saline as compared with uninjected vehicle controls (**Figure 4.12**). There were no changes in the

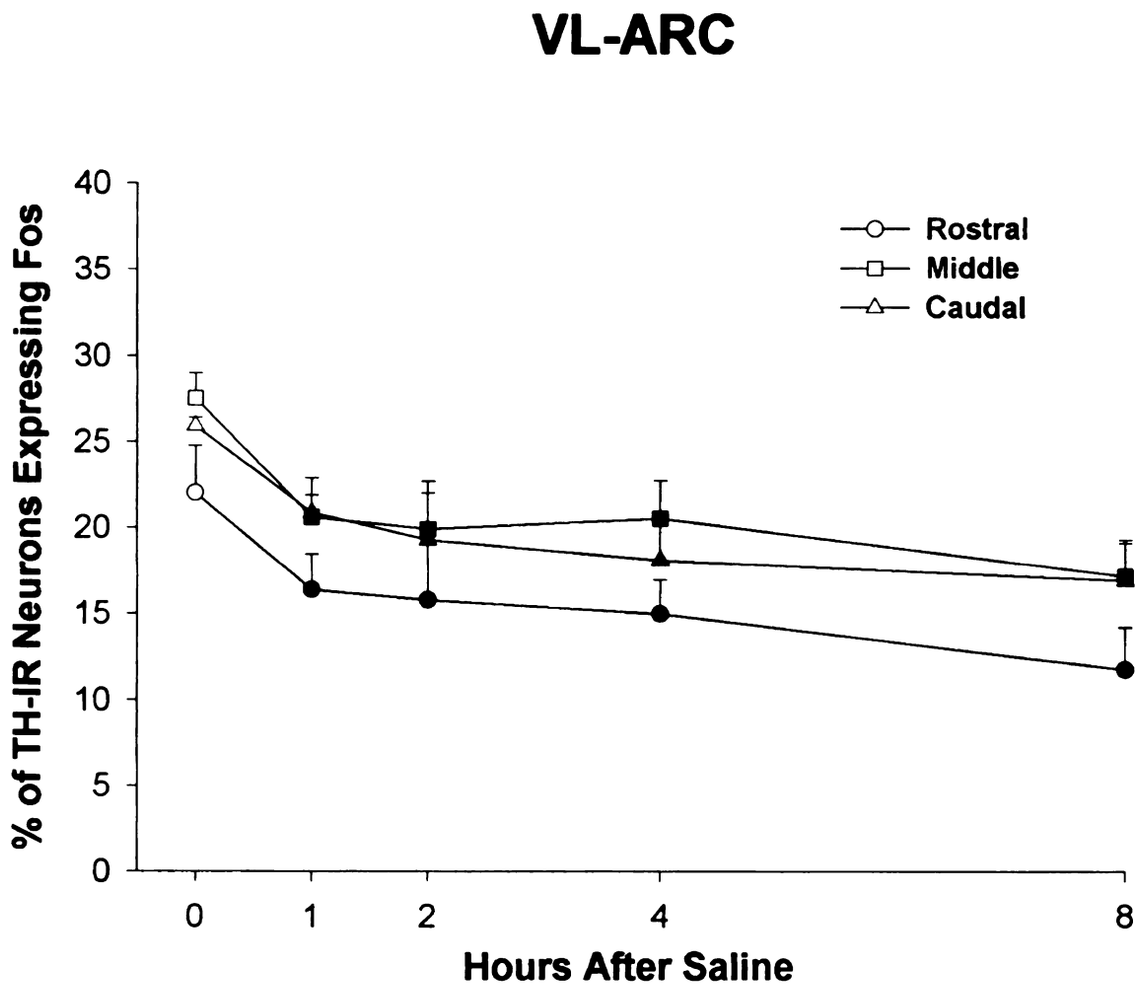

Figure 4.12 Time course effects of saline on the percentage of TH-IR neurons expressing Fos in the rostral (circles), middle (squares), and caudal (triangles) regions of the VL-ARC. Rats were injected with 0.9% saline (filled symbols; 1 ml/kg; ip) and sacrificed 1, 2, 4 or 8 h later. Zero time controls (open symbols) received no injection prior to sacrifice. Symbols represent the means and vertical lines ± 1 SEM from 6-8 animals.

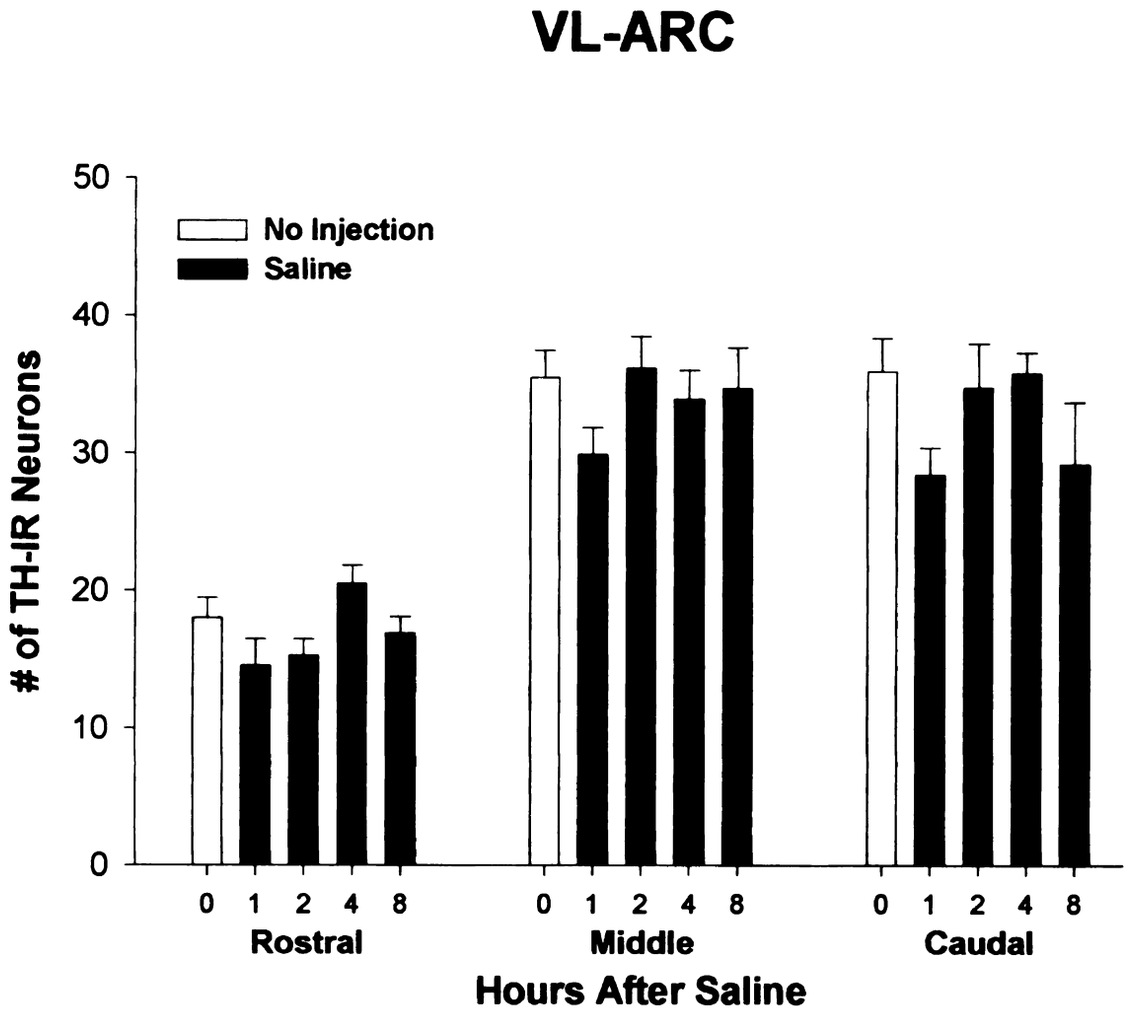

Figure 4.13 Time course effects of saline on the numbers of TH-IR neurons in the rostral, middle, and caudal regions of the VL-ARC. Rats were injected with 0.9% saline (filled columns; 1 ml/kg; ip) and sacrificed 1, 2, 4 or 8 h later. Zero time controls (open columns) received no injection prior to sacrifice. Columns represent the means and vertical lines + 1 SEM from 6-8 animals.

numbers of TH-IR neurons in the VL-ARC at any time point after saline administration (**Figure 4.13**). Time of day linear regression analysis revealed *r* values of -0.355 (rostral), -0.371 (middle), and -0.316 (caudal) in the VL-ARC. The *r* value is the correlation coefficient which represents the measure of the relationship between two variables. This number varies between -1 and +1. An *r* value of -1 indicates there is a perfect negative relationship between the two variables, with one always decreasing as the other increases. An *r* value of +1 indicates a perfect positive relationship between variables, with both always increasing together. When there is no relationship between variables, the *r* value is 0.

The correlation analysis demonstrated a negative correlation between time of day and Fos expression in the rostral and middle the VL-ARC, but not the caudal VL-ARC (**Figures 4.14-4.16**). Fos expression decreased as the day progressed. There was a gradual decrease in Fos expression in the middle and caudal DM-ARC following saline administration such that there was a significant decrease in the percentage of TH-IR neurons with Fos-IR nuclei at 8 h (**Figure 4.17**). There were no changes in the numbers of TH-IR neurons in the DM-ARC at any time point after saline administration (**Figure 4.18**). Time of day regression analysis revealed r values of 0.121 (rostral), -0.498 (middle) and -0.437 (caudal) in the DM-ARC. There was a negative correlation between time of day and Fos expression in the middle and caudal DM-ARC (**Figures 4.20 and 4.21**), but not in the rostral DM-ARC (**Figure 4.19**). Saline had no effect on the number of TH-IR neurons (**Figure 4.22**; **Inset**) or on the percentage of those

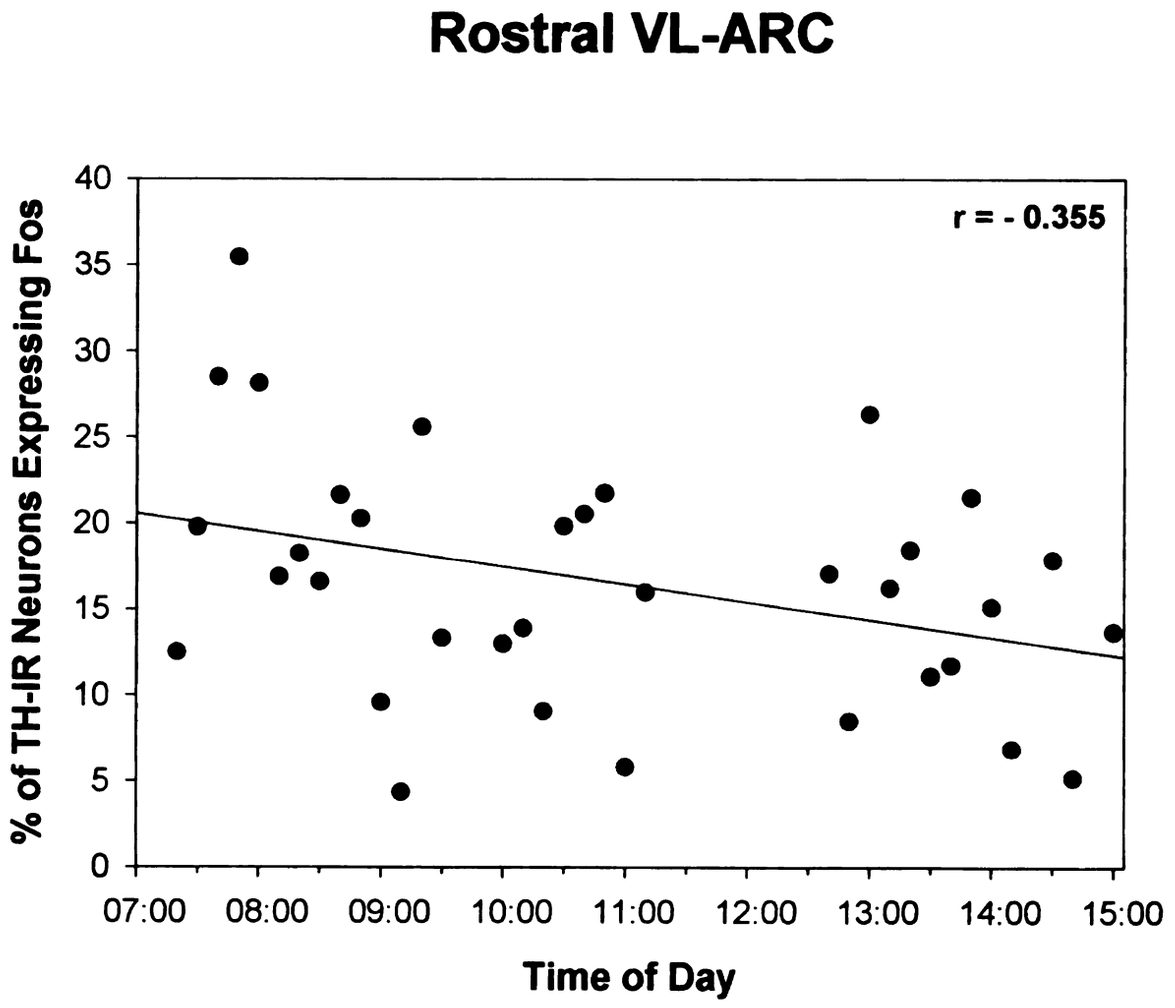

Figure 4.14 Effects of time of day on the percentage of TH-IR neurons expressing Fos of the rostral VL-ARC. Rats were injected with 0.9% saline (1 ml/kg; ip) and controls received no injection. Each circle represents the % of TH-IR neurons expressing Fos from a single animal. Analysis of the data by linear regression indicates that a significant decline in Fos expression occurred ($p<0.05$).

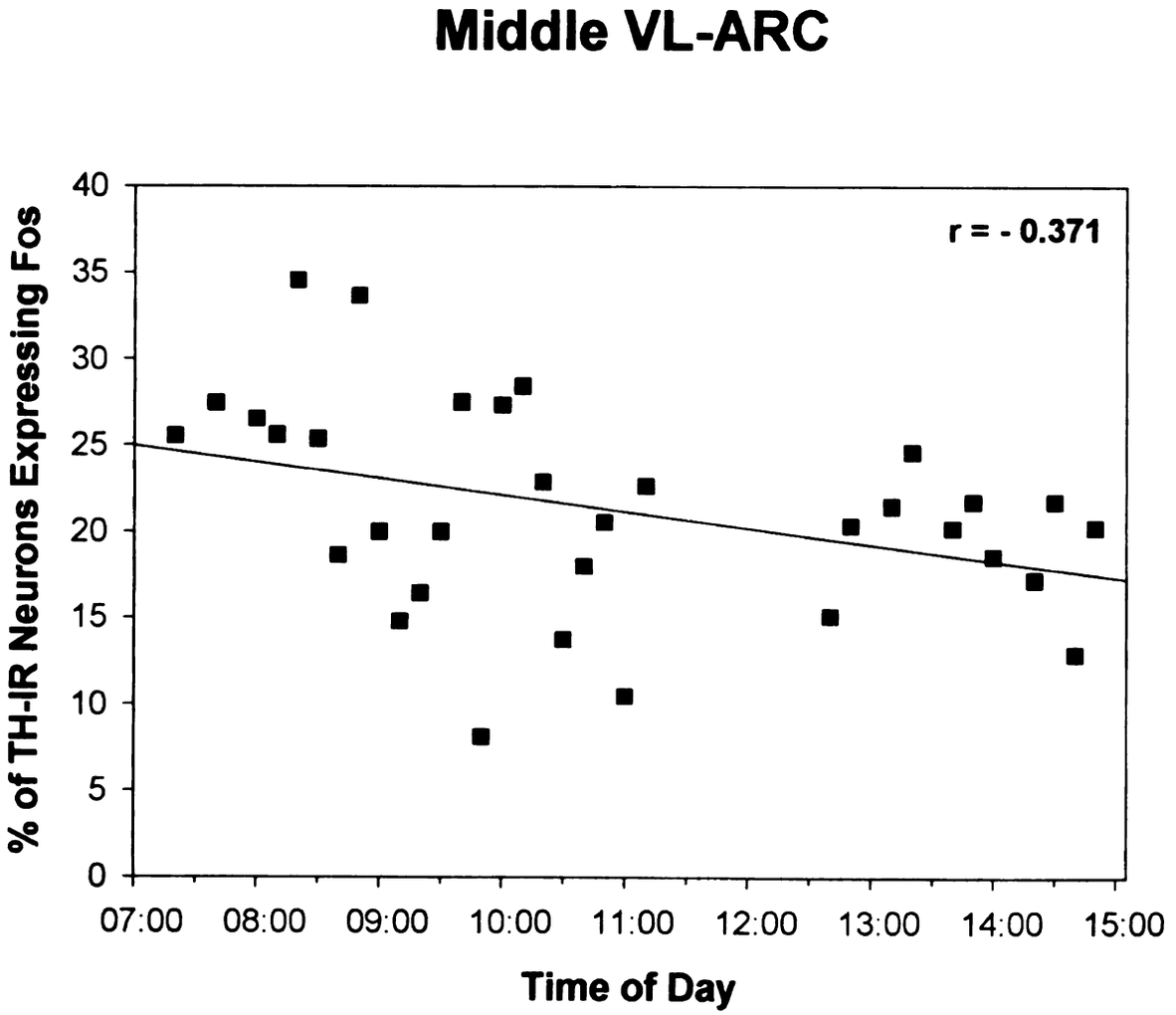

Figure 4.15 Effects of time of day on the percentage of TH-IR neurons expressing Fos of the middle VL-ARC. Rats were injected with 0.9% saline (1 ml/kg; ip) and controls received no injection. Each sqaure represents the % of TH-IR neurons expressing Fos from a single animal. Analysis of the data by linear regression indicates that a significant decline in Fos expression occurred ($p<0.05$).

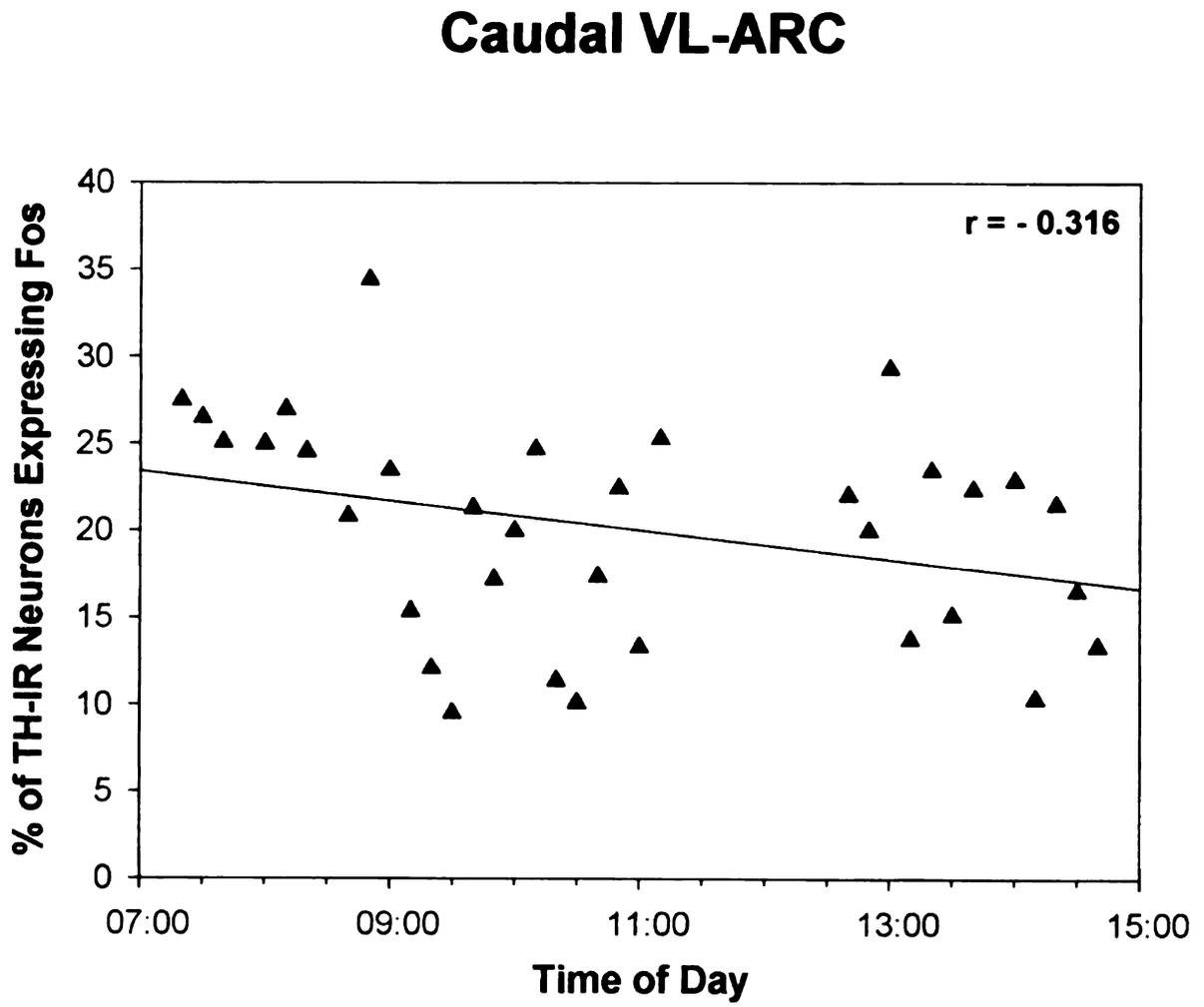

Figure 4.16 Effects of time of day on the percentage of TH-IR neurons expressing Fos of the caudal VL-ARC. Rats were injected with 0.9% saline (1 ml/kg; ip) and controls received no injection. Each triangle represents the % of TH-IR neurons expressing Fos from a single animal.

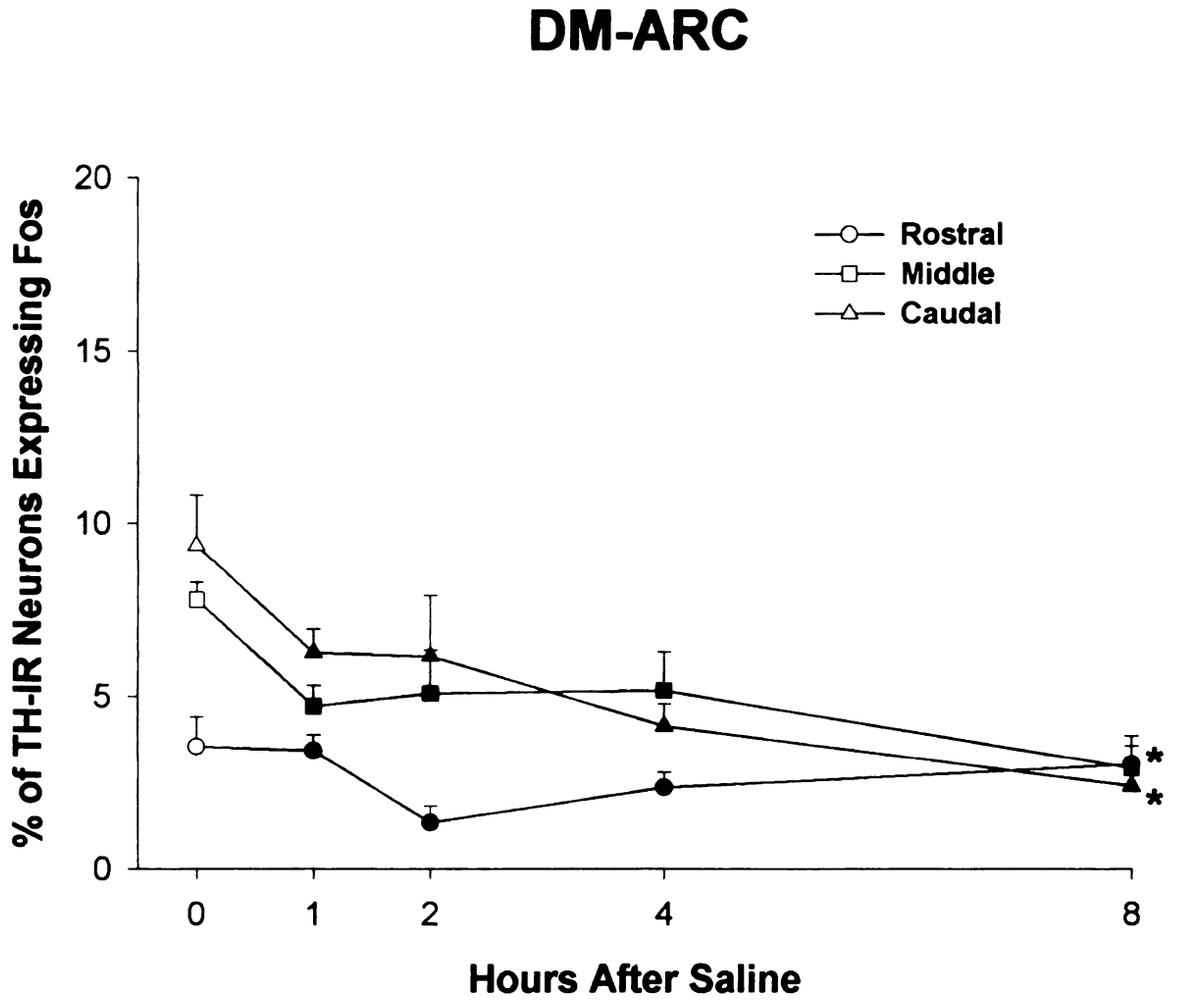

Figure 4.17 Time course effects of saline on the percentage of TH-IR neurons expressing Fos in the rostral (circles), middle (squares), and caudal (triangles) regions of the DM-ARC. Rats were injected with 0.9% saline (filled symbols; 1 ml/kg; ip) and sacrificed 1, 2, 4 or 8 h later. Zero time controls (open symbols) received no injection prior to sacrifice. Symbols represent the means and vertical lines ± 1 SEM from 6-8 animals.

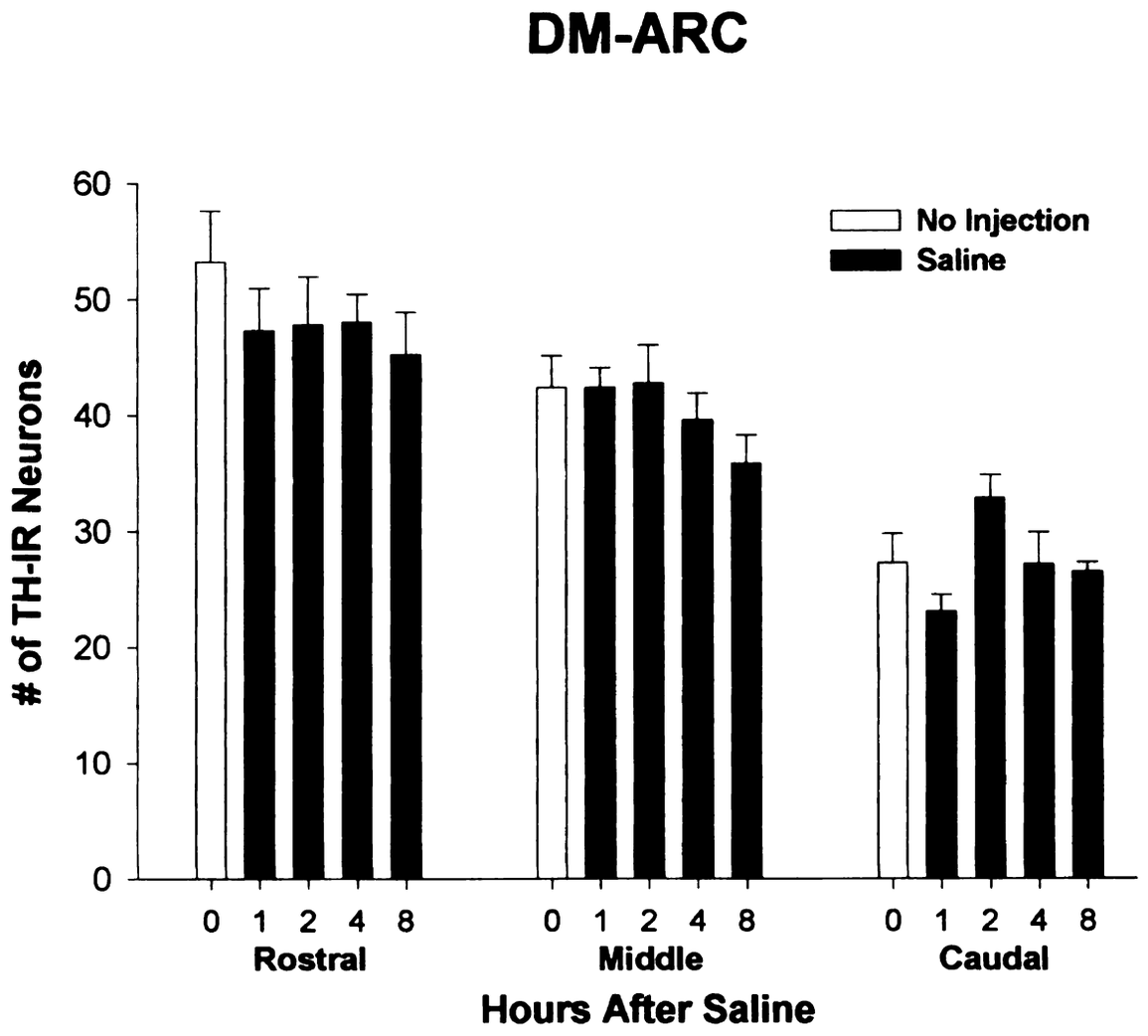

Figure 4.18 Time course effects of saline on the numbers of TH-IR neurons in the rostral, middle, and caudal regions of the DM-ARC. Rats were injected with 0.9% saline (filled columns; 1 ml/kg; ip) and sacrificed 1, 2, 4 or 8 h later. Zero time controls (open columns) received no injection prior to sacrifice. Columns represent the means and vertical lines + 1 SEM from 6-8 animals.

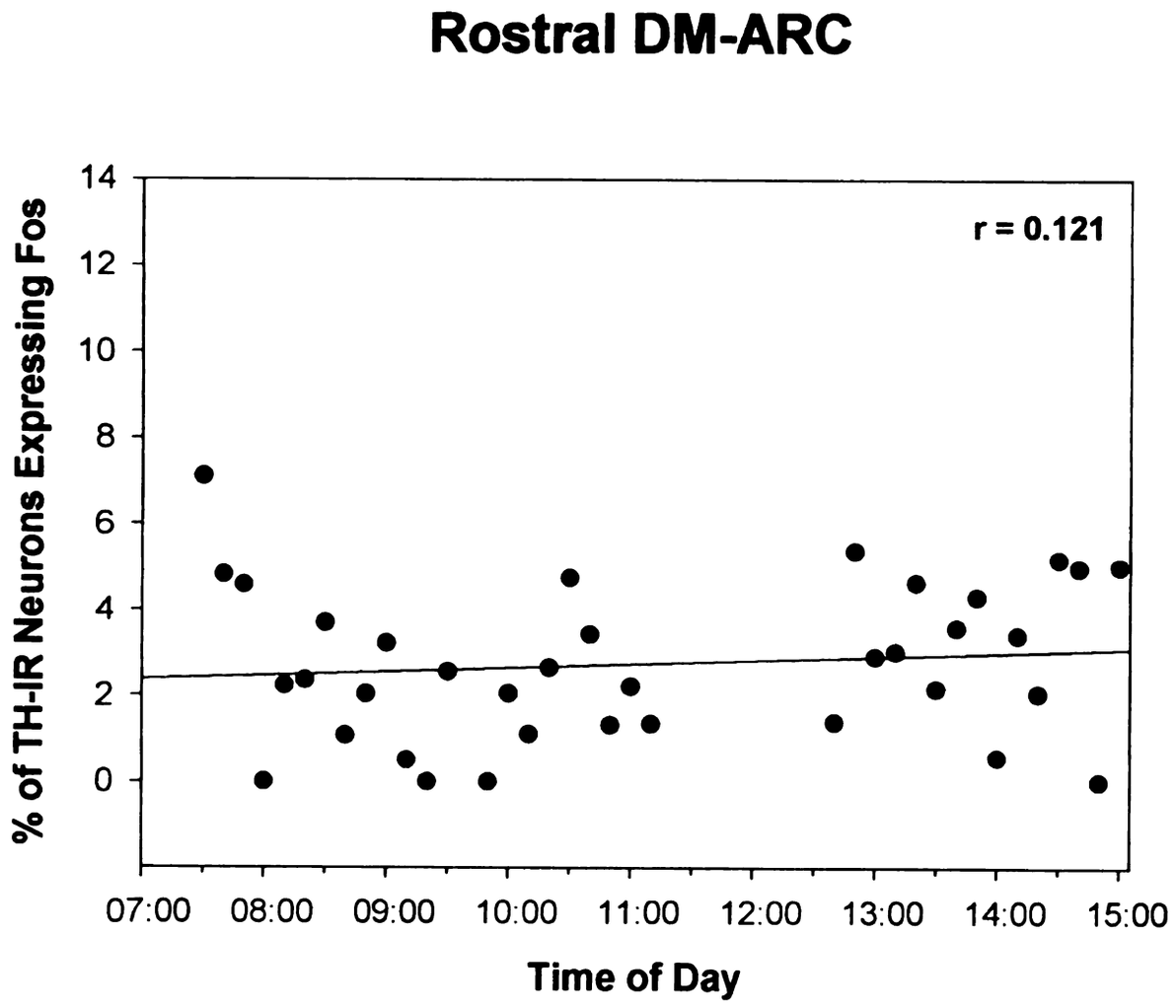

Figure 4.19 Effects of time of day on the percentage of TH-IR neurons expressing Fos of the rostral DM-ARC. Rats were injected with 0.9% saline (1 ml/kg; ip) and controls received no injection. Each circle represents the % of TH-IR neurons expressing Fos from a single animal.

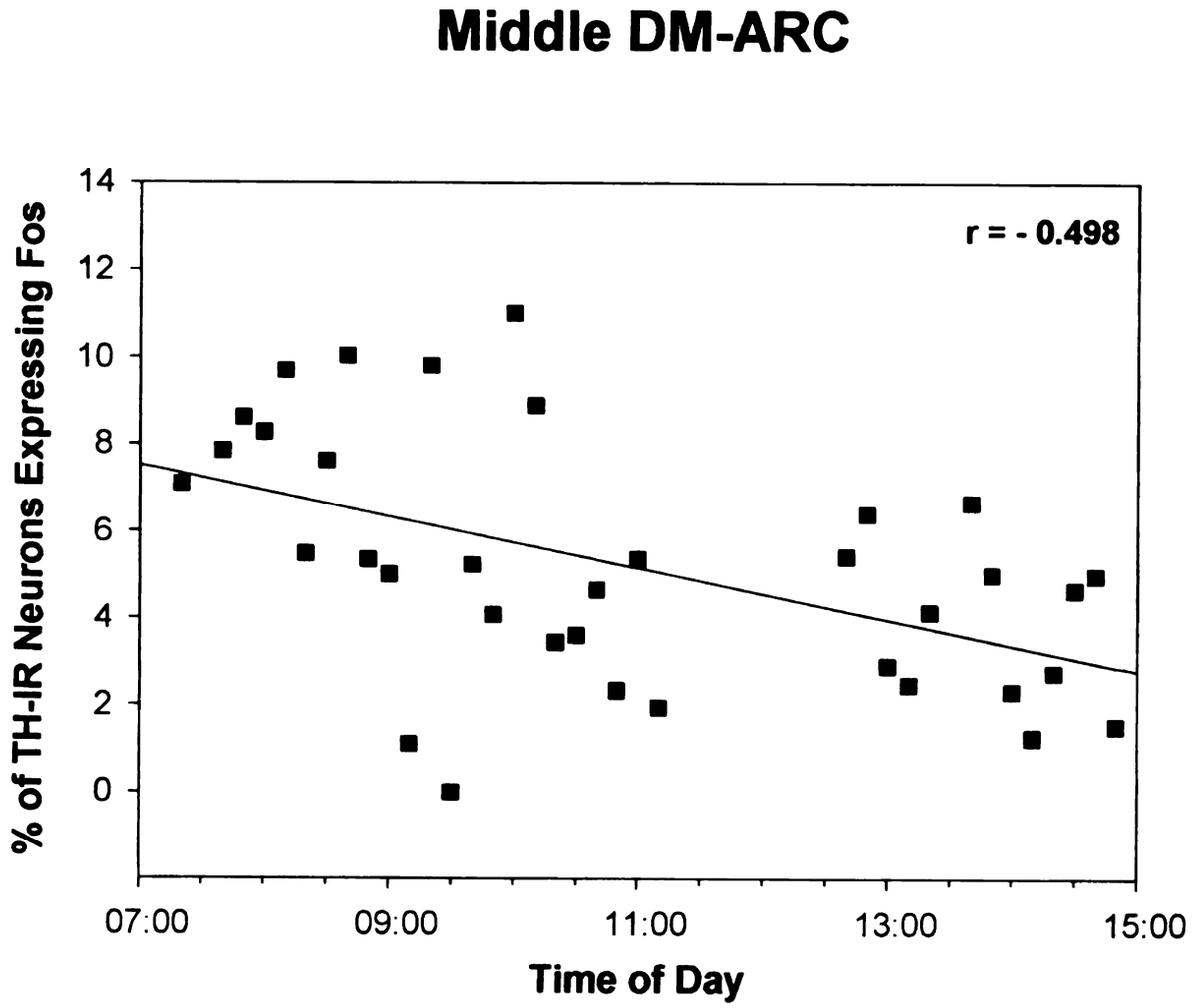

Figure 4.20 Effects of time of day on the percentage of TH-IR neurons expressing Fos of the middle DM-ARC. Rats were injected with 0.9% saline (1 ml/kg; ip) and controls received no injection. Each square represents the % of TH-IR neurons expressing Fos from a single animal. Analysis of the data by linear regression indicates that a significant decline in Fos expression occurred ($p<0.05$).

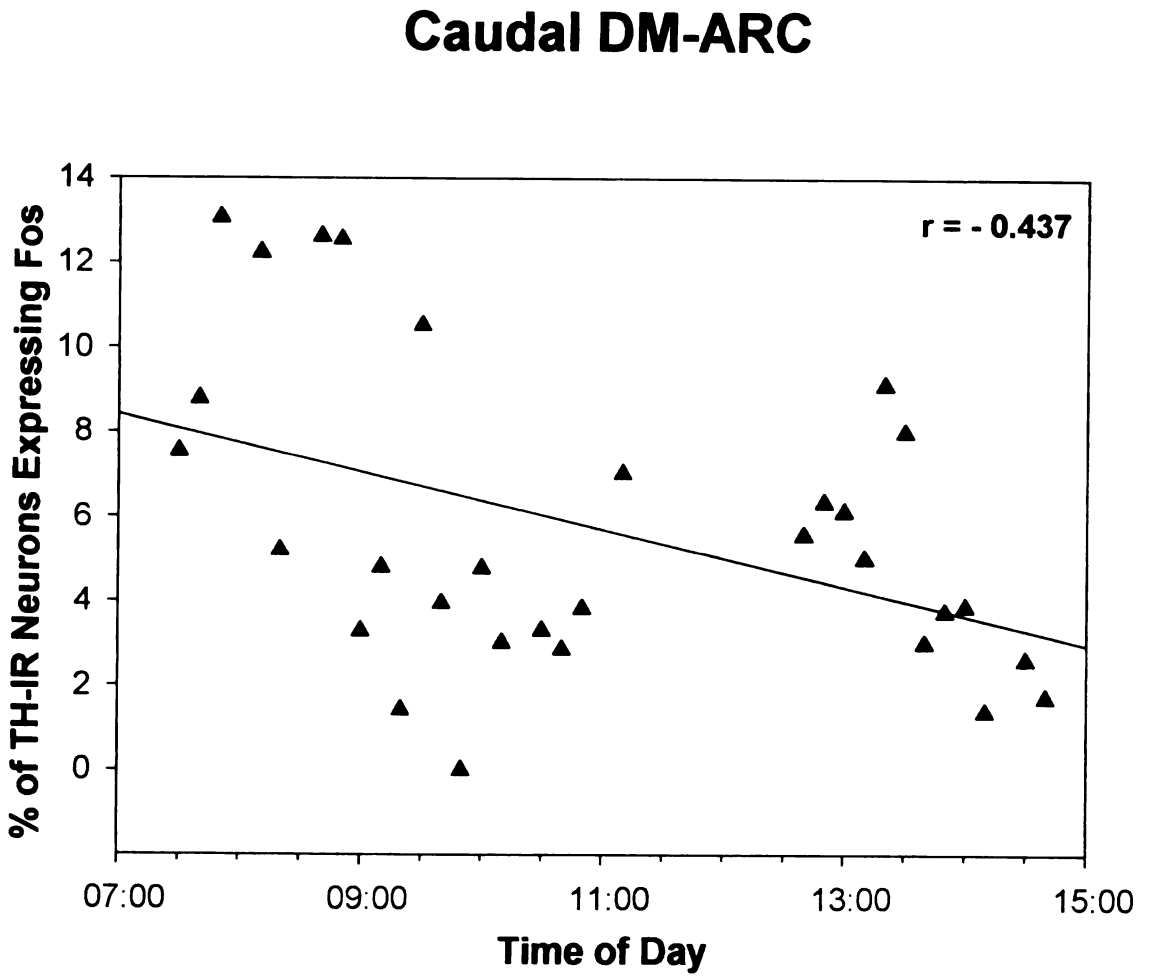

Figure 4.21 Effects of time of day on the percentage of TH-IR neurons expressing Fos of the caudal DM-ARC. Rats were injected with 0.9% saline (1 ml/kg; ip) and controls received no injection. Each triangle represents the % of TH-IR neurons expressing Fos from a single animal. Analysis of the data by linear regression indicates that a significant decline in Fos expression occurred ($p<0.05$).

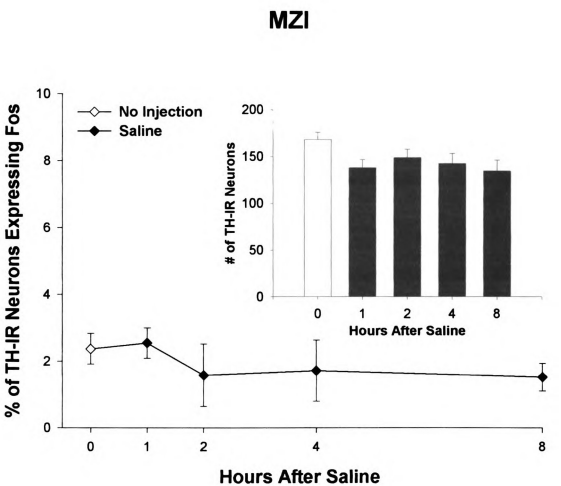

Figure 4.22 Time course effects of saline on the numbers of TH-IR neurons (**Inset**) and the percentage of these neurons expressing Fos in the MZI. Rats were injected with 0.9% saline (filled symbols and columns; 1 ml/kg; ip) and sacrificed 1, 2, 4 or 8 h later. Zero time controls (open symbols and columns) received no injection prior to sacrifice. Symbols and columns represent the means and vertical lines ± 1 SEM from 6-8 animals.

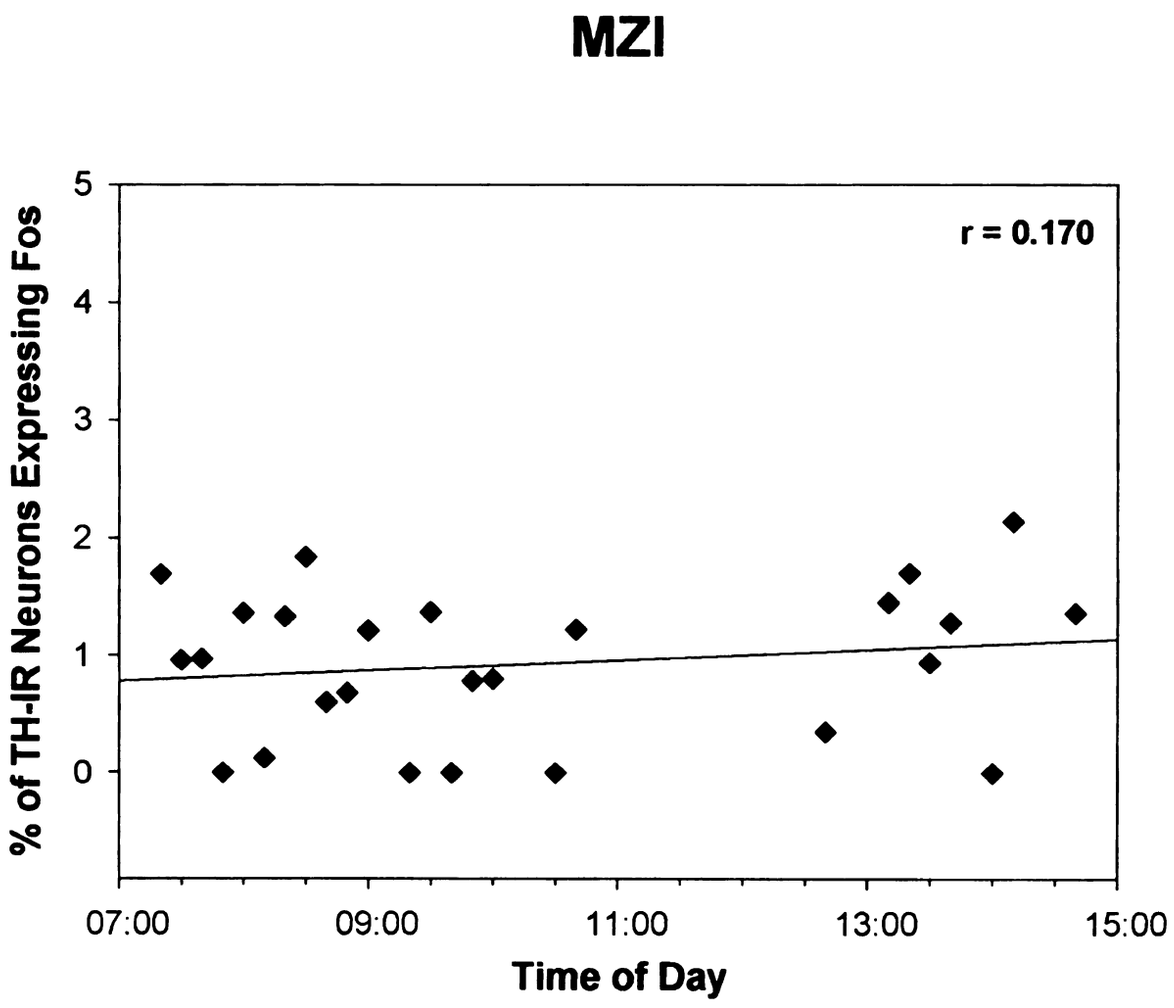

Figure 4.23 Effects of time of day on the percentage of TH-IR neurons expressing Fos of the MZI. Rats were injected with 0.9% saline (1 ml/kg; ip) and controls received no injection. Each diamond represents the % of TH-IR neurons expressing Fos from a single animal.

neurons expressing Fos in the MZI (**Figure 4.22**). The *r* value from the time of day regression analysis in the MZI was 0.170. There was no correlation between Fos expression and time of day (**Figure 4.23**).

Fos protein dimerizes with a Jun protein before binding to the AP-1 site. A common combination of heterodimers is Fos and c-Jun, so if there is an increase in Fos, there could also be an increase in c-Jun. To determine if this is the case, the effects of quinelorane on c-Jun expression in the ARC were examined. **Figure 4.24** illustrates the immunohistochemical labeling of c-Jun-IR nuclei and TH-IR neurons in the ARC. This photomicrograph demonstrates the extremely low numbers of co-localized c-Jun-IR nuclei in TH-IR neurons in the middle ARC 2 h after quinelorane administration. While c-Jun-IR was virtually lacking in the TH-IR neurons, it was present in areas of the VL-ARC devoid of TH-IR neurons. **Figure 4.25** illustrates the time course effects of quinelorane on the percentage of TH-IR neurons expressing c-Jun in the DM-ARC. The percentage of TH-IR neurons containing c-Jun-IR nuclei in the DM-ARC was less than 2% and remained unchanged throughout the time course. There were no changes in the numbers of TH-IR neurons in the DM-ARC (**Figure 4.25**; **Inset**). In the VL-ARC, quinelorane had no effect on the percentage of TH-IR neurons containing c-Jun-IR nuclei at any timepoint (**Figure 4.26**). The percentage of co-localization remained low as seen in the DM-ARC, below 3%. There were no changes in the numbers of TH-IR neurons in the VL-ARC (**Figure 4.26**; **Inset**). Quinelorane had no effect on the number of TH-IR neurons (**Figure 4.27**; **Inset**) or the percentage of those neurons expressing c-Jun (**Figure 4.27**) in the MZI.

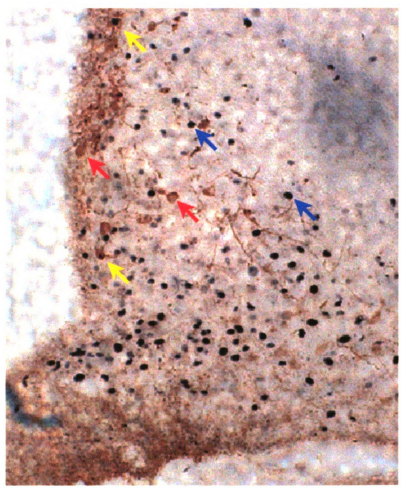

Figure 4.24 Medium power (200x) computer-captured image demonstrating c-Jun-IR nuclei (blue arrows), TH-IR neurons (red arrows) and colocalization of Jun-IR nuclei in TH-IR neurons (yellow arrows) of the middle DM-ARC following administration of quinelorane. Rats were injected with quinelorane (100 μg/kg; ip) and sacrificed 2 h later.

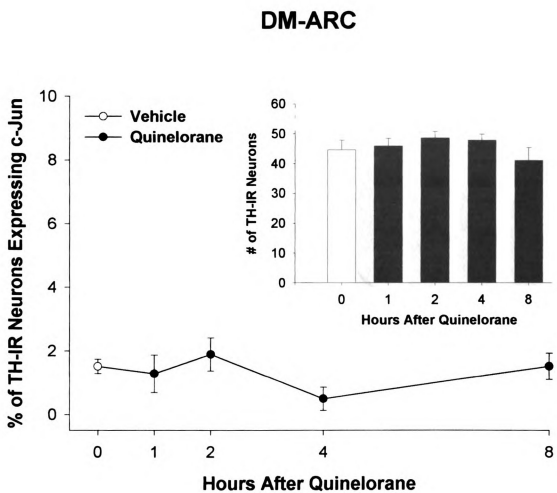

Figure 4.25 Time course effects of quinelorane on the numbers of TH-IR neurons (**Inset**) and the percentage of those neurons expressing c-Jun in the middle region of the DM-ARC. Rats were injected with quinelorane (filled symbols and columns; 100 μg/kg; ip) and sacrificed 1, 2, 4 or 8 h later. Zero time controls (open symbols and columns) were injected with 0.9% saline vehicle (1 ml/kg; ip) and sacrificed 2 h later. Symbols represent the means and vertical lines ± 1 SEM from 6-8 animals.

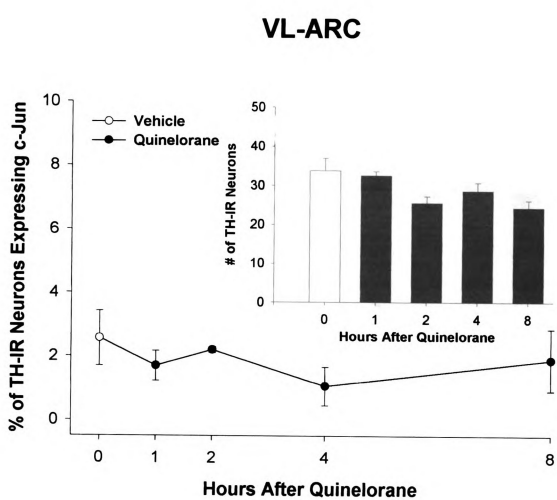

Figure 4.26 Time course effects of quinelorane on the numbers of TH-IR neurons (**Inset**) and the percentage of those neurons expressing c-Jun in the middle region of the VL-ARC. Rats were injected with quinelorane (filled symbols and columns; 100 μg/kg; ip) and sacrificed 1, 2, 4 or 8 h later. Zero times controls (open symbols and columns) were injected with 0.9% saline vehicle (1 ml/kg; ip) and sacrificed 2 h later. Symbols and columns represent the means and vertical lines ± 1 SEM from 6-8 animals.

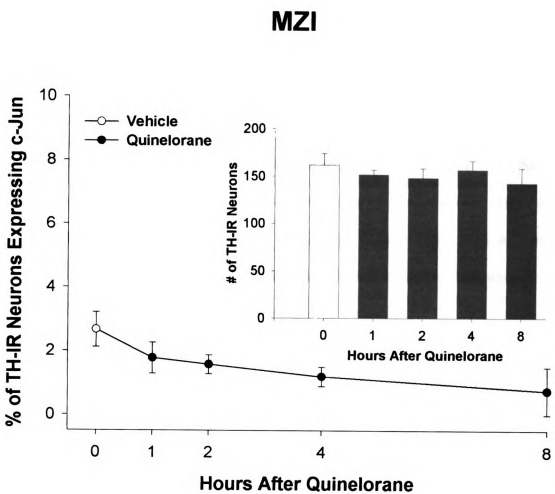

Figure 4.27 Time course effects of quinelorane on the numbers of TH-IR neurons (**Inset**) and the percentage of those neurons expressing c-Jun in the MZI. Rats were injected with quinelorane (filled symbols and columns; 100 μg/kg; ip) and sacrificed 1, 2, 4, or 8 h later. Zero time controls (open symbols and columns) were injected with 0.9% saline vehicle (1 ml/kg; ip) and sacrificed 2 h later. Symbols and columns represent the means and vertical lines ± 1 SEM from 6-8 animals.

Discussion

Quinelorane is a D2 receptor agonist that acutely decreases neuronal activity in the DA neurons of the mesotelencephalic system via action on autoreceptors and long loop neuronal feedback circuits. Interestingly, this agonist has the opposite action on TIDA neurons by increasing their activity via a mechanism that is independent of PRL (Eaton et al., 1993; Durham et al., 1996). The previous chapter demonstrated that the expression of FRA in the DM-ARC correlates with neuronal activity of TIDA nerve terminals in the ME. The aim of the present study was to determine if D2 receptors regulate Fos and c-Jun expression in TIDA neurons located in subdivisions of the rostral, middle, and caudal ARC.

The results from these studies reveal that activation of D2 receptors increases Fos expression in TIDA neurons throughout the rostral-caudal extent of the DM-ARC in a time dependent manner in a fixed population of TH-IR neurons. This increase in Fos is delayed and transitory (peaking at 2 h) compared to the rapid (occurring at 30 min) and prolonged effects (persisting for at least 8 h) of quinelorane on neuronal activity as estimated from neurochemical indices (Eaton et al., 1993). This delay of expression in the DM-ARC is characteristic of the induction of Fos and other immediate early genes. Fos protein has a half life of 90 to 120 min, with maximum levels appearing between 1 and 3 h, gradually disappearing from the nucleus by 4 to 6 h (Sonnenberg et al., 1989; Chan et al., 1993; Kovacs and Sawchenko, 1996). This time course of Fos expression is similar to that seen following PRL stimulation of TIDA neurons.

Exogenous PRL as well as haloperidol administration increases FRA expression in the DM-ARC with a peak response at 3 h (Hentschel et al., 2000).

Raclopride is able to block the stimulatory effect of quinelorane on Fos expression indicating that the actions of quinelorane are mediated through D2 receptors. These results correlate with the findings from neuronal activity studies demonstrating that D2 agonists induce an acute stimulatory response in TIDA neurons and this can be reversed with a D2 receptor antagonist (Eaton et al., 1993; Durham et al., 1997). The lack of effect of D2 receptor blockade on Fos expression in the DM-ARC suggests that D2 receptors do not tonically inhibit Fos expression in these neurons. If TIDA neurons were indeed regulated by presynaptic autoreceptors, one would expect a D2 receptor antagonist to have a stimulatory affect on Fos expression and a D2 agonist to be able to reverse the affects as has been demonstrated in the striatum (Merchant et al., 1994; Rogue and Vincendon, 1992).

The IHDA neurons of the MZI are regulated by DA receptors as are the DA neurons of the mesotelencephalic systems (Lookingland and Moore, 1984). DA agonists and locally applied DA decrease, while DA antagonists increase the activity of IHDA neurons (Lookingland and Moore, 1995; Eaton et al., 1992). If Fos correlates with neuronal activity, then blockade of D2 receptors on IHDA neurons should increase Fos expression. These studies demonstrate that this does occur. While quinelorane has no effect on Fos expression, it reverses the stimulatory effect of raclopride. These results demonstrate that Fos expression is regulated through D2 receptors. This is consistent with *in vitro* studies

performed in cultured TH-IR hypothalamic neurons demonstrating that D2 agonists can reverse stimulated Fos expression (Sim et al., 1994). These receptors are most likely located on IHDA cell bodies and/or dendrites as opposed to axon terminals. Antidromic stimulation of hypothalamic neurons does not induce immediate early gene expression for it bypasses the second messenger system necessary to induce them (Icard-Liepkalns et al., 1992; Luckman et al., 1994; Hoffman and Murphy, 2000). Thus, since Fos can be induced through D2 receptors, the receptors must be somatodentritic.

In the VL-ARC, the percentage of Fos levels in TH-IR neurons in the control group is higher than the DM-ARC (20% vs 5% respectively) suggesting that greater numbers of these neurons are tonically active. While quinelorane had no stimulatory effect on Fos expression in the VL-ARC at 2 h as in the DM-ARC, there was a decrease after 4 h. These results in the VL-ARC from the raclopride study demonstrated no effect at 2 h at a time when DM-ARC TH-IR neurons are activated suggesting that these neurons are not regulated through D2 receptors. This is in contrast to the specific effects of PRL on the TH-IR neurons of the VL-ARC.

PRL increases FRA levels in the VL-ARC in a transient pattern at 3 h (Hentschel et al., 2000) similar to that seen in the DM-ARC following quinelorane administration. The VL-ARC contains PRL receptors (Bakowska and Morrell, 1997) and thus Fos (and perhaps long term gene) expression may be regulated by PRL as opposed to DA receptors. However, unlike the neurons of the DM-ARC, those of the VL-ARC do not produce DD, thus only DOPA is synthesized

and released (Komori et al., 1991; Meister et al., 1988; Balan et al., 2000). Their function has not been completely elucidated, but evidence indicates that DOPA may be released and taken up and converted to DA in the ME or at the anterior pituitary (Meister et al., 1988; Misu et al., 1996). DD has been demonstrated in the walls of blood vessels, so it is possible that DOPA released into the portal blood system is converted to DA and can act at the anterior pituitary (Meister et al., 1988). These "DOPA-ergic" neurons co-express TH and neuropeptides (Chronwall 1985; Ershov et al., 2002) and DOPA may contribute to the regulation of peptide turnover (Everitt et al., 1996).

The decrease in Fos expression in the VL-ARC may be due to other factors such as stress (Lookingland et al., 1990; Campeau et al 1991; Persico et al., 1993) or circadian rhythms (Lerant and Freeman, 1997; Yang et al., 1999). Restraint stress has been demonstrated to decrease TIDA neuronal activity in female rats (Lookingland et al 1990) while handling of rats for the first time (Campeau et al., 1991) or acute intraperitoneal injection of saline results in a strong induction of Fos and FRA in the hypothalamus after 2 h (Ryabinin et al., 1999). There was no effect on Fos expression in the VL-ARC at any timepoint following the injection of saline suggesting that stress of injection or handling has no effect on Fos expression in TH-IR "DOPA-ergic" neurons in the VL-ARC.

A time of day analysis was also carried out to determine if there is a circadian rhythm influence on the expression of Fos in the ARC. There is evidence of circadian rhythm in TIDA neuronal activity in female rats. An endogenous rhythm exists in all adult female rats and is estrogen dependent.

There is a decrease in TIDA neuronal activity (Mai et al., 1994) as well as in FRA expression (Lerant and Freeman, 1997) in the late afternoon of proestrus which corresponds with an afternoon PRL surge. There are no similar studies examining activity of TIDA neurons in males. Interestingly, time of day analysis revealed a correlation with the percent of Fos expression and the time the rats were sacrificed in the middle and caudal portions of the DM-ARC as well as the rostral and middle portions of the VL-ARC. As the day progresses, Fos expression decreases in TIDA neurons, hinting at a circadian rhythm; however, a 24 h time course would need to be performed to make any further conclusions. This would be unique for male rats for previous studies have not demonstrated a circadian rhythm in the ARC (Pan, 1996).

In addition to Fos, Jun proteins can be induced following specific stimulation (Herdegen and Leah, 1998). Jun proteins are a family of immediate early genes consisting of c-Jun, JunB and JunD. Studying Jun proteins in conjunction with Fos appears to be a logical choice, for these two immediate early genes form heterodimers and bind to the AP-1 site on the TH gene promoter. Fos can regulate the transcriptional activity and increase transactivating potential of c-Jun. It has a similar half-life to c-Fos (90-120 min). *c-jun* mRNA and Jun proteins have been detected throughout the brain (Rogue and Vincendon, 1992; Hughes and Dragunow, 1995). In the hypothalamus, c-Jun–IR nuclei have been located in LHRH and magnocellular neurons and are co-expressed with c-Fos following such stimuli as proestrous LH surge and hypertonic saline (Hoffman et al., 1993).

Interestingly, however, the activation of D2 receptors did not result in an increase of c-Jun at any time point. The first possibility is that c-Jun is not the Jun protein that is co-expressed with Fos in TIDA neurons following D2 receptor activation. Indeed, c-Jun-IR nuclei were identified in the ARC, but the nuclei were located mostly in the parvocellular region of the ARC and in the medial portion of the VL-ARC where TH-IR neurons are the fewest, if not absent. Fos may form a heterodimer with JunB in TIDA neurons. Though thought to be less stable than c-Jun, JunB can be rapidly induced and has a half-life similar to c-Jun. Another possible explanation is that not all stimuli have the same effect on Fos and Jun family members. c-Jun is induced by serum, phorbol ester (which stimulates the protein kinase C pathway), growth factors and cytokines (such as platelet derived growth factor, epithelial growth factor, nerve growth factor, fibroblast growth factor), but not by increases of protein kinase A via membrane depolarization or stimulation of nicotinic receptors in PC12 cells. All of these stimuli, however, increase c-Fos and JunB expression (Hughes and Dragunow, 1995; Herdegen 2000). DA receptors are linked to cAMP and thus to protein kinase A. Keeping this in mind, it is conceivable that c-Jun would not be induced following quinelorane administration, and the Jun protein that may dimerize with Fos could be JunB.

Taken together the results presented in this chapter reveal that D2 receptors regulate Fos, but not c-Jun, expression in TIDA neurons throughout the rostral-caudal extent of the DM-ARC. These results correspond with the neurochemical studies examining the nerve terminal activity of the ME following

D2 receptor activation. Unlike the DM-ARC, however, Fos expression in TH-IR neurons in the VL-ARC is not regulated by D2 receptors.

CHAPTER FIVE

THE ROLE OF KAPPA OPIOID RECEPTORS IN D2 RECEPTOR REGULATION OF FOS EXPRESSION IN TH-IR NEURONS IN SUBDIVISIONS OF THE ARCUATE NUCLEUS

Introduction

As described in Chapter Four, immediate early gene expression in TIDA neurons can be modulated by a D2 receptor-mediated mechanism. This is evidenced by the finding that activation of D2 receptors increases the expression of Fos protein in the cell bodies of TIDA neurons in the DM-ARC. It is unlikely that this effect is due to a direct action on TIDA neurons since D2 receptors are inhibitory, leading to decreases in cAMP and Ca^{+2} conductance as well as increases in K^{+} conductance within target neurons (Vallone et al., 2000). A stimulatory response of TIDA neurons following activation of D2 receptors is not consistent with the response of neurons regulated by inhibitory autoreceptors located on DA terminals, cell bodies and dendrites.

Instead, D2 receptor-induced stimulation of TIDA neuronal activity is mediated through a neuronal system originating outside the mediobasal hypothalamus (Durham et al., 1996). This was demonstrated through studies involving mediobasal hypothalamic deafferentation surgeries. Those animals receiving the deafferentation surgery failed to demonstrate an increase in TIDA neuronal activity following the activation of D2 receptors, indicating that the D2 receptors must be located outside the mediobasal hypothalamus. There were two possibilities to explain this; 1) activation of a quiescent stimulatory neuronal system, or 2) suppression of a tonically active inhibitory neuronal system. Due to

their inhibitory effects on target cells, it is more likely that D2 receptors would "turn off" an already active system as opposed to triggering a stimulatory system to "turn on".

Dynorphin is an endogenous opioid neuropeptide highly selective for kappa opioid receptors (Chavkin et al., 1982) which exerts an inhibitory action on hypothalamic neurons (MacMillin and Clark, 1983; Lin and Pan, 1995). Several lines of pharmacological evidence suggest that the stimulatory effects of D2 receptors are mediated through the inhibition of tonically active dynorphin neurons that inhibit TIDA neurons via kappa opioid receptors. Blockade of kappa receptors with the antagonist nor-BNI, or immunoneutralization of endogenous dynorphin, both increase TIDA neuronal activity like the D2 agonist quinelorane (Manzanares et al., 1992a; Manzanares et al., 1992b; Durham et al., 1996). When co-administered, nor-BNI and quinelorane have no additive effect, suggesting they share a common pathway (Durham et al., 1996). In agreement, U50-488, a kappa receptor agonist, reverses the stimulatory effect of quinelorane on TIDA neurons (Durham et al., 1996). Taken together, these studies imply that tonically active inhibitory dynorphin neurons participate in DA receptor regulation of TIDA neurons.

While these studies do not prove that these dynorphin neurons are located within the mediobasal hypothalamus, microscopic analysis and immunoassay studies lead one to believe that this is the case. Dynorphin-IR and mRNA are located in the ARC and outside the mediobasal hypothalamus in the ventromedial hypothalamic nucleus (Zamir et al., 1983; Zamir et al., 1984;

Durham, 1999). When D2 receptors are stimulated with quinelorane, expression of dynorphin mRNA in the ARC is decreased, whereas the mRNA in the ventromedial hypothalamic nucleus is not (Durham, 1999). The downstream effect of this would be a decrease in synthesis and possibly release of dynorphin, which is consistent with the view that dynorphin neurons located in the ARC are selectively inhibited by D2 receptors via an unknown upstream neuron. Kappa receptor mRNA as well as binding sites are located in the ARC, indicating that not only do neurons produce the receptor mRNA, but they also express these receptors (Mansour et al., 1988; Mansour et al., 1995). Though these studies did not chemically identify the neurons with kappa receptors, other studies examined TIDA neurons specifically. Dynorphin terminals interact with and are concentrated around TIDA neurons, and electron microscopy has revealed synaptic vesicles and postsynaptic thickening at these terminals (Fitzsimmons et al., 1992). **Figure 5.1** illustrates this proposed neuronal pathway under basal conditions.

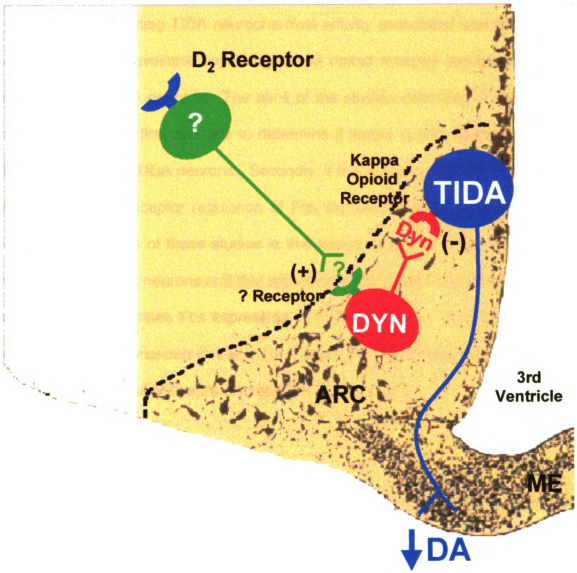

Figure 5.1 Frontal section schematic depicting the proposed neuronal pathway that mediates the stimulatory effects of D2 receptors on TIDA neuronal activity. Under basal conditions, a chemically unidentified neuron (depicted in green) located outside the mediobasal hypothalamus tonically stimulates dynorphin neurons located in the ARC. Dynorphin neurons in turn release dynorphin that acts at the kappa opioid receptor located on TIDA neurons to tonically inhibit DA release. Abbreviations: ?, unknown neuron/neurotransmitter/receptor; ARC, arcuate nucleus; DA, dopamine; DYN, dynorphin; ME, median eminence.

While there are several studies on the role of dynorphin and kappa opioid receptors in regulating TIDA neurochemical activity associated with DA release, no information is available regarding kappa opioid receptor regulation of gene expression in TIDA neurons. The aims of the studies described in this chapter are two fold. The first aim was to determine if kappa opioid receptors regulate Fos expression in TIDA neurons. Secondly, if this is the case, then what role do they play in D2 receptor regulation of Fos expression in TIDA neurons. The working hypothesis of these studies is that kappa receptors tonically inhibit Fos expression in TIDA neurons and that activation of D2 receptors inhibits dynorphin neurons and stimulates Fos expression in TIDA neurons. For comparison, the effects on Fos expression in the "DOPA-ergic" neurons in the VL-ARC and the IHDA neurons of the MZI were also studied.

Materials and Methods

Gonadally intact male rats were used in these experiments. Care and handling of the rats was carried out as described in the **Materials and Methods** in Chapter 2. Following appropriate treatments, rats were anesthetized with Equithesin and perfused with 4% paraformaldehyde. Brains were removed and sectioned as described in **Materials and Methods** in Chapter 2. The identification of TH-IR neurons using alkaline phosphatase and Fos-IR using nickel-intensified diaminobenzidine in the ARC and MZI was carried out using immunohistochemical procedures in **Materials and Methods** in Chapter 2. The ARC sections were sorted into rostral, middle and caudal regions and then

visually partitioned into DM-ARC and VL-ARC. Fos was localized with anti-Fos antiserum generated against residues 4 to 17 of human *fos* (Oncogene). The dilution used was 1:10,000 in TBS/TX containing 1.5% normal donkey serum. TH was detected using anti-TH serum (Chemicon) generated against rat adrenal medullary tumor tissue. The final dilution was 1:20,000 in TBS/TX containing 1.5% normal goat serum.

Results

Photomicrographs in **Figure 5.2** illustrate Fos expression in TH-IR neurons of middle DM-ARC 2 h after injection of either vehicle (**Top Panel**) or nor-BNI (**Bottom Panel**) to male rats. These images show an increase in colocalization of Fos-IR nuclei in TH-IR neurons following nor-BNI administration. **Figure 5.3** illustrates the time course effects of nor-BNI in the percentage of TH-IR neurons expressing Fos-IR nuclei in the DM-ARC. Nor-BNI significantly increased Fos expression in a time dependent manner reaching maximum levels at 2 h and returning to basal levels by 8 h in the rostral, middle, and caudal regions of the DM-ARC. There was a decrease in the numbers of TH-IR neurons throughout the rostrocaudal extent of the DM-ARC; however, there were no changes in the numbers of neurons within each region of the DM-ARC at any time point following nor-BNI (**Figure 5.4**). In contrast, in the VL-ARC nor-BNI had no effect on the percentage of TH-IR neurons containing Fos-IR nuclei (**Figure 5.5**). There was an increasing gradient in the numbers of TH-IR neurons in vehicle-treated rats that extended caudally in the VL-ARC. As in the DM-ARC,

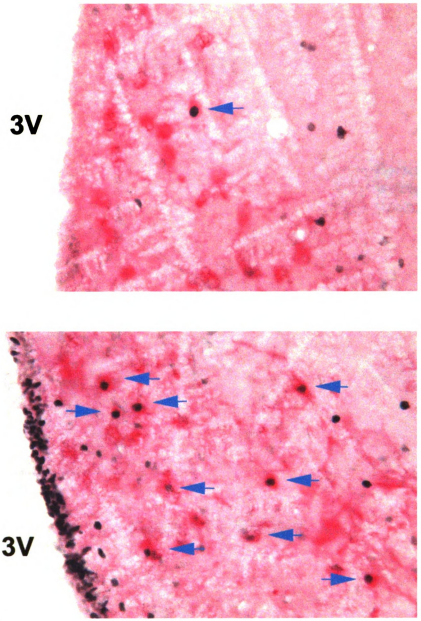

Figure 5.2 High power (400x) computer-captured images demonstrating increased Fos expression in TH-IR neurons of the DM-ARC 2 h following administration of nor-BNI. Rats were injected with either vehicle (**Top Panel**; ddH_2O; 3 μl/rat; icv) or nor-BNI (**Bottom Panel**; 12.5 μg/rat; icv) and sacrificed 2 h later. Arrows represent colocalization of pink TH-IR neurons containing black Fos-IR nuclei. 3V, third ventricle.

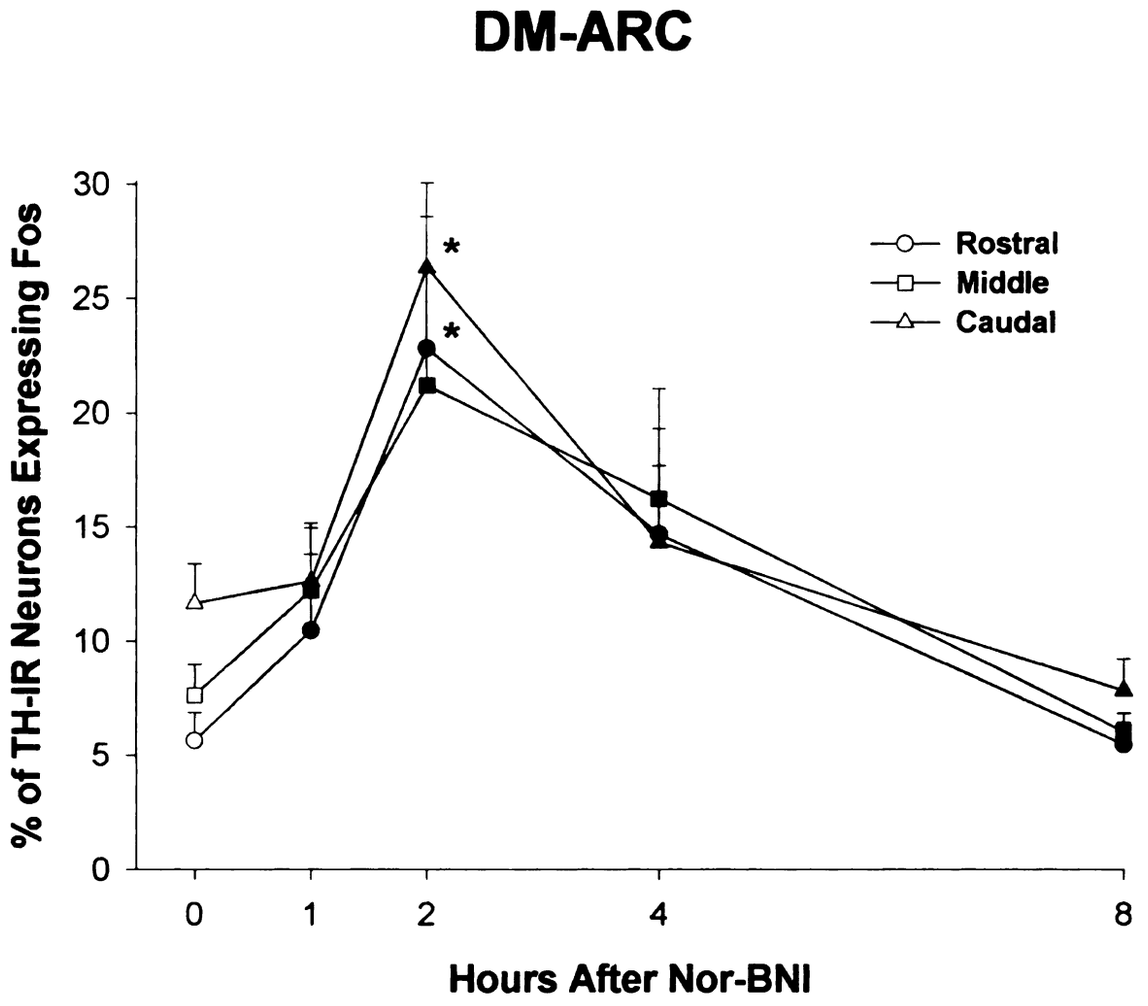

Figure 5.3 Time course effects of nor-BNI on the percentage of TH-IR neurons expressing Fos in the rostral (circles), middle (squares), and caudal (triangles) regions of the DM-ARC. Rats were injected with nor-BNI (filled symbols; 12.5 μg/rat; icv) and sacrificed 1, 2, 4, or 8 h later. Zero time controls (open symbols) were injected with ddH_2O vehicle (3 μl/rat; icv) and sacrificed 2 h later. Symbols represent the means and vertical lines + 1 SEM from 6-8 animals. *, Values for nor-BNI-treated rats that are significantly different ($p<0.05$) from vehicle-treated controls.

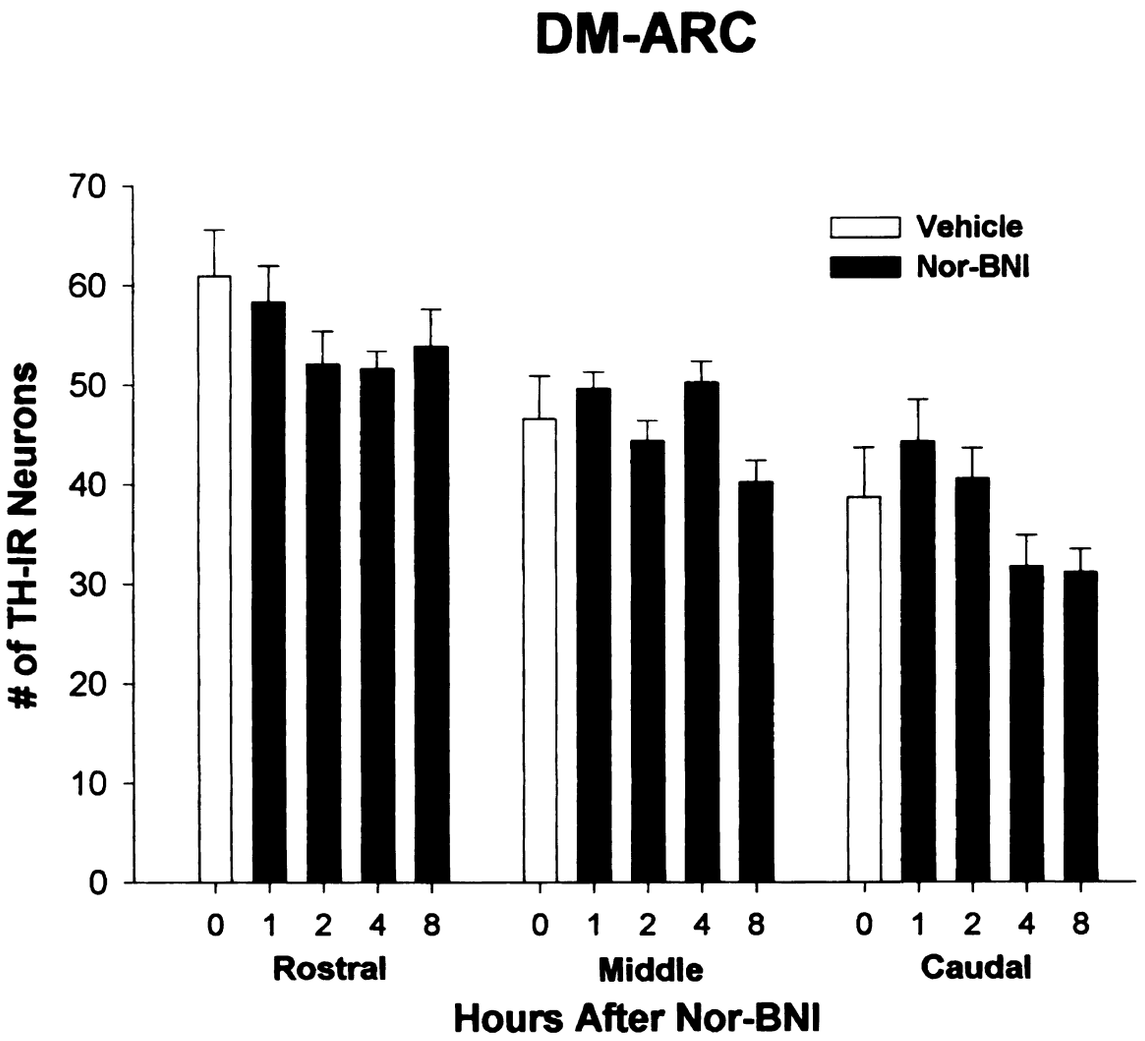

Figure 5.4 Time course effects of nor-BNI on the numbers of TH-IR neurons in the rostral, middle, and caudal regions of the DM-ARC. Rats were injected with nor-BNI (filled columns; 12.5 μg/rat; icv) and sacrificed 1, 2, 4, or 8 h later. Zero time controls (open columns) were injected with ddH_2O vehicle (3 μl/rat; icv) and sacrificed 2 h later. Columns represent the means and vertical lines + 1 SEM from 6-8 animals.

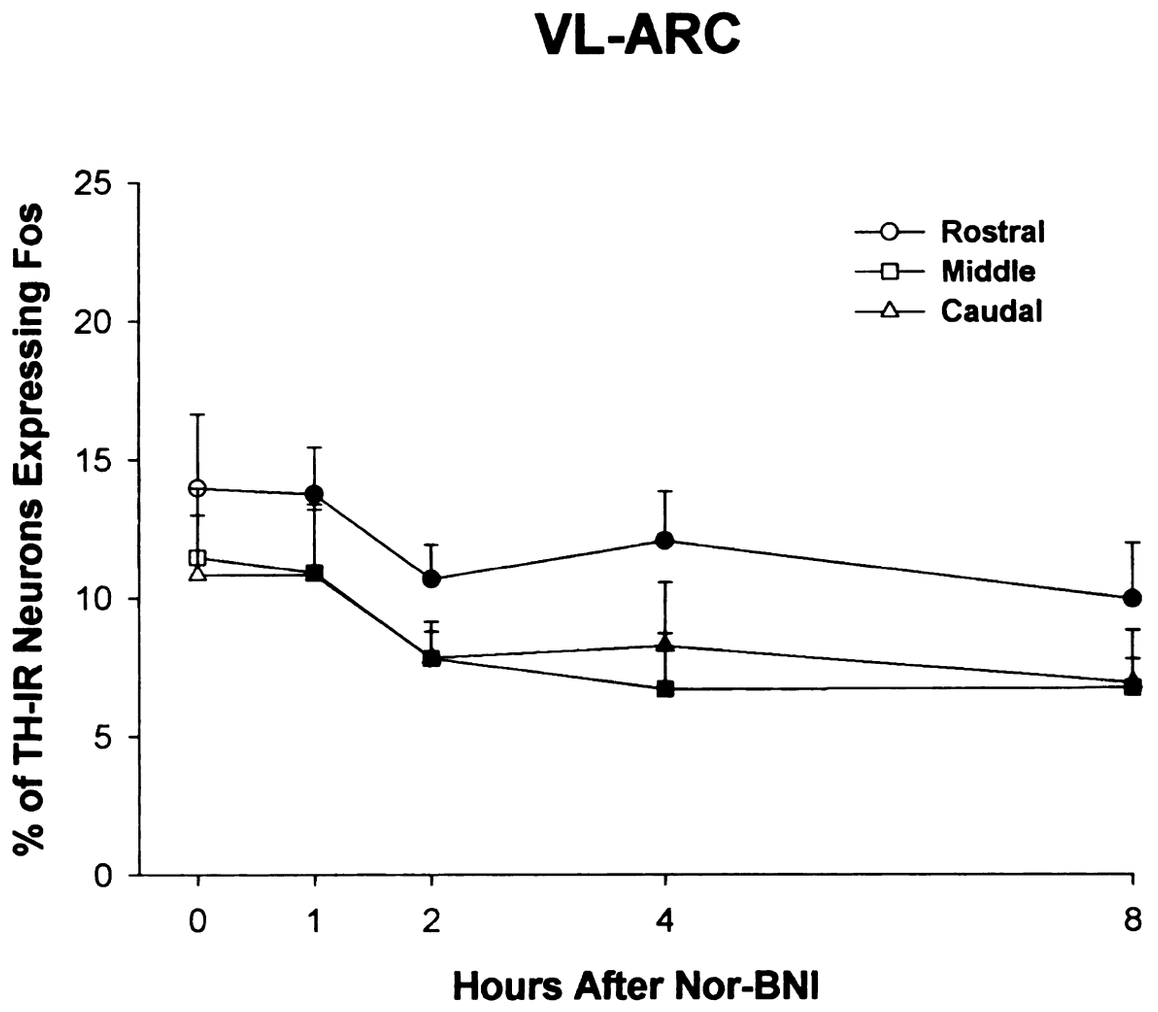

Figure 5.5 Time course effects of nor-BNI on the percentage of TH-IR neurons expressing Fos in the rostral (circles), middle (squares), and caudal (triangles) regions of the VL-ARC. Rats were injected with nor-BNI (filled symbols; 12.5 μg/rat; icv) and sacrificed 1, 2, 4, or 8 h later. Zero time controls (open symbols) were injected with ddH_2O vehicle (3 μl/rat; icv) and sacrificed 2 h later. Symbols represent the means and vertical lines + 1 SEM from 6-8 animals.

there were no changes in the numbers of TH-IR neurons at any time point within each region of the VL-ARC following nor-BNI administration (**Figure 5.6**). In the MZI, nor-BNI had no effect on the numbers of TH-IR neurons (**Figure 5.7; Bottom Panel**) or the percentage of those containing Fos-IR nuclei (**Figure 5.7; Top Panel**).

To determine if the effects of nor-BNI on Fos expression were mediated through kappa opioid receptors, a study was carried out using the kappa receptor agonist U50-488. Activation of kappa opioid receptors had no effect *per se*, but reversed the stimulatory effects of nor-BNI on Fos-IR nuclei throughout the rostrocaudal extent of the DM-ARC (**Figure 5.8**). There were no changes in the numbers of TH-IR neurons following U50-488 or nor-BNI administration (**Figure 5.9**). In the VL-ARC, U50-488 significantly decreased the percentage of TH-IR neurons containing Fos-IR nuclei and this effect was blocked by nor-BNI (**Figure 5.10**). Nor-BNI alone had no effect on the percentage of the TH-IR neurons containing Fos-IR nuclei in the VL-ARC. There were no changes in the numbers of TH-IR neurons in the VL-ARC following administration of either U50-488 or nor-BNI (**Figure 5.11**). In the MZI, neither nor-BNI nor U50-488 had any effect on the numbers of TH-IR neurons (**Figure 5.12; Bottom Panel**) or the percentage of those neurons containing Fos-IR nuclei (**Figure 5.12; Top Panel**).

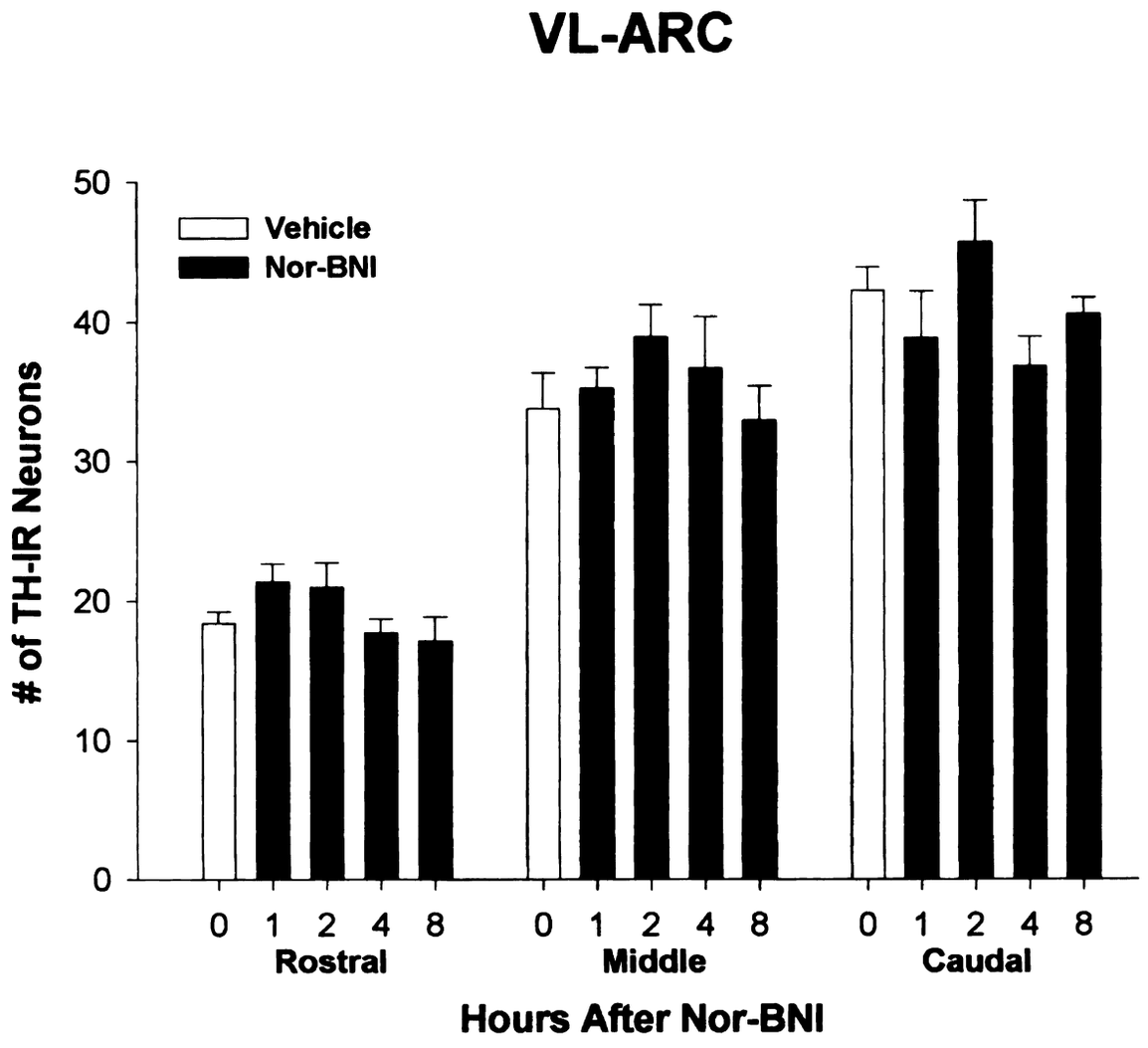

Figure 5.6 Time course effects of nor-BNI on the numbers of TH-IR neurons in the rostral, middle, and caudal regions of the VL-ARC. Rats were injected with nor-BNI (filled columns; 12.5 μg/rat; icv) and sacrificed 1, 2, 4, or 8 h later. Zero time controls (open columns) were injected with ddH_2O vehicle (3 μl/rat; icv) and sacrificed 2 h later. Columns represent the means and vertical lines + 1 SEM from 6-8 animals.

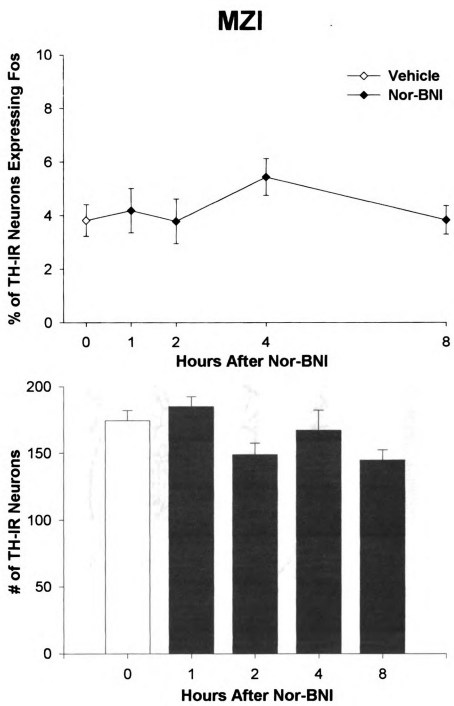

Figure 5.7 Time course effects of nor-BNI on the numbers of TH-IR neurons (**Bottom Panel**) and the percentage of these neurons expressing Fos (**Top Panel**) in the MZI. Rats were injected with nor-BNI (filled symbols and columns; 12.5 μg/rat; icv) and sacrificed 1, 2, 4, or 8 h later. Zero time controls (open symbols and columns) were injected with ddH_2O vehicle (3 μl/rat; icv) and sacrificed 2 h later. Symbols and columns represent the means and vertical lines ± 1 SEM from 6-8 animals.

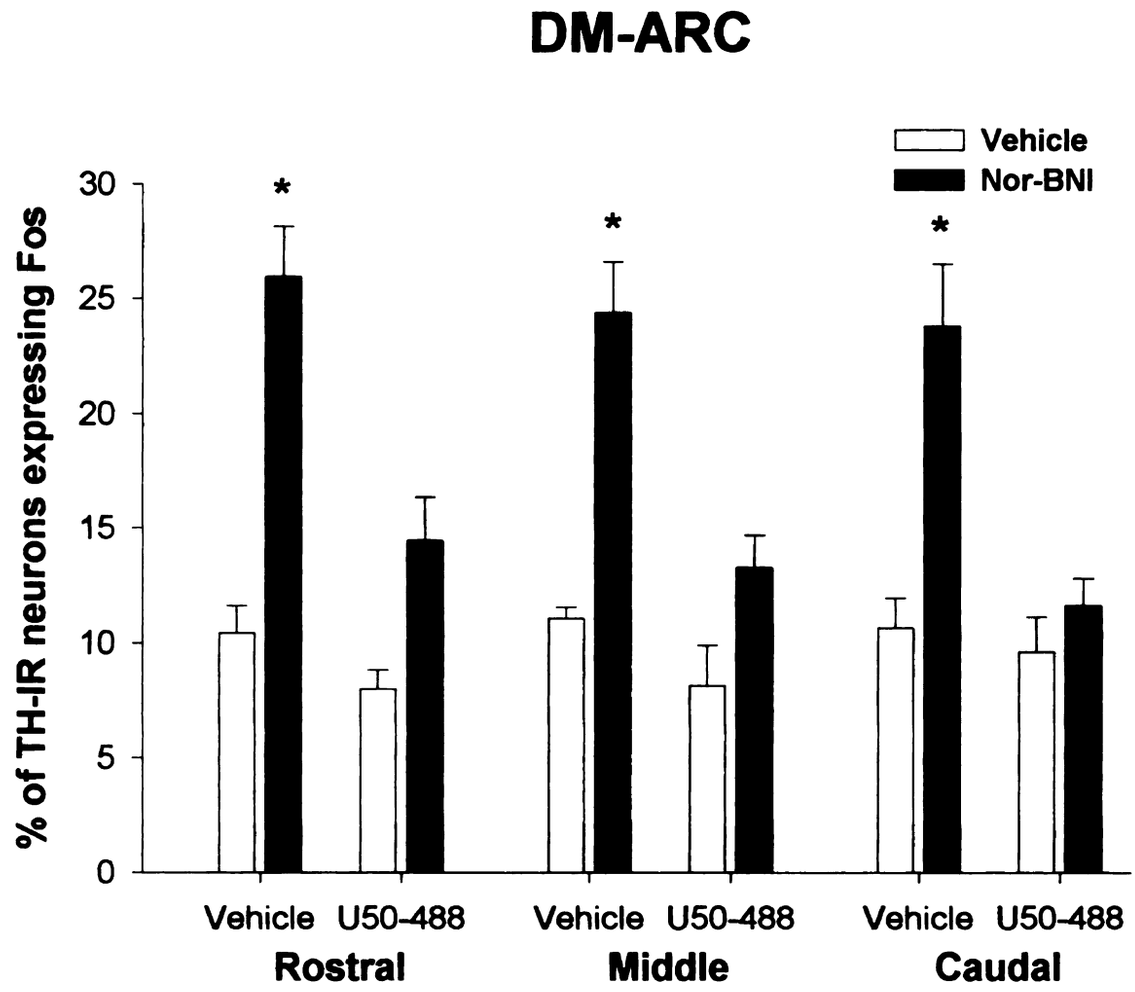

Figure 5.8 Effects of nor-BNI on the percentage of TH-IR neurons expressing Fos in the rostral, middle and caudal regions of the DM-ARC of vehicle- or U50488-treated rats. Rats were injected with either U50488 (10 mg/kg; sc) or its ddH_2O vehicle (1 ml/kg; sc) 2 h prior to sacrifice, and with either nor-BNI (12.5 μg/rat; icv) or its ddH_2O vehicle (3 μl/rat; icv) 2 h prior to sacrifice. Columns represent the means and vertical lines + 1 SEM from 6-8 vehicle- (open columns), and nor-BNI- (solid columns) treated rats. *, Values that are significantly different ($p < 0.05$) from vehicle-treated rats.

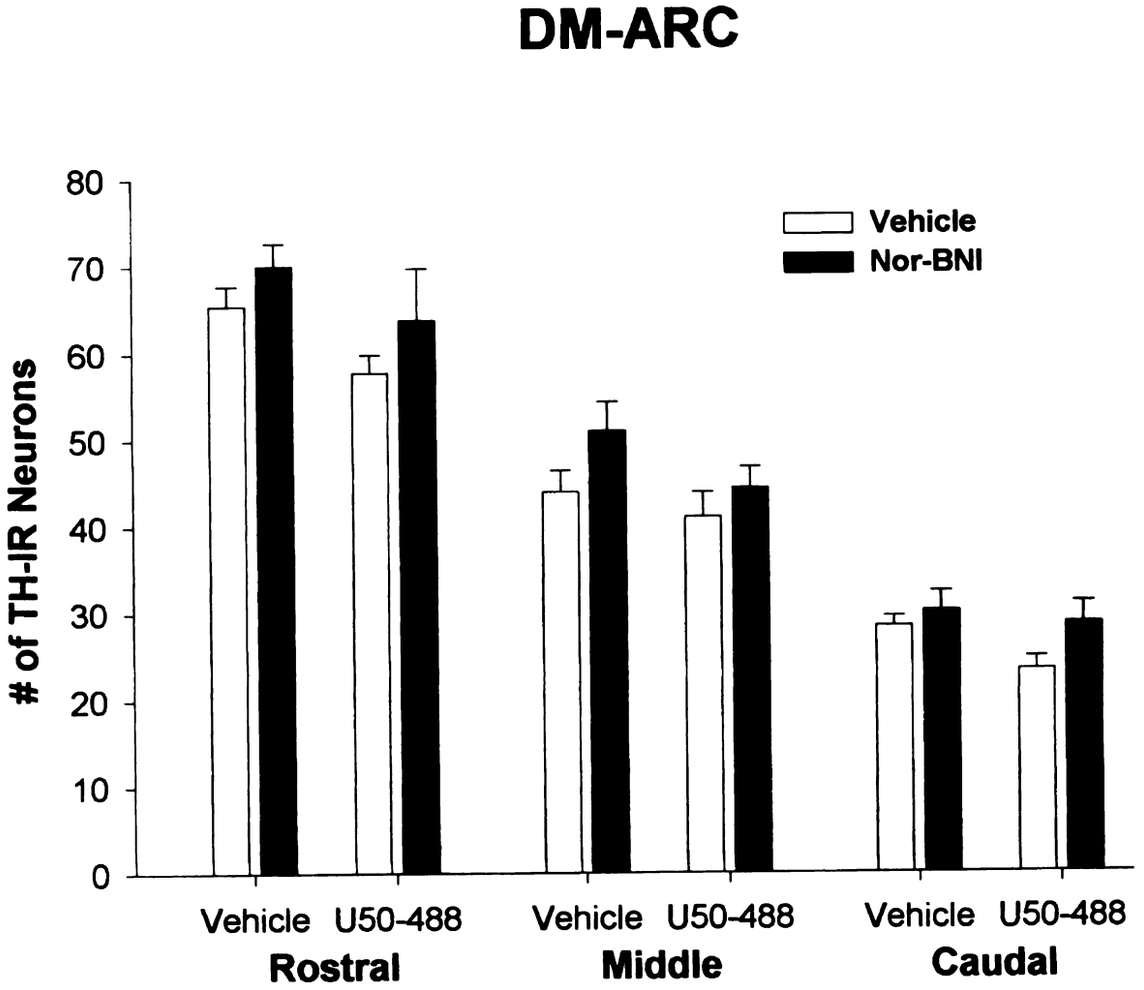

Figure 5.9 Effects of nor-BNI on the numbers of TH-IR neurons in the rostral, middle and caudal regions of the DM-ARC of vehicle- or U50488-treated rats. Rats were injected with either U50-488 (10 mg/kg; sc) or its ddH_2O vehicle (1 ml/kg; sc) 2 h prior to sacrifice, and with either nor-BNI (12.5 μg/rat; icv) or its ddH_2O vehicle (3 μl/rat; icv) 2 h prior to sacrifice. Columns represent the means and vertical lines + 1 SEM from 6-8 vehicle- (open columns), and nor-BNI- (solid columns) treated rats.

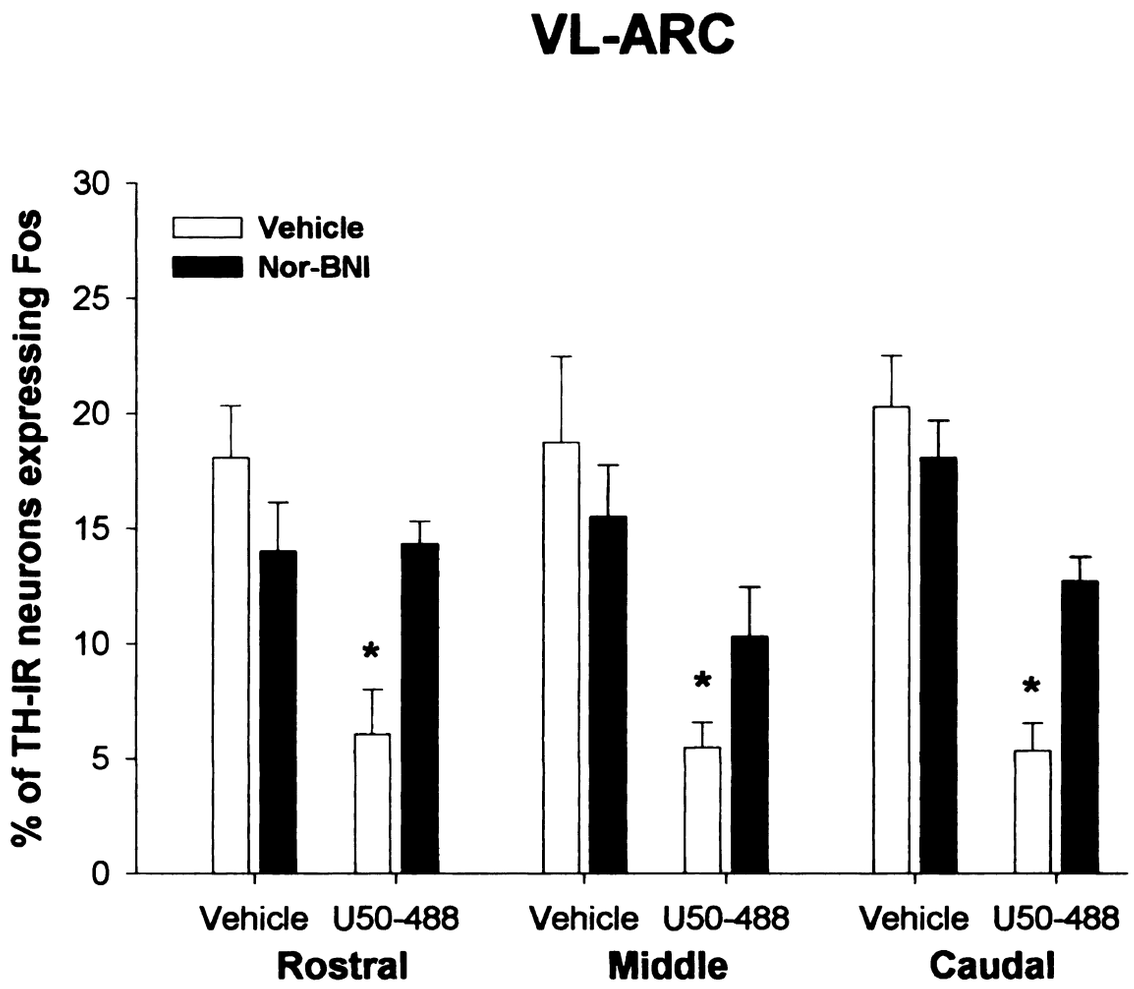

Figure 5.10 Effects of nor-BNI on the percentage of TH-IR neurons expressing Fos in the rostral, middle and caudal regions of the VL-ARC of vehicle- or U50488-treated rats. Rats were injected with either U50488 (10 mg/kg; sc) or its ddH_2O vehicle (1 ml/kg; sc) 2 h prior to sacrifice, and with either nor-BNI (12.5 μg/rat; icv) or its ddH_2O vehicle (3 μl/rat; icv) 2 h prior to sacrifice. Columns represent the means and vertical lines + 1 SEM from 6-8 vehicle- (open columns), and nor-BNI- (solid columns) treated rats. *, Values that are significantly different ($p < 0.05$) from vehicle-treated rats.

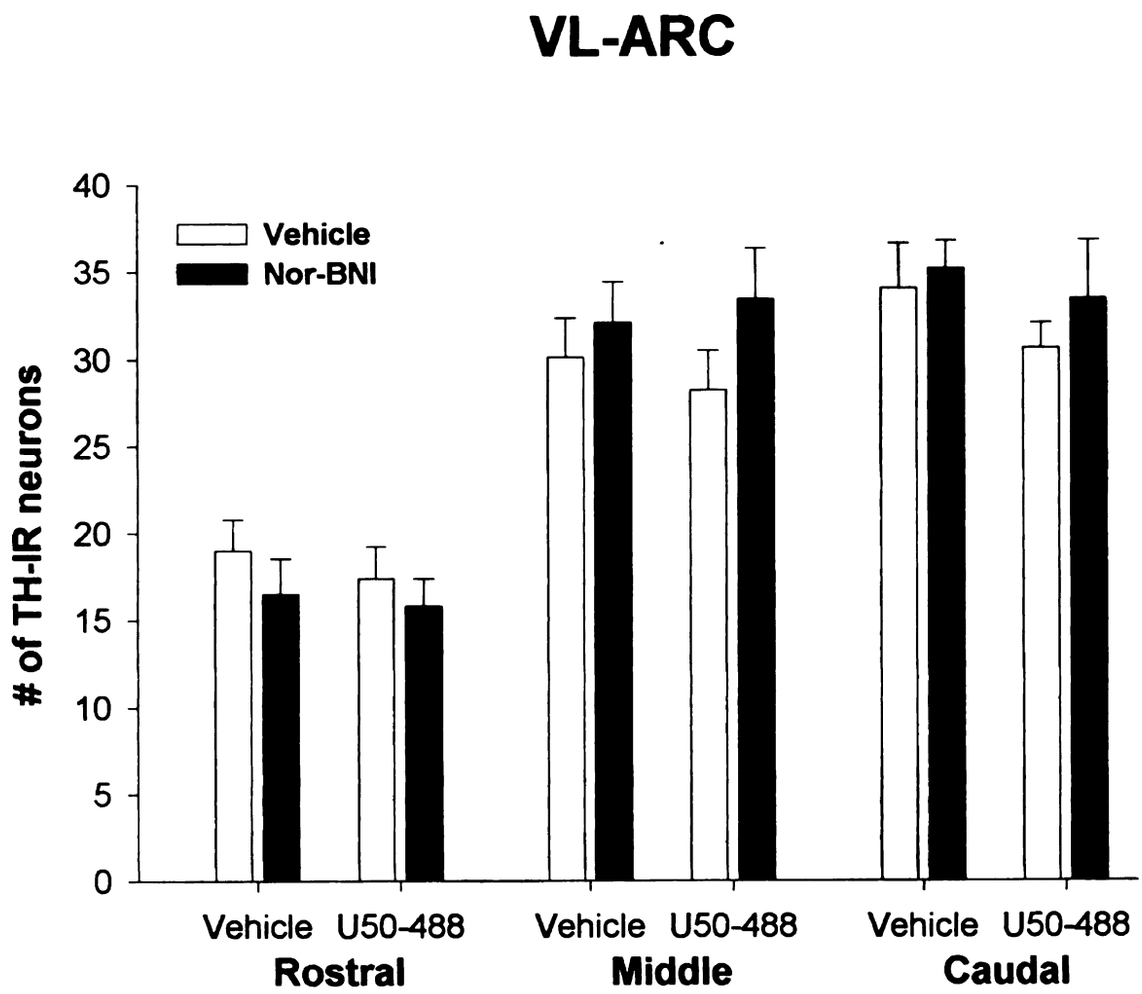

Figure 5.11 Effects of nor-BNI on the numbers of TH-IR neurons in the rostral, middle and caudal regions of the VL-ARC of vehicle- or U50488-treated rats. Rats were injected with either U50488 (10 mg/kg; sc) or its ddH_2O vehicle (1 ml/kg; sc) 2 h prior to sacrifice, and with either nor-BNI (12.5 μg/rat; icv) or its ddH_2O vehicle (3 μl/rat; icv) 2 h prior to sacrifice. Columns represent the means and vertical lines + 1 SEM from 6-8 vehicle- (open columns), and nor-BNI- (solid columns) treated rats.

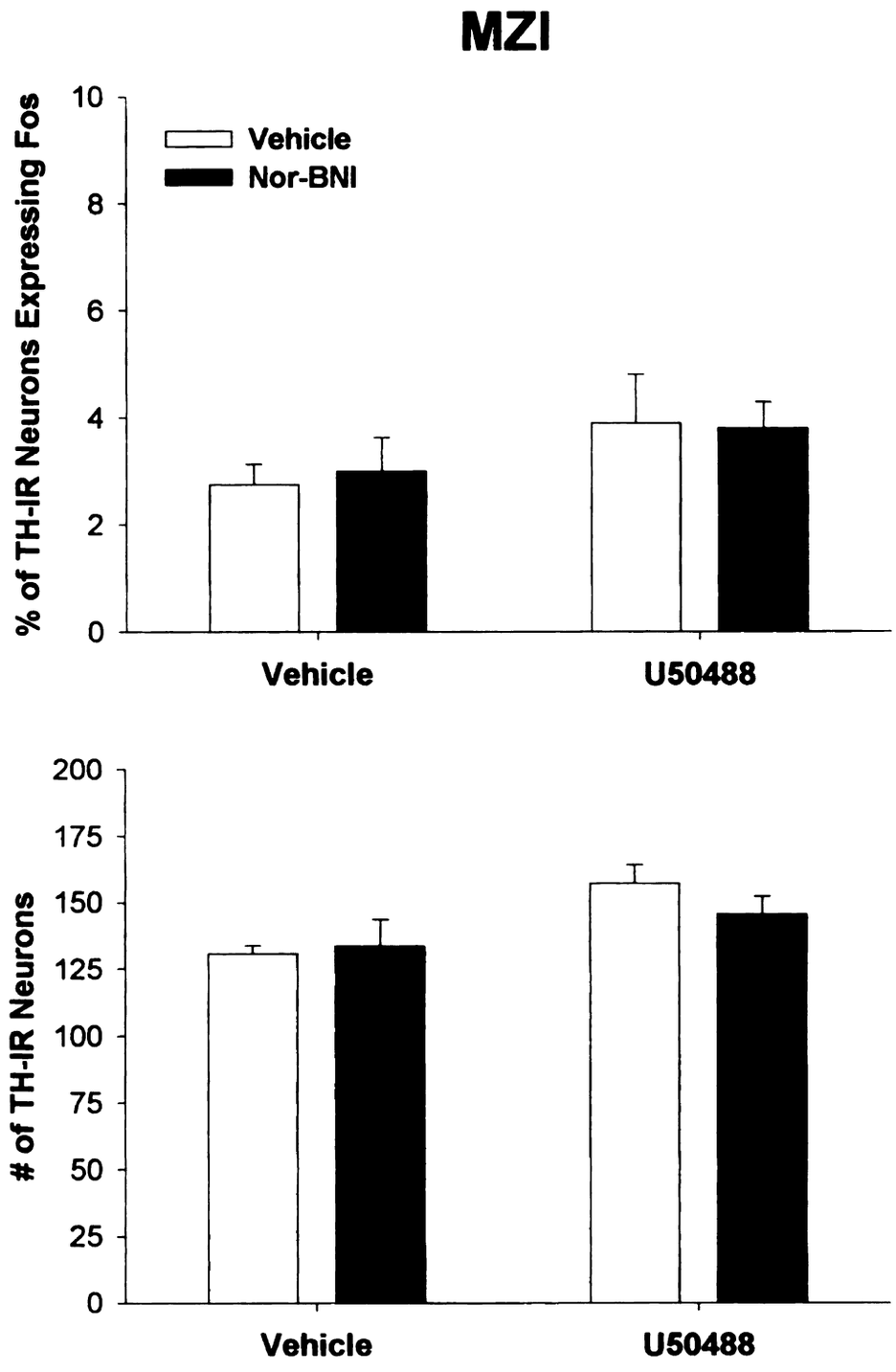

Figure 5.12 Effects of nor-BNI on the numbers of TH-IR neurons (**Bottom Panel**) and the percentage of these neurons expressing Fos (**Top Panel**) in the MZI of vehicle- or U50488-treated rats. Rats were injected with either U50488 (10 mg/kg; sc) or it ddH_2O vehicle (1 ml/kg; sc) 2 h prior to sacrifice, and with either nor-BNI (12.5 μg/rat; icv) or its ddH_2O vehicle (3 μl/rat; icv) 2 h prior to sacrifice. Columns represent the means and vertical lines + 1 SEM from 6-8 vehicle- (open columns) and nor-BNI- (solid columns) treated rats.

If quinelorane blocks the inhibitory effects of dynorphin at kappa receptors thereby increasing Fos expression in TIDA neurons, then the addition of a kappa receptor agonist should restore activity at kappa receptors and block the effects of quinelorane on Fos expression. U50-488 had no effect *per se*, but was able to reverse the stimulatory effects of quinelorane on the percentage of TH-IR neurons containing Fos-IR nuclei in the DM-ARC (**Figure 5.13**). There were no changes in the numbers of neurons after quinelorane or U50-488 (**Figure 5.14**). As shown in **Figure 5.15**, quinelorane significantly decreased the percentage of Fos-IR nuclei in TH-IR neurons throughout the rostrocaudal extent of the VL-ARC at an earlier time point than in Chapter 4. U50-488 alone also decreased the Fos expression, but there was no additive effect of quinelorane and U50-488. Neither quinelorane nor U50-488 had an effect on the numbers of TH-IR neurons within each region of the VL-ARC (**Figure 5.16**). In the MZI, quinelorane significantly decreased the expression of Fos in TH-IR neurons (**Figure 5.17; Top Panel**). U50-488 had no effect on the percentage of TH-IR neurons expression Fos or on the numbers of TH-IR neurons (**Figure 5.17; Bottom Panel**) in vehicle or quinelorane-treated animals.

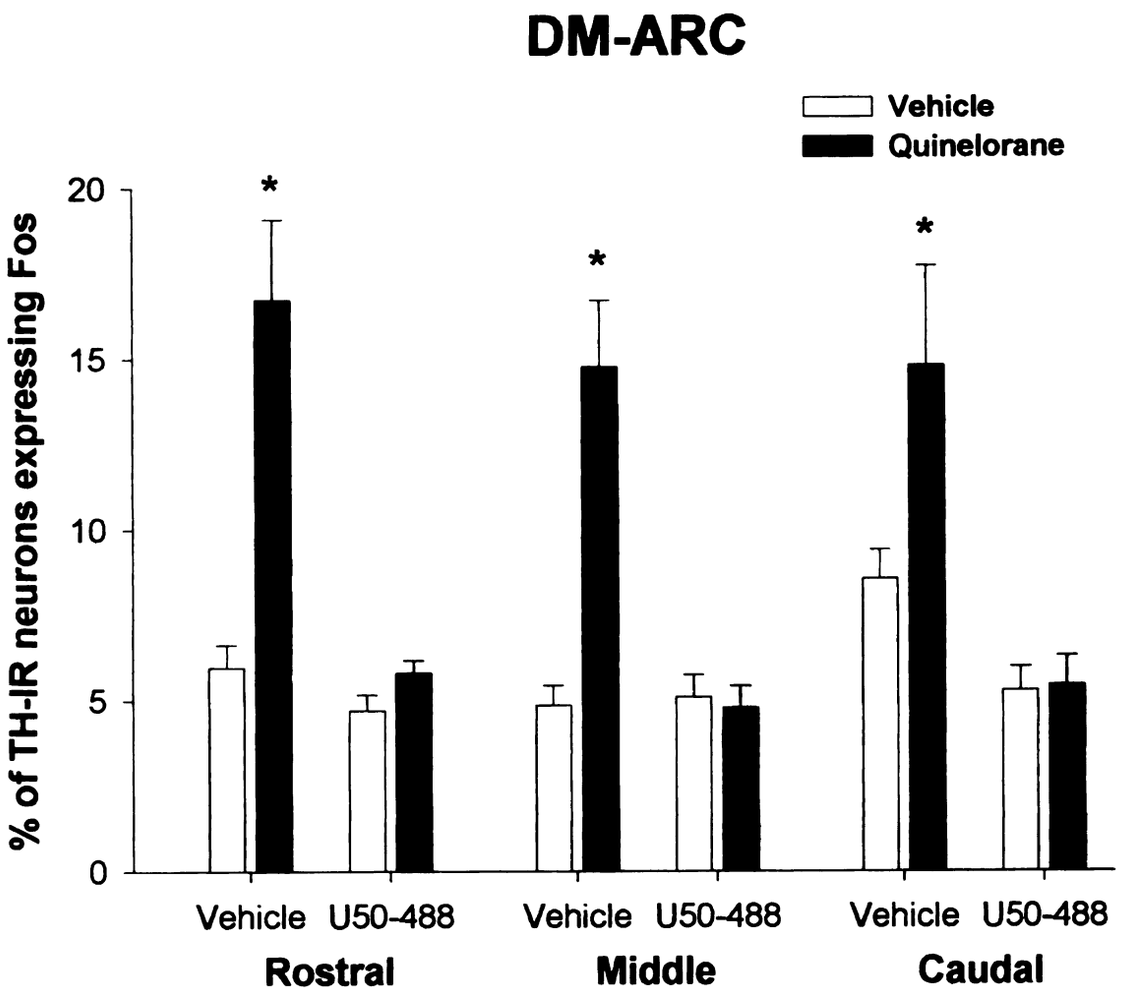

Figure 5.13 Effects of quinelorane on the percentage of TH-IR neurons expressing Fos in the rostral, middle and caudal regions of the DM-ARC of vehicle- or U50488-treated rats. Rats were injected with either U50488 (10 mg/kg; sc) or its ddH_2O vehicle (1 ml/kg; sc) 2 h prior to sacrifice, and with either quinelorane (100 μg/kg; ip) or its 0.9% saline vehicle (1 ml/kg; ip) 2 h prior to sacrifice. Columns represent the means and vertical lines + 1 SEM from 6-8 vehicle- (open columns), and quinelorane- (solid columns) treated rats. *, Values that are significantly different ($p < 0.05$) from vehicle-treated rats.

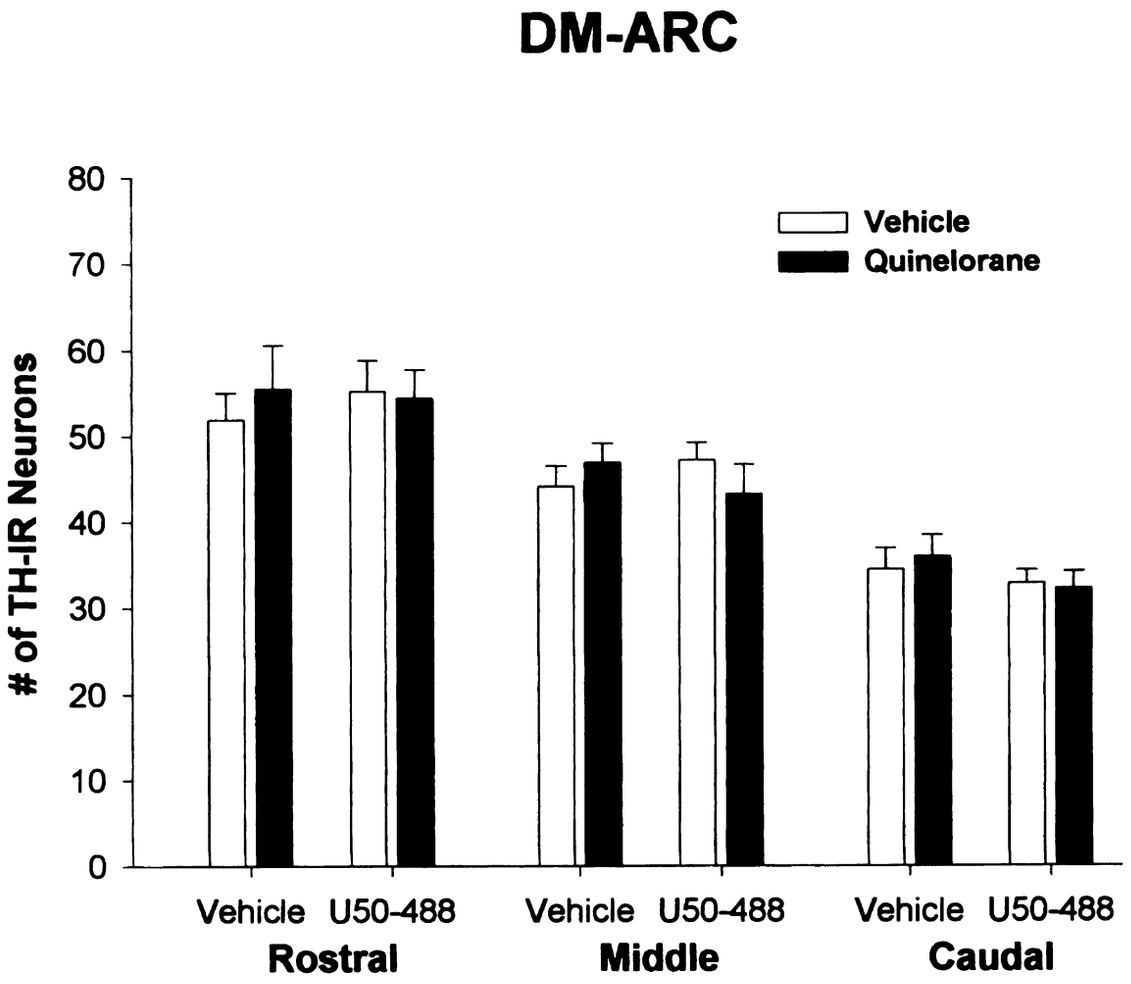

Figure 5.14 Effects of quinelorane on the numbers of TH-IR neurons in the rostral, middle and caudal regions of the DM-ARC of vehicle- or U50488-treated rats. Rats were injected with either U50488 (10 mg/kg; sc) or its ddH_2O vehicle (1 ml/kg; sc) 2 h prior to sacrifice, and with either quinelorane (100 μg/kg; ip) or its 0.9% saline vehicle (1 ml/kg; ip) 2 h prior to sacrifice. Columns represent the means and vertical lines + 1 SEM from 6-8 vehicle- (open columns), and quinelorane- (solid columns) treated rats.

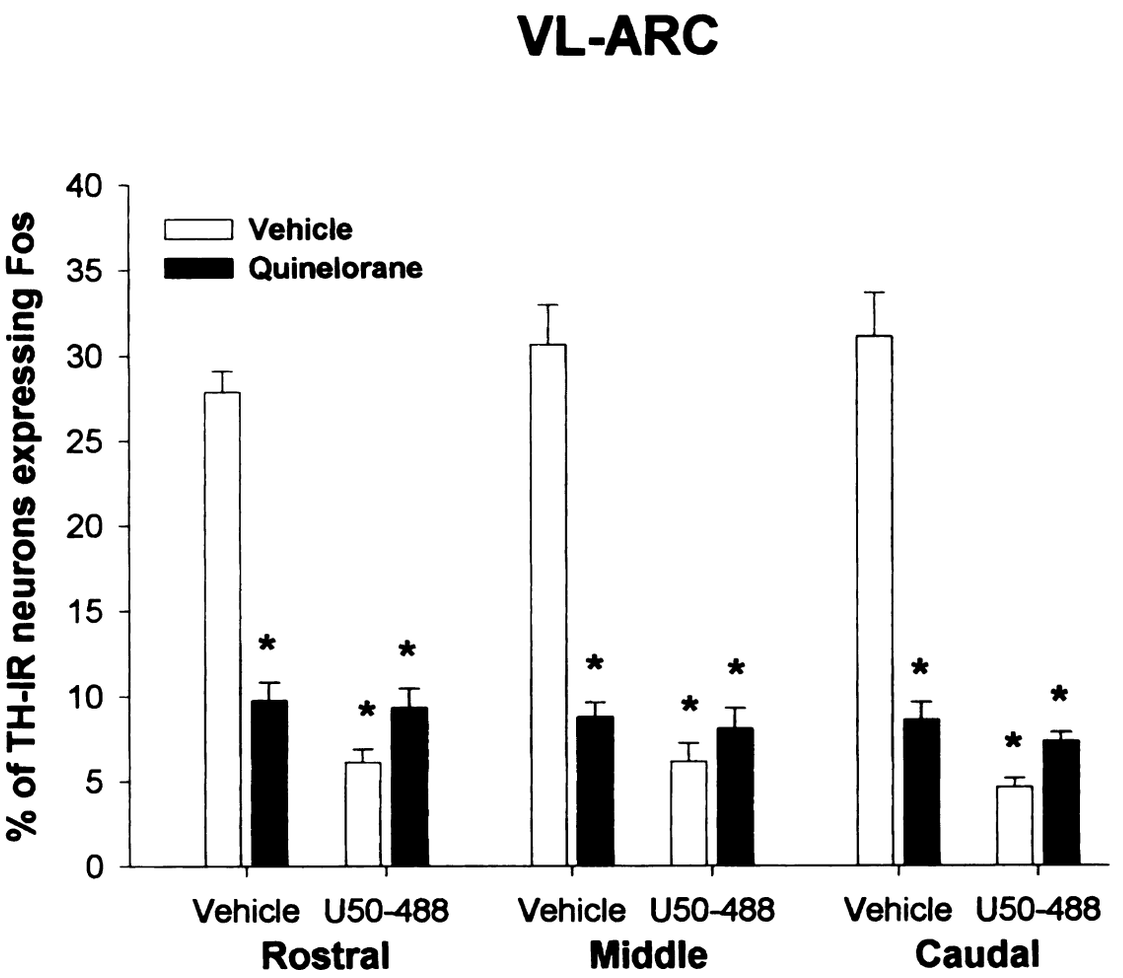

Figure 5.15 Effects of quinelorane on the percentage of TH-IR neurons expressing Fos in the rostral, middle and caudal regions of the VL-ARC of vehicle- or U50488-treated rats. Rats were injected with either U50488 (10 mg/kg; sc) or its ddH_2O vehicle (1 ml/kg; sc) 2 h prior to sacrifice, and with either quinelorane (100 μg/kg; ip) or its 0.9% saline vehicle (1 ml/kg; ip) 2 h prior to sacrifice. Columns represent the means and vertical lines + 1 SEM from 6-8 vehicle- (open columns), and quinelorane- (solid columns) treated rats. *, Values that are significantly different ($p < 0.05$) from vehicle-treated rats.

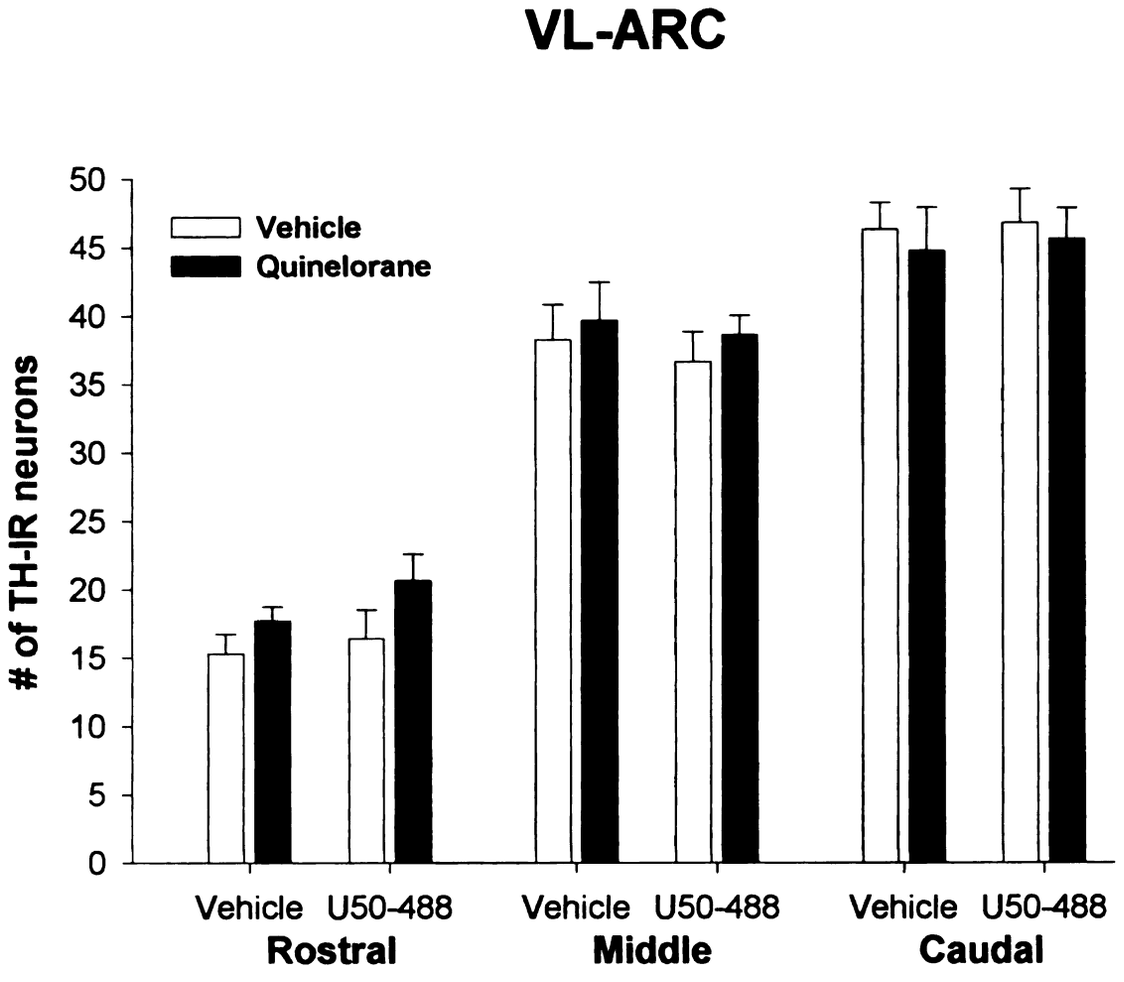

Figure 5.16 Effects of quinelorane on the numbers of TH-IR neurons in the rostral, middle and caudal regions of the VL-ARC of vehicle- or U50488-treated rats. Rats were injected with either U50488 (10 mg/kg; sc) or its ddH_2O vehicle (1 ml/kg; sc) 2 h prior to sacrifice, and with either quinelorane (100 μg/kg; ip) or its 0.9% saline vehicle (1 ml/kg; ip) 2 h prior to sacrifice. Columns represent the means and vertical lines + 1 SEM from 6-8 vehicle- (open columns), and quinelorane- (solid columns) treated rats.

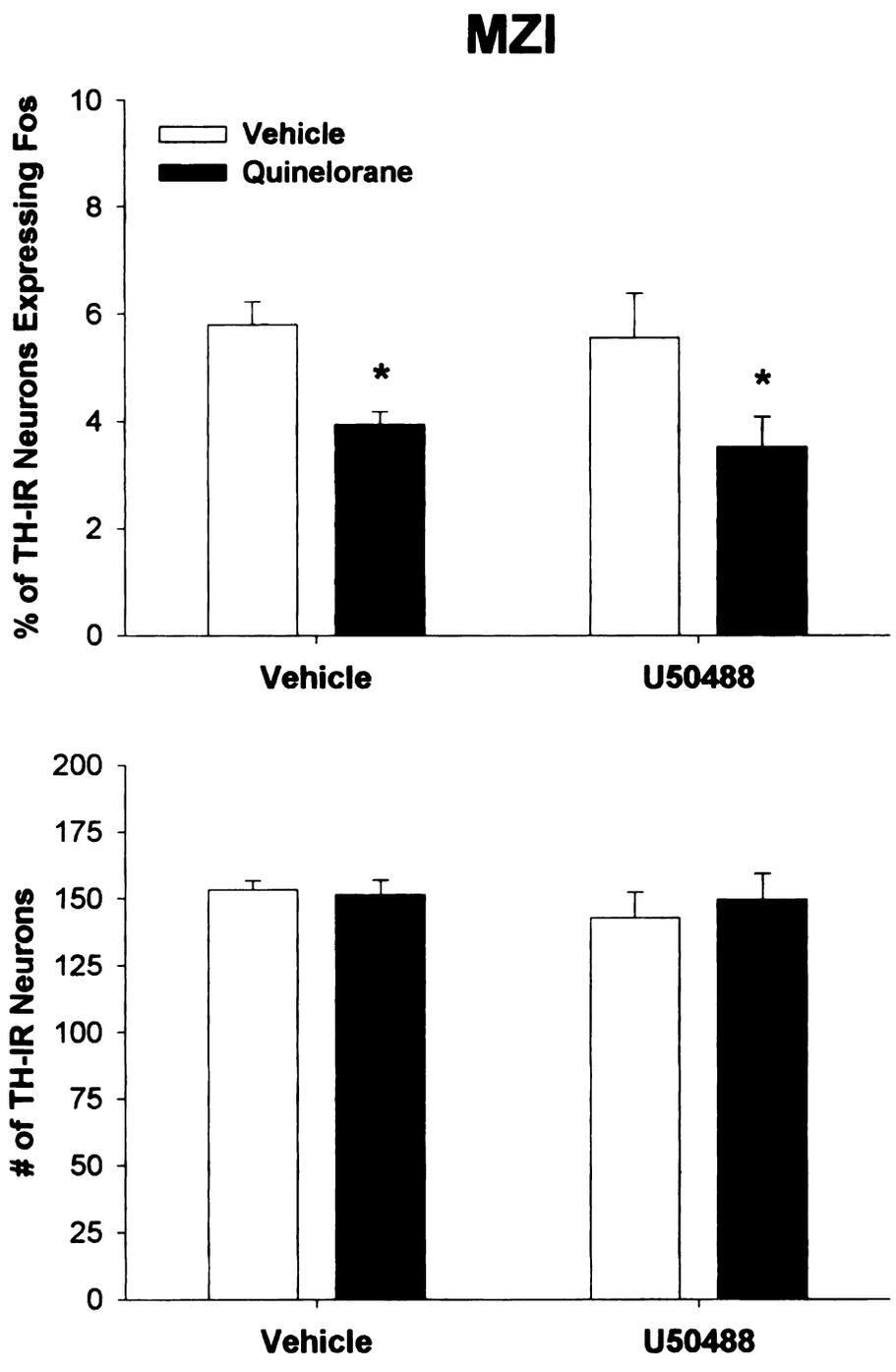

Figure 5.17 Effects of quinelorane on the numbers of TH-IR neurons (**Bottom Panel**) and the percentage of these neurons expressing Fos (**Top Panel**) in the MZI of vehicle- or U50488-treated rats. Rats were injected with either U50488 (10 mg/kg; sc) or it ddH_2O vehicle (1 ml/kg; sc) 2 h prior to sacrifice, and with either quinelorane (100 μg/kg; ip) or its 0.9% saline vehicle (1 ml/kg; ip) 2 h prior to sacrifice. Columns represent the means and vertical lines + 1 SEM from 6-8 vehicle- (open columns) and quinelorane- (solid columns) treated rats. *, Values that are significantly different ($p < 0.05$) from vehicle-treated rats.

DISCUSSION

The major finding of these studies is that opioid receptors regulate Fos expression in TIDA neurons of the DM-ARC. Blockade of kappa opioid receptors increases Fos expression in TIDA neurons throughout the rostrocaudal extent of the DM-ARC in a time dependent manner. This time frame is characteristic of the induction of Fos and other immediate early genes in a variety of tissues. Once induced, *c-fos* mRNA increases as early as 15 min and is subsequently translated into Fos protein (Herdegen and Leah, 1998). The half life of Fos protein is 90-120 min, with maximum levels reached between 1 and 3 h, and gradually disappearing from the nucleus by 4-6 h (Sonnenberg et al., 1989; Chan et al., 1993; Kovacs and Sawchenko, 1996). This rapid down-regulation of Fos is not fully understood, but there are three main processes that could account for this. First is down-regulation of transcription by Fos protein cis-repressing its own promoter (Sassone-Corsi et al., 1988). Secondly, the mRNA of *c-fos* and other oncogenes are not stable and contain elements that make them targets for exonucleases and thus rapid degradation (Veyrune et al., 1995). Thirdly, in addition to mRNA degradation, the protein itself is also rapidly broken down by lysosomes and proteasomes (Stancovski et al., 1995; Aniento et al., 1996).

This time course of Fos expression shown here is similar to that seen by others following the blockade of mu and kappa opioid receptors. For example, naloxone and nor-BNI both increase Fos expression in unidentified neurons in various areas of the brain 90 to 120 min following administration (Gestreau et al., 2000; Carr et al., 1999). Kappa opioid receptors are linked to G_i and G_o proteins,

which inhibit cAMP and hyperpolarize cell membranes (Childers, 1991; Childers et al., 1998; Takekoshi et al., 2000). These data suggest that kappa receptors tonically suppress Fos expression in TIDA neurons. Precedent for induction of immediate early genes through the loss of tonic opioid activity has been demonstrated in the central amygdala (Carr et al., 1999) and nucleus tractus solitarii (Gestreau et al., 2000). In this case, the blockade of dynorphin induces a disinhibition of TIDA neurons by a postsynaptic action which results in an increase in neuronal discharge and metabolic activities strong enough to induce Fos expression (Morgan and Curran, 1991).

In the DM-ARC, the time course of Fos expression in TH-IR neurons following blockade of kappa receptors is also identical to the time course following activation of D2 receptors shown in Chapter 4. In this respect blockade of kappa receptors mimics the effects of D2 receptor activation on Fos expression in TIDA neurons of the DM-ARC. These results, along with the neurochemical experiments using nor-BNI and U50-488, (Manzanares et al., 1992a and 1992b; Durham et al., 1996) further support a role of kappa receptors in mediating the effects of D2 receptor stimulation of Fos expression.

If expression of Fos is regulated by kappa opioid receptors, then a kappa receptor agonist should reverse the effects of a kappa opioid receptor antagonist. Indeed, U50-488 blocks the stimulatory effect of nor-BNI on Fos expression confirming that the actions of nor-BNI are mediated through kappa opioid receptors. These results correlated with findings from neuronal activity studies demonstrating that kappa antagonists induce an acute stimulatory response in

TIDA neurons and this can be reversed by a kappa receptor agonist (Manzanares et al., 1992). The lack of effect of a kappa agonist suggests that dynorphin neurons are tonically active and maximally inhibit Fos expression in TIDA neurons of the DM-ARC under basal conditions. In addition to TIDA neurons, the neurons of the periventricular DA system are also tonically inhibited by dynorphin as revealed by neurochemical studies (Manzanares et al., 1991). This is in contrast to the effects on the nigrostriatal and mesolimbic DA systems in neurochemical studies where there was no effect following the blockade or activation of kappa receptors on neuronal activity in these two systems (Manzanares et al., 1991). This suggests that nigrostriatal and mesolimbic neurons are not tonically inhibited by dynorphin.

Having established that Fos expression in TIDA neurons is regulated by kappa opioid receptors, the next aim was to determine if these receptors share a common pathway that mediates the stimulatory effects of D2 receptors on Fos expression. If quinelorane increases Fos expression in TIDA neurons by preventing dynorphin release and activation of kappa opioid receptors, then the administration of a kappa receptor agonist should restore activity at these receptors and prevent stimulation of Fos expression. The results from this study reveal that this is indeed the case, and correlate with previous neurochemical studies showing that U50-488 reverses the stimulatory effects of quinelorane on TIDA neuronal activity (Durham et al., 1996). These studies demonstrate that the D2 receptor-mediated neuronal regulation of Fos expression in the DM-ARC

of TIDA neurons occurs through the loss of tonic inhibition of dynorphin neurons via kappa opioid receptors.

This is the first time this type of regulation of Fos expression has been demonstrated in DA neurons. Kappa receptors are involved DA receptor-mediated regulation of immediate early genes, but in non-DA striatonigral neurons (striatal neurons which project to the substantia nigra). Dynorphin released in the ST from striatonigral neurons following D1-receptor stimulation acts locally on pre-synaptic kappa receptors on DA terminals or postsynaptic kappa receptors on the striatonigral neurons themselves to inhibit Fos and zif268 induction (Steiner and Gerfen, 1995, 1996 and 1998). In the substantia nigra and ventral tegmental areas, kappa receptor mRNA (Mansour et al., 1994) and receptor binding (Speciale et al., 1993) has been demonstrated, as well as dynorphin-IR terminals forming synapses with TH-labeled dendrites (Pickel et al., 1993). Dynorphin released in the substantia nigra from striatonigral terminals could act to inhibit nigrostriatal neurons; however, none of these studies examined Fos immunoreactivity in these DA neurons. Only one study has been reported to examine the effects of kappa receptor blockade on Fos expression in the ventral tegmental area (Carr et al., 1999). Unlike TIDA neurons in the DM-ARC, nor-BNI had no effect on neurons in the ventral tegmental area suggesting that mesolimbic DA neurons are not tonically suppressed by dynorphin.

Figure 5.18 illustrates the proposed pathway following D2 receptor activation with quinelorane. From the available evidence it is likely that the D2 receptors are located outside the mediobasal hypothalamus, whereas dynorphin

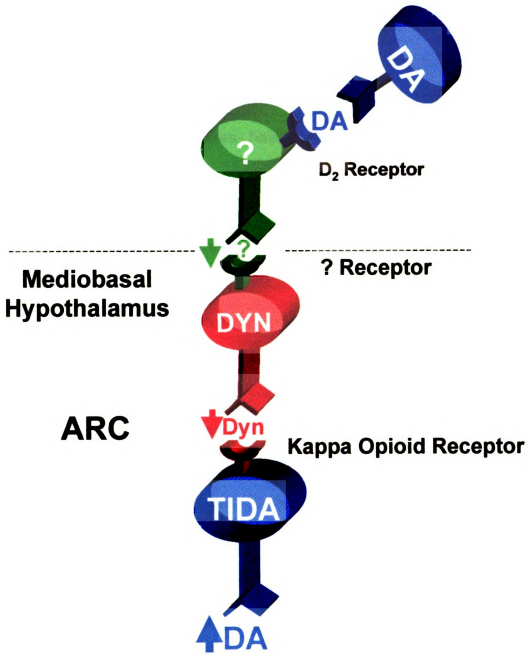

Figure 5.18 Schematic depicting the proposed neuronal pathway following D2 receptor activation. DA acts at a D2 receptor on the chemically unidentified neurons (depicted in green) located outside the mediobasal hypothalamus. In turn, there is a decrease in the release of stimulatory neurotransmitter which leads to inhibition of dynorphin neurons. The decrease in dynorphin at the kappa opioid receptor leads to a disinhibition of TIDA neurons and subsequent increase in DA release. Abbreviations: ?, unknown neuron/neurotransmitter/receptor; ARC, arcuate nucleus; DA, dopamine; DYN, dynorphin; ME, median eminence.

neurons are located in the ARC and terminate at kappa opioid receptors on TIDA neurons. There are still several unknowns in this pathway; 1) the origin of DA, 2) location of the D2 receptor-expressing target cells, 3) the neurochemical identity of the target cell and its receptors on dynorphin neurons.

Although no thorough studies have been carried to answer these questions, it is tempting to speculate about what these unknowns might be. One area of the hypothalamus that may be involved in this neuronal pathway is the dorsomedial hypothalamic nucleus. Electrical stimulation of this nucleus stimulates DA release from TIDA neurons (Gunnet and Moore, 1988). Since current spread to the ARC was ruled out in these studies it is likely that the stimulation causes DA release from an unknown source that, in turn, activates D2 receptors and mimics the stimulatory effect of quinelorane. The DMN also contains extensive dendritic processes from the IHDA neurons of the MZI (Chan-Palay et al., 1984), therefore a possible origin of DA is the MZI. The IHDA neurons project to the paraventricular nucleus, the horizontal diagonal band, and the central amygdala (Eaton et al., 1994; Wagner et al., 1995), hence it is possible that one of these areas contains the D2 receptor expressing target cell.

If the proposed pathway is correct, then the neuron targeted by DA should originate outside the mediobasal hypothalamus and be stimulatory in nature, tonically activating dynorphin neurons. One clue to the identity of this stimulatory neuron is that activation of its target receptor should mimic the effects of dynorphin neurons and tonically inhibit TIDA neurons. Though it is not known what the neuron might be, there are certain neurotransmitter and receptor systems that can certainly be ruled out. For example, several lines of evidence demonstrate that the neuropeptide neurotensin is not involved. First, neurotensin activates TIDA neurons (Berry and Gudelsky, 1990) and mediates the stimulatory effects of PRL on the activation of these neurons (Hentschel et al., 1998). In addition, co-administration of a neurotensin receptor antagonist has no effect on the quinelorane-induced increases in TIDA neuronal activity (Durham, 1999).

Two neurotransmitters that tonically inhibit TIDA neurons are GABA (acting at $GABA_A$ receptors; Wagner et al., 1994a) and glutamate (acting at AMPA receptors; Wagner et al., 1994b). However, GABA is an inhibitory neurotransmitter so if the unidentified neuron were GABAergic it would inhibit (rather that stimulate) dynorphin neurons thus leading to activation of TIDA neurons. Interestingly, blockade of AMPA receptors increases the activity of TIDA neurons (Wagner et al., 1994) thus mimicking the effect of quinelorane. However, this increase is not reversed by activating kappa opioid receptors as it is by a $GABA_A$ receptor agonist (Wagner et al., 1994c). Therefore, the AMPA receptor-mediated tonic inhibition of TIDA neurons occurs by a mechanism involving $GABA_A$ receptors and not kappa receptors.

The results of the VL-ARC reveal that "DOPA-ergic" neurons are not regulated by kappa opioid receptors under basal conditions. In these TH-IR neurons, activation of kappa opioid receptors decreased Fos expression while blockade of the receptors had no effect. Thus, kappa opioid receptors do not tonically inhibit these neurons. There is evidence that there are dynorphin nerve terminals in the ARC (Fitzsimmons, et al., 1992); however, those studies do not differentiate between the VL-ARC vs. DM-ARC. There are also dynorphin neurons in the ventromedial nucleus (VMN) of the hypothalamus (Zamir et al.,1983), and like "DOPA-ergic" neurons, these neurons are not regulated by D2 receptors (Durham, 1999). Though no studies are available concerning the projection of dynorphin neurons of the VMN, it is possible they regulate "DOPA-ergic" neurons. While it is possible that these neurons have kappa receptors, it cannot be concluded from these studies if or whether or not the effect of dynorphin on "DOPA-ergic" neurons is direct or indirect.

In these experiments, quinelorane decreased Fos expression in the "DOPA-ergic" cells of the VL-ARC at an earlier time point compared to results reported in Chapter 4. One possibility for this difference in response is time of day influences. However, the animals of the quinelorane groups in these studies and in Chapter 4 followed the same dosing schedule and were sacrificed at the same time of day. Thus, time of day influences do not account for this difference. The response of "DOPA-ergic" neurons to the D2 receptor agonist has been variable throughout, reiterating that, unlike the TIDA neurons in the DM-ARC, D2

receptors do not regulate these neurons. The significance of this finding remains to be elucidated.

The results for the IHDA neurons of the MZI demonstrate that there is no tonic kappa opioid receptor regulation of Fos expression, nor is there any response to the kappa agonist. This is in agreement with neurochemical studies demonstrating a lack of kappa opioid receptor regulation of IHDA neuronal activity (Tian et al., 1992). Thus, it is concluded that there is no kappa opioid receptor regulation of gene expression in the IHDA neurons of the MZI.

It is interesting to note that quinelorane significantly decreases Fos expression in these neurons. Recall in Chapter 4 quinelorane alone had no effect on Fos expression in the IHDA neurons at 2 h. One possibility for this difference in response is time of day influences. However, the animals receiving quinelorane in these studies and in Chapter 4 were sacrificed at the same time of day. Thus, time of day influences can not account for this difference.

The percentage of neurons expressing Fos in the vehicle groups is higher in this experiment (approximately 6%) compared to previous studies (approximately 4% or less). In the raclopride/quinelorane study in Chapter 4 (**Figure 4.11**), blockade of D2 receptors with raclopride increased the expression of Fos in the MZI to about 6% and this was reversed with quinelorane. It is possible that, for a reason not explained or due to some natural variation, the IHDA neurons were slightly more active and thus expressing more Fos at the time of this experiment. If the D2 receptors were not fully occupied, quinelorane may have been able to bind and decrease Fos expression.

In conclusion, dynorphin neurons projecting to TIDA neurons are tonically active, and they regulate Fos expression via kappa opioid receptors in TIDA neurons in the DM-ARC. The expression of Fos in "DOPA-ergic" neurons of the VL-ARC is regulated by kappa receptors as well; however, this regulation is not present under basal conditions. Finally, D2 receptor mediated regulation of Fos in TIDA neurons in DM-ARC occurs via a mechanism involving inhibition of endogenous dynorphin release and loss of tonic inhibition of gene expression by kappa opioid receptors.

CHAPTER SIX

D2 RECEPTOR REGULATION OF TH GENE EXPRESSION IN SUBDIVISIONS OF THE ARCUATE NUCLEUS

Introduction

In Chapter 4, immunohistochemical techniques were utilized to characterize D2 receptor-mediated changes in Fos expression in TIDA neurons. These studies revealed that following D2 receptor activation, Fos increases throughout the rostral-caudal extent of the DM-ARC in a time dependent manner, but not in the VL-ARC. These results correlated with previous neurochemical studies examining D2 receptor-mediated stimulation of TIDA nerve terminal activity in the ME (Eaton et al., 1993). Activation of D2 receptors increases DA synthesis and turnover in these neurons within 30 min and persists for at least 8 h (Eaton et al., 1993; Durham et al., 1996).

TH is the rate limiting enzyme in the catecholamine biosynthesis pathway. The catalytic activity of this molecule determines the synthetic rate of DA in the TIDA system (Wang et al., 1993). TH can be regulated by activation of the existing enzyme, such as through phosphorylation (Porter, 1986a) and by increased synthesis of the enzyme beginning at the transcription level (Biguet et al., 1991; Kumer and Vrana, 1996).

There are several lines of evidence demonstrating a correlation between TH neuronal activity and TH mRNA expression in TIDA neurons regulated by PRL. Chronic administration of pharmacological agents that cause changes in PRL levels results in corresponding changes in TIDA neuronal activity and TH

mRNA expression (Arbogast and Voogt, 1991). Also, afferent neuronally-mediated physiological stimuli originating from suckling rat pups decreases TIDA neuronal activity and TH mRNA expression in dams, which can be reversed with the removal of the pups (Wang et al., 1993; Berghorn et al., 2001). However, the acute effects of DA receptor activation on TH gene expression in TIDA neurons have not been studied.

The specific aim of these studies was to determine if an acute increase in neuronal activity caused by activation of D2 receptors was associated with changes in the expression of the long term gene TH in TIDA neurons. The working hypothesis is that acute activation of DA release from TIDA neurons is accompanied by an increase of TH mRNA expression in these neurons. To this end, the time course of effects of quinelorane on TH mRNA expression were determined in the DM-ARC and for comparison, "DOPA-ergic" neurons in the VL-ARC and IHDA neurons in the MZI.

Materials and Methods

Gonadally intact male rats were used in these experiments. Care and handling of the rats was carried out as described in **Materials and Methods** in Chapter 2. Following appropriate treatments, rats were decapitated and brains were quickly frozen. Brains were sectioned using a cryostat as described in **Materials and Methods** in Chapter 2. The identification of neurons containing TH mRNA in the ARC and MZI was carried out using *in situ* hybridization procedures in **Materials and Methods** in Chapter 2. Results from studies

presented earlier demonstrated that the stimulation of Fos expression was consistent throughout the rostrocaudal extent of the DM-ARC. Because there were no differences in this response, the *in situ* studies focused on the rostral and middle ARC. The rostral and middle ARC sections were chosen and then visually partitioned into DM-ARC and VL-ARC. TH mRNA was localized with a TH oligonucleotide probe labeled with ^{35}S.

Results

Photomicrographs in **Figure 6.1** illustrate TH mRNA expression in neurons in the middle DM-ARC 4 h after the injection of either vehicle (**Left Panel**) or quinelorane (**Right Panel**). There is an increase in grain density of TH mRNA following quinelorane administration. **Figure 6.2** illustrates the time course effects of quinelorane on the labeling density ratio of TH mRNA expression per neuron in the DM-ARC. Quinelorane significantly increased TH mRNA expression in a time dependent manner reaching maximum levels at 4 h and remained elevated for at least 24 h in the DM-ARC. There were no changes in the numbers of neurons containing TH mRNA within the DM-ARC at any timepoint following quinelorane administration (**Figure 6.3**). In contrast, in the VL-ARC quinelorane had no effect on the labeling density ratio of TH mRNA per neuron (**Figure 6.4**). As in the DM-ARC, there were no changes in the numbers of neurons containing TH mRNA at any timepoint within the VL-ARC following quinelorane administration (**Figure 6.5**). In the MZI, quinelorane had no effect on

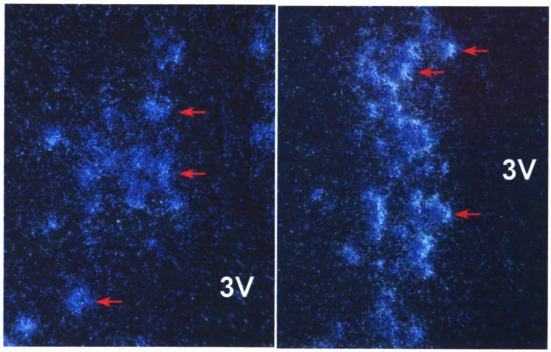

Figure 6.1 High power (400x) computer-captured images demonstrating increased TH mRNA expression in neurons of the DM-ARC 4 h following administration of quinelorane. Rats were injected with either vehicle (Left Panel; 0.9% saline; 1 ml/kg; ip) or quinelorane (Right Panel; 100 μg/kg; ip) and sacrificed 4 h later. Arrows represent silver grains localized over the cell bodies of neurons containing TH mRNA. 3V, third ventricle.

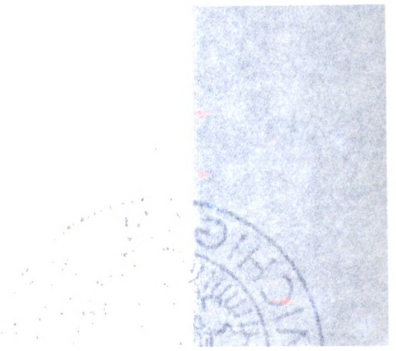

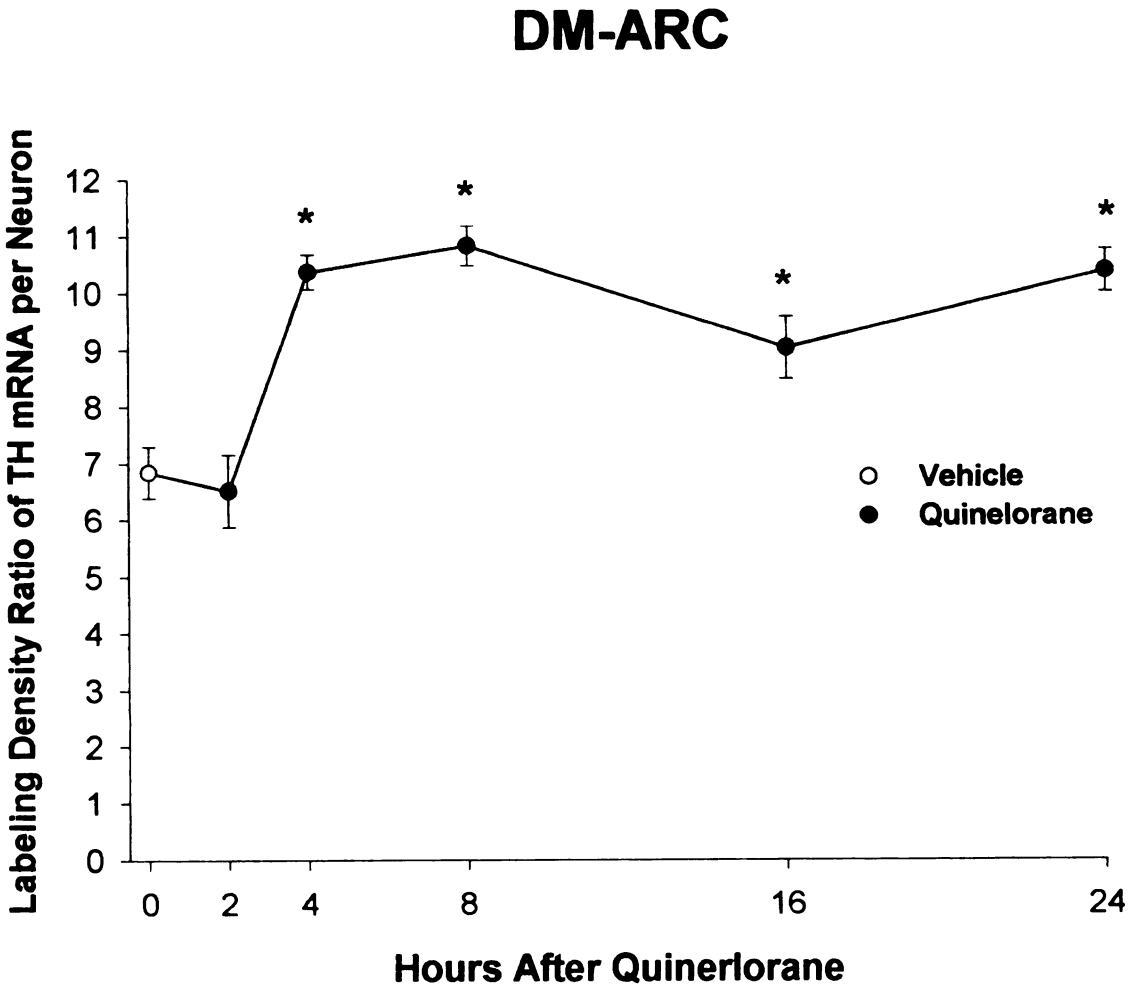

Figure 6.2 Time course effects of quinelorane on the labeling density ratio of TH mRNA expression per neuron in the DM-ARC. Rats were injected with quinelorane (filled symbols; 100 μg/kg; ip) and sacrificed 2, 4, 8, 16, or 24 h later. Zero time controls (open symbols) were injected with 0.9% saline vehicle (1 ml/kg; ip) and sacrificed 2 h later. Symbols represent the means and vertical lines ± 1 SEM from 6-8 animals. *, Values for quinelorane-treated rats that are significantly different ($p<0.05$) from vehicle-treated controls.

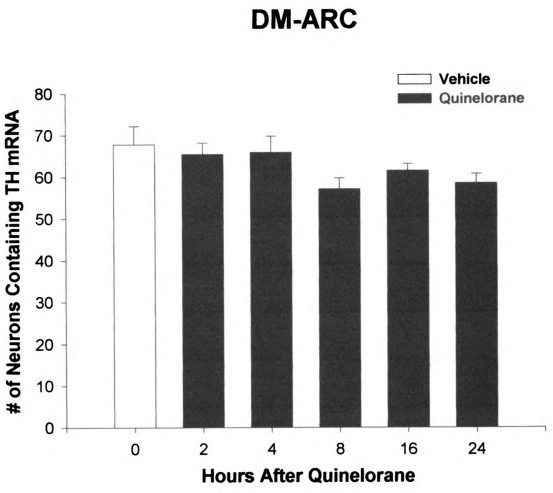

Figure 6.3 Time course effects of quinelorane on the number of neurons containing TH mRNA in the DM-ARC. Rats were injected with quinelorane (filled columns; 100 μg/kg; ip) and sacrificed 2, 4, 8, 16, or 24 h later. Zero time controls (open columns) were injected with 0.9% saline vehicle (1 ml/kg; ip) and sacrificed 2 h later. Columns represent the means and vertical lines + 1 SEM from 6-8 animals.

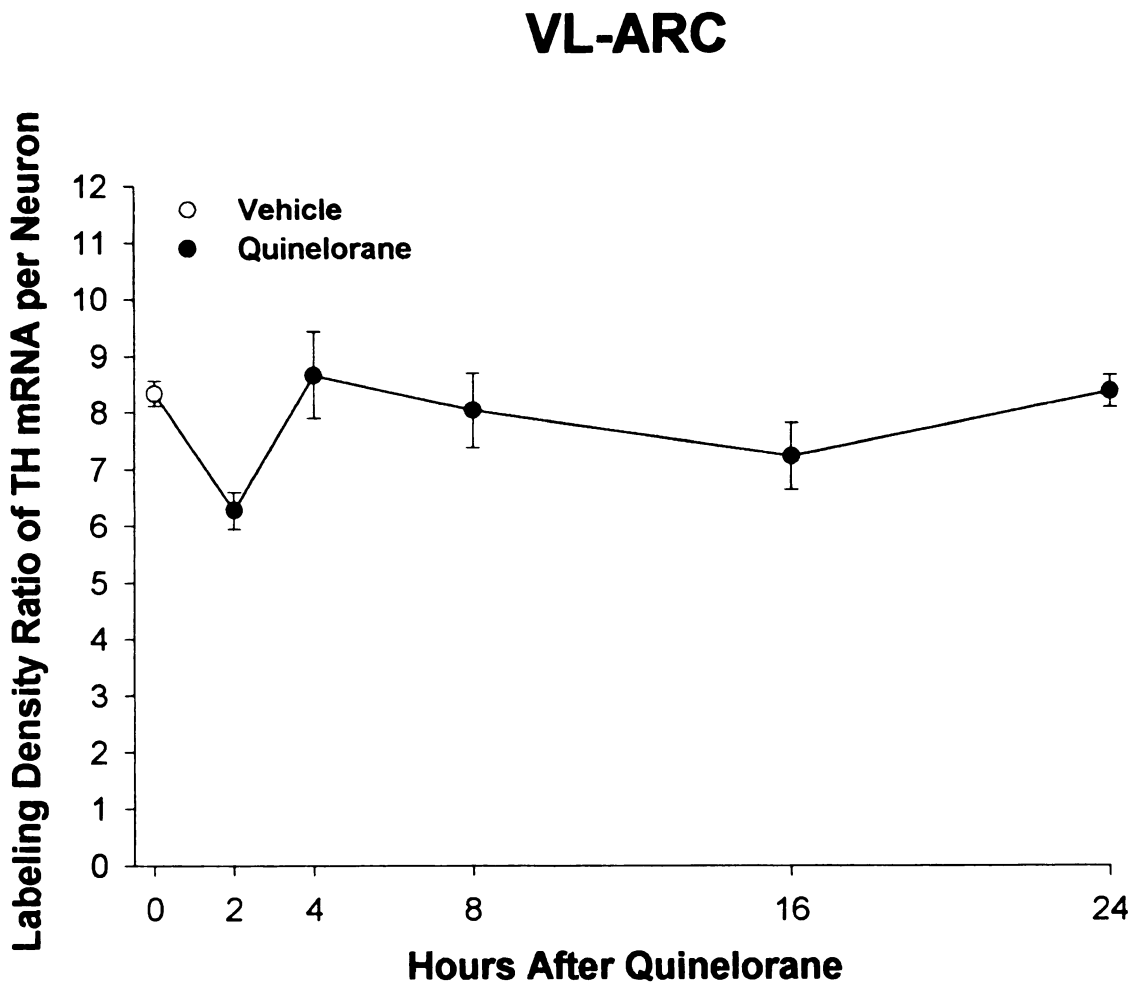

Figure 6.4 Time course effects of quinelorane on the labeling density ratio of TH mRNA per neuron in the VL-ARC. Rats were injected with quinelorane (filled symbols; 100 μg/kg; ip) and sacrificed 2, 4, 8, 16, or 24 h later. Zero time controls (open symbols) were injected with 0.9% saline vehicle (1 ml/kg; ip) and sacrificed 2 h later. Symbols represent the means and vertical lines ± 1 SEM from 6-8 animals.

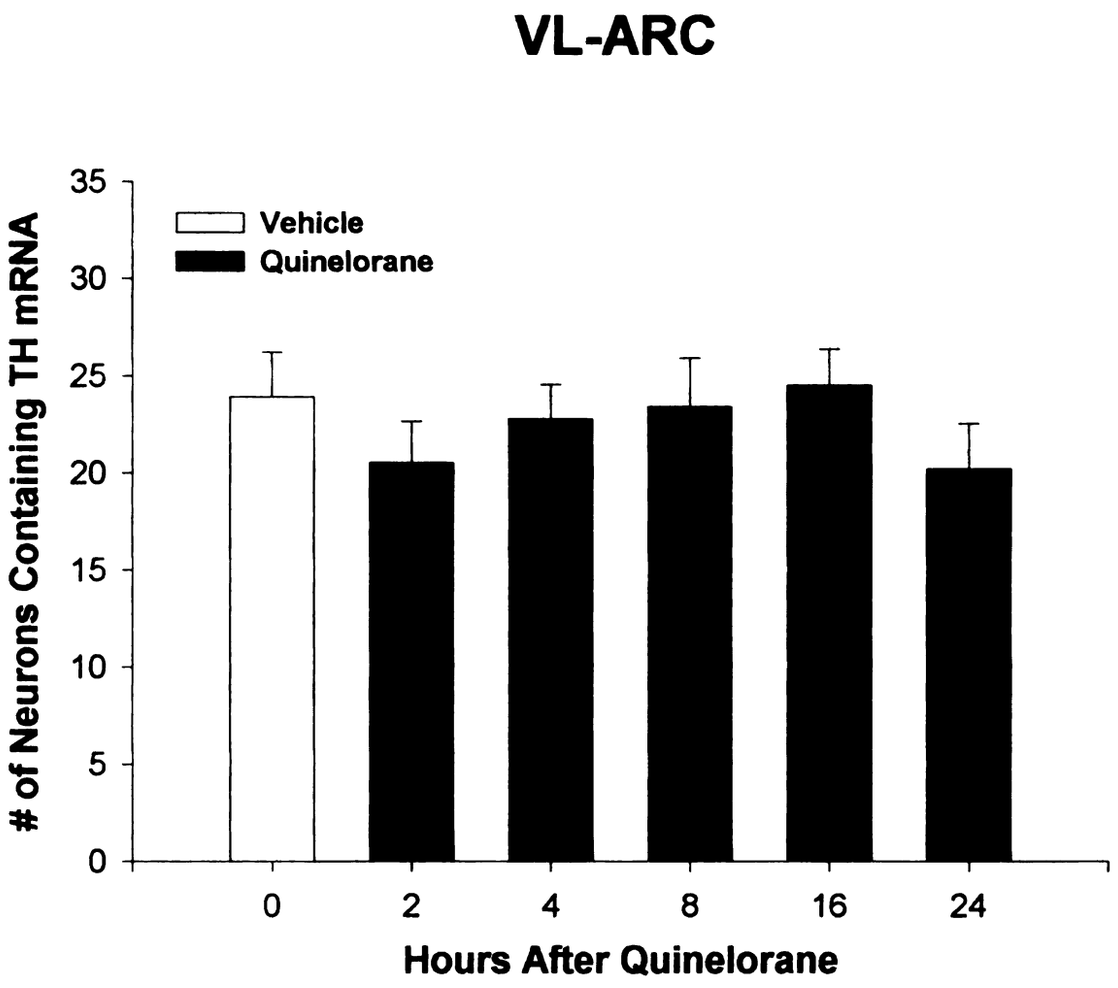

Figure 6.5 Time course effects of quinelorane on the numbers of neurons containing TH mRNA in the VL-ARC. Rats were injected with quinelorane (filled columns; 100 μg/kg; ip) and sacrificed 2, 4, 8, 16 or 24 h later. Zero time controls (open columns) were injected with 0.9% saline vehicle (1 ml/kg; ip) and sacrificed 2 h later. Columns represent the means and vertical lines + 1 SEM from 6-8 animals.

the numbers of neurons containing TH mRNA (**Figure 6.6; Bottom Panel**) or the labeling density ratio of TH mRNA (**Figure 6.6; Top Panel**).

To determine if the effects of quinelorane on TH mRNA were mediated by D2 receptors, a study was carried out using the D2 receptor antagonist raclopride. Blockade of D2 receptors had no effect *per se*, but reversed the stimulatory effects of quinelorane on TH mRNA expression in the DM-ARC (**Figure 6.7**). There were no changes in the numbers of neurons containing TH mRNA following raclopride or quinelorane administration (**Figure 6.8**). In the VL-ARC, neither quinelorane nor raclopride had any effect on the numbers of neurons containing TH mRNA (**Figure 6.10**) or on the labeling density ratio of TH mRNA of those neurons (**Figure 6.9**). In the MZI, neither quinelorane nor raclopride had any effect on the numbers of neurons containing TH mRNA (**Figure 6.11; Bottom Panel**) or the labeling density ratio of TH mRNA of those neurons (**Figure 6.11; Top Panel**).

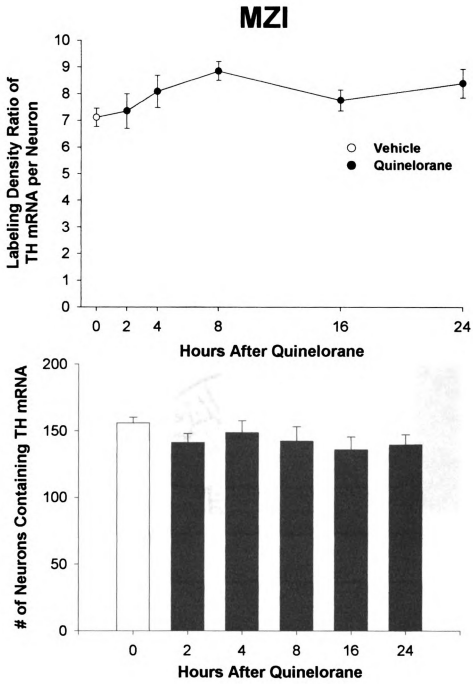

Figure 6.6 Time course effects of quinelorane on the numbers of neurons containing TH mRNA (**Bottom Panel**) and the labeling density ratio of TH mRNA per neuron (**Top Panel**) in the MZI. Rats were injected with quinelorane (filled symbols and columns; 100 μg/kg; ip) and sacrificed 2, 4, 8, 16, or 24 h later. Zero time controls (open symbols and columns) were injected with 0.9% saline vehicle (1 ml/kg; ip) and sacrificed 2 h later. Symbols and columns represent the means and vertical lines + 1 SEM from 6-8 animals.

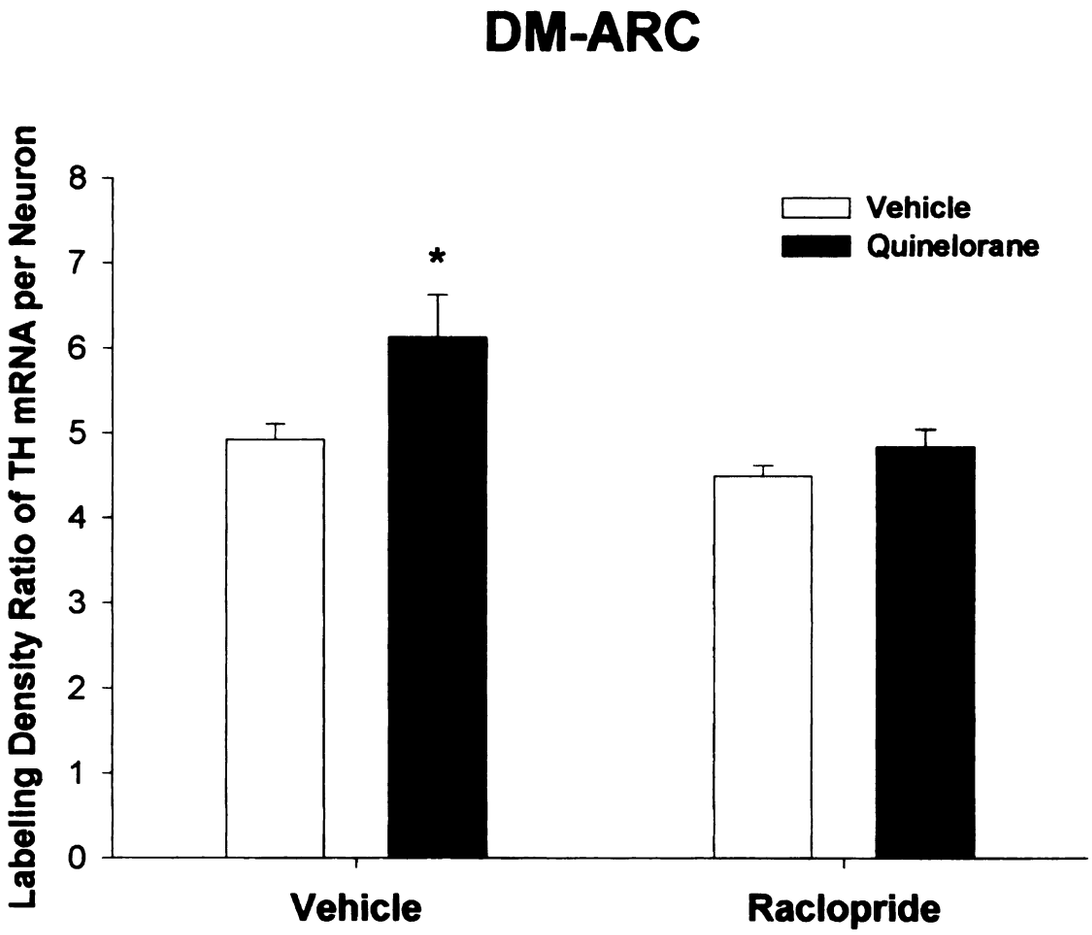

Figure 6.7 Effects of quinelorane on the labeling density ratio of TH mRNA per neuron in the DM-ARC of vehicle- or raclopride-treated rats. Rats were injected with either raclopride (3 mg/kg; ip) or its 0.9% saline vehicle (1 ml/kg; ip) 4 h prior to sacrifice, and with either quinelorane (100 μg/kg; ip) or its 0.9% saline vehicle (1 ml/kg; ip) 4 h prior to sacrifice. Columns represent the means and vertical lines + 1 SEM from 6-8 vehicle- (open columns) and quinelorane- (solid columns) treated rats. *, Values that are significantly different ($p<0.05$) from vehicle-treated rats.

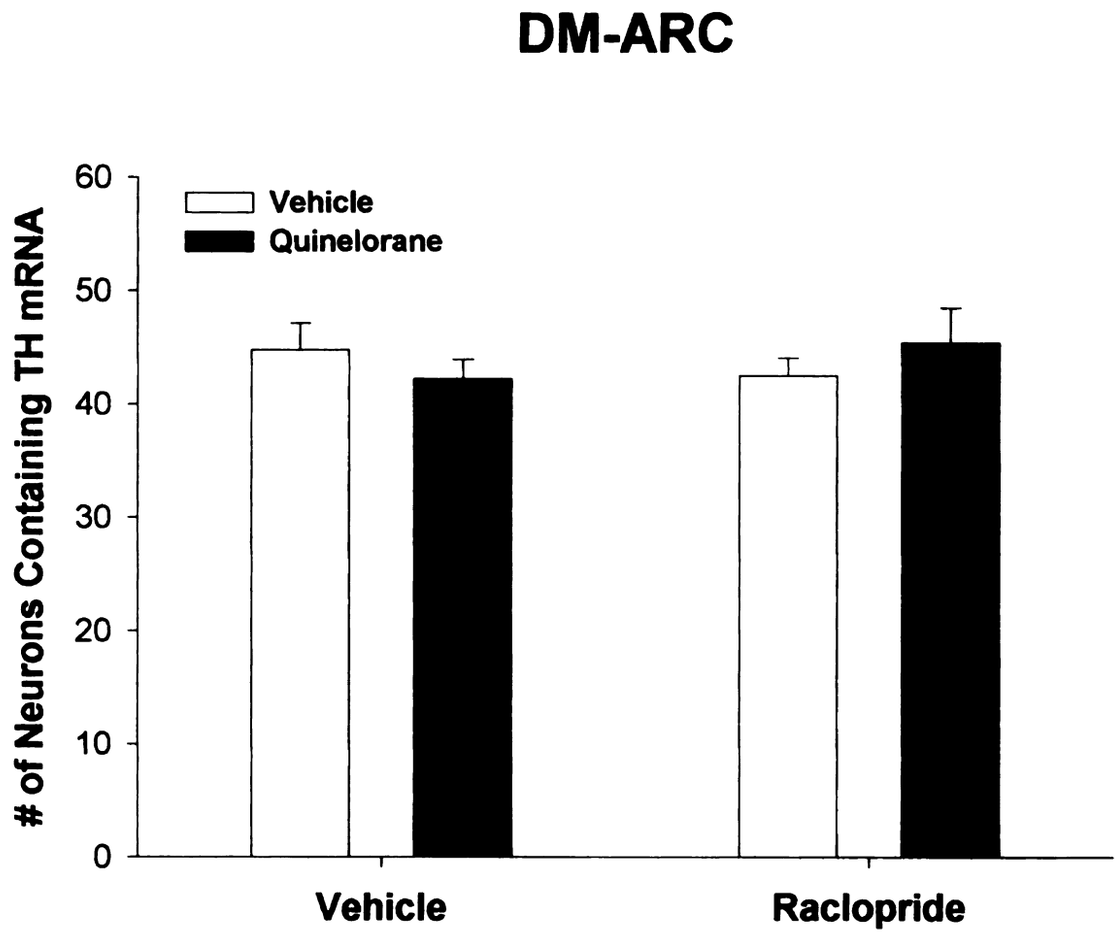

Figure 6.8 Effects of quinelorane on the numbers of neurons containing TH mRNA in the DM-ARC of vehicle- or raclopride-treated rats. Rats were injected with either raclopride (3 mg/kg; ip) or its 0.9% saline vehicle (1 ml/kg; ip) 4 h prior to sacrifice, and with either quinelorane (100 μg/kg; ip) or its 0.9% saline vehicle (1 ml/kg; ip) 4 h prior to sacrifice. Columns represent the means and vertical lines + 1 SEM from 6-8 vehicle- (open columns) and quinelorane- (solid columns) treated rats.

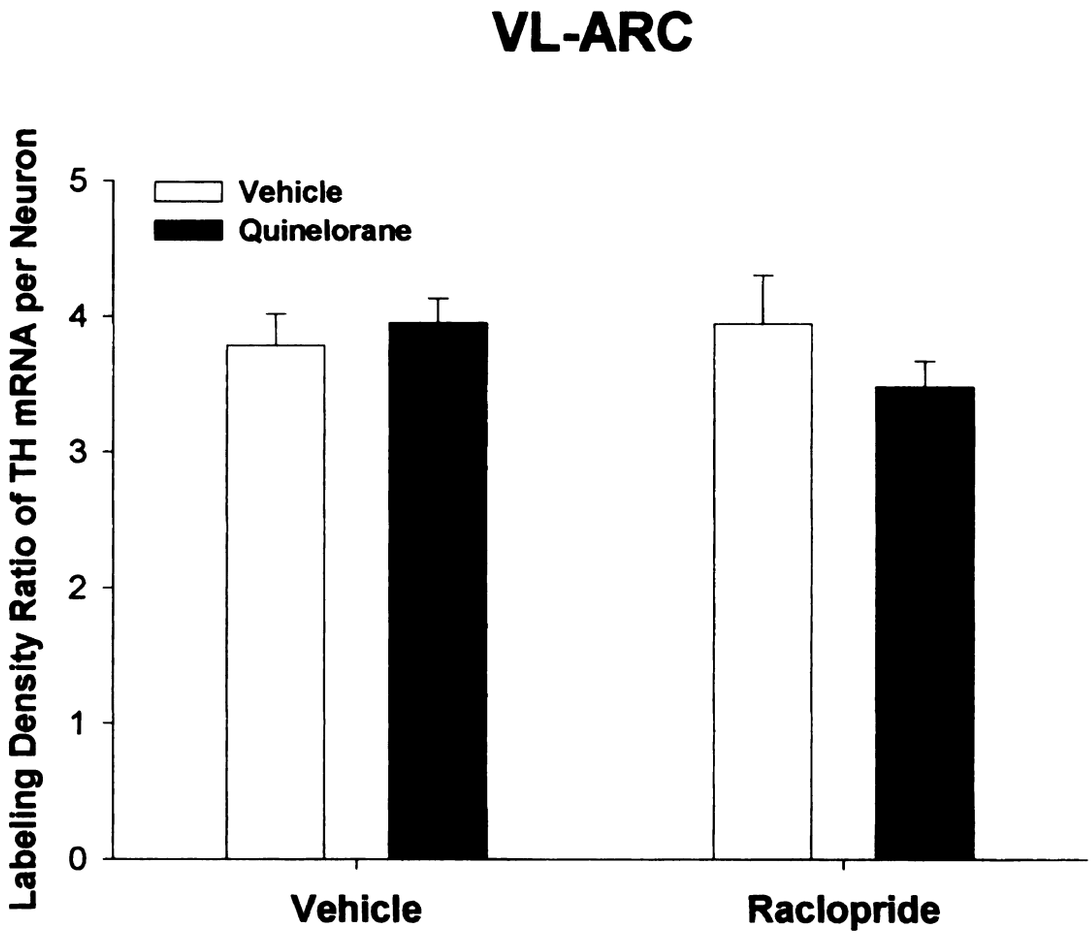

Figure 6.9 Effects of quinelorane on the labeling density ratio of TH mRNA per neuron in the VL-ARC of vehicle- or raclopride-treated rats. Rats were injected with either raclopride (3 mg/kg; ip) or its 0.9% saline vehicle (1 ml/kg; ip) 4 h prior to sacrifice, and with either quinelorane (100 μg/kg; ip) or its 0.9% saline vehicle (1 ml/kg; ip) 4 h prior to sacrifice. Columns represent the means and vertical lines + 1 SEM from 6-8 vehicle- (open columns) and quinelorane- (solid columns) treated rats.

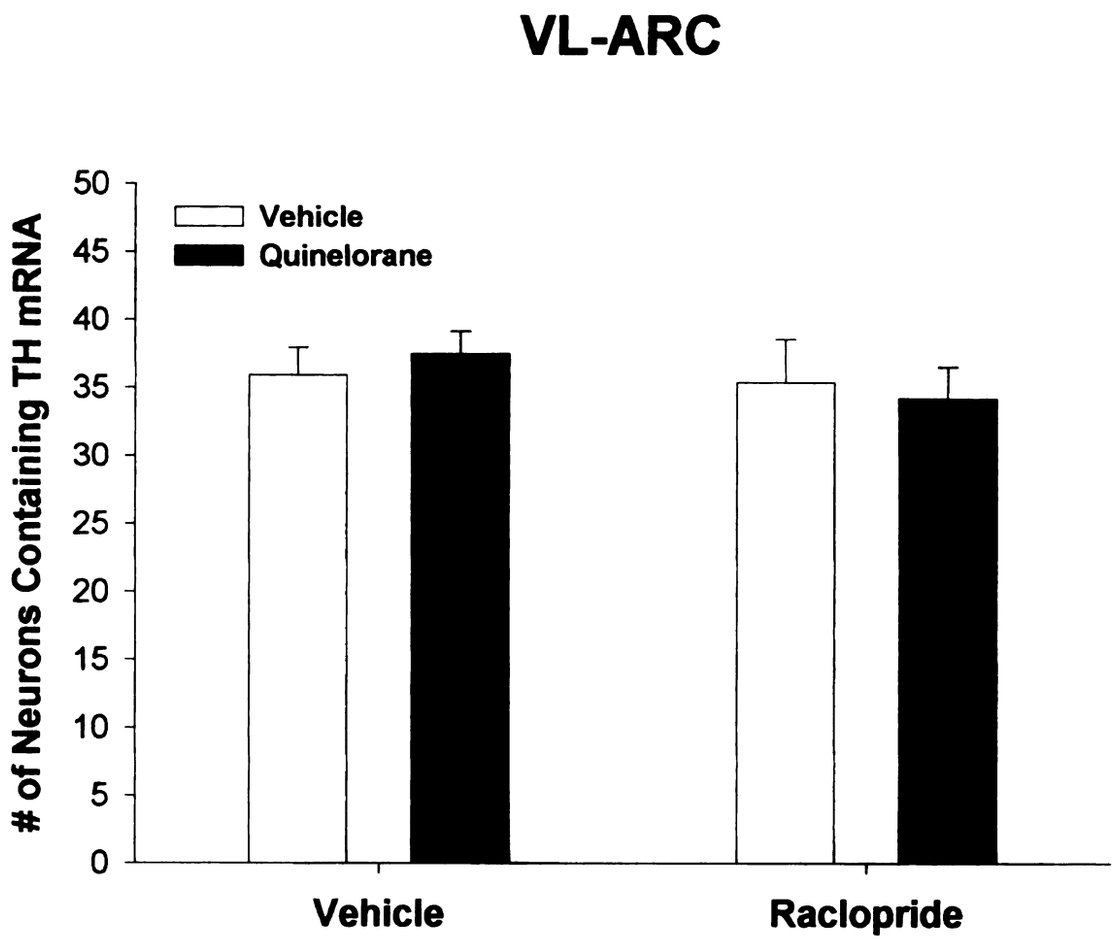

Figure 6.10 Effects of quinelorane on the numbers of neurons containing TH mRNA in the VL-ARC of vehicle- or raclopride-treated rats. Rats were injected with either raclopride (3 mg/kg; ip) or its 0.9% saline vehicle (1 ml/kg; ip) 4 h prior to sacrifice, and with either quinelorane (100 μg/kg; ip) or its 0.9% saline vehicle (1 ml/kg; ip) 4 h prior to sacrifice. Columns represent the means and vertical lines + 1 SEM from 6-8 vehicle- (open columns) and quinelorane- (solid columns) treated rats.

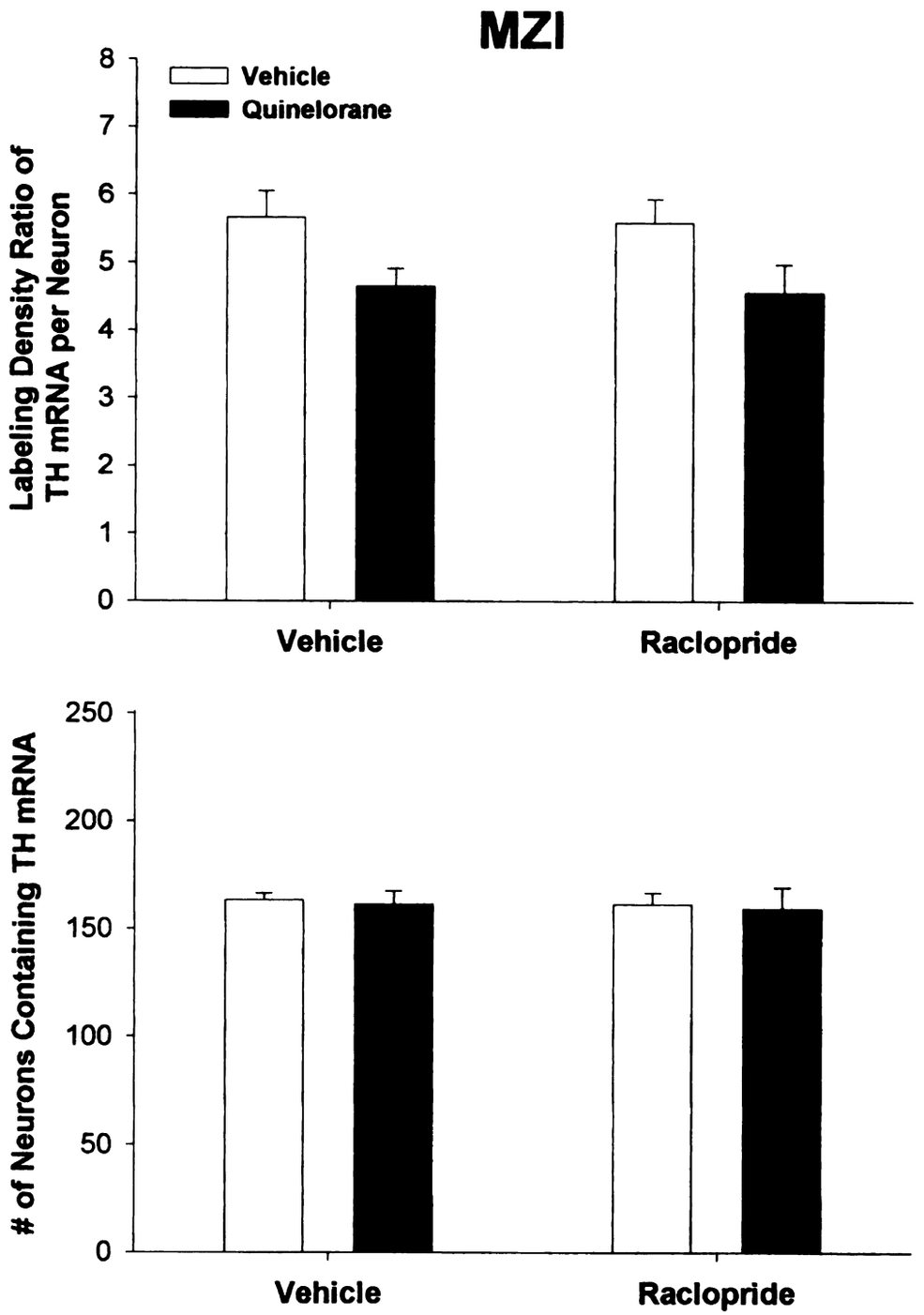

Figure 6.11 Effects of quinelorane on the numbers of neurons containing TH mRNA (**Bottom Panel**) and the labeling density ratio of TH mRNA per neuron (**Top Panel**) in the MZI of vehicle- or raclopride-treated rats. Rats were injected with either raclopride (3 mg/kg; ip) or its 0.9% saline vehicle (1 ml/kg; ip) 4 h prior to sacrifice, and with either quinelorane (100 μg/kg; ip) or its 0.9% saline vehicle (1 ml/kg; ip) 4 h prior to sacrifice. Columns represent the means and vertical lines + 1 SEM from 6-8 vehicle- (open columns) and quinelorane- (solid columns) treated rats. *, Values that are significantly different ($p<0.05$) from vehicle-treated rats.

DISCUSSION

The aim of the present study was to determine if D2 receptors regulate TH gene expression in TIDA neurons located in DM-ARC. The results from these studies reveal that activation of D2 receptors increases TH mRNA expression in a time dependent manner in a fixed population of TIDA neurons.

There were no changes in the numbers of neurons containing TH mRNA at any time point. This is in agreement with other *in situ* hybridization studies of TIDA neurons demonstrating a constant number of neurons expressing TH mRNA following exposure to bromocriptine, haloperidol, and PRL (Arbogast and Voogt, 1991) and during the estrous cycle (Arbogast and Voogt, 1994). The numbers of neurons containing TH mRNA is consistent with the numbers of TH-IR neurons counted in the immunohistochemical studies in Chapter 4. These results indicate that the amount of TH mRNA is increasing per neuron, as opposed to an increase in the numbers of neurons expressing TH mRNA.

This is different from Fos expression. There are increases in the actual numbers of TH-IR neurons containing Fos protein. This implies that there is a subset of TIDA neurons that are responsive to D2 receptor activation. These results can also be explained in part by the technique used for analyzing TH mRNA. All the neurons that contained TH mRNA were counted (which is equivalent to the numbers of TH-IR neurons found in immunohistochemical studies presented in Chapters 3, 4, and 5). However, for the analysis of the amount of TH mRNA present, not all neurons labeled with TH mRNA were evaluated. Only 10 of the "brightest" neurons were chosen (i.e. those neurons

that visually had the greatest amount of silver grains). While it is possible to determine the amount of TH mRNA expressed in each neuron (though time-prohibitive), it is not known if those neurons that were considered the brightest were also the neurons expressing Fos. Fos binds to the AP-1 site on the TH gene promoter, which can regulate the synthesis of TH. Therefore, it's very plausible that those neurons with increased Fos expression also have an increase in expression of TH mRNA.

D2 receptor-mediated activation of TH mRNA expression is delayed (4 h) and persistent (24 h) compared to D2 receptor-mediated activation of TIDA neuronal activity which increases rapidly (30 min) and is less prolonged (at least 8 h). The time course for the induction of TH mRNA varies depending on the experimental model and design. Many studies have used cell cultures for examining TH mRNA expression. *In vitro* studies using fetal hypothalamic cell cultures stimulated with forskolin (which induces the PKA pathway) also increases TH mRNA expression at 3 and 6 h (Tohei et al., 2000). However, studies using PC12 cells find TH mRNA expression as early as 1 h following stimulation with nerve growth factor and epidermal growth factor (Gizang-Ginsberg and Ziff, 1990 and 1994).

The results of the studies presented here are in contrast to Arbogast and Voogt (1995) who examined the effects of bromocriptine, a DA receptor agonist, on TH mRNA expression in TIDA neurons. Exposure to bromocriptine for 4 h decreases PRL and TH catalytic activity, but not TH mRNA expression. Other studies examining the induction of TH mRNA looked at chronic manipulations. In

the ARC, chronic administration of DA antagonist haloperidol increases PRL and TIDA neuronal activity as well as TH mRNA (Arbogast and Voogt, 1991), while chronic administration of bromocriptine results in decreases in these parameters (Arbogast and Voogt, 1991 and 1995). While bromocriptine is a DA receptor agonist and haloperidol a DA receptor antagonist, they are not selective for D2 receptors as are quinelorane and raclopride, respectively. Their effects on TIDA neurons are through their actions on PRL and not a direct effect on TIDA neurons.

D2 receptor induced activation of TH mRNA expression in TIDA neurons is unique in that a single acute stimulus induces a long term response, which has not been demonstrated in other dopaminergic systems (Arbogast and Voogt, 1991; Sirinathsinghji et al., 1994; Iwata et al., 2000). D2 receptor-mediated activation of TIDA neuronal activity last 8 h, but TH mRNA levels remained elevated for at least 16 more hours. Indeed, removal of suckling pups induced changes in TH mRNA expression in a similar time course as quinelorane administration (Wang et al., 1993; Berghorn et al., 2001); however, what should be noted is that the suckling pups were absent for the full 48 h of experiment. The response of TH mRNA expression following the return of suckling was not studied. Therefore, this study has a chronic stimulus, unlike the acute stimulation of D2 receptors.

Expression of TH mRNA is very prolonged after the acute activation of D2 receptors. However, under basal conditions, the half life of TH mRNA in the ARC is 6-7 h as estimated by transcription inhibition studies in slice explant cultures

(Maurer and Wray, 1997). TH can be regulated through a variety of mechanisms such as transcriptional regulation of mRNA levels, alternative RNA processing, regulation of RNA stability, translational regulation, feedback inhibition, allosteric regulation by polyanions, enzyme phosphorylation and enzyme stability (Kumer and Vrana, 1996). Though it is not possible to determine exactly what specific regulation of TH can account for the sustained TH mRNA expression, it is most likely regulation of transcription or mRNA stability. Transcription regulation can be mediated through changes in the transcription rate (due to the physiological state of the animal or various pharmacological agents) and/or through cell type-specific expression (Kumer and Vrana, 1996). Indeed other mechanisms of regulation of TH may be occurring under these experimental conditions; however, these mechanisms would most likely not be reflected as increases in mRNA.

The D2 receptor antagonist raclopride is able to reverse the stimulatory effect of quinelorane on TH mRNA expression indicating that the actions of quinelorane are mediated through D2 receptors. The lack of effect following blockade of D2 receptors also indicates that these neurons are not tonically inhibiting TH expression. These results correlate with the finding from neuronal activity studies demonstrating that D2 agonists induce an acute stimulatory response in TIDA neurons and this can be reversed with a D2 receptor antagonist (Eaton et al., 1993; Durham et al., 1997). This also correlates with the immunohistochemical findings in Chapter 4 showing that D2 receptors mediate

Fos expression in the DM-ARC in a time-dependent manner, and this increase precedes the increase in TH mRNA.

Taken together, these results suggest a causal relationship between D2 receptor-mediated stimulation of DA release from TIDA neurons and Fos-induced activation of TH synthesis. The increase in TH mRNA following activation of D2 receptors is delayed and prolonged compared to Fos expression as illustrated in Chapter 4. Neuronal activity increases 30 min following D2 receptor activation followed by immediate early gene expression at 2 h. This time course is similar to the effects of lactation and subsequent removal of suckling pups. Lactation inhibits TIDA neuronal activity, and FRA and TH mRNA expression. When suckling pups are removed from the mother, there is an increase in maternal TIDA neuronal activity (Selmanoff and Wise, 1981; de-Greef et al., 1981), followed by increases in FRA expression at 3 h (Hoffman et al., 1984) and TH mRNA at 6 h (Wang et al., 1993; Berghorn et al., 2001). These studies demonstrate a temporal effect of a stimulus: the induction of neuronal activity followed by an increase in immediate early gene expression and then an increase in long term gene expression. **Figure 6.12** summarizes the sequences of neuronal activity and gene expression following the activation of D2 receptors.

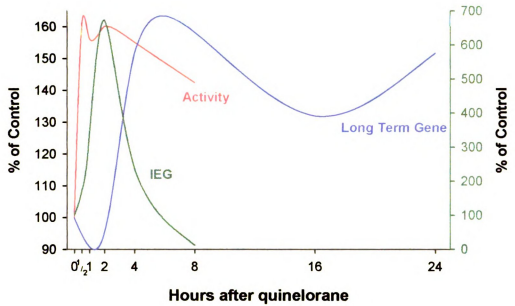

Figure 6.12 Sequence of TIDA neuronal activity and gene expression following activation of D2 receptors. D2 receptor-mediated DA release (red) precedes the stimulation of immediate early (green) and long term gene expression (blue) in the DM-ARC of TIDA neurons. Abbreviations: IEG, immediate early gene.

First there is a rapid increase in neuronal activity; associated with this is an increase in immediate early gene (Fos) expression. This is transitory and decreases in the face of sustained activity of the neurons. Following the induction and synthesis of Fos protein, it dimerizes with a Jun protein and binds to the AP-1 site (Curran and Franza, 1988; Angel and Karin, 1991) located within the TH gene promoter of DA neurons (Biguet et al., 1991; Icard-Liepkalns et al., 1992; Kumer and Vrana, 1996). Binding of the AP-1 site regulates the transcription and translation of TH. The increase in Fos is then followed by an increase in expression of the long term gene product, TH mRNA. This D2 receptor-mediated DA release precedes the stimulation of immediate early and

long term gene expression in the DM-ARC of TIDA neurons. This temporal sequence of events also supports a role for Fos in the regulation of TH mRNA in TIDA neurons.

In the VL-ARC, activation of D2 receptors has no effect on TH mRNA gene expression which coincides with the lack of stimulation of Fos expression in "DOPA-ergic" neurons in this region. Furthermore, the levels of TH mRNA remain relatively constant in the VL-ARC throughout the time course of the experiment, which is in contrast with the expression of Fos. As demonstrated in Chapter 4, there is a significant decrease in Fos expression at the 4 and 8 h time points. This decrease in Fos does not appear to have an effect on the level of TH mRNA. The results presented here demonstrate that "DOPA-ergic" neurons of the VL-ARC are regulated differently than the TIDA neurons of the DM-ARC. Studies pertaining to gene expression in the VL-ARC are very limited, thus no definitive conclusions can be made concerning the function or regulation of these neurons.

The IHDA neurons of the MZI are regulated by DA receptors as are the DA neurons of the mesotelencephalic systems (Lookingland and Moore, 1984). DA agonists and locally applied DA all decrease, while DA antagonists increase the activity of IHDA neurons (Moore and Lookingland, 1995; Eaton et al, 1992). Interestingly, the results from the present studies reveal that TH gene expression is not mediated through D2 receptors in IHDA neurons. Similar findings were found following administration of DA agonists (apomorphine and bromocriptine) and DA antagonists (eticlopride or haloperidol) (Arbogast and Voogt, 1991;

Sirinathsinghji et al., 1994; Iwata et al., 2000). There were no changes in the expression of TH mRNA in the IHDA neurons in the MZI following treatment with either bromocriptine or haloperidol (Arbogast and Voogt, 1991).

In the mesolimbic and nigrostriatal DA systems, time course studies examining the effects of the DA antagonist eticlopride on TH mRNA revealed no changes in expression at any time point (5 min to 24 h) in the ventral tegmental area or substantia nigra (Sirinathsinghji et al., 1994). Other studies determined that TH protein and TH mRNA are inhibited by chronic continuous infusion, but not intermittent injection of DA agonist apomorphine (Iwata et al., 2000). Chronic infusion of a DA agonist works at post-synaptic receptors via a long-loop feedback circuit to exert negative feedback on the DA neurons (Roth and Elsworth, 1995). This continuous negative feedback can lead to decreases in TH mRNA. A single injection of DA agonist or antagonist is capable to altering DA neuronal activity in the IHDA neurons of the MZI through pre-synaptic autoreceptors (Lookingland and Moore, 1984); however, TH mRNA is not affected by acute actions because antidromic stimulation (i.e. stimulation at pre-synaptic autoreceptors) does not effect gene expression (Icard-Liepkalns et al., 1992).

Taken together the results presented in this chapter reveal that D2 receptors regulate TH mRNA expression and support a role for Fos in this regulation in TIDA neurons in the DM-ARC. In addition, TH gene expression in the "DOPA-ergic" neurons in the VL-ARC and in IHDA neurons in the MZI is not regulated by D2 receptors.

CHAPTER SEVEN

THE ROLE OF FOS IN THE REGULATION OF TH GENE EXPRESSION IN TIDA NEURONS IN SUB DIVISIONS OF THE ARCUATE NUCLEUS

Introduction

In Chapter Four, it was demonstrated that stimulation of D2 receptors can increase expression of Fos in a time dependent manner in TIDA neurons located in the DM-ARC. These same neurons, as illustrated in Chapter Six, also have increases in TH mRNA following the activation of D2 receptors. The TH gene promoter contains an AP-1 site (**Figure 7.1**), and it has been well documented through *in vitro* studies that the Fos family of proteins dimerize with the Jun family of proteins and bind to the AP-1 site (Bohmann et al., 1987; Franza et al., 1988; Rauscher et al., 1988; Gizang-Ginsberg and Ziff, 1994) and thereby regulate TH transcription (Gizang-Ginsberg and Ziff, 1990; Icard-Liepkalns et al., 1992; Nagamoto-Combs et al., 1997; Sun and Tank, 2002). Indirect evidence has shown *in vivo* that increases in TH mRNA in TIDA neurons occur after the induction of FRA expression, suggesting that FRA may play a role in the regulation of TH in these neurons (Wang et al., 1993; Hoffman et al., 1994). There have not, however, been any *in vivo* studies examining a direct link between expression of Fos and TH.

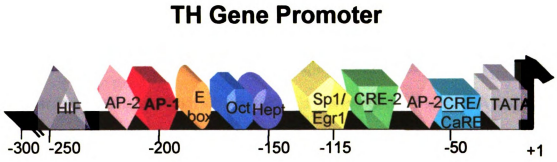

Figure 7.1 A schematic representation of the rat TH proximal gene promoter. The putative and functional elements involved in regulation of TH transcription are shown. **HIF:** Binding site for hypoxia-induced protein. **AP-2:** Binding site for AP-2 transcription factor found in adrenergic and noradrenergic neurons. **AP-1:** Highlighted in **red**; functional binding site for Fos/Jun; involved in stimulated expression. **E box:** Overlaps with AP-1 site and is involved with cell specificity. **Oct/Hept:** Binding site for Oct-2; represses expression. **Sp1/Egr1:** Binding sites for Sp1 and Egr1; involved in basal and stimulated expression. **CRE-2:** Binding site for CREB, involved in stimulated expression, works as a modulator possibly with CRE. **CRE/CaRE:** Binding site for cyclic AMP response element binding protein (CREB), regulates basal and cyclic AMP induced expression. **TATA box:** Conserved A•T-rich core promoter site. Abbreviations: AP, activated protein; CaRE, calcium response element; CRE, cAMP response element; Egr, early growth response; Hept, heptamer; HIF, hypoxia-inducible factor; Oct, octamer; Sp, specificity protein. Modified from Papanikolaou and Sabban, 2000.

The specific aim of these studies was to assess the role of Fos in the regulation of TH gene expression in TIDA neurons. The working hypothesis is that Fos mediates quinelorane-induced activation of TH mRNA expression in TIDA neurons. To determine a role for Fos, an experimental technique needed to be developed that could remove the influence of Fos. The use of antisense oligonucleotide probes provides a way to transiently "knock out" proteins, such as Fos by preventing the translation of specific mRNA's (Chiasson et al., 1992; Merchant, 1994; Hooper et al., 1994).

A gene is comprised of a specific sequence of bases. In order for a gene to be expressed a strand of mRNA must be copied from DNA that encodes the gene of interest. In double stranded DNA, one strand is the coding strand while the other is the template from which mRNA is transcribed. The mRNA sequence is thus complimentary to the DNA template strand and identical to the coding strand. Normally after the mRNA is transcribed, a ribosome can attach and carry out translation of proteins (Pilowsky and Suzuki, 1994). The objective of antisense oligonucleotides is to interfere with gene expression by preventing the translation of proteins from mRNA. Two of the primary mechanisms of antisense, translational arrest and activation of RNase H, are depicted in **Figure 7.2.**

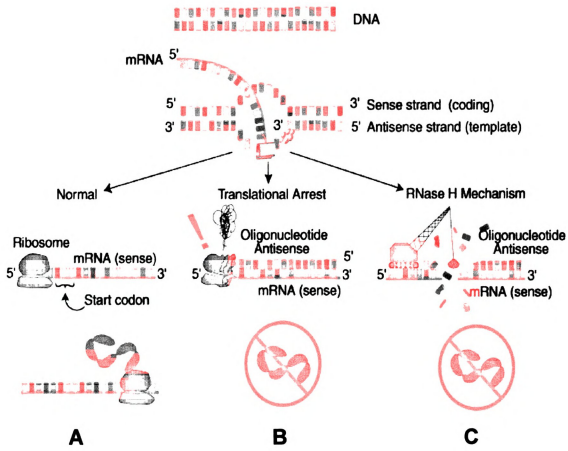

Figure 7.2 A schematic representation of the process of normal gene expression and two of the possible mechanisms by which antisense can attenuate translation of protein from mRNA. DNA consists of two complimentary strands: a coding strand and a template strand. mRNA is transcribed from the template strand so that its sequence is identical to the coding strand. Under normal conditions a ribosome attaches to the mRNA and carries out translation of the protein **(A)**. Antisense oligonucleotides bind to the mRNA and block the ribosome causing translational arrest **(B)** or induce RNase H which degrades RNA/DNA hybrids **(C)**. Modified from Pilowsky and Suzuki, 1994 and Zon, 1995.

An antisense oligonucleotide has a sequence that is complimentary to a portion of the mRNA of interest. The antisense and mRNA hybridize to form a complex that inhibits the ribosome and halts the translation of the desired protein (Pilowsky and Suzuki, 1994). RNase H is an endonuclease that recognizes RNA-DNA complexes and selectively cleaves the RNA strand (Zon, 1995). Once the RNA is cleaved, the antisense oligonucleotide is thought to dissociate from the duplex and become available to bind to a second target mRNA (Myers and Dean, 2000). In addition, it is possible for the antisense to enter the nucleus and interact directly with the gene of interest by forming a triple helix which would prevent transcription from taking place (Miller and Das, 1998). Intron-exon junction sites are also possible targets of antisense leading to inhibition of proper splicing and consequently the maturation of the transcript (Phillips and Gyurko, 1995; Koller et al., 2000).

Certain aspects need to be considered when employing antisense oligonucleotides including the route of administration, dose, and time course of action. The route of administration can either be directly into the target brain tissue (intracerebral) or into the cerebrospinal fluid of the ventricle (intracerebroventricular; icv). Several studies have examined the effects of *c-fos* antisense in the striatum using a direct intracerebral route of administration (Chiasson et al., 1992; Merchant, 1994; Dragunow et al., 1993). The injection of antisense intracerebrally causes tissue damage and necrosis, and consequently this route is best used in a brain region that is relatively large (like the striatum) where adequate viable tissue remains to detect a response. Icv administration is

more appropriate when multiple brain regions are to be studied or the target region of interest is small and difficult to reach without causing extensive tissue damage.

The proper dose of antisense is in accordance with the route of administration and certain characteristics of the target gene. Small doses of only 1 or 2 nmol are sufficient for intracerebral injections (Chiasson et al., 1992) since the oligonucleotide is injected directly into the tissue and concentrated in a small area. Larger doses ranging from 10-50 nmol are necessary for icv administration due to dilution in the CSF (Chiu et al., 1994). If the gene of interest has low basal expression and turns over rapidly (such as Fos) one injection may be sufficient (Merchant, 1994). However, if the basal expression of the gene is high and the turnover is low (such as a receptor), then multiple dosing is usually necessary before effective protein depletion is observed (Qin et al., 1995). The timing of administration of *c-fos* antisense has been examined from 4-72 hours with 10-12 hours being the most successful at consistently preventing the translation of Fos protein (Hooper et al., 1994; Morrow et al., 1999).

Preliminary studies for this thesis were carried out to determine the most appropriate route of administration that would assure delivery of Fos antisense oligonucleotide to the ARC. Intracerebral injections resulted in extensive tissue damage from the cannula and fluid pressure from the injection of antisense. It was concluded that the ARC is too small to be suited for intracerebral injections. Accordingly, one aim of the studies included in this chapter was to establish the effective dose of antisense oligonucleotide probe when administered via icv route

of administration. Initial experiments established the time course effect of *c-fos* antisense and its specificity in preventing Fos expression in quinelorane-stimulated TIDA neurons. The last experiment used these parameters to determine the effect of *c-fos* antisense on TH mRNA in TIDA neurons under basal conditions and following activation of D2 receptors. For comparison, the effects of icv *c-fos* antisense administration on Fos and TH mRNA expression in the "DOPA-ergic" neurons of the VL-ARC and the IHDA neurons of the MZI were also studied.

Materials and Methods

Gonadally intact male rats were used in these experiments. Care and handling of the rats was carried out as described in **Materials and Methods** in Chapter 2. Following appropriate treatments in the first set of experiments, rats anesthetized with Equithesin and perfused with 4% paraformaldehyde. Brains were removed and sectioned as described in **Materials and Methods** in Chapter 2. The identification of TH-IR neurons and Fos-IR nuclei in the ARC and MZI was carried out using immunohistochemical procedures in **Materials and Methods** in Chapter 2. The ARC sections were sorted into rostral, middle, and caudal regions and then visually partitioned into DM-ARC and VL-ARC.

For the last experiment, rats were decapitated and brains were quickly frozen and sectioned. The identification of neurons containing TH mRNA in the ARC and MZI was carried out using *in situ* hybridization procedures as described in **Materials and Methods** in Chapter 2. Results from studies presented earlier

demonstrated that the stimulation of Fos expression was consistent throughout the rostrocaudal extent of the DM-ARC. Because there were no differences in this response, the *in situ* studies focused on the middle ARC. The middle ARC sections were chosen and then visually partitioned into DM-ARC and VL-ARC.

c-fos antisense, *c-fos* "sense", and *c-fos* "nonsense" probes were prepared as described in **Material and Methods** in Chapter 2. The antisense probe sequence was complimentary to the translation start site of *c-fos* mRNA. The "sense" probe sequence consisted of the same sequence as the translation start site, and the "nonsense" probe had the same G:C:T:A content of the antisense probe but had a mismatched sequence of bases.

Results

Figure 7.3 depicts the time course effects of *c-fos* antisense on the percentage of quinelorane-stimulated TH-IR neurons containing Fos-IR nuclei in the DM-ARC. Quinelorane significantly increased Fos expression in the rostral, middle and caudal regions of the DM-ARC as previously demonstrated in Chapters 4 and 5. *c-fos* antisense significantly blocked quinelorane-induced Fos expression in a time dependent manner, effective by 6 h in the rostral and middle regions, and by 12 h in the caudal region of the DM-ARC. As seen in previous studies, the distribution of TH-IR neurons declines through the rostral-caudal extent of the DM-ARC, but there were no changes in the numbers of TH-IR neurons at any time point following *c-fos* antisense administration within each

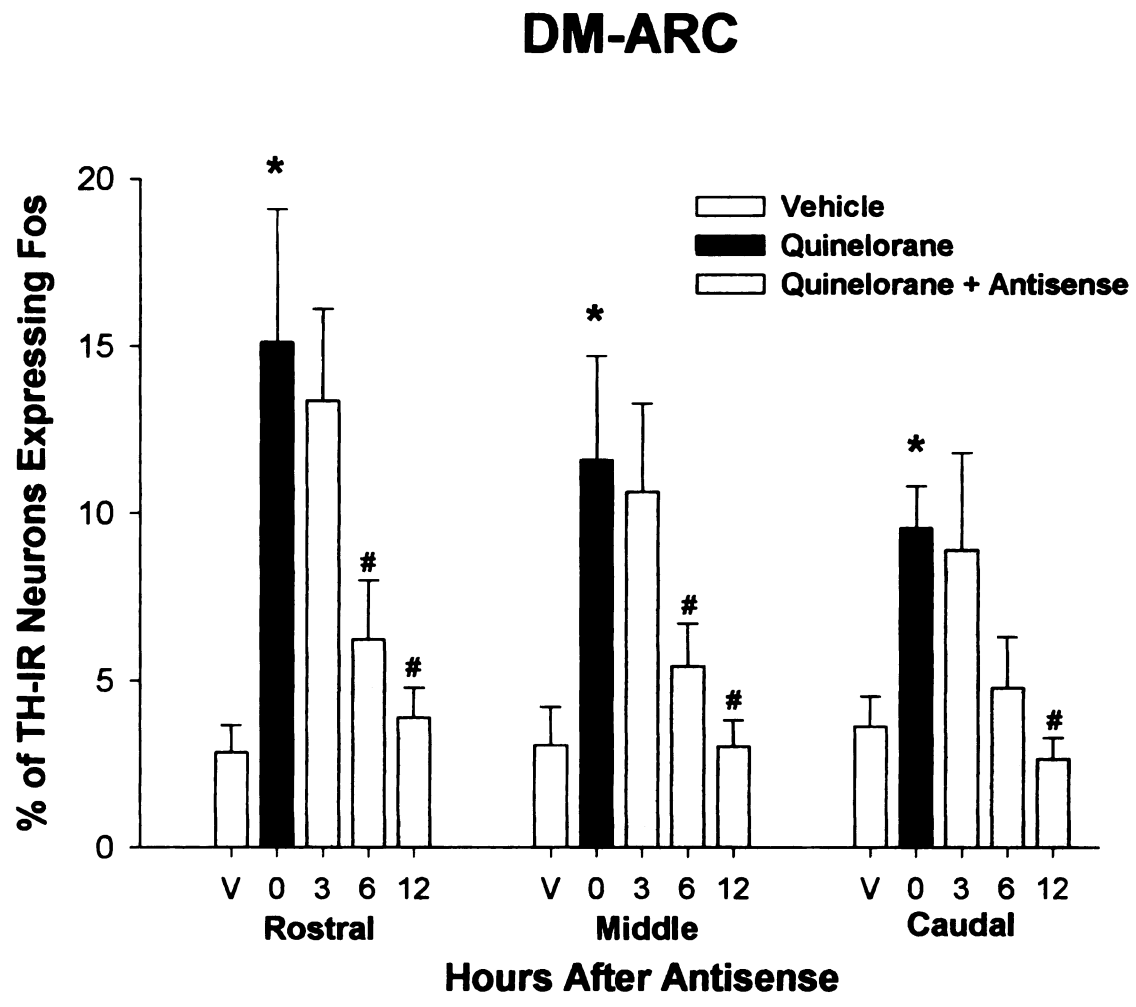

Figure 7.3 Time course effects of *c-fos* antisense oligonucleotide on the percentage of TH-IR neurons expressing Fos in the rostral, middle, and caudal regions of the DM-ARC in quinelorane-treated rats. Rats were injected with *c-fos* antisense (gray columns; 40 nmol/rat; icv) 3, 6 or 12 h prior to sacrifice and with quinelorane (100 μg/kg; ip) 2 h prior to sacrifice. Zero time controls (black columns) were injected with 0.9% saline vehicle (3 μl/rat; icv) 12 h prior to sacrifice and with quinelorane (100 μg/kg; ip) 2 h prior to sacrifice. Vehicle controls (open columns) were injected with 0.9% saline vehicle (3 μl/rat; icv) 12 h prior to sacrifice and again with 09% saline (1 ml/kg; ip) 2 h prior to sacrifice. Columns represent the means and vertical lines + 1 SEM from 6-8 animals. *, Values for quinelorane-treated rats that are significantly different ($p<0.05$) from vehicle-treated controls. #, Values for antisense-treated rats that are significantly different ($p<0.05$) from quinelorane-treated rats.

region of the DM-ARC (**Figure 7.4**). In contrast, *c-fos* antisense had no effect on the percentage of TH-IR neurons expressing Fos (**Figure 7.5**) or the numbers of TH-IR neurons throughout the rostral-caudal extent of the VL-ARC in quinelorane-treated animals (**Figure 7.6**). In the MZI, there were no changes in the numbers of TH-IR neurons (**Figure 7.7; Bottom panel**) or in the percentage of those neurons containing Fos-IR nuclei (**Figure 7.7; Top panel**) at any timepoint following *c-fos* antisense administration.

To characterize the specificity of *c-fos* antisense in preventing Fos expression, a study was carried out using *c-fos* "sense" and *c-fos* "nonsense" oligonucleotides. While *c-fos* antisense was able to block the stimulatory effects of quinelorane on the percentage of TH-IR neurons expressing Fos, *c-fos* "sense" and *c-fos* "nonsense" probes had no effect (**Figure 7.8**). There were no changes in the numbers of TH-IR neurons following the administration of quinelorane or the three different *c-fos* oligonucleotides (**Figure 7.9**). In the VL-ARC, quinelorane significantly decreased the percentage of TH-IR neurons expressing Fos in the middle and caudal regions; however, *c-fos* antisense, "sense" and "nonsense" had no effect in quinelorane-treated animals (**Figure 7.10**). There were no changes in the numbers of TH-IR neurons within each rostrocaudal region of the VL-ARC following any of the treatments (**Figure 7.11**). In the MZI, there were no changes in the numbers of TH-IR neurons (**Figure 7.12**; **Bottom panel**) or in the percentage of those neurons containing Fos-IR nuclei (**Figure 7.12; Top panel**) following any of the treatments.

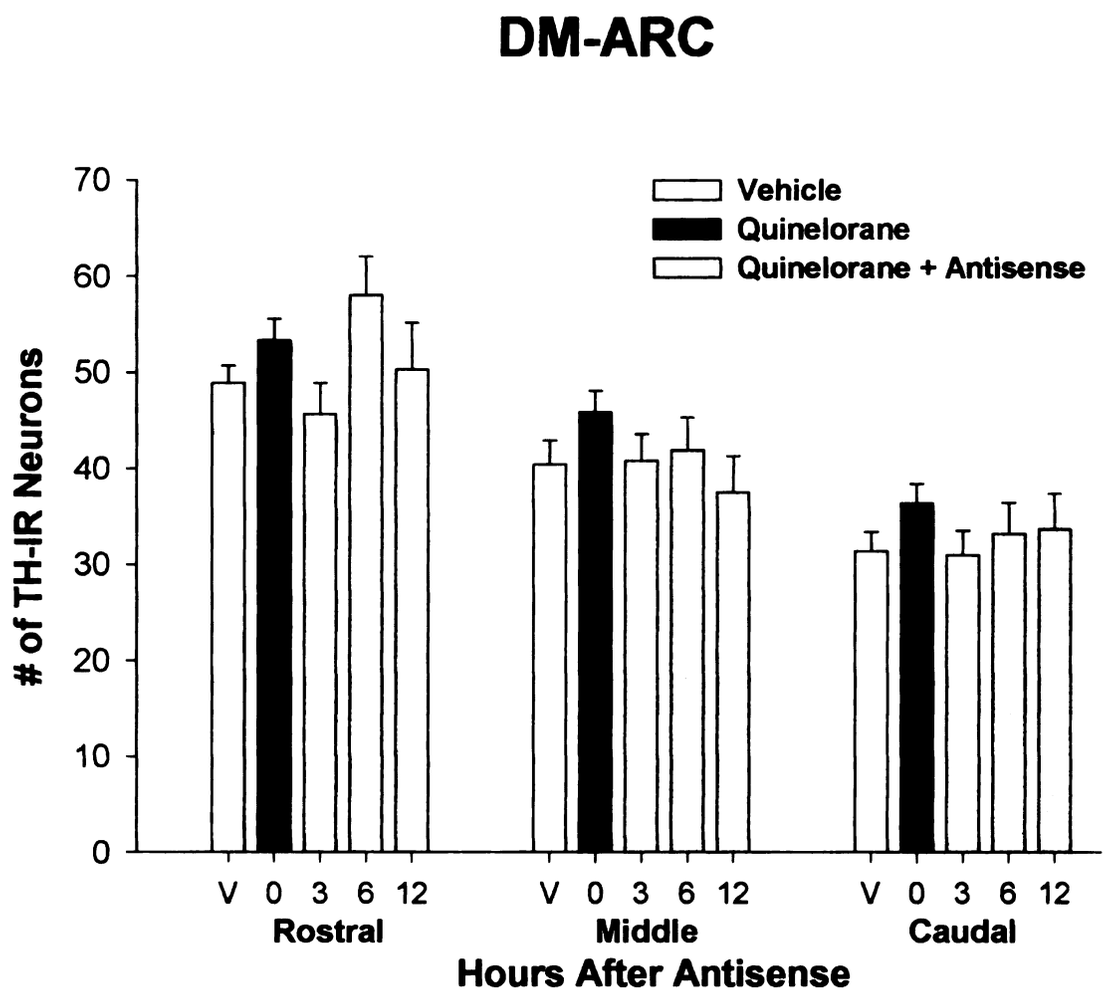

Figure 7.4 Time course effects of *c-fos* antisense oligonucleotide on the numbers of TH-IR neurons in the rostral, middle, and caudal regions of the DM-ARC in quinelorane-treated rats. Rats were injected with *c-fos* antisense (gray columns; 40 nmol/rat; icv) 3, 6 or 12 h prior to sacrifice and with quinelorane (100 μg/kg; ip) 2 h prior to sacrifice. Zero time controls (black columns) were injected with 0.9% saline vehicle (3 μl/rat; icv) 12 h prior to sacrifice and with quinelorane (100 μg/kg; ip) 2 h prior to sacrifice. Vehicle controls (open columns) were injected with 0.9% saline vehicle (3 μl/rat; icv) 12 h prior to sacrifice and again with 09% saline (1 ml/kg; ip) 2 h prior to sacrifice. Columns represent the means and vertical lines + 1 SEM from 6-8 animals.

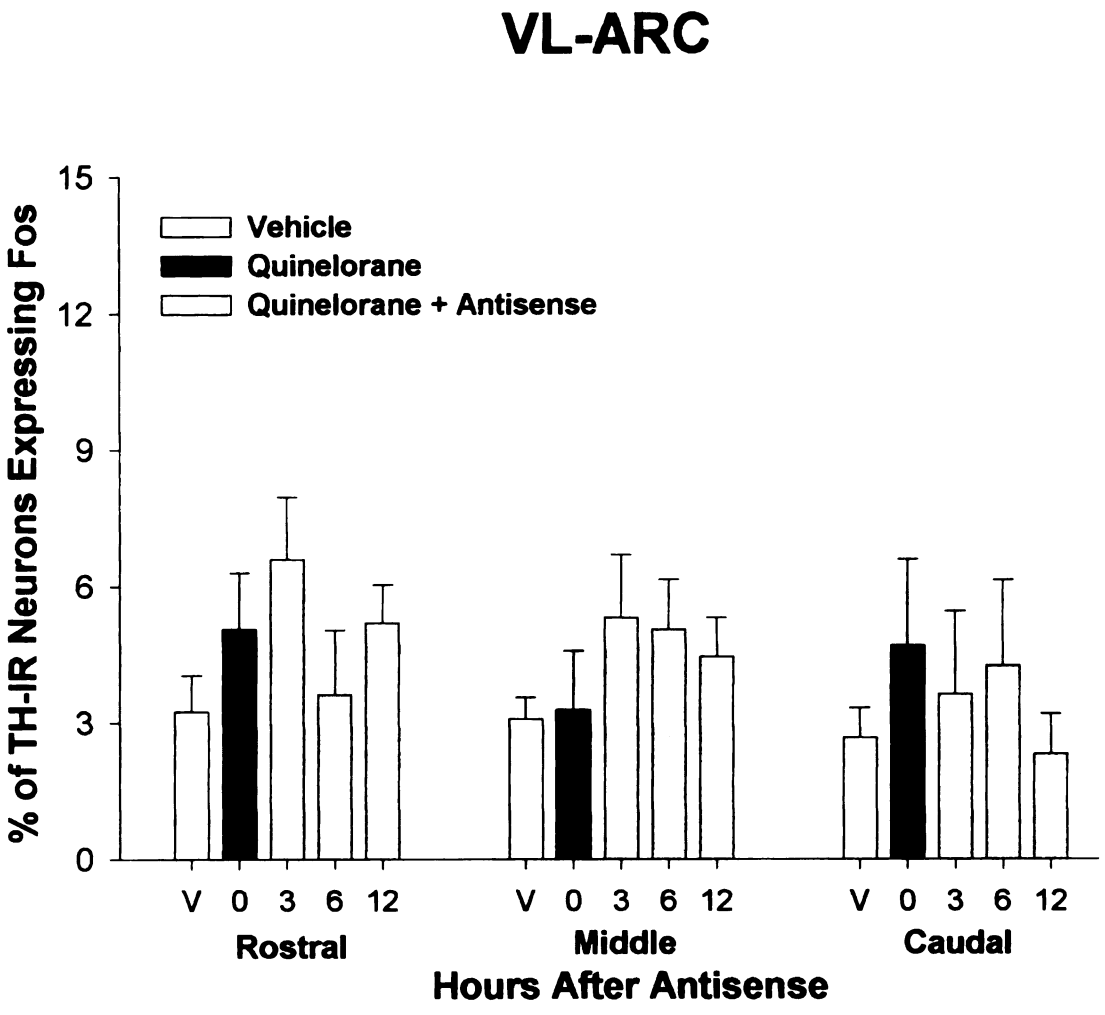

Figure 7.5 Time course effects of *c-fos* antisense oligonucleotide on the percentage of TH-IR neurons expressing Fos in the rostral, middle, and caudal regions of the VL-ARC in quinelorane-treated rats. Rats were injected with *c-fos* antisense (gray columns; 40 nmol/rat; icv) 3, 6 or 12 h prior to sacrifice and with quinelorane (100 μg/kg; ip) 2 h prior to sacrifice. Zero time controls (black columns) were injected with 0.9% saline vehicle (3 μl/rat; icv) 12 h prior to sacrifice and with quinelorane (100 μg/kg; ip) 2 h prior to sacrifice. Vehicle controls (open columns) were injected with 0.9% saline vehicle (3 μl/rat; icv) 12 h prior to sacrifice and again with 09% saline (1 ml/kg; ip) 2 h prior to sacrifice. Columns represent the means and vertical lines + 1 SEM from 6-8 animals.

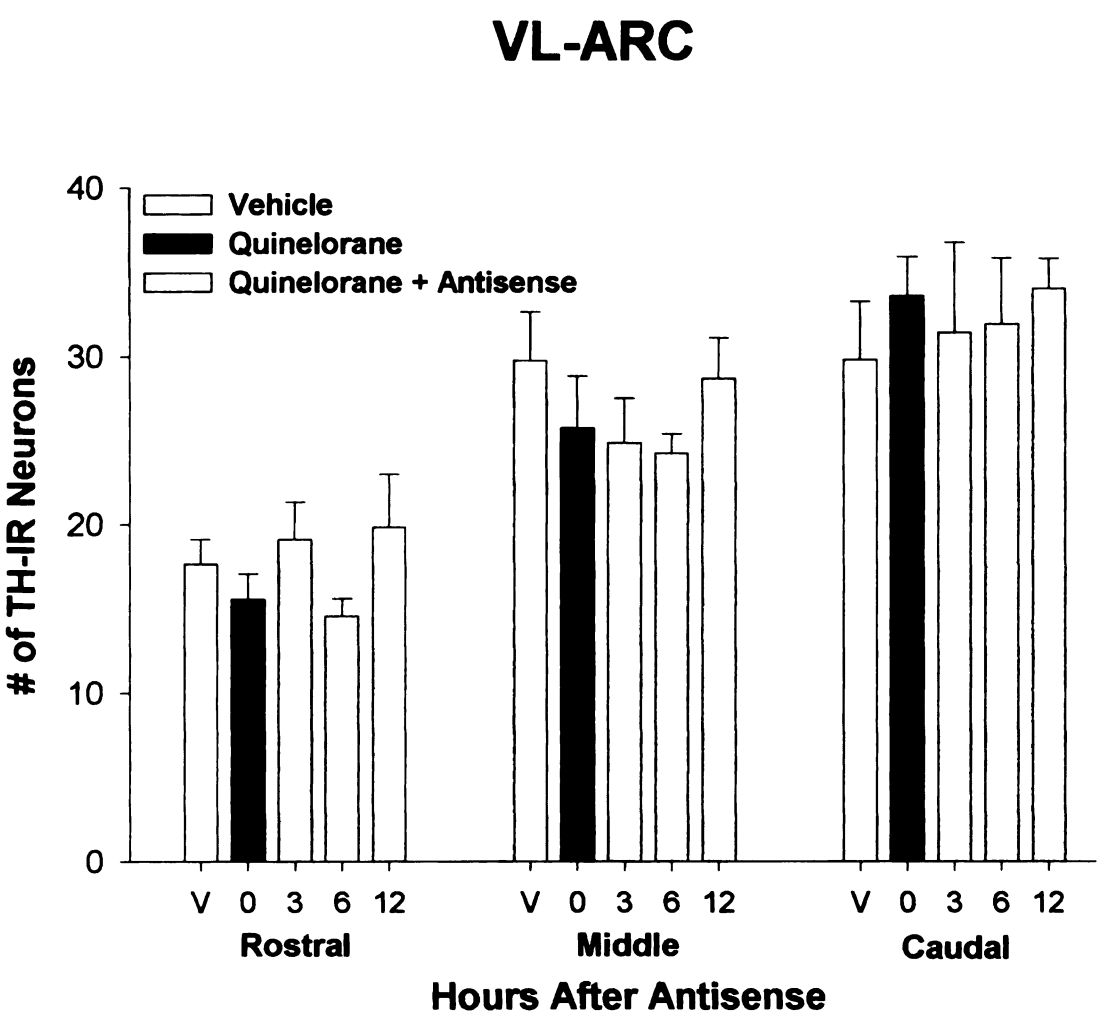

Figure 7.6 Time course effects of *c-fos* antisense oligonucleotide on the numbers of TH containing neurons in the rostral, middle, and caudal regions of the VL-ARC in quinelorane-treated rats. Rats were injected with *c-fos* antisense (gray columns; 40 nmol/rat; icv) 3, 6 or 12 h prior to sacrifice and with quinelorane (100 μg/kg; ip) 2 h prior to sacrifice. Zero time controls (black columns) were injected with 0.9% saline vehicle (3 μl/rat; icv) 12 h prior to sacrifice and with quinelorane (100 μg/kg; ip) 2 h prior to sacrifice. Vehicle controls (open columns) were injected with 0.9% saline vehicle (3 μl/rat; icv) 12 h prior to sacrifice and again with 09% saline (1 ml/kg; ip) 2 h prior to sacrifice. Columns represent the means and vertical lines + 1 SEM from 6-8 animals.

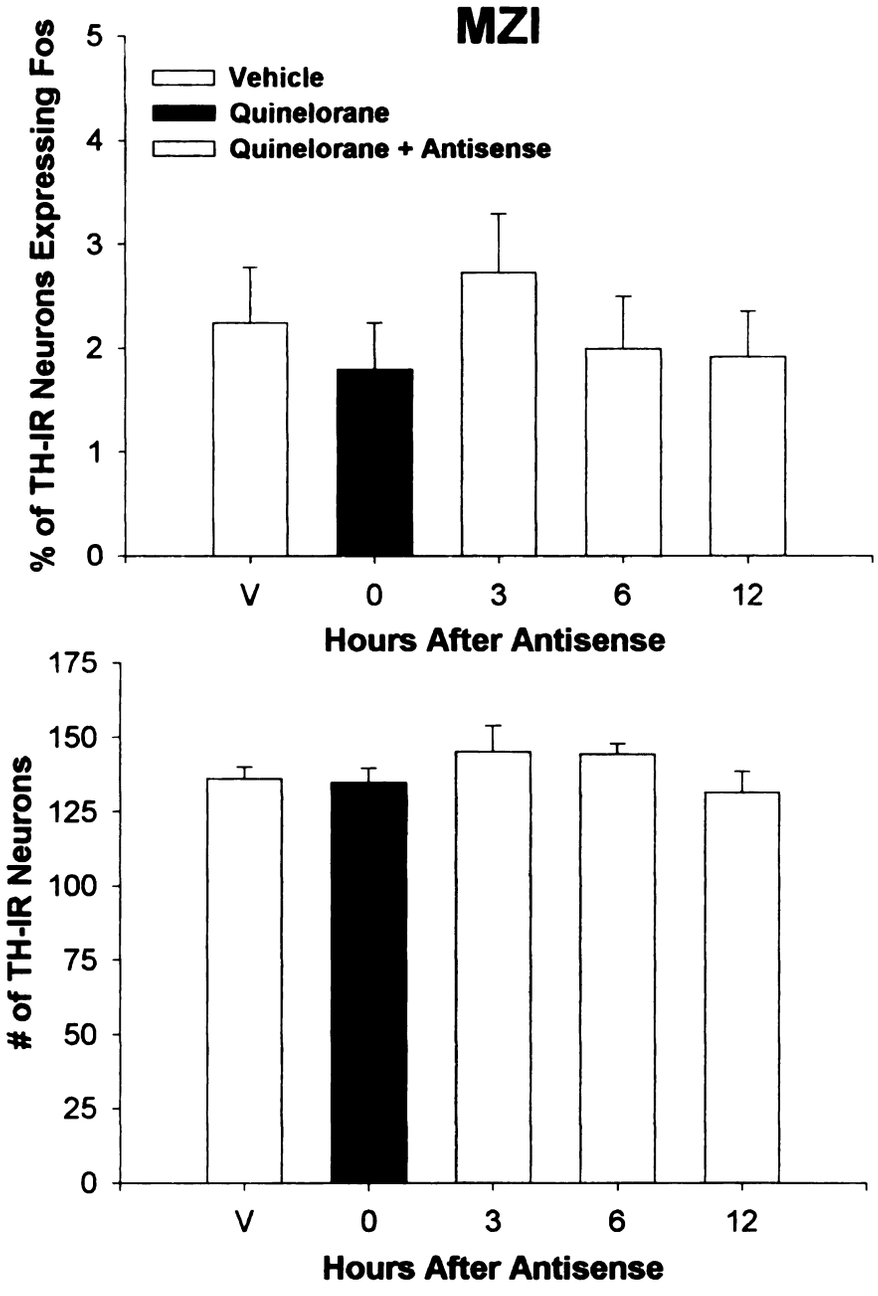

Figure 7.7 Time course effects of *c-fos* antisense oligonucleotide on the numbers of TH-IR neurons (**Bottom Panel**) and the percentage of these neurons expressing Fos (**Top Panel**) in the MZI in quinelorane-treated rats. Rats were injected with *c-fos* antisense (gray columns; 40 nmol/rat; icv) 3, 6 or 12 h prior to sacrifice and with quinelorane (100 μg/kg; ip) 2 h prior to sacrifice. Zero time controls (black columns) were injected with 0.9% saline vehicle (3 μl/rat; icv) 12 h prior to sacrifice and with quinelorane (100 μg/kg; ip) 2 h prior to sacrifice. Vehicle controls (open columns) were injected with 0.9% saline vehicle (3 μl/rat; icv) 12 h prior to sacrifice and again with 09% saline (1 ml/kg; ip) 2 h prior to sacrifice. Columns represent the means and vertical lines + 1 SEM from 6-8 animals.

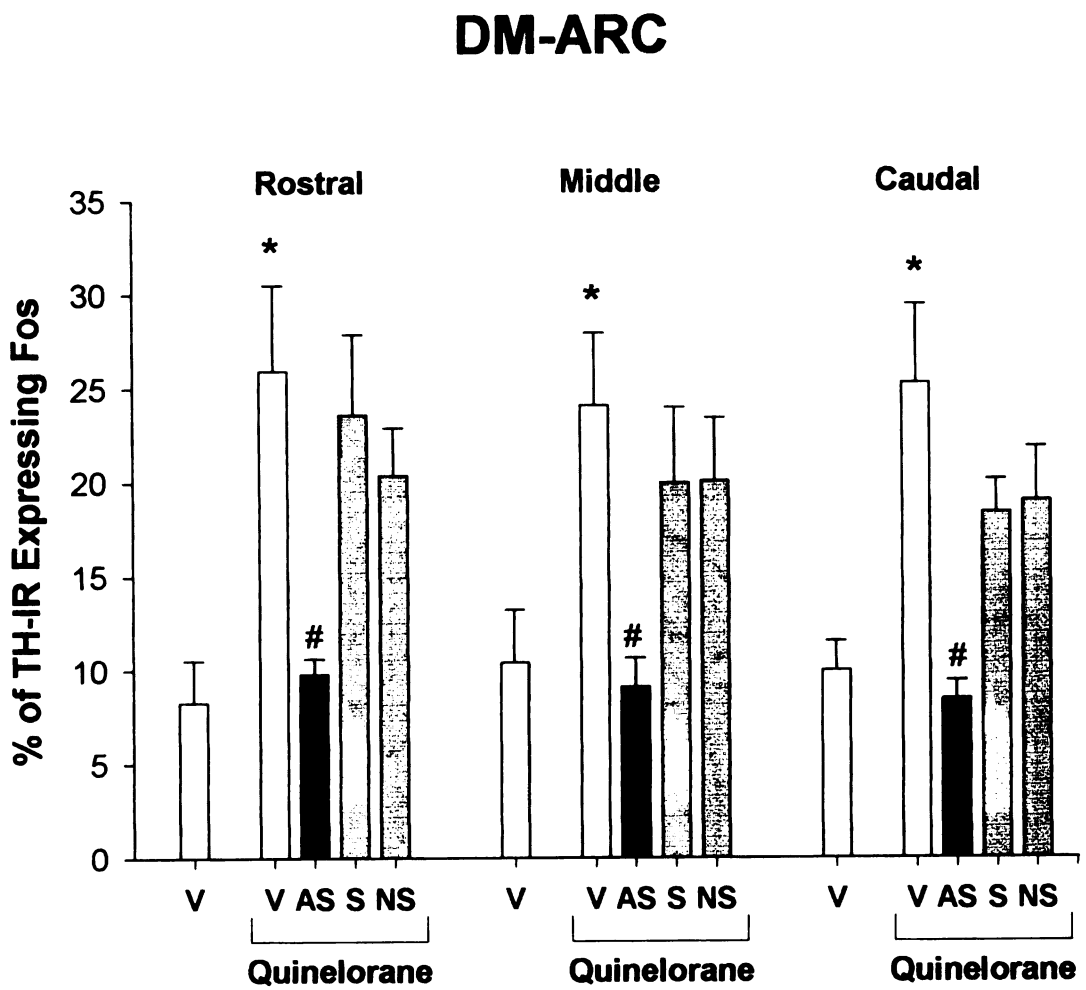

Figure 7.8 Effects of *c-fos* antisense, sense, and nonsense oligonucleotides on the percentage of TH-IR neurons expressing Fos in the rostral, middle, and caudal regions of the DM-ARC in quinelorane-treated rats. Rats were injected with *c-fos* antisense (AS; 40 nmol/rat; icv), *c-fos* sense (S; 40 nmol/rat; icv), or *c-fos* nonsense (NS; 40 nmol/rat; icv) 12 h prior to sacrifice and with quinelorane (100 μg/kg; ip) 2 h prior to sacrifice. Controls were injected with 0.9% saline vehicle (3 μl/rat; icv) 12 h prior to sacrifice and with either quinelorane (V; 100 μg/kg; ip) or 0.9% saline (V; 1 ml/kg; ip) 2 h prior to sacrifice. Columns represent the means and vertical lines + 1 SEM from 6-8 animals. *, Values that are significantly different ($p<0.05$) from vehicle-treated controls. #, Values that are significantly different ($p<0.05$) from quinelorane-treated controls. Abbreviations: AS, antisense; NS, nonsense; S, sense; V, vehicle.

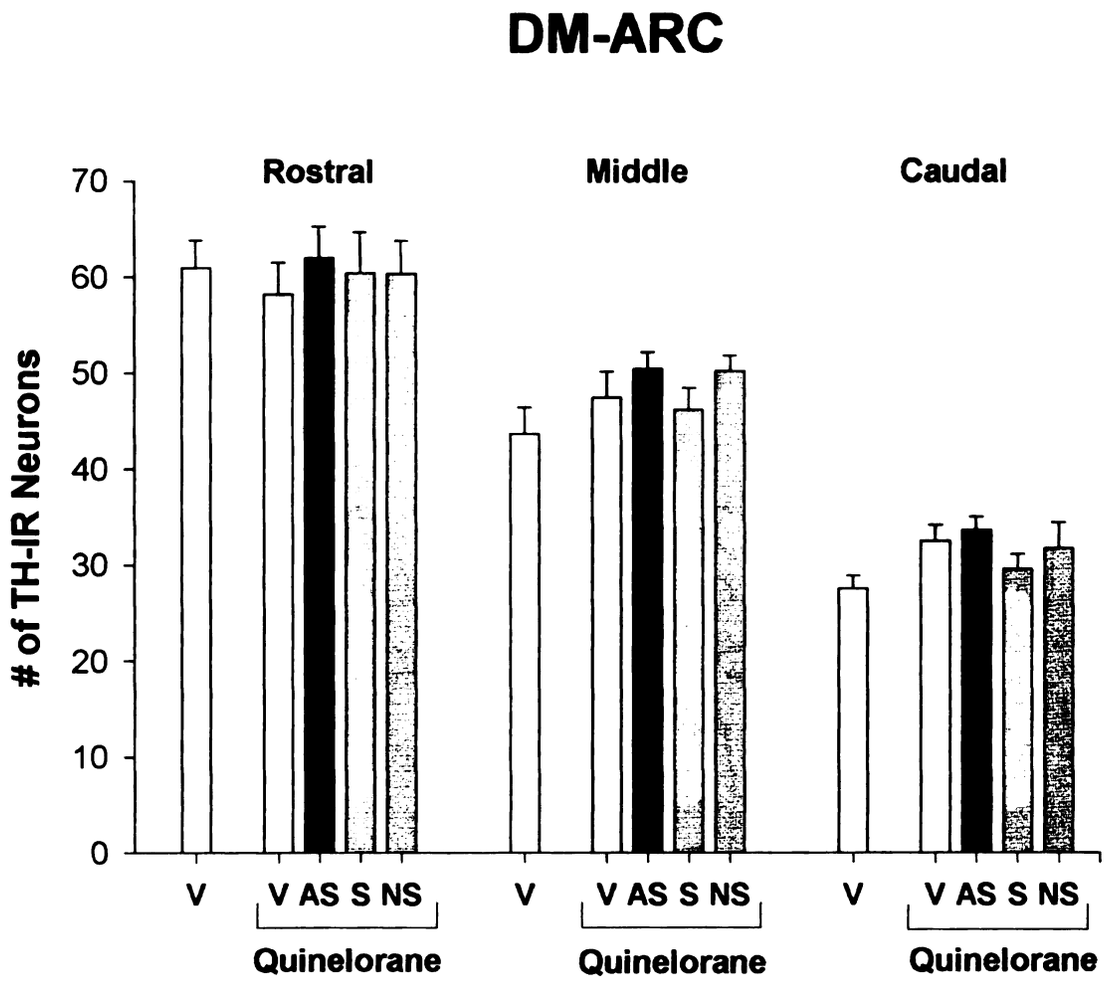

Figure 7.9 Effects of *c-fos* antisense, sense, and nonsense oligonucleotides on the numbers of TH containing neurons in the rostral, middle, and caudal regions of the DM-ARC in quinelorane-treated rats. Rats were injected with *c-fos* antisense (AS; 40 nmol/rat; icv), *c-fos* sense (S; 40 nmol/rat; icv) or *c-fos* nonsense (NS; 40 nmol/rat; icv) 12 h prior to sacrifice and with quinelorane (100 μg/kg; ip) 2 h prior to sacrifice. Controls were injected with 0.9% saline vehicle (3 μl/rat; icv) 12 h prior to sacrifice and with either quinelorane (V; 100 μg/kg; ip) or saline (V; 1 ml/kg; ip) 2 h prior to sacrifice. Columns represent the means and vertical lines + 1 SEM from 6-8 animals. Abbreviations: AS, antisense; NS, nonsense; S, sense; V, vehicle.

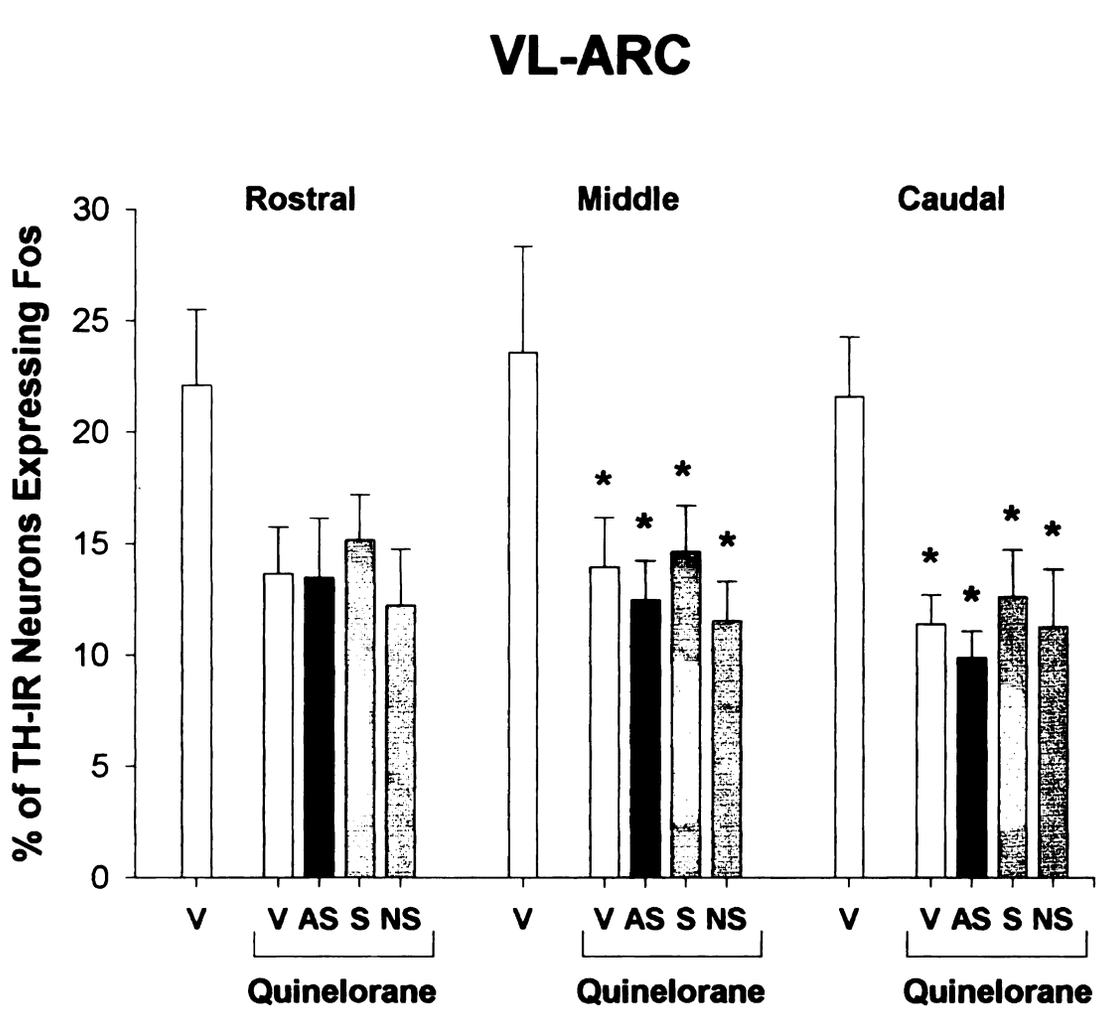

Figure 7.10 Effects of *c-fos* antisense, sense, and nonsense oligonucleotides on the percentage of TH-IR neurons expressing Fos in the rostral, middle, and caudal regions of the VL-ARC in quinelorane-treated rats. Rats were injected with *c-fos* antisense (AS; 40 nmol/rat; icv), *c-fos* sense (S; 40 nmol/rat; icv), or *c-fos* nonsense (NS; 40 nmol/rat; icv) 12 h prior to sacrifice and with quinelorane (100 μg/kg; ip) 2 h prior to sacrifice. Controls were injected with 0.9% saline vehicle (3 μl/rat; icv) 12 h prior to sacrifice and with either quinelorane (V; 100 μg/kg; ip) or 0.9% saline (V; 1 ml/kg; ip) 2 h prior to sacrifice. Columns represent the means and vertical lines + 1 SEM from 6-8 animals. *, Values that are significantly different ($p<0.05$) from vehicle-treated controls. Abbreviations: AS, antisense; NS, nonsense; S, sense; V, vehicle.

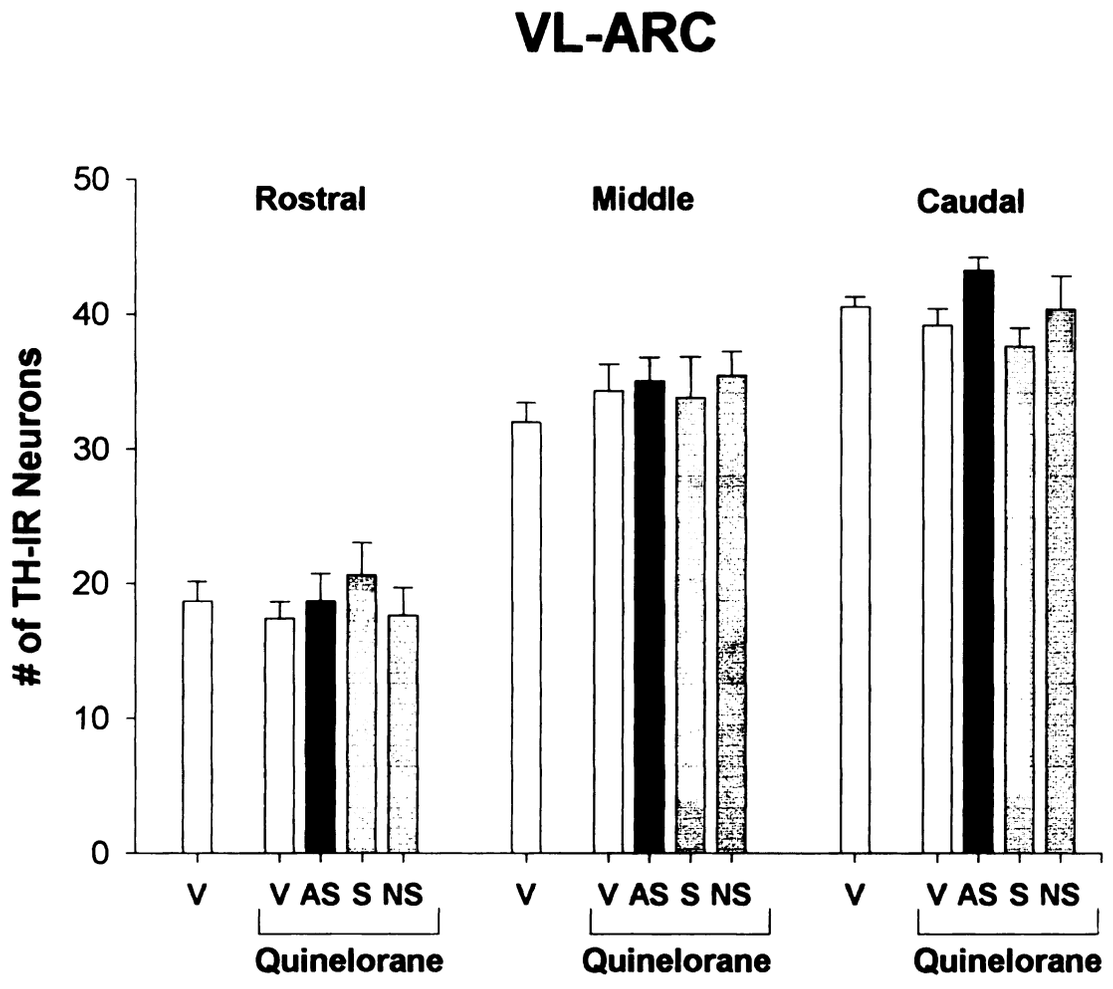

Figure 7.11 Effects of *c-fos* antisense, sense, and nonsense oligonucleotides on the numbers of TH-IR neurons in the rostral, middle, and caudal regions of the VL-ARC in quinelorane-treated rats. Rats were injected with *c-fos* antisense (AS; 40 nmol/rat; icv), *c-fos* sense (S; 40 nmol/rat; icv) or *c-fos* nonsense (NS; 40 nmol/rat; icv) 12 h prior to sacrifice and with quinelorane (100 μg/kg; ip) 2 h prior to sacrifice. Controls were injected with 0.9% saline vehicle (3 μl/rat; icv) 12 h prior to sacrifice and with either quinelorane (V; 100 μg/kg; ip) or saline (V; 1 ml/kg; ip) 2 h prior to sacrifice. Columns represent the means and vertical lines + 1 SEM from 6-8 animals. Abbreviations: AS, antisense; NS, nonsense; S, sense; V, vehicle.

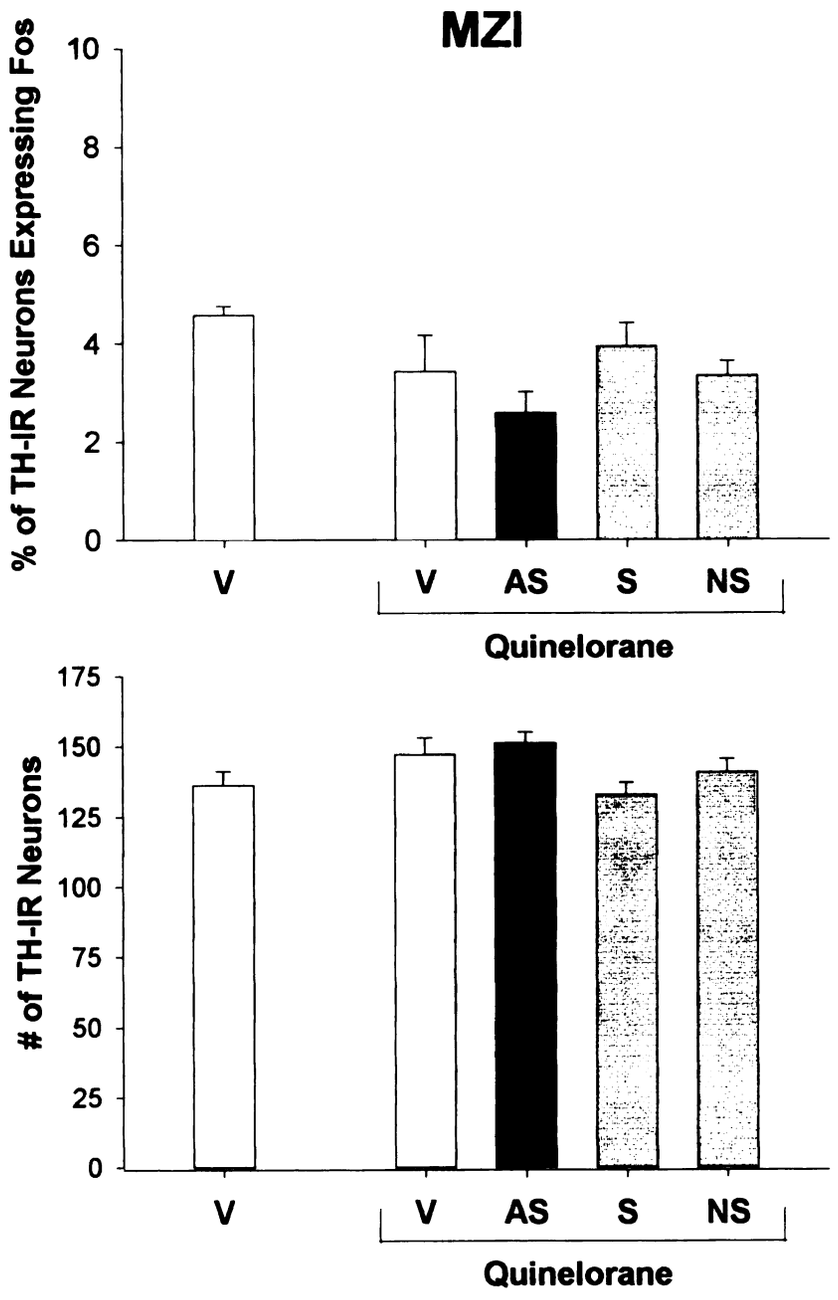

Figure 7.12 Effects of *c-fos* antisense, sense, and nonsense oligonucleotides on the numbers of TH-IR neurons (**Bottom Panel**) and the percentage of these neurons expressing Fos (**Top Panel**) in the MZI in quinelorane-treated rats. Rats were injected with *c-fos* antisense (AS; 40 nmol/rat; icv), *c-fos* sense (S; 40 nmol/rat; icv) or *c-fos* nonsense (NS; 40 nmol/rat; icv) 12 h prior to sacrifice and with quinelorane (100 μg/kg; ip) 2 h prior to sacrifice. Controls were injected with 0.9% saline vehicle (3 μl/rat; icv) 12 h prior to sacrifice and with either quinelorane (V; 100 μg/kg; ip) or saline (V; 1 ml/kg; ip) 2 h prior to sacrifice. Columns represent the means and vertical lines + 1 SEM from 6-8 animals. Abbreviations: AS, antisense; NS, nonsense; S, sense; V, vehicle.

Once the *c-fos* antisense was determined to block Fos expression, a study was carried out to determine if Fos mediates quinelorane-induced stimulation of TH mRNA expression in TIDA neurons. Quinelorane significantly increased the labeling density ratio of TH mRNA per cell in the DM-ARC (**Figure 7.13**). *c-fos* antisense in the absence of quinelorane had no effect on the labeling density ratio of TH mRNA in the DM-ARC; however, it was able to block quinelorane-induced increases in the labeling density ratio. The "sense" and "nonsense" oligonucleotide probes had no effect. There were no changes in the numbers of neurons that contain TH mRNA in the DM-ARC following any of the treatments (**Figure 7.14**). In the VL-ARC, there were no changes in the labeling density ratio (**Figure 7.15**) or in the numbers of neurons containing TH mRNA following any of the treatments (**Figure 7.16**). Similarly, there were no changes in the labeling density ratio (**Figure 7.17; Top Panel**) or in the number of neurons containing TH mRNA (**Figure 7.17; Bottom Panel**) in the IHDA neurons of the MZI.

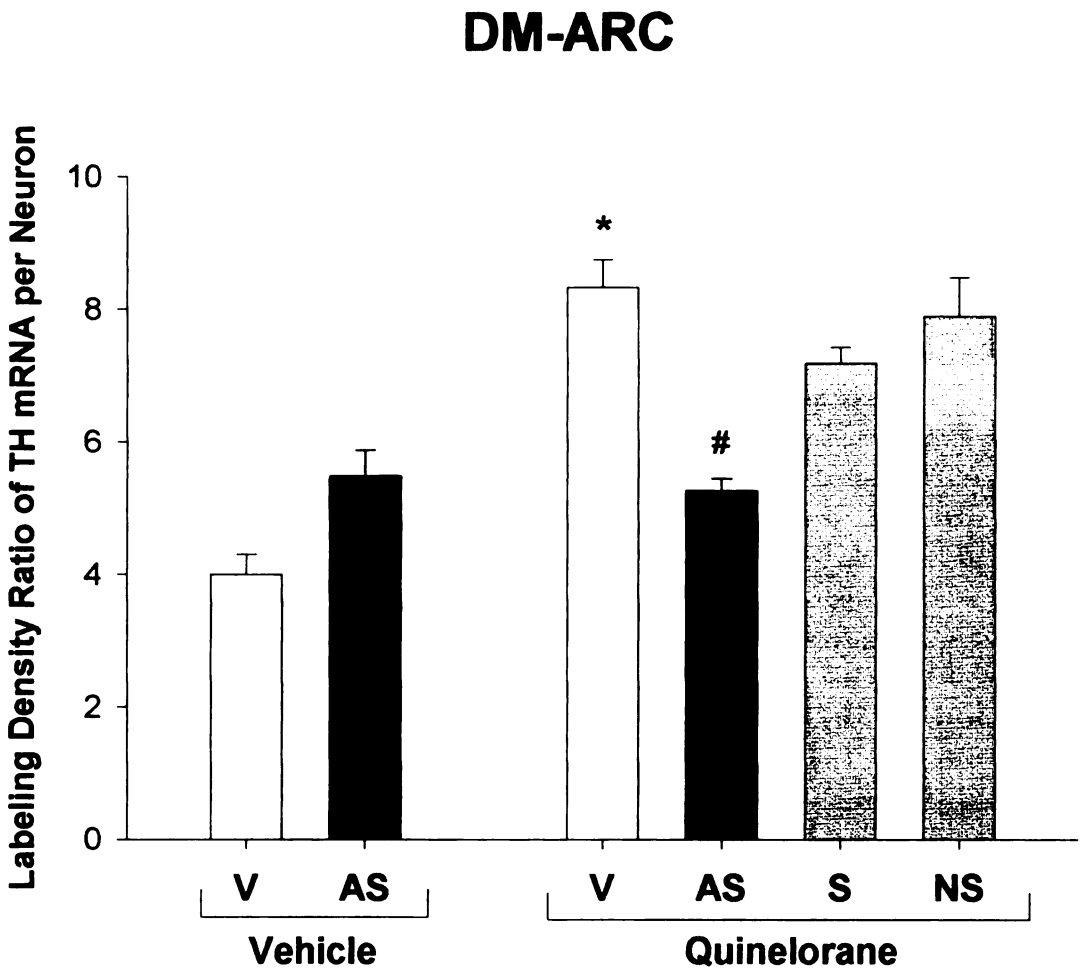

Figure 7.13 Effects of *c-fos* antisense, sense, and nonsense oligonucleotides on the labeling density ratio of TH mRNA per neuron in the DM-ARC in quinelorane-treated rats. Rats were injected with *c-fos* antisense (AS; 40 nmol/rat; icv), *c-fos* sense (S; 40 nmol/rat; icv), or *c-fos* nonsense (NS; 40 nmol/rat; icv) 14 h prior to sacrifice and with quinelorane (100 μg/kg; ip) 4 h prior to sacrifice. Controls were injected with 0.9% saline vehicle (3 μl/rat; icv) 14 h prior to sacrifice and with either quinelorane (V; 100 μg/kg; ip) or 0.9% saline (V; 1 ml/kg; ip) 4 h prior to sacrifice. Columns represent the means and vertical lines + 1 SEM from 6-8 animals. *, Values that are significantly different ($p<0.05$) from vehicle-treated controls. #, Values that are significantly different ($p<0.05$) from quinelorane-treated controls. Abbreviations: AS, antisense; NS, nonsense; S, sense; V, vehicle.

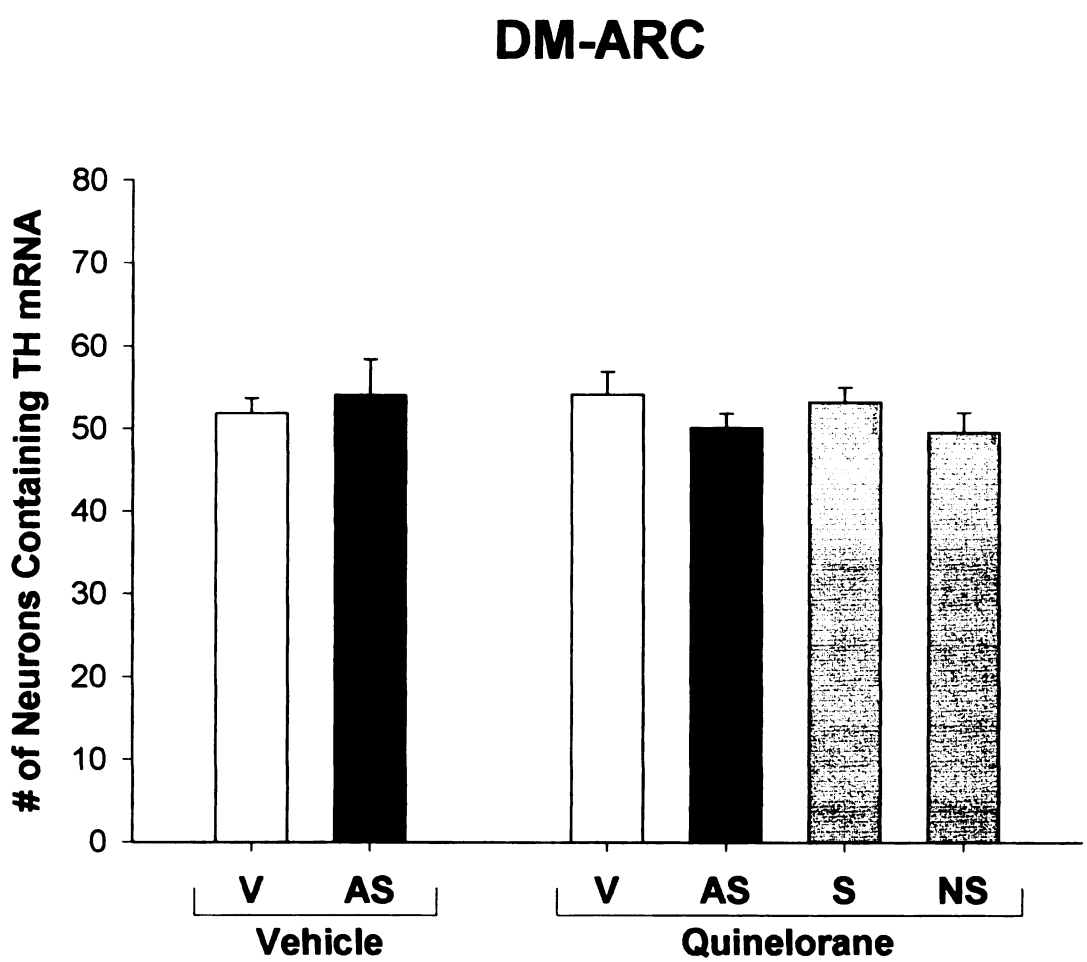

Figure 7.14 Effects of *c-fos* antisense, sense, and nonsense oligonucleotides on the numbers of neurons expressing TH mRNA in the rostral, middle, and caudal regions of the DM-ARC in quinelorane-treated rats. Rats were injected with *c-fos* antisense (AS; 40 nmol/rat; icv), *c-fos* sense (S; 40 nmol/rat; icv) or *c-fos* nonsense (NS; 40 nmol/rat; icv) 14 h prior to sacrifice and with quinelorane (100 μg/kg; ip) 4 h prior to sacrifice. Controls were injected with 0.9% saline vehicle (3 μl/rat; icv) 14 h prior to sacrifice and with either quinelorane (V; 100 μg/kg; ip) or saline (V; 1 ml/kg; ip) 4 h prior to sacrifice. Columns represent the means and vertical lines + 1 SEM from 6-8 animals. Abbreviations: AS, antisense; NS, nonsense; S, sense; V, vehicle.

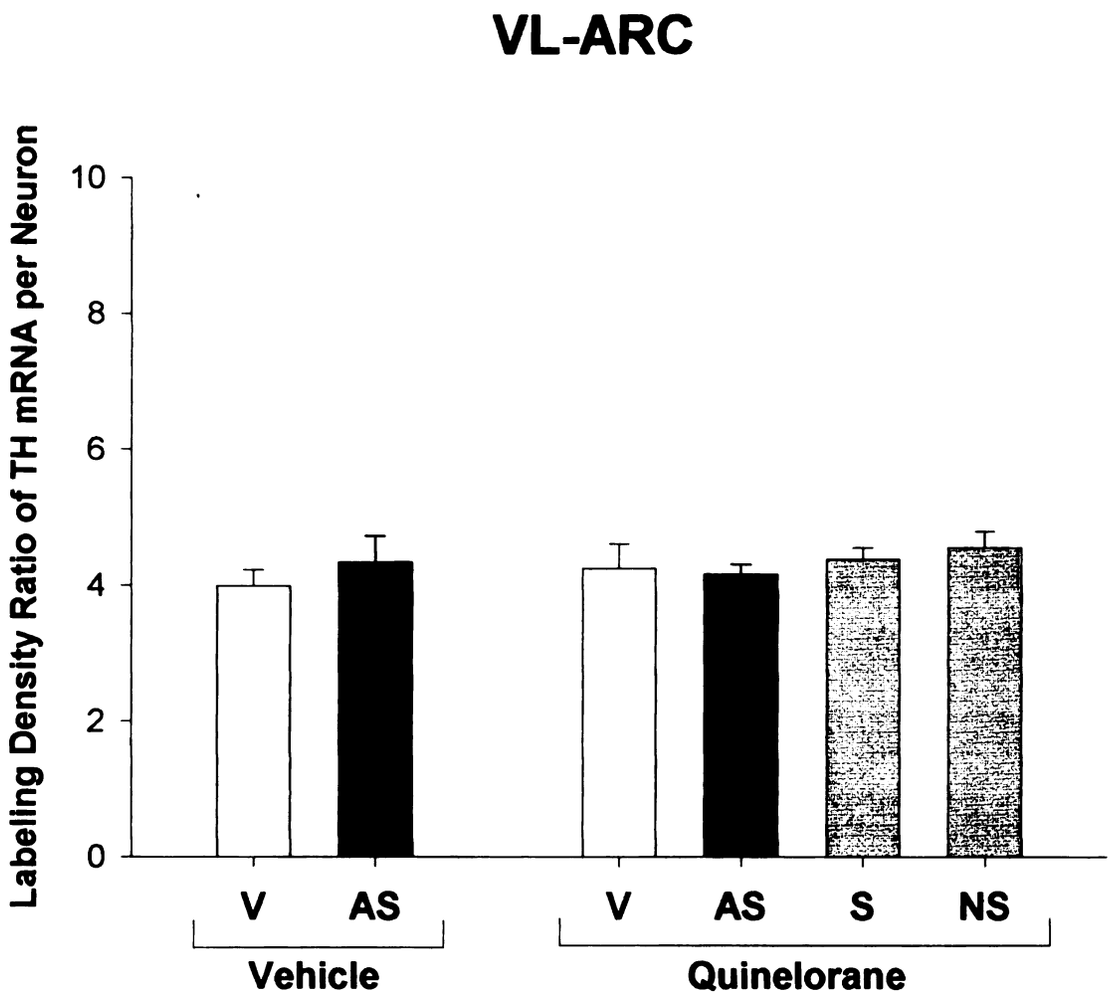

Figure 7.15 Effects of *c-fos* antisense, sense, and nonsense oligonucleotides on the labeling density ratio of TH mRNA per neuron in the rostral, middle, and caudal regions of the VL-ARC in quinelorane-treated rats. Rats were injected with *c-fos* antisense (AS; 40 nmol/rat; icv), *c-fos* sense (S; 40 nmol/rat; icv), or *c-fos* nonsense (NS; 40 nmol/rat; icv) 14 h prior to sacrifice and with quinelorane (100 μg/kg; ip) 4 h prior to sacrifice. Controls were injected with 0.9% saline vehicle (3 μl/rat; icv) 14 h prior to sacrifice and with either quinelorane (V; 100 μg/kg; ip) or 0.9% saline (V; 1 ml/kg; ip) 4 h prior to sacrifice. Columns represent the means and vertical lines + 1 SEM from 6-8 animals. Abbreviations: AS, antisense; NS, nonsense; S, sense; V, vehicle.

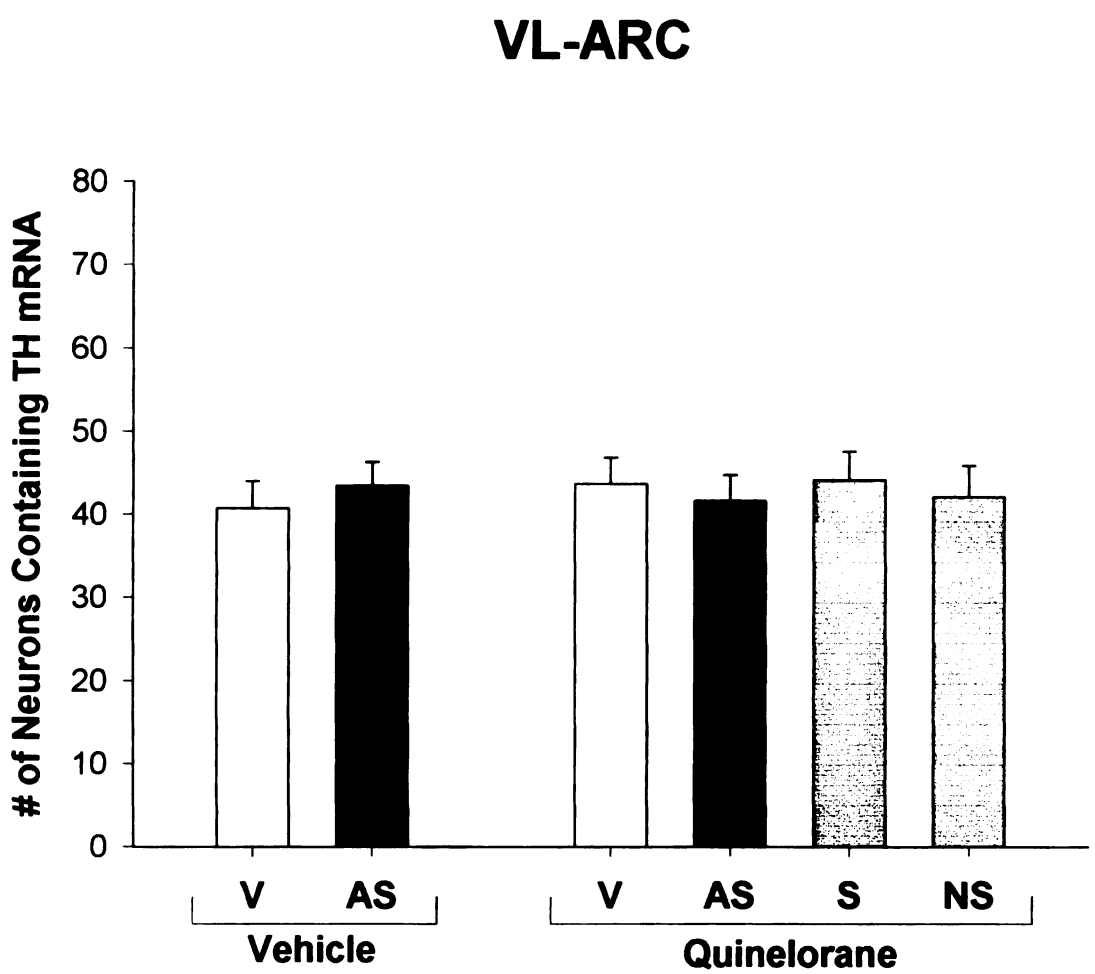

Figure 7.16 Effects of *c-fos* antisense, sense, and nonsense oligonucleotides on the numbers of neurons expressing TH mRNA in the rostral, middle, and caudal regions of the VL-ARC in quinelorane-treated rats. Rats were injected with *c-fos* antisense (AS; 40 nmol/rat; icv), *c-fos* sense (dark gray; 40 nmol/rat; icv) or *c-fos* nonsense (light gray; 40 nmol/rat; icv) 14 h prior to sacrifice and with quinelorane (100 μg/kg; ip) 4 h prior to sacrifice. Controls were injected with 0.9% saline vehicle (3 μl/rat; icv) 14 h prior to sacrifice and with either quinelorane (V; 100 μg/kg; ip) or saline (V; 1 ml/kg; ip) 4 h prior to sacrifice. Columns represent the means and vertical lines + 1 SEM from 6-8 animals. Abbreviations: AS, antisense; NS, nonsense; S, sense; V, vehicle.

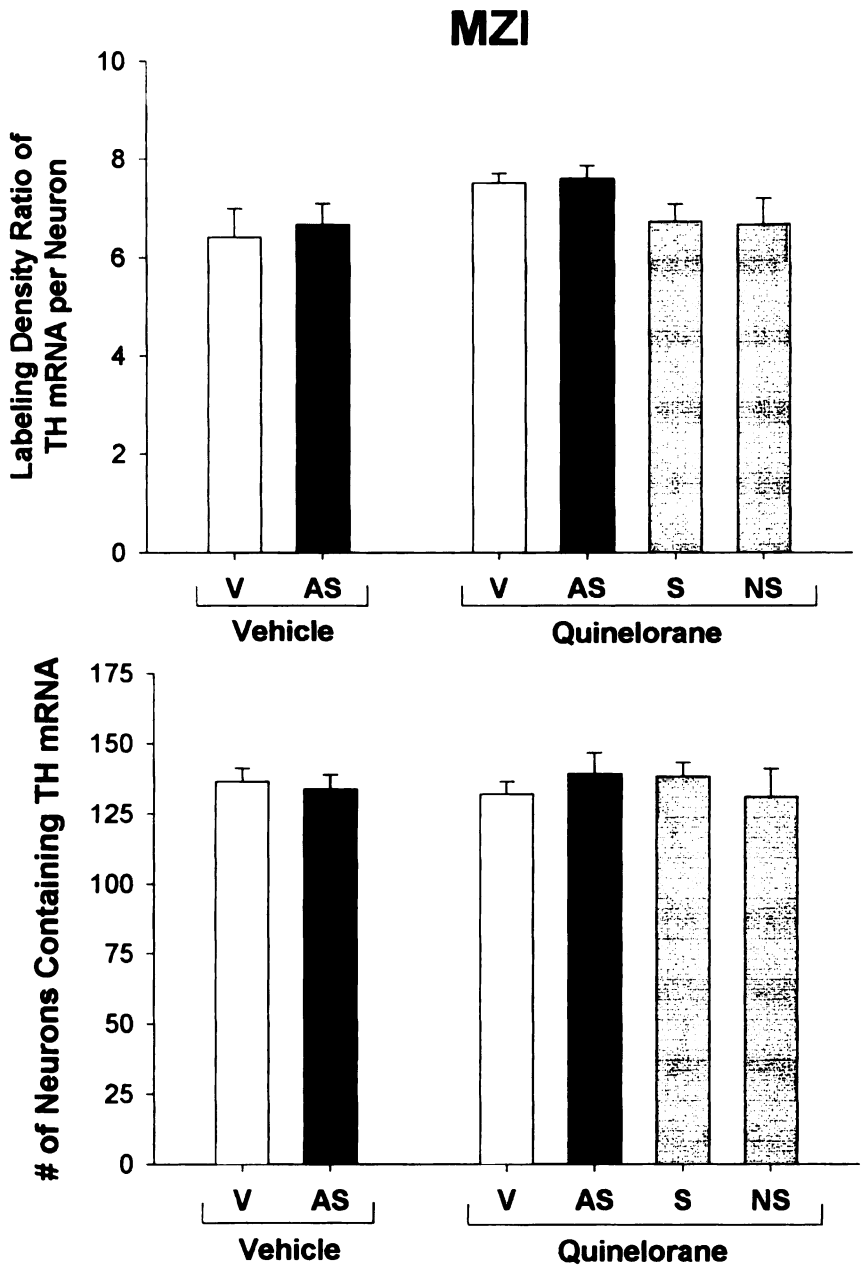

Figure 7.17 Effects of *c-fos* antisense, sense, and nonsense oligonucleotides on the numbers of neurons expressing TH mRNA (**Bottom Panel**) and the labeling density ratio of TH mRNA of these neurons (**Top Panel**) in the MZI in quinelorane-treated rats. Rats were injected with *c-fos* antisense (AS; 40 nmol/rat; icv), *c-fos* sense (dark gray; 40 nmol/rat; icv) or *c-fos* nonsense (light gray; 40 nmol/rat; icv) 14 h prior to sacrifice and with quinelorane (100 μg/kg; ip) 4 h prior to sacrifice. Controls were injected with 0.9% saline vehicle (3 μl/rat; icv) 14 h prior to sacrifice and with either quinelorane (V; 100 μg/kg; ip) or saline (V; 1 ml/kg; ip) 4 h prior to sacrifice. Columns represent the means and vertical lines + 1 SEM from 6-8 animals. Abbreviations: AS, antisense; NS, nonsense; S, sense; V, vehicle.

DISCUSSION

These studies reveal that Fos mediates, at least in part, D2 receptor activation of TH expression in TIDA neurons. Indeed, a single icv injection of *c-fos* antisense is capable of blocking Fos protein expression in quinelorane-stimulated TIDA neurons of the DM-ARC in a time-dependent manner. These results establish that a single injection of 40 nmol of antisense oligonucleotide into the lateral ventricle is concentrated enough to travel in the cerebrospinal fluid to the third ventricle and penetrate into the adjacent DM-ARC. This is consistent with other studies demonstrating that single injection of phosphorothioated antisense (identical to that employed here) follows bulk flow from the lateral ventricle through to the third and fourth ventricle finally to the subarachnoid spaces (Yaida and Nowak, 1995).

These results are consistent with a previous report showing that oligonucleotides can penetrate 1 to 2 mm into the tissue surrounding the lateral ventricles and approximately 1 mm into the tissue surrounding the third and fourth ventricle (Grzanna et al., 1998). This is in contrast to studies utilizing phosphodiester (or unmodified) oligonucleotides that are subject to rapid degradation by exonucleases and do not remain in the tissue long enough to exert anti-translational effects (Szklarczyk and Kaczmarek, 1995; Yaida and Nowak, 1995; Broberger et al., 2000). The phosphorothioated (or fully modified) antisense has a modified backbone; the oxygen atoms in the phosphodiester bond between nucleotides are replaced with sulfur atoms which impart a greater stability in biological fluids (Phillips and Gyurko, 1995). The half life of a 15-mer

phosphorothioated oligonucleotide probe can be up to 19 h *in vitro* in CSF (Campbell et al., 1990).

The results of the present study demonstrate that for *c-fos* antisense to have its anti-translational effects it must be present for at least six hours. This is consistent with previous reports demonstrating that *c-fos* antisense is capable of blocking Fos protein expression between 6 to 18 h after its administration (Chiasson et al., 1992; Dragunow et al., 1993; Hooper et al., 1994; Liu et al., 1994; Grzanna et al., 1998; Morrow et al., 1999). This delayed action of antisense suggests that it takes at least 6 h for the antisense oligonucleotide to diffuse through tissue, internalize within neurons, and hybridize to the target mRNA (Hooper et al., 1994; Liu et al., 1994; Phillips and Gyurko, 1995; Yaida and Nowak, 1995; Grzanna et al., 1998; Cui et al., 1999). Although the precise mechanism of how antisense gets into the cell is not known, it is believed to enter through fluid phase pinocytosis and/or absorptive endocytosis (Loke et al., 1989; Phillips and Gyurko, 1995; Myers and Dean, 2000). There is also evidence that a membrane-bound receptor may internalize antisense when present in low concentrations (Yakubov et al., 1989). This has been supported by the identification of 30 kDA, 66 kDA and 80 kDA proteins that mediate the uptake of oligonucleotides (Miller and Das, 1998; de Diesbach et al., 2000).

The antisense oligonucleotide probe used in these experiments was phosphorothioated to increase its stability. Some studies have reported side effects in animals following the use of modified oligonucleotides including lethargy, piloerection and frequent urination (Cirelli et al., 1995; Schobitz et al.,

1997; Ho et al., 1998). In addition, this modification confers a charge to the molecule that may cause it to interact with proteins in a nonselective fashion (Perez et al., 1994; Szklarczyk and Kaczmarek, 1999; Eckstein, 2000). Accordingly, an experiment was carried out to determine if the anti-translational effects of *c-fos* antisense were indeed specific, and this was tested by using *c-fos* "sense" and "nonsense" oligonucleotides. The *c-fos* "sense" oligonucleotide has the same sequence of nucleotides found in the segment of targeted *c-fos* mRNA. There are no base pairs that it can bind with so this oligonucleotide does not prevent Fos expression (Phillip and Gyurko, 1995; Pilowsky and Suzuki, 1994). The *c-fos* "nonsense" oligonucleotide is a jumbled sequence that has the same base composition as the antisense oligonucleotide, but has no homology to any known mRNA and likewise has no effect on Fos expression (Pilowsky and Suzuki, 1994). The three oligonucleotide sequences were also run through GenBank,® an NIH genetic sequence database, to determine if the sequence of *c-fos* antisense was specific for the *c-fos* gene (and not *fosb*, *fra1* or *fra2*) of the rat, and that the *c-fos* "sense" and "nonsense" sequences were not found on any other mRNA.

The results from this experiment demonstrate that the effect of *c-fos* antisense is specific. Antisense was able to attenuate quinelorane-induced Fos expression in TH-IR neurons in the DM-ARC, whereas "sense" and "nonsense" oligonucleotides were ineffective. These results also confirm and coincide with other studies (Cirelli et al., 1995) that the behavioral effects (lethargy, piloerection and urination) are specific to the antisense and not due to the phosphorothioation

or nonspecific protein binding, for the animals receiving the "sense" and "nonsense" probes do not exhibit these behavioral effects.

It is important to note that throughout the antisense experiments the numbers of neurons in each region of the DM-ARC remained constant which is consistent with the conclusion that the effects of phosphorothioated *c-fos* antisense is not toxic or damaging to these neurons. Thus, the decrease in the expression of Fos caused by this oligonucleotide is not due to destruction of neurons expressing Fos, but rather to a true blockade of protein synthesis.

Many studies have been carried out using antisense probes to block immediate early genes, neuropeptides, as well as receptors. The link between immediate early genes and long term genes has been insinuated, but studies demonstrating this are few. With the route of administration and the time course ascertained for employing *c-fos* antisense to block D2 receptor stimulation of Fos protein synthesis, the next step was to establish a link between Fos and TH gene expression. If Fos mediates the stimulatory effects of D2 receptor activation on TH mRNA, then *c-fos* antisense should prevent this increase in TH mRNA.

The results of this study reveal this is the case. Fos antisense blocks quinelorane-induced activation of TH mRNA expression in neurons in the DM-ARC. Evidently, antisense blocks the translation of Fos protein, and there is no Fos to dimerize with Jun protein, resulting in decreased binding of the dimer at the AP-1 site on the TH promoter. These results also suggest that other proteins of the Fos family such as FosB, FRA1 or FRA2 are not part of the dimerization. The *c-fos* antisense is specific for the translation start site of *c-fos* mRNA and

does not bind to *fosB*, *fra1* or *fra2* mRNA (GenBank,®). If FosB, FRA1 or FRA2 were involved in D2 receptor activation of TH mRNA expression, then accelerated translation of these proteins and dimerization with Jun would activate TH mRNA expression even in the presence of *c-fos* antisense. By eliminating Fos expression, TH mRNA does not increase following quinelorane administration. This is a specific action of the antisense since *c-fos* "sense" and "nonsense" probes do not alter the expression of TH mRNA. The oligonucleotides and phosphorothioation are not toxic or destructive to the cells containing TH mRNA, for there are no changes in their numbers.

Antisense alone has no effect on the levels of TH mRNA being expressed by neurons in the DM-ARC revealing that blockade of constitutively expressed Fos has no impact on basal TH gene expression. This implies that other transcription factors may be involved. It has been demonstrated that the CRE site and SP-1 site on the proximal TH gene promoter are necessary for the basal expression of TH mRNA in neuroblastoma cell lines (Kim et al., 1993; Yang et al., 1998). Studies in PC-18 cells (rat pheochromocytoma cells derived from PC-12 cells) have revealed that induction of Fos is sufficient to stimulate the TH gene transcription rate and that this is in part dependent on the AP1 site within the TH proximal promoter (Sun and Tank, 2002). Taken together, these results suggest that the induction of Fos is necessary for the increase in TH mRNA following D2 receptor activation of TIDA neurons, but the AP-1 may not play a prominent role in promoting basal levels of TH mRNA synthesis. Thus, it can be hypothesized

that an antisense to CREB or SP-1 may very well decrease the basal expression of TH mRNA in TIDA neurons.

While various studies have been carried out using *c-fos* antisense to study the effects of Fos protein expression, only a few studies have examined antisense effects on other markers *in vivo*. *c-fos* antisense is capable of blocking behaviors associated with fear and anxiety (Moller et al., 1994) as well as preventing alcohol tolerance (Szabo et al., 1996). One study demonstrated the ability of *c-fos* antisense to block haloperidol-stimulated neurotensin mRNA induction in the striatum and ischemia-induced nerve growth factor mRNA stimulation in the dentate gyrus, indicating a role of Fos in the regulation of neurotensin gene and nerve growth factor, respectively (Merchant, 1994; Cui et al., 1999). However, this is the first time that a link has been established between Fos and the TH gene *in vivo*.

c-fos antisense has no effect on Fos expression in "DOPA-ergic" neurons of the VL-ARC. One possibility could be that the antisense does not diffuse into the VL-ARC. However, oligonucleotides have been shown to diffuse approximately 1 mm into tissue from the third ventricle (Yaida and Nowak, 1995; Grzanna et al., 1998), so it seems unlikely that the oligonucleotide failed to penetrate into the VL-ARC.

In the time course study, the percentage of neurons TH-IR neurons expressing Fos in the control group is only 3%, much lower than in previous experiments (which have ranged from 15-30%). The actual numbers of TH-IR neurons in each rostrocaudal region is similar to what has been reported in

previous experiments, so the lower percentage of Fos-IR is not due to a lack of neurons present. Quinelorane has no stimulatory effect on Fos expression in the VL-ARC, which correlates with the results shown in Chapters 4 and 5.

In the specificity study, the expression of Fos in the VL-ARC in the control group is consistent with previous studies. In this experiment, quinelorane significantly decreases the percentage of TH-IR neurons expressing Fos in the middle and caudal regions of the VL-ARC. In rostral region there is a decrease in the percentage of Fos expression, but it is not significant most likely due to variability. Interestingly, antisense had no further effect on the expression of Fos in these neurons. The percentage of TH-IR neurons expressing Fos following the administration of *c-fos* antisense was still between 10 and 15%, similar to that determined after quinelorane administration. Although it would seem logical to anticipate that antisense would further decrease Fos expression, it is possible that the inhibitory effect of quinelorane attenuated the transcription of *c-fos* mRNA sufficiently that antisense had very little *c-fos* mRNA to react with. As in the DM-ARC, there are no changes in the numbers of TH-IR neurons in the VL-ARC indicating that antisense, "sense" and "nonsense" have no deleterious effect on the viability of the "DOPA-ergic neurons" of the VL-ARC.

The levels of TH mRNA in VL-ARC "DOPA-ergic" neurons were unchanged regardless of the treatment. These neurons are not regulated by D2 receptors, thus the lack of a stimulatory effect of quinelorane on TH mRNA is consistent with the results presented in Chapter 6. It is interesting to note that when quinelorane decreases Fos expression in the VL-ARC (though this effect is

variable), there is no corresponding change in TH mRNA. It is possible that if the CRE and SP-1 sites on the TH gene promoter are involved in the basal levels of TH mRNA expression, then decreased levels of Fos would not have an affect on gene expression.

In the MZI, the overall percentage of Fos expression in TH-IR neurons in the control groups is low. Moreover, antisense administration had no effect on Fos expression in these neurons. One reason could be that the antisense failed to diffuse to the MZI in adequate amounts. Icv injections can diffuse about 1-2 mm from the ventricles (Yaida and Nowak, 1995; Grzanna et al., 1998), but the MZI is greater than 2 mm from the lateral and third ventricles. Also, similar to the VL-ARC, basal Fos expression may be so low that the *c-fos* antisense has no or very little *c-fos* mRNA to bind to, thus no appreciable difference could be determined in Fos protein expression. The numbers of IHDA neurons in the MZI remain the same indicating that if the oligonucleotide probe diffused to the MZI then it has no effect on the viability of these DA neurons.

As in the VL-ARC, TH mRNA expression remained unaffected in the IHDA neurons of the MZI following Fos antisense administration. The labeling density ratio of TH mRNA per cell is greater in the MZI compared to the VL-ARC indicating that the basal level of TH mRNA content is greater in the MZI. This correlates with the staining of the neurons in the immunohistochemistry studies; the greater the intensity of the staining, the greater the protein content (Hoffman and Murphy, 2000). In these studies, the TH immunostaining in the MZI is darker than in the VL-ARC. While the MZI has greater basal levels of TH mRNA,

antisense alone was without effect. This indicates that Fos does not play a role in the basal expression of TH gene expression, implying that other transcription factors are involved such as CREB or SP-1.

In conclusion, these experiments reveal that *c-fos* antisense specifically prevents the D2 receptor-mediated stimulation of Fos and TH gene expression in TIDA neurons of the DM-ARC, but not the VL-ARC. With the use of *c-fos* antisense, a link has been established between the immediate early gene Fos and the long term gene TH. These results also reveal that the AP-1 site is not involved with the basal expression of TH mRNA in the ARC or in IHDA neurons of the MZI.

CHAPTER EIGHT

GENERAL SUMMARY

This body of work was aimed at determining if an acute increase in neuronal activity caused by stimulation of D2 receptors was associated with the regulation of gene expression in TIDA neurons. To this end, studies herein detailed the sexual differences in the distribution of TIDA neurons and basal level of FRA expression in subdivisions of the ARC, the temporal effects of D2 receptor stimulation on immediate early gene expression in TIDA neurons, the role of kappa opioid receptors in D2 receptor regulation, the temporal effects of D2 receptor stimulation on TH gene expression and the role of Fos in TH gene expression. The major points from these studies are summarized below.

DM-ARC

There are no sexual differences in the numbers of TH-IR neurons located within the rostral-caudal extent of the DM-ARC, but the number of TH-IR neurons in both females and males is higher in the rostral than in either the middle or caudal regions. The percentage of TH-IR neurons containing FRA-IR nuclei was 2-3 times higher in females versus males only in the rostral DM-ARC.

A single injection of D2 receptor agonist quinelorane causes a delayed (2 h) and transient (through 4 h) increase in the percentage of TH-IR neurons expressing Fos throughout the rostral-caudal extent of the DM-ARC. The blockade of D2 receptors with the antagonist raclopride has no effect *per se,* but

reverses the stimulatory effects of quinelorane. These results reveal that D2 receptors regulate Fos expression in TIDA neurons in the DM-ARC.

Blockade of kappa opioid receptors with the antagonist nor-BNI increases the percentage of TH-IR neurons expressing Fos in a delayed and transient manner similar to quinelorane throughout the rostral-caudal extent of the DM-ARC. Activation of kappa opioid receptors with the agonist U50-488 reverses the stimulatory effects of nor-BNI, indicating that kappa opioid receptors regulate Fos expression. U50-488 also blocks the stimulatory effects of quinelorane on percentage of TH-IR neurons expressing Fos in the DM-ARC. The results suggest that kappa opioid receptors mediate D2 receptor regulation of Fos expression.

Quinelorane significantly increases the labeling density ratio of TH mRNA per neuron in the DM-ARC at 4 h and remains elevated for at least 24 h, but has no effect on the numbers of neurons containing TH mRNA at any timepoint. Blockade of D2 receptors with raclopride has no effect *per se*, but reverses the stimulatory effects of quinelorane on TH mRNA expression. *c-fos* antisense, which specifically blocks Fos expression, prevents quinelorane-induced increases in the labeling density ratio of TH mRNA per neuron in the DM-ARC. The *c-fos* "sense" and "nonsense" oligonucleotide probes have no effect. There is no change in the numbers of neurons that contain TH mRNA in the DM-ARC following any of the treatments. These results reveal that D2 receptors regulate TH gene expression in TIDA neurons in the DM-ARC and that Fos, at least in part, mediates this activation of TH gene expression.

VL-ARC

There are no sexual differences in the numbers of TH-IR neurons in the rostral VL-ARC, but the number of TH-IR neurons in the middle and caudal VL-ARC were higher in males than in females. There were no sexual differences in the percentage of TH-IR neurons containing FRA-IR nuclei.

While there is no effect 2 h following quinelorane administration, there is a decrease at 4h in the percentage of TH-IR neurons expressing Fos throughout the rostral-caudal extent of the VL-ARC. Blockade of D2 receptors with raclopride has no significant effect on Fos expression. These results suggest that "DOPA-ergic" neurons of the VL-ARC are not regulated by D2 receptors.

In contrast to the DM-ARC, activation of kappa opioid receptors with U50-488 significantly decreases the percentage of TH-IR neurons containing Fos-IR nuclei throughout the rostral-caudal extent of the VL-ARC. While nor-BNI has no effect *per se,* it reverses the inhibitory effects of U50-488. These results indicate that while kappa opioid receptors regulate Fos expression, it is not under basal conditions as seen in the DM-ARC.

Neither quinelorane nor raclopride has an effect on the labeling density ratio of TH mRNA per neuron in the VL-ARC, indicating that D2 receptors do not regulate TH gene expression in "DOPA-ergic" neurons. *c-fos* antisense, "sense," and "nonsense" oligonucleotide probes have no effect on the labeling density ratio or on the numbers of neurons containing TH mRNA in the VL-ARC. These results reveal that D2 receptors do not regulate TH gene expression in "DOPA-

ergic" neurons in the VL-ARC and Fos does not play a role in TH gene expression.

MZI

There is no sexual difference in the numbers of TH-IR neurons or in the percentage of those neurons expressing FRA in the MZI.

As in the VL-ARC, quinelorane has no effect at 2 h; however, it does decrease the percentage of TH-IR neurons containing Fos-IR nuclei at 8 h. Blockade of D2 receptors with raclopride increases the percentage of TH-IR neurons containing Fos-IR nuclei in the MZI, and this is reversed by the administration of quinelorane. These studies demonstrate that Fos expression in IHDA neurons of the MZI are regulated by D2 autoreceptors.

In contrast to the ARC, neither activation nor blockade of kappa opioid receptors has any effect on the percentage of TH-IR neurons containing Fos-IR nuclei, indicating that kappa opioid receptors do not regulate Fos expression in the IHDA neurons of the MZI.

D2 receptors do not regulate TH gene expression in IHDA neurons of the MZI, as demonstrated by the lack of effect of raclopride and quinelorane on the labeling density ratio of TH mRNA. *c-fos* antisense, "sense," and "nonsense" oligonucleotide probes have no effect on the labeling density ratio in the MZI suggesting that Fos does not play a role in the basal expression of TH gene expression.

CONCLUDING DISCUSSION

DM-ARC

To review, D2 receptors are inhibitory and systemic administration of selective D2 agonists decreases neuronal activity, including DA neuronal systems regulated by DA autoreceptors or feedback neuronal circuits (Foreman et al., 1989; Eaton et al., 1994a). TIDA neurons are unique in that activation of D2 receptors stimulates TIDA neuronal activity (Berry and Gudelsky, 1991; Eaton et al., 1993). This response is independent of PRL and is instead mediated through an afferent neuronal system involving the inhibition of tonically active dynorphin via kappa opioid receptors (Durham et al., 1996). The goal of these studies was to determine if this mechanism is involved in the regulation of gene expression in TIDA neurons.

For well over a decade, inducible transcription factors have been studied and utilized as a tool for mapping neuronal activity. Under basal conditions Fos expression is low, but is induced following transsynaptic activation. Immediate early genes are stimulated within minutes to hours through depolarization or ligand-mediated activation of membrane receptors located on neuronal cell bodies or dendrites. This triggers a second messenger system and phosphorylation cascade involving protein kinases and constitutive transcription factors (Sheng and Greenberg, 1990; Sim et al., 1994). The constitutive transcription factors induce the transcription and translation of immediate early genes. The immediate early genes then bind to their DNA binding elements to

regulate transcription and translation of long-term genes (Gizang-Ginsberg and Ziff, 1990; Icard-Liepkalns et al., 1992).

The studies described in this dissertation demonstrated that activation of D2 receptors increases Fos expression in TIDA neurons throughout the rostral-caudal extent of the DM-ARC. This is mediated through the release of inhibition from tonically active dynorphin neurons via kappa opioid receptors. The origin of the DA and the location of the D2 receptor-expressing target cells have yet to be determined. From the available evidence described earlier, it has been suggested that the D2 receptors are located outside the mediobasal hypothalamus (Durham et al., 1996). The dorsomedial hypothalamic nucleus may be one area of the hypothalamus that may be involved in the afferent neuronal pathway. Electrical stimulation in this area increases TIDA neuronal activity, mimicking the effect of quinelorane (Gunnet and Moore, 1988). Within the dorsomedial nucleus are extensive dendritic processes from IHDA neurons of the MZI (Chan-Palay et al., 1984), thus the MZI may be the origin of the DA. Areas of the brain to be considered for the location of the D2 receptor-expressing target cell are the paraventricular nucleus, the horizontal diagonal band, and the central amygdala, the three areas to which the IHDA neurons project (Eaton, et al., 1994; Wagner et al., 1995).

The neurochemical identity of the target cell and its receptors on dynorphin neurons has yet to be elucidated. One characteristic that is required of this upstream neuron is the ability to mimic the effect of dynorphin on TIDA neurons. In addition, it is most likely a stimulatory neuron given that D2

receptors are inhibitory and activation of these receptors would most likely "turn off" a stimulatory neuronal system. Neurotensin is a neuropeptide that stimulates, rather than inhibits, TIDA neurons and is involved in mediating the effects of PRL on the activation of these neurons (Hentschel et al., 1998). GABA (acting at $GABA_A$ receptors; Wagner et al., 1994a) and glutamate (acting at AMPA receptors; Wagner et al., 1994b) tonically inhibit TIDA neurons. However, GABA is an inhibitory neurotransmitter and would inhibit dynorphin neurons under basal conditions resulting in increased activity of TIDA neurons. Blockade of AMPA receptors increases the activity of TIDA neurons, mimicking the effect of quinelorane; however, this mechanism involves $GABA_A$ receptors and not kappa opioid receptors (Wagner et al., 1994c).

The blockade of D2 receptors had no effect on Fos expression suggesting a lack of tonic activation of these receptors. This might suggest that the DA pathway that serves as a source of DA for these receptors may be active only during specific situations (e.g. during different endocrinological states, stress, etc.). Alternatively, these D2 receptors may not be activated by endogenous DA, but respond only to exogenously administered DA agonists. There is precedent for this; for example, the activation of DA receptors in the area postrema.

Dynorphin neurons are located in the hypothalamus including the ventromedial nucleus and ARC as demonstrated by microscopic analysis and immunoassay studies and are concentrated around TIDA neurons (Zamir et al., 1983 and 1984; Fitzsimmons et al., 1992; Durham, 1999). To help determine the possible location of the unknown projection neurons future studies could include

retrograde tract tracing studies in conjunction with immunohistochemistry or *in situ* hybridization. Dynorphin neurons located in the DM-ARC could be identified using immunohistochemical or *in situ* hybridization techniques. The tracer could be injected into the DM-ARC to identify nerve terminals clustered around the dynorphin neurons and then examine where these projections to the DM-ARC originate. If a specific area or nucleus of the brain could be identified, this may assist in determining the identity of the interneuron. Immunohistochemical studies could then be carried out using appropriate agonists and antagonists to determine if that neurotransmitter mimics the effect of dynorphin on Fos expression in TIDA neurons.

Dynorphin acts at kappa opioid receptors, which have been identified in the ARC. Kappa opioid receptors are linked to Gi/o protein, inhibiting cAMP (Childers, 1991; Childers et al., 1998b, Takekoski et al., 2000). If the theoretical pathway is correct, under basal conditions the interneuron stimulates dynorphin release, which acting at kappa opioid receptors inhibits TIDA neuronal activity and the expression of Fos. Activation of D2 receptors would inhibit the interneuron, thus releasing the inhibitory action of dynorphin on TIDA neuronal activity and on Fos expression. The lack of dynorphin at kappa opioid receptors may lead to increases in the cAMP and begin the second messenger cascade eventually leading to an increase in the transcription and translation of Fos.

In addition to a correlation between TIDA neuronal activity and immediate early gene expression, there is also a correlation between neuronal activity and TH mRNA expression (Arbogast and Voogt, 1991; Wang et al., 1993; Berghorn

et al., 2001). Acute increases in neuronal activity caused by activation of D2 receptors were associated with increases in the expression of the TH gene in TIDA neurons. Follow up studies could determine if kappa opioid receptors mediate D2 receptor regulation of TH gene expression using *in situ* hybridization. If this is true, blockade of kappa opioid receptors should increase TH gene expression mimicking the effects of quinelorane, and activation of kappa receptors should reverse the stimulatory effects of quinelorane.

The expression of TH is delayed, occurring after the induction of TIDA neuronal activity and the expression of Fos. Following the induction and synthesis of Fos protein, it dimerizes with a Jun protein and binds to the AP-1 site (Curran and Franza, 1988; Angel and Karin, 1991) located within the TH gene promoter of DA neurons (Biguet et al., 1991; Icard-Liepkalns, et al., 1992; Kumer and Vrana, 1996). Thus, the AP-1 site regulates the transcription and translation of TH.

The last set of experiments for this dissertation utilizing *c-fos* antisense determined that Fos, at least in part, mediates D2 receptor activation of TH expression in TIDA neurons. *c-fos* antisense blocks the translation of Fos protein resulting in a lack of Fos to dimerize with Jun and decreases binding of the dimer at the AP-1 site on the TH promoter. *c-fos* antisense alone has no effect on TH gene expression implying that the AP-1 site does not play a major role in the basal expression of TH. While there is some expression of Fos under basal conditions that presumably binds to the AP-1 site with a Jun protein, other factors may be needed to induce TH gene transcription. The E box is adjacent to the

AP-1 site and is believed to be involved with cell specificity (Papanikolaou and Sabban, 2000). It is possible this site and/or other modulators or enhancers must be present in addition to the binding of Fos/Jun dimers for AP-1 to induce transcription of TH in this system. The Hept and Oct sites on the TH gene promoter are repressor sites specificity (Papanikolaou and Sabban, 2000). Under basal conditions, these or other repressor sites may interfere with the binding of Fos to the AP-1 site. Studies have demonstrated that the CRE and SP-1 sites on the proximal TH gene promoter are necessary for the basal expression of TH (Kim et al., 1993; Yang et al., 1998). Additional studies could examine the effects of a CREB or SP-1 antisense on the expression of TH. If these binding sites are involved in the basal regulation of TH expression, then an antisense to their respective binding proteins should decrease the basal expression of TH.

This pathway of D2 receptor-mediated activity of TIDA neurons is separate from the PRL pathway. First, coadministration of exogenous PRL and quinelorane has an additive effect on TIDA neuronal activity (Durham et al., 1996). Indeed PRL increases FRA expression in a time dependent manner similar to the time course following the activation of D2 receptors (Hentschel et al., 2000b). However, TIDA neuronal activity increases 6 – 12 h following PRL administration (Hentschel et al., 2000a), but only 30 min following the activation of D2 receptors (Eaton et al., 1993). Thus FRA expression precedes the increases in PRL-induced TIDA neuronal activity, while Fos expression occurs after quinelorane-induced neuronal activity.

VL-ARC

The neurons of the VL-ARC do not contain DD and thus can not synthesize DA, but only the precursor DOPA. These neurons are not true TIDA neurons as in the DM-ARC, but can be considered "DOPA-ergic" neurons. Unlike the DM-ARC, D2 receptors do not regulate Fos expression in "DOPA-ergic" neurons in the VL-ARC. Fos expression may instead be regulated by PRL. The VL-ARC contains PRL receptors (Bakowska and Morrell, 1997) and administration of exogenous PRL increases FRA expression in a time dependent manner (Hentschel et al., 2000). The function of "DOPA-ergic" neurons is not completely understood, but DOPA may be released into the portal blood system where it is converted to DA by DD found in the walls of blood vessels (Meister et al., 1988; Misu et al., 1996).

Fos expression in "DOPA-ergic" neurons is regulated by kappa opioid receptors but this is not present under basal conditions. While there is evidence of dynorphin neurons and nerve terminals being present in the ARC, dynorphin neurons are also present in the ventromedial hypothalamic nucleus. Ventromedial nucleus dynorphin neurons are not regulated by D2 receptors (Durham, 1999) so it is possible that the "DOPA-ergic" neurons of the VL-ARC are regulated by them. Future studies could include tract tracing studies to determine the hypothalamic nucleus of origin of the dynorphin nerve terminals found in the ARC in conjunction with immunohistochemical labeling of the dynorphin neurons and "DOPA-ergic" neurons.

As with Fos expression, TH gene expression in "DOPA-ergic" neurons also is not regulated by D2 receptors. What is interesting to note is the levels of TH mRNA remain relatively constant and are not greater than in the DM-ARC in light of the fact that Fos expression is greater in the VL-ARC under basal conditions and decreases following D2 receptor activation. Fos does not appear to have an effect on the level of TH mRNA in these neurons. "DOPA-ergic" neurons co-express TH and neuropeptides (Chronwall 1985; Ershov et al., 2002). The AP-1 site is found on other proximal gene promoter in addition to the TH gene. It is possible that Fos may bind to an AP-1 site located on a promoter of a neuropeptide gene coexpressed in "DOPA-ergic" neurons.

c-fos antisense has no effect on Fos or TH gene expression in quinelorane-treated "DOPA-ergic" neurons. In these studies, activation of D2 receptors resulted in decreases in Fos expression at 2 h. Although it would seem logical that antisense would further decrease Fos expression, it is possible that the inhibitory effect of quinelorane attenuated the transcription of *c-fos* mRNA sufficiently that antisense had very little *c-fos* mRNA to hybridize to.

MZI

The IHDA neurons of the MZI are regulated by DA receptors as are the DA neurons of the mesotelencephalic systems (Lookingland and Moore, 1984). D2 receptor agonists decrease while antagonists increase DA neuronal activity (Lookingland and Moore, 1995; Eaton et al., 1992). The studies in this dissertation demonstrate that D2 receptors agonists are without effect, but D2

antagonists increase Fos expression in IHDA neurons. The D2 receptors are most likely located on IHDA cell bodies and/or dendrites as opposed to axon terminals, for antidromic stimulation of hypothalamic neurons does not induce immediate early gene expression (Icard-Liepkalns et al., 1992; Luckman et al., 1994; Hoffman and Murphy, 2000).

Although Fos expression is regulated by acute activation of D2 receptors, TH gene expression is not. Various studies in the mesolimbic and nigrostriatal DA systems have demonstrated that chronic continuous infusions, but not intermittent injections of DA agonists inhibit TH mRNA expression (Sirinathsinghji et al., 1994; Iwata et al., 2000). Chronic infusion of apomorphine a very short acting DA agonist works at post-synaptic receptors via a long-loop feedback circuit to exert negative feedback on the DA neurons (Roth and Elsworth, 1995). This continuous negative feedback can lead to decreases in TH mRNA. While these studies were carried out in the mesolimbic and nigrostriatal DA systems, it is logical to anticipate the same is for the IHDA neurons. To test this hypothesis, quinelorane, a long acting DA agonist, could be administered to assess the effect on TH gene expression in IHDA neurons. If this hypothesis is correct, chronic injections of quinelorane should decrease the expression of TH mRNA. A single injection of DA agonist or antagonist is capable to altering DA neuronal activity in the IHDA neurons of the MZI through pre-synaptic autoreceptors (Lookingland and Moore, 1984); however, TH mRNA is not affected by acute actions because antidromic stimulation (i.e. stimulation at pre-synaptic autoreceptors) does not effect gene expression (Icard-Liepkalns et al., 1992).

The results of these final studies demonstrate that Fos does not play a role in TH gene expression in IHDA neurons following the acute activation of D2 receptors. There are several possible reasons for this. First acute activation or blockade of D2 receptors does not alter TH gene expression. Secondly, the expression of Fos is low in IHDA neurons under basal conditions and following quinelorane administration thus no appreciable difference could be determined in Fos expression following c-fos antisense administration. To determine if Fos plays a role in TH gene expression, the IHDA neurons would first need to be stimulated with a D2 receptor antagonist to stimulate Fos. To ensure changes in the TH gene expression chronic injections of the antagonist may not increases Fos expression but increases FRA-1 or FRA-2 expression (which are induced following chronic stimulation). Thus even under the proper conditions, Fos may not mediate the expression of the TH gene.

In conclusion, the results of studies described in this thesis demonstrate that D2 receptors regulate the expression of the immediate early gene Fos in TIDA neurons of the DM-ARC. This is mediated through the release of inhibition of tonically active dynorphin neurons via kappa opioid receptors It is believed that the removal of the inhibitory effect by dynorphin on adenylate cyclase and cAMP is a potent enough stimulus to induce Fos expression. In addition to regulation of Fos, stimulation of D2 receptors also leads to increases in the expression of TH mRNA. Fos, at least in part, plays a role in the regulation of TH gene expression, a gene that is essential to maintain DA synthesis and PRL inhibitory function of these TIDA neurons.

BIBLIOGRAPHY

Abate,C., Luk,D., Gentz,R., Rauscher,F.J.I., CURRAN,T., 1990. Expression and purification of the leucine zipper and DNA-binding domains of Fos and Jun: both Fos and Jun contact DNA directly. Proceedings of the National Academy of Sciences of the United States of America 87, 1032-1036.

Ajika,K., Hokfelt,T., 1973. Ultrastructural identification of catecholamine neurons in the hypothalamic periventricular-arcuate nucleus-median eminence complex with special reference to quantitative aspects. Brain Research 57, 97-117.

Angel,P., Karin,M., 1991. The role of Jun, Fos and the AP-1 complex in cell-proliferation and transformation. Biochimica et Biophysica Acta 1072, 129-157.

Aniento,F., Papavassiliou,A.G., Knecht,E., Roche,E., 1996. Selective uptake and degradation of c-fos and v-fos by rat liver lysosomes. FEBS Letters 390, 47-52.

Annunziato,L., Leblanc,P., Kordon,C., Weiner,R.I., 1980. Differences in the kinetics of dopamine uptake in synaptosome preparations of the median eminence relative to other dopaminergically innervated brain regions. Neuroendocrinology 31, 316-320.

Arbogast,L.A., Voogt,J.L., 1995. Hypoprolactinemia decreases tyrosine-hydroxylase activity in the tuberoinfundibular dopaminergic-neurons acutely by protein dephosphorylation and chronically by changes in gene-expression. Endocrine 3, 801-806.

Arbogast,L.A., Voogt,J.L., 1990. Sex-related alterations in hypothalamic tyrosine hydroxylase after neonatal monosodium glutamate treatment. Neuroendocrinology 52, 460-467.

Arbogast,L.A., Voogt,J.L., 1991. Hyperprolactinemia increases and hypoprolactinemia decreases tyrosine hydroxylase messenger ribonucleic acid levels in the arcuate nuclei, but not the substantia nigra or zona incerta. Endocrinology 128, 997-1005.

Arbogast,L.A., Voogt,J.L., 1994. Progesterone suppresses tyrosine hydroxylase messenger ribonucleic acid levels in the arcuate nucleus on proestrus. Endocrinology 135, 343-350.

Bakowska,J.C., Morrell,J.I., 1997. Atlas of the neurons that express mRNA for the long form of the prolactin receptor in the forebrain of the female rat. The Journal of Comparative Neurology 386, 161-177.

Balan,I.S., Ugrumov,M.V., Calas,A., Mailly,P., Krieger,M., Thibault,J., 2000. Tyrosine hydroxylase-expressing and/or aromatic l-amino acid decarboxylase-expressing neurons in the mediobasal hypothalamus of perinatal rats: Differentiation and sexual dimorphism. The Journal of Comparative Neurology 425, 167-176.

Baruchin,A., Weisberg,F.P., Miner,L.L., Ennis,D., Nisenbaum,L.K., Naylor,E., Stricker,E.M., Zigmound,M.J., Kaplan,B.B., 1990. Effects of cold exposure on rat adrenal tyrosine hydroxylase: an analysis of RNA, protein, enzyme activity, and cofactor levels. Journal of Neurochemistry 54, 1769-1775.

Berghorn,K.A., Le,W.W., Sherman,T.G., Hoffman,G.E., 2001. Suckling stimulus suppresses messenger RNA for tyrosine hydroxylase in arcuate neurons during lactation. Journal of Comparative Neurology 438, 423-432.

Berry,S.A., Gudelsky,G.A., 1991. Effect of D2 dopamine agonists on tuberoinfundibular dopamine neurons. Neuropharmacology 30, 961-965.

Berry,S.A., Gudelsky,G.A., 1990. D1 receptors function to inhibit the activation of tuberoinfundibular dopamine neurons. The Journal of Pharmacology and Experimental Therapeutics 254, 677-682.

Berry,S.A., Gudelsky,G.A., 1991. Effect of D2 dopamine agonists on tuberoinfundibular dopamine neurons. Neuropharmacology 30, 961-965.

Best,J.A., Chen,Y., Piech,K.M., Tank,A.W. The Response of the Tyrosine Hydroxylase Gene to Cyclic AMP Is Mediated by Two Cyclic AMP-Response Elements. Journal of Neurochemistry 65[5], 1934. 1995.

Best,J.A., Tank,A.W., 1998. The THCRE2 site in the rat tyrosine hydroxylase gene promoter is repsonsive to phorbol ester. Neuroscience Letters 258, 131-134.

Biguet,N.F., Vyas,S., Mallet,J., 1991. In vitro and in vivo regulation of the expression of the tyrosine hydroxylase gene. Journal de Physiologie 85, 105-109.

Bishop,J.M., 1985. Viral oncogenes. Cell 42, 23-38.

Björklund,A., Lindvall,O., Nobin,A., 1975. Evidence of an incerto-hypothalamic dopamine neuronal system in the rat. Brain Research 89, 29-42.

Björklund,A., Nobin,A., 1973. Fluorescence histochemical and microspectrofluorometric mapping of dopamine and noradrenalin cell groups in the rat diencephalon. Brain Research 51, 193-205.

Bohmann,D., Bos,T.J., Admon,A., Nishimura,T., Vogt,P.K., Tjian,R., 1987. Human proto-oncogene c-jun encodes a DNA binding protein with structural and functional properties of transcription factor AP-1. Science 238, 1386-1392.

Broberger,C., Nylander,I., Geijer,T., Terenius,L., Hokfelt,T., Georgieva,J., 2000. Differential effects of intrastriatally infused fully and endcap phosphorothioate antisense oligonucleotides on morphology, histochemistry, and prodynorphin expression in rat brain. Molecular Brain Research 75, 25-45.

Brown,L.L., Siegel,H., Etgen,A.M., 1996. Global sex differences in stress-induced activation of cerebral metabolism revealed by 2-deoxyglucose autoradiography. Hormones and Behavior 30, 611-617.

Campbell,D.G., Hardie,D.G., Vulliet,P.R., 1986. Indentification of the four phosphorylation sites in the N-terminal region of tyrosine hydroxylase. J. Biol. Chem. 261, 10489-10492.

Campbell,J.-M., Bacon,T.-A., Wickstrom,E., 1990 Oligodeoxynucleoside phosphorothioate stability in subcellular extracts, culture media, sera and cerebrospinal fluid. Journal of Biochemical and Biophysical Methods 20, 259-267.

Campeau,S., Hayward,M.D., Hope,B.T., Rosen,J.B., Nestler,E.J., Davis,M., 1991. Induction of the c-fos proto-oncogene in rat amygdala during unconditioned and conditioned fear. Brain Research 565, 349-352.

Carlsson,A., Davis,J.N., Kehr,W., Lindqvist,M., Atack,C.V., 1972. Simultaneous measurement of tyrosine and tryptophan hydroxylase activities in brain in vivo using an inhibitor of the aromatic amino acid decarboxylase. Naunyn-Schmiedebergs Archives of Pharmacology 275, 153-168.

Carr,K.D., Kutchukhidze,N., Park,T.H., 1999. Differential effects of □ and κ opioid antagonists on Fos-like immunoreactivity in extended amygdala. Brain Research 822, 34-42.

Chan-Palay,V., Zaborszky,L., Kohler,C., Goldstein,M., Palay,S.L., 1984. Distribution of tyrosine-hydroxylase-immunoreactive neurons in the hypothalamus of rats. The Journal of Comparative Neurology 227, 467-496.

Chan,R.K., Brown,E.R., Ericsson,A., Kovacs,K.J., Sawchenko,P.E., 1993. A comparison of two immediate-early genes, c-fos and NGFI-B, as markers for functional activation in stress-related neuroendocrine circuitry. Journal of Neuroscience. 13, 5126-5138.

Chan-Palay,V., Zaborszky,L., Kohler,C., Goldstein,M., Palay,S.L., 1984. Distribution of tyrosine-hydroxylase-immunoreactive neurons in the hypothalamus of rats. The Journal of Comparative Neurology 227, 467-496.

Chavkin,C., James,I.F., Goldstein,A., 1982. Dynorphin is a specific endogenous ligand of the κ receptor. Science 215, 413-415.

Chen,Y., Best,J.A., Nagamoto,K., Tank,A.W., 1996. Regulation of tyrosine hydroxylase gene expression by the m1 muscarinic acetylcholine receptor in rat pheochromocytoma cells. Molecular Brain Research 40, 42-54.

Cheng,J., Roques,B.P., Gacel,G.A., Huang,E., Pasternak,G.W., 1992. Kappa 3 opiate receptor binding in the mouse and rat. European Journal of Pharmacology 226, 15-20.

Cheung,S., Ballew,J.R., Moore,K.E., Lookingland,K.J., 1998. Contribution of dopamine neurons in the medial zona incerta to the innervation of the central nucleus of the amygdala, horizontal diagonal band of Broca and hypothalamic paraventricular nucleus. Brain Research 808, 174-181.

Cheung,S., Johnson,J.D., Moore,K.E., Lookingland,K.J., 1997a. Dopamine receptor-mediated regulation of expression of Fos and its related antigens (FRA) in somatostatin neurons in the hypothalamic periventricular nucleus. Brain Research 770, 176-183.

Cheung,S., Will,Y.M., Hentschel,K., Moore,K.E., Lookingland,K.J., 1997b. Role of gonadal steroids in determining sexual differences in expression of Fos-related antigens in tyrosine hydroxylase-immunoreactive neurons in subdivisions of the hypothalamic arcuate nucleus. Endocrinology 138, 3804-3810.

Chiason,B.J., Hooper,M.L., Murphy,P.R., Robertson,H.A., 1992. Antisense oligonucleotide eliminates in vivo expression of c-fos in mammalian brain. European Journal of Pharmacology 227, 451-453.

Childers,S.R., 1991. Opioid receptor-coupled second messenger systems. Life Sciences 48, 1991-2003.

Childers,S.R., Xiao,R.Y., Vogt,L., Sim,L.J., 1998a. Lack of evidence of kappa(2)-selective activation of G-proteins - kappa opioid receptor stimulation of [S-35]GTPγS binding in guinea pig brain. Biochemical Pharmacology 56, 113-120.

Childers,S.R., Xiao,R., Vogt,L., Sim,L.J., 1998b. κ opioid receptor stimulation of [^{35}S] GTPγS binding in guinea pig brain. Biochemical Pharmacology 56, 113-123.

Chiu,T.H., Dun,S.L., Tang,H., Dun,N.J., 1994. c-fos antisense attenuates Fos expression in rat central neurons induced by hemorrhage. Neuroreport 5, 2178-2180.

Chronwall,B.M., 1985. Anatomy and physiology of the neuroendocrine arcuate nucleus. Peptides 6, 1-11.

Cirelli,C., Pompeiano,M., Tononi,G., 1995. In vivo antisense approaches to the role of immediate early gene expression in the brain. Regulatory Peptides 59, 151-162.

Cone,R.I., Weber,E., Barchas,J.D., Goldstein,A., 1983. Regional distribution of dynorphin and neo-endorphin peptides in rat brain, spinal cord, and pituitary. Journal of Neuroscience 3, 2146-2152.

Cui,J.-K., Hsu,C.Y., Liu,P.K., 1999. Suppression of postischemic hippocampal nerve growth factor expression by a c-fos antisense oligodeoxynucleotide. Journal of Neuroscience 19, 1335-1344.

Curran,T., MacConnell,W.P., van-Straaten,F., Verma,I.M., 1983. Structure of the FBJ murine osteosarcoma virus genome: molecular cloning of its associated helper virus and the cellular homolog of the v-fos gene from mouse and human cells. Molecular and Cellular Biology 3, 914-921.

Curran,T., Teich,N.M., 1982. Identification of a 39,000-dalton protein in cells transformed by the FBJ murine osteosarcoma virus. Virology 116, 221-235.

Curran,T., Franza,B.R.Jr., 1988. Fos and Jun: The AP-1 connection. Cell 55, 395-397.

Curran,T., Morgan,J.I., 1995. Fos: An immediate-early transcription factor in neurons. Journal of Neurobiology 26, 403-412.

Czyzyk-Krzeska,M.F., Dominski,Z., Kole,R., Millhorn,D.E., 1994a. Hypoxia stimulates binding of a cytoplasmic protein to a pyrimidine- rich sequence in the 3'-untranslated region of rat tyrosine hydroxylase mRNA. J. Biol. Chem. 269, 9940-9945.

Czyzyk-Krzeska,M.F., Furnari,B.A., Lawson,E.E., Millhorn,D.E., 1994b. Hypoxia increases rate of transcription and stability of tyrosine hydroxylase mRNA in pheochromocytoma (PC12) cells. J. Biol. Chem. 269, 760-764.

Dahlstrom,A., Fuxe,K., 1964. Evidence of the existence of monoamine containing neurons in the central nervous system. 1. Demonstration of monoamines in the cell bodies of brainstem neurons. Acta Physiologica Scandinavica 232, 1-55.

Daubner,S.C., Fitzpatrick,P.F., 1993. Alleviation of catecholamine inhibition by tyrosine hydroxylase by phosphorylation at serine-40. Advances in Experimental Medicine and Biology 338, 87-92.

Daubner,S.C., Piper,M.M., 1995. Deletion mutants of tyrosine hydroxylase identify a region critical for heparin binding. Protein Science 4, 538-541.

Dawson,S.J., Yoon,S.O., Chikaraishi,D.M., Lillycrop,K.A., Latchman,D.S., 1994. The Oct-2 transcription factor represses tyrosine hydroxylase expression via a heptamer TAATGARAT-like motif in the gene promoter. Nucl. Acids. Res. 22, 1023-1028.

de-Greef,W.J., Plotsky,P.M., Neill,J.D., 1981. Dopamine levels in hypophyseal stalk plasma and prolactin levels in peripheral plasma of the lactating rat: effects of a simulated suckling stimulus. Neuroendocrinology 32, 229-233.

Demarest,K.T., Moore,K.E., 1979. Comparison of dopamine synthesis regulation in the terminals of nigrostriatal, mesolimbic, tuberoinfundibular and tuberohypophyseal neurons. Journal of Neural Transmission 46, 263-277.

Demarest,K.T., McKay,D.W., Riegle,G.D., Moore,K.E., 1981. Sexual differences in tuberoinfundibular dopamine nerve activity induced by neonatal androgen exposure. Neuroendocrinology 32, 108-113.

Demarest,K.T., Moore,K.E., 1981. Sexual differences in the sensitivity of tuberoinfundibular dopamine neurons to the actions of prolactin. Neuroendocrinology 33, 230-234.

Demarest,K.T., Riegle,G.D., Moore,K.E., 1984. Prolactin-induced activation of tuberoinfundibular dopaminergic neurons: evidence for both a rapid "tonic" and a delayed "induction" component. Neuroendocrinology 38, 467-475.

Demarest,K.T., Riegle,G.D., Moore,K.E., 1985. The interrelationship between the rapid "tonic" and the delayed "induction" components of the prolactin-induced activation of tuberoinfundibular dopamine neurons. In: MacLeod,R.M., Thorner,M.O., Scapagnini,U. (Eds.), Prolactin. Basic and clinical correlates. Liviana Press, Padova, Vol. 1, pp. 533-542.

Demarest,K.T., Riegle,G.D., Moore,K.E., 1986. The rapid "tonic" and the delayed "induction" components of the prolactin-induced activation of tuberoinfundibular dopaminerigc neurons following the systemic administration of prolactin. Neuroendocrinology 43, 291-299.

Demarest,K.T., Moore,K.E., 1979a. Comparison of dopamine synthesis regulation in the terminals of nigrostriatal, mesolimbic, tuberoinfundibular and tuberohypophyseal neurons. Journal of Neural Transmission 46, 263-277.

Demarest,K.T., Moore,K.E., 1979b. Lack of a high affinity transport system for dopamine in the median eminence and posterior pituitary. Brain Research 171, 545-551.

Dhawan,B.N., Cesselin,F., Raghubir,R., Reisine,T., Bradley,P.B., Portoghese,P.S., Hamon,M., 1996. International union of pharmacology. XII. Classification of opioid receptors. The American Society for Pharmacology and Experimental Therapeutics 48, 567-592.

Diesbach,P.D., Berens,C., N'Kuli,F., Monsigny,M., Sonveaux,E., Wattiez,R., Courtoy,P.J., 2000. Identification, purification and partial characterization of an oligonucleotide receptor in membranes of HepG2 cells. Nucleic Acids Research. 28, 868-874.

Dragunow,M., Robertson,G.S., Faull,R.L.M., Robertson,H.A., Jansen,K., 1990. D2 dopamine receptor antagonists induce Fos and related proteins in rat striatal neurons. Neuroscience 37, 287-294.

Dragunow,M., Tse,C., Glass,M., Lawlor,P., 1994. c-fos antisense reduces expression of Krox 24 in rat caudate and neocortex. Cellular and Molecular Neurobiology 14, 395-405.

Dragunow,M., Hughes,P., 1995. Induction of immediate-early genes and the control of neurotransmitter-regulated gene expression within the nervous system. Pharmacological Reviews 47, 133-178.

Dragunow,M., Lawlor,P., Chiason,B.J., Robertson,H.A., 1993. c-fos antisense generates apomorphine and amphetamine-induced rotation. Neuroreport 5, 305-306.

Durham,R.A. Dopamine Receptor-Mediated Regulation of Tuberoinfundibular Dopaminergic Neurons (Dissertation). 1-209. 1999. Michigan State University.

Durham,R.A., Eaton,M.J., Moore,K.E., Lookingland,K.J., 1997. Effects of selective activation of dopamine D2 and D3 receptors on prolactin secretion and the activity of tuberoinfundibular dopamine neurons. European Journal of Pharmacology 335, 37-42.

Durham,R.A., Johnson,J.D., Moore,K.E., Lookingland,K.J., 1996. Evidence that D2 receptor-mediated activation of hypothalamic tuberoinfundibular dopaminergic neurons in the male rat occurs via inhibition of tonically active afferent dynorphinergic neurons. Brain Research 732, 113-120.

Eaton,M.J., Cheung,S., Moore,K.E., Lookingland,K.J., 1996. Dopamine receptor-mediated regulation of corticotropin-releasing hormone neurons in the hypothalamic paraventricular nucleus. Brain Research 738, 60-66.

Eaton,M.J., Gopalan,C., Kim,E., Lookingland,K.J., Moore,K.E., 1993. Comparison of the effects of the dopamine D2 agonist quinelorane on tuberoinfundibular dopaminergic neuronal activity in male and female rats. Brain Research 629, 53-58.

Eaton,M.J., Lookingland,K.J., Moore,K.E., 1994a. Effects of the selective dopaminergic d2 agonist quinelorane on the activity of dopminergic and noradrenergic neurons projecting to the diencephalon of the rat. The Journal of Pharmacology and Experimental Therapeutics 268, 645-652.

Eaton,M.J., Tian,Y., Lookingland,K.J., Moore,K.E., 1992. Remoxipride and raclopride differentially alter the activity of incertohypothalamic dopaminergic neurons. Neuropharmacology 31, 1121-1126.

Eaton,M.J., Wagner,C.K., Moore,K.E., Lookingland,K.J., 1994. Neurochemical identification of A13 dopaminergic neuronal projections from the medial zona incerta to the horizontal limb of the diagonal band of Broca and the central nucleus of the amygdala. Brain Research 659, 201-207.

Eckstein,F., 2000. Phosphorothioate oligonucleotides: What is their origin and what is unique about them? Antisense & Nucleic Acid Drug Development 10, 117-121.

Eells,J.B., Clough,R.W., Miller,J.W., Jobe,P.C., Browning,R.A., 2000. Fos expression and 2-deoxyglucose uptake following seizures in developing genetically epilepsy-prone rat. Brain Research Bulletin 52, 379-389.

Ershov,P.V., Ugrumov,M.V., Calas,A., Krieger,M., Thibault,J., 2002. Differentiation of tyrosine hydroxylase-synthesizing and/or aromatic L-amino acid decarboxylase-synthesizing neurons in the rat mediobasal hypothalamus: Quantitative double-immunofluorescence study. The Journal of Comparative Neurology 446, 114-122.

Everitt,B., Meister,B., Hokfelt,T., Melander,T., Terenius,L., Rokaeus,A., Theodorsson-Norheim,E., Dockray,G., Edwardson,J., Cuello,A.C., Elde,R., Goldstein,M., Hemmings,H., Ouimet,C., Walaas,I., Greengard,P., Vale,W., Weber,E., Wu,J.-Y., Chang,K.-J., 1986. The hypothalamic arcuate nucleus-median eminence complex: Immunohistochemistry of transmitters, peptides and DARPP-32 with special reference to coexistence in dopamine neurons. Brain Research Reviews 11, 97-155.

Ferland,L., Labrie,F., Euvrard,C., Raymond,J.P., 1979. Antidopaminergic activity of estrogens on prolactin release at the pituitary level in vivo. Molecular and Cellular Endocrinology 14, 199-206.

Finkel,M.P., Biskis,B.O., Jinkins,P.B., 1966. Virus induction of osteosarcoma in mice. Science 151, 698-701.

Fisch,T.M., Prywes,R., Roeder,R.G., 1987. c-fos sequence necessary for basal expression and induction by epidermal growth factor, 12-O-tetradecanoyl phorbol-13-acetate and the calcium ionophore. Molecular and Cellular Biology 7, 3490-3502.

Fitzsimmons,M.D., Olschowka,J.A., Wiegand,S.J., Hoffman,G.E., 1992. Interaction of opioid peptide-containing terminals with dopaminergic perikarya in the rat hypothalamus. Brain Research 581, 10-18.

Foreman,M.M., Fuller,R.W., Hynes,M.D., Gidda,J.S., Nichols,C.L., Schaus,J.M., Kornfield,E.C., Clemens,J.A., 1989. Preclinical studies on quinelorane, a potent and highly selective D2-dopaminergic agonist. The Journal of Pharmacology and Experimental Therapeutics 250, 227-235.

Fossom,L.H., Sterling,C.R., Tank,A.W., 1992. Regulation of tyrosine-hydroxylase gene-transcription rate and tyrosine-hydroxylase messenger-rna stability by cyclic-AMP and glucocorticoid. Mol Pharmacol 42, 898-908.

Fowler,C.J., Fraser,G.L., 1994. Mu-, delta-, kappa-opioid receptors and their subtypes. A critical review with emphasis on radioligand binding experiments. Neurochemistry International 24, 401-426.

Fox,C.A., Mansour,A., Thompson,R.C., Bunzow,J.R., Civelli,O., Watson,S.J., 1993. The distribution of dopamine D2 receptor heteronuclear RNA (hnRNA) in the rat brain. Journal of Chemical Neuroanatomy 6, 363-373.

Franza,B.R., Rauscher,F.J., Josephs,S.F., Curran,T., 1988. The Fos complex and Fos-related antigens recognize sequence elements that contain AP-1 binding sites. Science 239, 1150-1153.

Fuxe,K., Agnati,L.F., Kalia,M., Goldstein,M., Andersson,K., Härfstrand,A., 1985. Dopaminergic systems in the brain and pituitary. In: Flückiger,E., Müller,E.E., Thorner,M.O. (Eds.), The Dopaminergic System. Springer-Verlag, New York, pp. 11-25.

Gahn,L.G., Roskoski,R.Jr., 1995. Thermal stability and CD analysis of rat tryosine hydroxylase. Biochemistry 34, 252-256.

Gestreau,C., Le Guen,S., Besson,J.-M., 2000. Is there tonic activity in the endogenous opioid systems? A c-fos study in the rat central nervous system after intravenous injection of naloxone or naloxone-methiodide. The Journal of Comparative Neurology 427, 285-301.

Gizang-Ginsberg,E., Ziff,E.B., 1990. Nerve growth factor regulates tyrosine hydroxylase gene transcription through a nucleoprotein complex that contains c-fos. Genes and Development 4, 477-491.

Gizang-Ginsberg,E., Ziff,E.B., 1994. Fos family members successively occupy the tyrosine hydroxylase gene AP-1 site after nerve growth factor or epidermal growth factor stimulation and can repress transcription. Molecular Endocrinology 8, 249-262.

Goc,A., Stachowiak,M.K., 1994. Bovine tyrosine hydroxylase gene-promoter regions involved in basal and angiotensin II-stimulated expression in nontransformed adrenal medullary cells. Journal of Neurochemistry 62, 834-843.

Goldstein,A., Fischli,W., Lowney,L.I., Hunkapiller,M., Hood,L., 1981. Porcine pituitary dynorphin: complete amino acid sequence of the biologically active heptadecapeptide. Proceedings of the National Academy of Sciences of the United States of America 78, 7219-7223.

Goldstein,A., Tachibana,S., Lowney,L.I., Hunkapiller,M., Hood,L., 1979. Dynorphin-(1-13), an extraordinarily potent opioid peptide. Proceedings of the National Academy of Sciences of the United States of America 76, 6666-6670.

Gonzalez,G.A., Montminy,M.R., 1989. Cyclic AMP stimulates somatostatin gene transcription by phosphorylation of CREB at serine 133. Cell 59, 675-680.

Grima,B., Lamouroux,A., Blanot,F., Biguet,N.F., Mallet,J., 1985. Complete coding sequence of rat tyrosine-hydroxylase messenger-RNA. Proceedings of the National Academy of Sciences of the United States of America 82, 617-621.

Grzanna,R., Dubin,J.R., Dent,G.W., Ji,Z., Zhang,W., Ho,S.P., Hartig,P.R., 1998. Intrastriatal and intraventricular injections of oligodeoxynucleotides in the rat brain: tissue penetration, intracellular distribution and c-fos antisense effects. Molecular Brain Research 63, 35-52.

Gudelsky,G.A., Annunziato,L., Moore,K.E., 1978. Localization of the site of the haloperidol-induced, prolactin-mediated increase of dopamine turnover in the median eminence: studies in rats with complete hypothalamic deafferentations. Journal of Neural Transmission 42, 181-192.

Gudelsky,G.A., Moore,K.E., 1976. Differential drug effects on dopamine concentrations and rates of turnover in the median eminence, olfactory tubercle and corpus striatum. Journal of Neural Transmission 38, 95-105.

Gudelsky,G.A., Porter,J.C., 1980. Release of dopamine from tuberoinfundibular neurons into pituitary stalk blood after prolactin or haloperidol administration. Endocrinology 106, 526-529.

Gudelsky,G.A., Porter,J.C., 1981. Sex-related difference in the release of dopamine into the hypophyseal portal blood. Endocrinology 109, 1394-1398.

Gunnet,J.W., Lookingland,K.J., Lindley,S.E., Moore,K.E., 1987. Effect of electrical stimulation of the arcuate nucleus on neurochemical estimates of tuberoinfundibular and tuberohypophyseal dopaminergic neuronal activities. Brain Research 424, 371-378.

Gunnet,J.W., Lookingland,K.J., Moore,K.E., 1986a. Comparison of the effects of castration and steroid replacement on incertohypothalamic dopaminergic neurons in male and female rats. Neuroendocrinology 44, 269-275.

Gunnet,J.W., Lookingland,K.J., Moore,K.E., 1986b. Effects of gonadal steroids on tuberoinfundibular and tuberohypophyseal dopaminergic neuronal activity in male and female rats. Proceedings of the Society for Experimental Biology and Medicine 183, 48-53.

Gunnet,J.W., Moore,K.E., 1988. Effect of electrical stimulation of the ventromedial nucleus and the dorsomedial nucleus on the activity of tuberoinfundibular dopaminergic neurons. Neuroendocrinology 47, 20-26.

Halász,B., Fuxe,K., Agnati,L.F., Kalia,M., Goldstein,M., Andersson,K., Härfstrand,A., Clark,B.J., 1985. The Dopaminergic System. Springer-Verlag, Berlin.

Haycock,J.W., 1990. Phosphorylation of tyrosine hydroxylase in situ at serine 8, 19, 31, and 40. J. Biol. Chem. 265, 11682-11691.

Haycock,J.W., Wakade,A.R., 1992. Activation and multiple-site phosphorylation of tyrosine hydroxylase in perfused rat adrenal glands. Journal of Neurochemistry 58, 67-64.

Hentschel,K. Mechanisms Underlying Prolactin-Induced Activation of Tuberoinfundibular Dopaminergic Neurons (Dissertation). 1-205. 2000. Michigan State University.

Hentschel,K., Cheung,S., Moore,K.E., Lookingland,K.J., 1998. Pharmacological evidence that neurotensin mediates prolactin-induced activation of tuberoinfundibular dopamine neurons. Neuroendocrinology 68, 71-76.

Hentschel,K., Fleckenstein,A.E., Toney,T.W., Lawson,D.M., Moore,K.E., Lookingland,K.J., 2000a. Prolactin regulation of tuberoinfundibular dopaminergic neurons: Immunoneutralization studies. Brain Research 852, 28-36.

Hentschel,K., Moore,K.E., Lookingland,K.J., 2000b. Effects of prolactin on expression of fos related antigens in tyrosine hydroxylase-immunoreactive neurons in subdivisions of the arcuate nucleus. Brain Research 857, 110-118.

Herdegen,T., Leah,J.D., 1998. Inducible and constitutive transcription factors in the mammalian nervous system: control of gene expression by Jun, Fos, and Krox, and CREB/ATF proteins. Brain Research Reviews 28, 370-490.

Hirai,S.I., Bourachot,B., Yaniv,M., 1990. Both Jun and Fos contribute to transcription activation by the heterodimer. Oncogene 5 , 39-46.

Ho,S.P., Livanov,V., Zhang,W., Li,J., Lesher,T., 1998. Modification of phosphorothioate oligonucleotides yields potent analogs with minimal toxicity for antisense experiments in the CNS. Molecular Brain Research 62, 1-11.

Hoffman,G.E., Le,W.-W., Abbud,R., Lee,W.-S., Smith,M.S., 1994. Use of Fos-related antigens (FRA's) as markers of neuronal activity: FRA changes in dopamine neurons during proestrus, pregnancy and lactation. Brain Research 654, 207-215.

Hoffman,G.E., Murphy,A.Z., 2000. Anatomical markers of activity in hypothalamic systems. In: Conn,P.M., Freeman,M.E. (Eds.), Neuroendocrinology in Physiology and Medicine. Humana Press, Totowa, N.J., pp. 541-552.

Hoffman,G.E., Smith,M.S., Fitzsimmons,M.D., 1992. Detecting steroidal effects of immediate early gene expression in the hypothalamus. Neuroprotocols 1, 52-66.

Hoffman,G.E., Smith,M.S., Verbalis,J.G., 1993. c-Fos and related immediate early gene products as markers of activity in neuroendocrine systems. Frontiers in Neuroendocrinology 14, 173-213.

Hooper,M.L., Chiason,B.J., Robertson,H.A., 1994. Infusion into the brain of an antisense oligonucleotide to the immediate-early gene c-fos suppresses production of Fos and produces a behavioral effect. Neuroscience 63, 917-924.

Hsu,S.-M., Raine,L., Fanger,H., 1981. Use of avidin-biotin-peroxidase complex (ABC) in immunoperoxidase techniques. The Journal of Histochemistry and Cytochemistry 29, 577-580.

Hsu,S.-M., Soban,E., 1982. Color modification of diaminobenzidine (DAB) precipitation by metallic ions and its application for double immunohistochemistry. The Journal of Histochemistry and Cytochemistry 30, 1079-1082.

Icard-Liepkalns,C., Faucon Biguet,N., Vyas,S., Robert,J.J., Sassone-Corsi,P., Mallet,J., 1992. AP-1 complex and c-fos transcription are involved in TPA provoked and trans-synaptic inductions of the tyrosine hydroxylase gene: Insights into long-term regulatory mechanisms. Journal of Neuroscience Research 32, 290-298.

Iwata,S., Nomoto,M., Kaseda,S., Tanoue,S.S.M., Fukuda,T., 2000. TH protein and mRNA in nigrostriatal dopaminergic neurons are down-regulated by continuous but not intermittent apomorphine. Molecular Brain Research 82, 133-136.

Iyengar,S., Kim,H.S., Wood,P.L., 1986. Effects of kappa opiate agonists on neurochemical and neuroendocrine indices: Evidence for kappa receptor subtypes. Life Sciences 39, 637-644.

James,M.D., MacKenzie,F.J., Tuohy-Jones,P.A., Wilson,C.A., 1987. Dopaminergic neurons in the zona incerta exert a stimulatory control on gonadotropin release via D1 dopamine receptors. Neuroendocrinology 43, 348-355.

Kaneda,N., Sasaoka,T., Kobayashi,K., Kiuchi,K., Nagatsu,I., Kurosawa,Y., Fujita,K., Yokoyama,M., Nomura,T., Katsuki,M., Nagatsu,T., 1991. Tissue-specific and high-level expression of the human tyrosine-hydroxylase gene in transgenic mice. Neuron 6, 583-594.

Kebabian,J.W., Calne,D.B., 1979. Multiple receptors for dopamine. Nature 277, 93-96.

Kedzierski,W., Aguila-Mansilla,N., Kozlowski,G.P., Porter,J.C., 1994. Expression of Tyrosine Hydroxylase Gene in Cultured Hypothalamic Cells: Roles of Protein Kinase A and C. J Neurochem 62, 431-437.

Kim,K., Tinti,C., Song,B., Cubells,J., Joh,T., 1994. Cyclic AMP-dependent protein kinase regulates basal and cyclic AMP-stimulated but not phorbol ester-stimulated transcription of the tyrosine hydroxylase gene. J Neurochem 63, 834-842.

Kim,K.S., Lee,M.K., Carroll,J., Joh,T.H., 1993. Both the basal and inducible transcription of the tyrosine hydroxylase gene are dependent upon a cAMP response element. J. Biol. Chem. 268, 15689-15695.

Koller,E., Gaarde,W.A., Monia,B.P., 2000. Elucidating cell signaling mechanisms using antisense technology. Trends in Pharmacological Sciences 21, 142-147.

Komisaruk,B.R., Rosenblatt,J.S., Barona,M.L., Chinapen,S., Nissaanov,J., O'Bannon,R.T.I., Johnson,B.M., Rodriguez Del Cerro,M.C., 2000. Combined c-fos and 14C-2-deoxyglucose method to differentiate site-specific excitation from disinhibition: Analysis of maternal behavior in the rat. Brain Research 859, 262-272.

Komori,K., Fujii,T., Nagatsu,I., 1991. Do some tyrosine hydroxylase-immunoreactive neurons in the human ventrolateral arcuate nucleus and globus pallidus produce only L-DOPA? Neuroscience Letters 133, 203-206.

Kouzarides,T., Ziff,E., 1988. The role of the leucine zipper in the fos-jun interaction. Nature 336, 646-651.

Kouzarides,T., Ziff,E., 1989. Leucine zippers of fos, jun and GCN4 dictate dimerization specificity and thereby control DNA binding. Nature 340, 568-571.

Kovács,K.J., Sawchenko,P.E., 1996. Sequence of stress-induced alterations in indices of synaptic and transcriptional activation in parvocellular neurosecretory neurons. Journal of Neuroscience 16, 262-273.

Kovács,K.J., 1998. c-Fos as a transcription factor: a stressful (re)view from a functional map. Neurochemistry International 33, 287-297.

Kumer,S.C., Vrana,K.E., 1996. Intricate regulation of tyrosine hydroxylase activity and gene expression. Journal of Neurochemistry 67, 443-462.

Lerant,A., Freeman,M.E., 1997. Dopaminergic neurons in periventricular and arcuate nuclei of proestrous and ovariectomized rats: Endogenous diurnal rhythm of Fos-related antigens expression. Neuroendocrinology 65, 436-445.

Lewis,D.A., Melchitzky,D.S., Haycock,J.W., 1993. Four isoforms of tyrosine hydroxylase are expressed in human brain. Neuroscience 54, 477-492.

Li,B.-H., Rowland,N.E., 1996. Peripherally and centrally administered bombesin induce Fos-like immunoreactivity in different brain regions in rats. Regulatory Peptides 62, 167-172.

Lin,J.-Y., Li,C.-S., Pan,J.-T., 1993. Effects of various neuroactive substances on single-unit activities of hypothalamic arcuate neurons in brain slices. Brain Research Bulletin 31, 587-594.

Lin,J.-Y., Pan,J.-T., 1995. Effects of endogenous opioid peptides and their analogs on the activities of hypothalamic arcuate neurons in brain slices from diestrous and ovariectomized rats. Brain Research Bulletin 36, 225-233.

Lin,J.-Y., Pan,J.-T., 1999. Single-unit activity of dorsomedial arcuate neurons and diurnal changes of tuberoinfundibular dopaminergic neuron activity in female rats with neonatal monosodium glutamate treatment. Brain Research Bulletin 48, 103-108.

Lindvall,O., Björklund,A., 1978. Anatomy of the dopaminergic neuron systems in the rat brain. Advances in Biochemical Psychopharmacology 19, 1-23.

Liu,P.K., Salminen,A., He,Y.Y., Liu,J.S., Hsu,C.Y., Jiang,M.H., Xue,J.J., 1994. Suppression of ischemia-induced Fos expression and AP-1 activity by an antisense oligodeoxynucleotide to c-fos messenger-RNA. Annals of Neurology 36, 566-576.

Lofstrom,A., Jonsson,G., Wiesel,F.-A., Fuxe,K., 1976. Microfluorometric quantitation of catecholamine fluorescence in rat median eminence. II. Turnover changes in hormonal states. Journal of Histochemistry and Cytochemistry 24, 430-442.

Loke,S.L., Stein,C.A., Zhang,X.H., Mori,K., Nakanishi,M., Subasinghe,C., Cohen,J.S., Neckers,L.M., 1989. Characterization of oligonucleotide transport into living cells. Proceedings of the National Academy of Sciences of the United States of America 86, 3474-3478.

Lookingland,K.J., Gunnet,J.W., Toney,T.W., Moore,K.E., 1990. Comparison of the effects of ether and restraint stress on the activity of tuberoinfundibular dopaminergic neurons in female and male rats. Neuroendocrinology 52, 99-105.

Lookingland,K.J., Jarry,H.D., Moore,K.E., 1987. The metabolism of dopamine in the median eminence reflects the activity of tuberoinfundibular neurons. Brain Research 419, 303-310.

Lookingland,K.J., Moore,K.E., 1984. Dopamine receptor-mediated regulation of incertohypothalamic dopaminergic neurons in the male rat. Brain Research 304, 329-338.

Lookingland,K.J., Moore,K.E., 1988. Comparison of the effects of restraint stress on the activities of tuberoinfundibular and tuberohypophyseal dopaminergic neurons. In: Beart,P.M., Woodruff,G.N., Jackson,D.M. (Eds.), Pharmacology and Functional Regulation of Dopaminergic Neurons. MacMillan Press, pp. 289-294.

Luckman,S.M., Dyball,R.E., Leng,G., 1994. Induction of c-fos expression in hypothalamic magnocellular neurons requires synaptic activation and not simply increased spike activity. Journal of Neuroscience 14, 4825-4830.

Ma,T.P., Johnson,J.C., Hoskins,G.A., 1997. Organization of the zona incerta in the macaque: an electron microscopic study. Anatomical Record 249, 259-275.

MacKenzie,F.J., Hunter,A.J., Daily,C., Wilson,C.A., 1984. Evidence that the dopaminergic incerto-hypothalamic tract has a stimulatory effect on ovulation and gonadotropin release. Neuroendocrinology 39, 289-295.

Mal,L.M., Shieh,K.R., Pan,J.T., 1994. Circadian changes of serum prolactin levels and tuberoinfundibular dopaminergic neuron activities in ovariectomized rats treated with or without estrogen - The role of the suprachiasmatic nuclei. Neuroendocrinology 60, 520-526.

Mansour,A., Fox,C.A., Burke,S., Meng,F., Thompson,R.C., Akil,H., Watson,S.J., 1994. Mu-opioid, delta-opioid, and kappa-opioid receptor messenger-RNA expression in the rat CNS - An in-situ hybridization study. Journal of Comparative Neurology 350, 412-438.

Mansour,A., Fox,C.A., Akil,H., Watson,S.J., 1995. Opioid-receptor mRNA expression in the rat CNS: anatomical and functional implications. Trends in Neurosciences 18, 22-29.

Mansour,A., Khachaturian,H., Lewis,M.E., Akil,H., Watson,S.J., 1988. Anatomy of CNS opioid receptors. Trends in Neurosciences 11, 308-314.

Manzanares,J., Wagner,E.J., LaVigne,S.D., Lookingland,K.J., Moore,K.E., 1992a. Sexual differences in kappa opioid receptor-mediated regulation of tuberoinfundibular dopaminergic neurons. Neuroendocrinology 55, 301-307.

Manzanares,J., Lookingland,K.J., LaVigne,S.D., Moore,K.E., 1991a. Activation of tuberohypophyseal dopamine neurons following intracerebroventricular administration of the selective kappa opioid receptor antagonist nor-binaltorphimine. Life Sciences 48, 1143-1149.

Manzanares,J., Lookingland,K.J., Moore,K.E., 1991b. Kappa opioid receptor-mediated regulation of dopaminergic neurons in the rat brain. The Journal of Pharmacology and Experimental Therapeutics 256, 500-505.

Manzanares,J., Wagner,E.J., Lookingland,K.J., Moore,K.E., 1992b. Effects of immunoneutralization of dynorphin$_{1-17}$ and dynorphin$_{1-8}$ on the activity of central dopaminergic neurons in the male rat. Brain Research 587, 301-305.

Maurer,J.A., Wray,S., 1997. Neuronal dopamine subpopulations maintained in hypothalamic slice explant cultures exhibit distinct tyrosine hydroxylase mRNA turnover rates. Journal of Neuroscience 17, 4552-4561.

Meister,B., Hokfelt,T., Steinbusch,H.W.M., Skagerberg,G., Lindvall,O., Geffard,M., Joh,T.H., Cuello,A.C., Goldstein,M., 1988. Do tyrosine hydroxylase-immunoreactive neurons in the ventrolateral arcuate nucleus produce dopamine or only L-DOPA? Journal of Chemical Neuroanatomy 1, 59-64.

Merchant,K.M., 1994. c-fos antisense oligonucleotide specifically attenuates haloperidol-induced increases in neurotensin/neuromedin N mRNA expression in rat dorsal striatum. Molecular and Cellular Neurosciences 5, 336-344.

Merchenthaler,I., Maderdrut,J.L., Cianchetta,P., Shughrue,P., Bronstein,D., 1997. In situ hybridization histochemical localization of prodynorphin messenger RNA in the central nervous system of the rat. Journal of Comparative Neurology 384, 211-232.

Mezey,É., Palkovits,M., 1982. Two-way transport in the hypothalamo-hypophyseal system. In: Ganong,W.F., Martini,L. (Eds.), Frontiers in Neuroendocrinology. Raven Press, New York, Vol. 7, pp. 1-29.

Miller,K.J., Das,S.K., 1998. Antisense oligonucleotides: strategies for delivery. Pharmaceutical Science and Technology Today 1, 377-386.

Misu,Y., Goshima,Y., Ueda,H., Okamura,H., 1996. Neurobiology of L-DOPAergic systems. Progress in Neurobiology 49, 415-454.

Moller,C., Bing,O., Heilig,M., 1994. c-fos expression in the amygdala: In vivo antisense modulation and role in anxiety. Cellular and Molecular Neurobiology 14, 415-423.

Moore,K.E., 1987. Hypothalamic dopaminergic neuronal systems. In: Meltzer,H.Y. (Ed.), Psychopharmacology: The Third Generation of Progress. Raven Press, New York, pp. 127-139.

Moore,K.E., Demarest,K.T., Johnston,C.A., 1980. The Actions of Prolactin on Tuberoinfundibular Dopaminergic Neurons in Male and Female Rats. In: Brambilla,F., Racagni,G., de Wied,D. (Eds.), Progress in Psychoneuroendocrinology. Elsevier/North-Holland Biomedical Press, pp. 359-366.

Moore,K.E., Lookingland,K.J., 1995. Dopaminergic neuronal systems in the hypothalamus. In: Bloom,F.E., Kupfer,D.J. (Eds.), Psychopharmacology: The Fourth Generation of Progress. Raven Press, New York, pp. 245-256.

Moore,K.E., Lookingland,K.J., Gunnet,J.W., 1987. Effects of gonadal steroids and pituitary hormones on the activity of tuberoinfundibular dopaminergic neurons. In: Genazzani,A.R., Montemagno,U., Nappi,C., Petraglia,F. (Eds.), The Brain and Female Reproductive Function. The Parthenon Publishing Group, Park Ridge, N.J., pp. 117-125.

Moore,K.E., Riegle,G.D., Demarest,K.T., 1985. Effects of long-term treatment with estradiol and haloperidol on serum concentrations of prolactin and tuberoinfundibular dopaminergic neuronal activity. In: MacLeod,R.M., Thorner,M.O., Scapagnini,U. (Eds.), Prolactin, Basic and Clinical Correlates. Liviana Press, Padova, Vol. 1, pp. 543-549.

Morgan,W.W., Herbert,D.C., Pfeil,K.A., 1982. The effect of hypophysectomy and subsequent prolactin replacement or of elevated prolactin alone on median eminence noradrenaline and dopamine in the rat. Endocrinology 110, 1584-1591.

Morrow,B.A., Elsworth,J.D., Inglis,F.M., Roth,R.H., 1999. An antisense oligonucleotide reverses the footshock-induced expression of Fos in the rat medial prefrontal cortex and the subsequent expression of conditioned fear-induced immobility. The Journal of Neuroscience 19, 5666-5673.

Myers,K.J., Dean,N.M., 2000. Sensible use of antisense: how to use oligonucleotides as research tools. Trends in Pharmacological Sciences 21, 19-23.

Nagamoto-Combs,K., Piech,K.M., Best,J.A., Sun,B., Tank,A.W., 1997. Tyrosine hydroxylase gene promoter activity is regulated by both cyclic-AMP-responsive element and AP1 sites following calcium influx. The Journal of Biological Chemistry 272, 6051-6058.

Najimi,M., Robert,J.J., Mallet,J., Rostene,W., Forgez,P., 2002. Neurotensin induces tyrosine hydroxylase gene activation through nitric oxide and protein kinase C signaling pathways. Mol Pharmacol 62, 647-653.

Nakashima,A., Ota,A., Sabban,E.L., 2003. Interactions between Egr1 and AP1 factors in regulation of tyrosine hydroxylase transcription. Molecular Brain Research 112, 61-69.

Nielsen,J.A., Moore,K.E., 1982. Effects of chloral hydrate, γ-butyrolactone, and equithesin on the efflux of dopamine and 5-hydroxytryptamine metabolites into cerebroventricular perfusates of Rats. Journal of Neurochemistry 39, 235-238.

Norris,M.L., Millhorn,D.E., 1995. Hypoxia-induced protein binding to oxygen-responsive sequences on the tyrosine hydroxylase gene. J. Biol. Chem. 270, 23774-23779.

Okuno,H., Fujisawa,H., 1991. Conversion of tyrosine hydroxylase to stable and inactive form by the end products. Journal of Neurochemistry 57, 53-60.

Palkovits,M., Mezey,É., Kanyicska,B., Fekete,M.I.K., 1982. Distribution of monoamines within the median eminence in rats. Endocrinologia Experimentalis 16, 207-216.

Pan,J.T., Lookingland,K.J., Moore,K.E., 1995. Differential effects of corticotropin-releasing hormone on central dopaminergic and noradrenergic neurons. Journal Of Biomedical Science 2, 50-56.

Pan,J.-T., 1996. Neuroendocrine functions of dopamine. In: Stone,T.W. (Ed.), CNS Neurotransmitters and Neuromodulators: Dopamine. CRC Press, Inc., Boca Raton, Florida, pp. 213-231.

Pan,J.-T., Kow,L.-M., Pfaff,D.W., 1986. Single-unit activity of hypothalamic arcuate neurons in brain tissue slices. Neuroendocrinology 43, 189-196.

Pan,J.-T., Lai,C.-J., Yen,S.-H., 1996. Effects of natriuretic peptides and dopamine on single-unit activity of dorsomedial arcuate neurons in rat brain slices. Brain Research 737, 78-82.

Papanikolaou,N.A., Sabban,E.L., 2000. Ability of Egr-1 to activate tyrosine hydroxylase transcription in PC12 cells. The Journal of Biological Chemistry 275, 26683-26689.

Paxinos,G., Watson,C., 1986. The Rat Brain in Stereotaxic Coordinates, 2nd edition. Academic Press, New York.

Paxinos,G., Watson,C. The Rat Brain in Stereotaxic Coordinates CD ROM. 4th edition. 1998. Academic Press.

Perez,J.R., Li,Y., Stein,C.A., Majumder,S., Oorschot,A.V., Narayanan,R., 1994. Sequence-independent induction of Sp1 transcription factor activity by phosphorothioate oligodeoxynucleotides. Proceedings of the National Academy of Sciences of the United States of America 91, 5957-5961.

Persico,A.M., Schindler,C.W., Ohara,B.F., Brannock,M.T., Uhl,G.R., 1993. Brain transcription factor expression - effects of acute and chronic amphetamine and injection stress. Molecular Brain Research 20, 91-100.

Phillips,M.I., Gyurko,R., 1995. In vivo applications of antisense oligonucleotides for peptide research. Regulatory Peptides 59, 131-141.

Pickel,V.M., Chan,J., Sesack,S.R., 1993. Cellular substrates for interactions between dynorphin terminals and dopamine dendrites in rat ventral tegmental area and substantia-nigra. Brain Research 602, 275-289.

Piech-Dumas,K.M., Best,J.A., Chen,Y., Nagamoto-Combs,K., Osterhout,C.A., Tank,A.W., 2001. The cAMP responsive element and CREB partially mediate the response of the tyrosine hydroxylase gene to phorbol ester. Journal of Neurochemistry 76, 1376.

Piech-Dumas,K.M., Tank,A.W., 1999. CREB mediates the cAMP-responsiveness of the tyrosine hydroxylase gene: use of an antisense RNA strategy to produce CREB-deficient PC12 cell lines. Molecular Brain Research 70, 219-230.

Pilowsky,P.M., Suzuki,S., 1994. Antisense oligonucleotides: A new tool in neuroscience. Clinical and Experimental Pharmacology and Physiology 21, 935-944.

Porter,J.C., 1986a. In situ activity and phosphorylation of tyrosine hydroxylase in the median eminence. Molecular and Cellular Endocrinology 46, 21-27.

Porter,J.C., 1986b. Relationship of age, sex, and reproductive status to the quantity of tyrosine hydroxylase in the median eminence and superior cervical ganglion of the rat. Endocrinology 118, 1426-1432.

Qin,Z.-H., Zhou,L.-W., Zhang,S.-P., Wang,Y., Weiss,B., 1995. D2 dopamine receptor antisense oligodeoxynucleotide inhibits the synthesis of a functional pool of D2 dopamine receptors. Molecular Pharmacology 46, 730-737.

Rauscher,F.J., Cohen,D.R., Curran,T., Bos,T.J., Vogt,P.K., Bohmann,D., Tjian,R., Franza,B.R., 1988. Fos-associated protein p39 is the product of the jun proto-oncogene. Science 240[4855], 1010-1016.

Ringstedt,T., Tang,L.-Q., Persson,H., Lendahl,U., Lagercrantz,H., 1995. Expression of c-fos, Tyrosine Hydroxylase, and Neuropeptide mRNA in the Rat Brain around Birth: Effects of Hypoxia and Hypothermia. Pediatric Research 37, 15-20.

Rodriguez-Gomez,J.A., Romero-Ramos,M., Vizuete,M.L., Venero,J.L., Cano,J., Machado,A., 1997. Increased Activity and Expression of Tyrosine Hydroxylase in the Rat Substantia Nigra after Chronic Treatment with Nomifensine. Molecular Pharmacology 52, 641.

Rogue,P., Vincendon,G., 1992. Dopamine D2 receptor antagonists induce immediate early genes in the rat striatum. Brain Research Bulletin 29, 469-472.

Roth,R.H., Elsworth,J.D., 1995. Biochemical pharmacology of midbrain dopamine neurons. In: Bloom,F.E., Kupfer,D.J. (Eds.), Psychopharmacology: The Fourth Generation of Progress. Raven Press, New York.

Ryabinin,A.E., Wang,Y.M., Finn,D.A., 1999. Different levels of Fos immunoreactivity after repeated handling and injection stress in two inbred strains of mice. Pharmacology Biochemistry and Behavior 63, 143-151.

Ryder,K., Lau,L.F., Nathans,D., 1988. A gene activated by growth factors is related to the oncogene v-jun. Proceedings of the National Academy of Sciences of the United States of America 85, 1487-1491.

Sagar,S.M., Sharp,F.R., Curran,T., 1988. Expression of c-fos Protein in Brain: Metabolic Mapping at the Cellular Level. Science 240, 1328-1331.

Sanghera,M.K., Anselmofranci,J., McCann,S.M., 1991. Effect of medial zona incerta lesions on the ovulatory surge of gonadotropins and prolactin in the rat. Neuroendocrinology 54, 433-438.

Sassone-Corsi,P., Sisson,J.C., Verma,I.M., 1988. Transcriptional autoregulation of the proto-oncogene fos. Nature 334, 314-319.

Schobitz,B., Pezeshki,G., Probst,J.C., Reul,J.M.H.M., Skutella,T., Stohr,T., Holsboer,F., Spanagel,R., 1997. Centrally administered oligodeoxynucleotides in rats: occurrence of non-specific effects. European Journal of Pharmacology 331, 97-107.

Selmanoff,M., Shu,C., Hartman,R.D., Barraclough,C.A., Petersen,S.L., 1991. Tyrosine-hydroxylase and POMC messenger-RNA in the arcuate region are increased by castration and hyperprolactinemia. Molecular Brain Research 10, 277-281.

Selmanoff,M., 1981. The lateral and medial median eminence: Distribution of dopamine, norepinephrine, and luetinizing hormone-releasing hormone and the effect of prolactin on catecholamine turnover. Endocrinology 108, 1716-1722.

Selmanoff,M., Wise,P.M., 1981. Decreased dopamine turnover in the median eminence in response to suckling in the lactating rat. Brain Research 212, 101-115.

Sharp,F.R., Sagar,S.M., Swanson,R.A., 1993. Metabolic mapping with cellular resolution: c-fos vs. 2-deoxyglucose. Critical Reviews in Neurobiology 7, 205-228.

Sheng,M., Thompson,M.A., Greenberg,M.E., 1991. CREB: a Ca(2+)-regulated transcription factor phosphorylated by calmodulin-dependent kinases. Science 252, 1427-1430.

Sheng,M., Greenberg,M.E., 1990. The regulation and function of c-fos and other immediate early genes in the nervous system. Neuron 4, 477-485.

Shull,J.D., Gorski,J., 1989. Estrogen regulation of prolactin gene transcription in vivo: paradoxical effects of 17β-estradiol dose. Endocrinology 124, 279-285.

Sim,L.J., Selley,D.E., Tsai,K.P., Morris,M., 1994a. Calcium and cAMP mediated stimulation of Fos in cultured hypothalamic tyrosine hydroxylase-immunoreactive neurons. Brain Research 653, 155-160.

Sim,L.J., Selley,D.E., Tsai,K.P., Morris,M., 1994b. D2 inhibition of stimulated Fos immunoreactivity in cultured tyrosine hydroxylase-IR hypothalamic neurons. Brain Research 651, 311-316.

Sirinathsinghji,D.J.S., Schuligoi,R., Heavens,R.P., Dixon,A., Iversen,S.D., Hill,R.G., 1994. Temporal changes in the messenger RNA levels of cellular immediate early genes and neurotransmitter/receptor genes in the rat neostriatum and substantia nigra after acute treatment with eticlopride, a dopamine D2 receptor antagonist. Neuroscience 62, 407-423.

Sonnenberg,J.L., MacGregorleon,P.F., Curran,T., Morgan,J.I., 1989. Dynamic alterations occur in the levels and composition of transcription factor AP-1 complexes after seizure. Neuron 3, 359-365.

Spano,P.F., Govoni,S., Trabucchi,M., 1978. Studies on the pharmacological properties of dopamine receptors in various areas of the central nervous system. Advances in Biochemistry and Psychopharmacology 19, 155-165.

Speciale,S.G., Manaye,K.F., Sadeq,M., German,D.C., 1993. Opioid receptors in midbrain dopaminergic regions of the rat. 2. Kappa-receptor and delta-receptor autoradiography. Journal of Neural Transmission-General Section 91, 53-66.

Stancovski,I., Gonen,H., Orian,A., Schwartz,A.L., Ciechanover,A., 1995. Degradation of the proto-oncogene product c-fos by the ubiquity proteolytic system in-vivo and in-vitro - identification and characterization of the conjugating enzymes. Molecular and Cellular Biology 15, 7106-7116.

Stehelin,D., Varmus,H.E., Bishop,J.M., Vogt,P.K., 1976. DNA related to the transforming gene(s) of avian sarcoma viruses is present in normal avian DNA. Nature 260, 170-173.

Steiner,H., Gerfen,C.R., 1995. Dynorphin opioid inhibition of cocaine-induced, D1 dopamine receptor-mediated immediate-early gene-expression in the striatum. Journal of Comparative Neurology 353, 200-212.

Steiner,H., Gerfen,C.R., 1996. Dynorphin regulates D1 dopamine receptor-mediated responses in the striatum: Relative contributions of pre- and postsynaptic mechanisms in dorsal and ventral striatum demonstrated by altered immediate-early gene induction. Journal of Comparative Neurology 376, 530-541.

Steiner,H., Gerfen,C.R., 1998. Role of dynorphin and enkephalin in the regulation of striatal output pathways and behavior. Experimental Brain Research 123, 60-76.

Sun,B.Y., Tank,A.W., 2002. Overexpression of c-fos is sufficient to stimulate tyrosine hydroxylase (TH) gene transcription in rat pheochromocytoma PC18 cells. Journal of Neurochemistry 80, 295-306.

Sun,B.Y., Tank,A.W., 2003. c-Fos is essential for the response of the tyrosine hydroxylase gene to depolarization or phorbol ester. J Neurochem 85, 1421-1430.

Suzuki,T., Okuno,H., Yoshida,T., Endo,T., Nishina,H., Iba,H., 1991. Difference in transcriptional regulatory function between c-Fos and Fra-2. Nucl. Acids. Res. 19, 5537-5542.

Szabo,G., Nunley,K.R., Hoffman,P.L., 1996. Antisense oligonucleotide to c-fos blocks the ability of arginine vasopressin to maintain ethanol tolerance. European Journal of Pharmacology 306, 67-72.

Szklarczyk,A., Kaczmarek,L., 1995. Antisense oligodeoxyribonucleotides: Stability and distribution after intracerebral injection into rat brain. Journal of Neuroscience Methods 69, 181-187.

Szklarczyk,A.W., Kaczmarek,L., 1999. Brain as a unique antisense environment. Antisense & Nucleic Acid Drug Development 9, 105-116.

Takekoshi,K., Ishii,K., Kawakami,Y., Isobe,K., Nakai,T., 2000. κ-opioid inhibits catecholamine biosynthesis in PC12 rat pheochromocytoma cell. FEBS Letters 477, 273-277.

Tian,Y., Eaton,M.J., Manzanares,J., Lookingland,K.J., Moore,K.E., 1992. Characterization of opioid receptor-mediated regulation of incertohypothalamic dopamine neurons: Lack of evidence for a role of 5-hydroxytryptaminergic neurons in mediating the stimulatory effects of morphine. Brain Research 591, 116-121.

Tian,Y., Lookingland,K.J., Moore,K.E., 1991. Contribution of noradrenergic neurons to 3,4-dihydroxyphenuylacetic acid concentrations in the regions of the rat brain containing incertohypothalamic dopaminergic neurons. Brain Research 555, 135-140.

Timmerman,W., Deinum,M.E., Westerink,B.H.C., Schuiling,G.A., 1995. Lack of evidence for dopamine autoreceptors in the mediobasal hypothalamus - A microdialysis study in awake rats. Neuroscience Letters 195, 113-116.

Tohei,A., VandeGarde,B., Arbogast,L.A., Voogt,J.L., 2000. Calcitonin inhibition of prolactin secretion in lactating rats: Mechanism of action. Neuroendocrinology 71, 327-332.

Toney,T.W., Lookingland,K.J., Moore,K.E., 1991. Role of testosterone in the regulation of tuberoinfundibular dopaminergic neurons in the male rat. Neuroendocrinology 54, 23-29.

Toney,T.W., Pawsat,D.E., Fleckenstein,A.E., Lookingland,K.J., Moore,K.E., 1992. Evidence that prolactin mediates the stimulatory effects of estrogen on tuberoinfundibular dopamine neurons in female rats. Neuroendocrinology 55, 282-289.

Treisman,R., 1986. Identification of a protein-binding site that mediates transcriptional response of the c-fos gene to serum factors. Cell 46, 567-574.

Treisman,R., 1992. The serum response element. Trends in Biochemical Sciences 17, 423-426.

Vallone,D., Picetti,R., Borrelli,E., 2000. Structure and function of dopamine receptors. Neuroscience and Biobehavioral Reviews 24, 125-132.

Van Den Pol,A.N., Herbst,R.S., Powell,J.F., 1984. Tyrosine hydroxylase-immunoreactive neurons of the hypothalamus: A light and electron microscopic study. Neuroscience 13, 1117-1156.

Veyrune,J.L., Carillo,S., Vie,A., Blanchard,J.M., 1995. c-fos messenger-RNA instability determinants present within both the coding and the 3'-non-coding region link the degradation of this messenger-RNA to its translation. Oncogene 11, 2127-2134.

Vogt,P.K., Bos,T.J., 1990. jun: Oncogene and transcription factor. Advances in Cancer Research 55, 1-35.

Vyas,S., Faucon Biguet,N., Mallet,J., 1990. Transcriptional and post-transcriptional regulation of tyrosine hydroxylase gene by protein kinase C. EMBO J. 9, 3707-3712.

Wagner,C.K., Eaton,M.J., Moore,K.E., Lookingland,K.J., 1995. Efferent projections from the region of the medial zona incerta containing A13 dopaminergic neurons: a PHA-L anterograde tract-tracing study in the rat. Brain Research 677, 229-237.

Wagner,E.J., Goudreau,J.L., Moore,K.E., Lookingland,K.J., 1994a. GABAergic regulation of tuberoinfundibular dopaminergic neurons in the male rats. Brain Research 659, 194-200.

Wagner,E.J., Manzanares,J., Moore,K.E., Lookingland,K.J., 1994b. Neurochemical evidence that estrogen-induced suppression of kappa-opioid receptor-mediated regulation of tuberoinfundibular dopaminergic neurons is prolactin-independent. Neuroendocrinology 59, 197-201.

Wagner,E.J., Moore,K.E., Lookingland,K.J., 1994c. Neurochemical evidence that AMPA receptor-mediated tonic inhibition of hypothalamic dopaminergic neurons occurs via activation of inhibitory interneurons. Brain Research 660, 319-322.

Wagner,E.J., Moore,K.E., Lookingland,K.J., 1994d. Non-NMDA receptor-mediated regulation of hypothalamic dopaminergic neurons in the rat. European Journal of Pharmacology 254, 105-112.

Wagner,E.J., Ronnekleiv,O.K., Grandy,D.K., Kelly,M.J., 1998. The peptide orphan FQ Inhibits β-endorphin neurons and neurosecretory Cells in the hypothalamic arcuate nucleus by activating an inwardly-rectifying K+ conductance. Neuroendocrinology 67, 73-82.

Wahlestedt,C., 1994. Antisense oligonucleotide strategies in neuropharmacology. TIPS 15, 42-46.

Wang,H.-J., Hoffman,G.E., Smith,M.S., 1993. Suppressed tyrosine hydroxylase gene expression in the tuberoinfundibular dopaminergic system during lactation. Endocrinology 133, 1657-1663.

Weiner,D.M., Levey,A.I., Sunahara,R.K., Niznik,H.B., Odowd,B.F., Seeman,P., Brann,M.R., 1991. D1 and D2 dopamine receptor messenger-RNA in rat brain. Proceedings of the National Academy of Sciences of the United States of America 88, 1859-1863.

Wyke,J., 1983. Evolution of oncogenes: From c-src to v-src. Nature 304, 491-492.

Yaida,Y., Nowak,T.S.Jr., 1995. Distribution of phosphodiester and phosphorothioate oligonucleotides in rat brain after intraventricular and intrahippocampal administration determined by in situ hybridization. Regulatory Peptides 59, 193-199.

Yang,C., Kim,H.-S., Seo,H., Kim,K.-S., 1998. Identification and characterization of potential cis-regulatory elements governing transcriptional activation of the rat tyrosine hydroxylase gene. Journal of Neurochemistry 71, 1358-1368.

Yang,S.-P., Lee,Y., Voogt,J.L., 1999. Fos expression in the female rat brain during the proestrous prolactin surge and following mating. Neuroendocrinology 69, 281-289.

Young,W.S., Warden,M., Mezey,E., 1987. Tyrosine-hydroxylase messenger-RNA is increased by hyperosmotic stimuli in the paraventricular and supraoptic nuclei. Neuroendocrinology 46, 439-444.

Zamir,N., Palkovits,M., Brownstein,M.J., 1983. Distribution of immunoreactive dynorphin in the central nervous system of the rat. Brain Research 280, 81-93.

Zamir,N., Palkovits,M., Brownstein,M.J., 1984. Distribution of immunoreactive dynorphin A1-8 in discrete nuclei of the rat brain: Comparison with dynorphin A. Brain Research 307, 61-68.

Zon,G., 1995. Brief Overview of control of genetic expression by antisense oligonucleotides and in vivo applications. Molecular Neurobiology 10, 219-229.

Zukin,R.S., Eghbali,M., Olive,D., Unterwald,E.M., Tempel,A., 1988. Characterization and visualization of rat and guinea pig brain κ opioid receptors: Evidence of κ1 and κ2 opioid receptors. Proceedings of the National Academy of Sciences of the United States of America 85, 4061-4065.